

# QCD Sum Rules Approach to the $X$ , $Y$ and $Z$ States

Raphael M. Albuquerque<sup>a</sup>, Jorgivan M. Dias<sup>b</sup>, K. P. Khemchandani<sup>c</sup>, A. Martínez Torres<sup>b</sup>, Fernando S. Navarra<sup>b</sup>,  
Marina Nielsen<sup>b,\*</sup>, Carina M. Zanetti<sup>a</sup>

<sup>a</sup>*Faculdade de Tecnologia, Universidade do Rio de Janeiro (FAT, UERJ), Rod. Presidente Dutra Km 298, 27537-000, Resende, RJ, Brazil*

<sup>b</sup>*Instituto de Física, Universidade de São Paulo, Rua do Matão, Travessa R187, 05508-090 São Paulo, São Paulo, Brazil*

<sup>c</sup>*Universidade Federal de São Paulo, C.P. 01302-907, Diadema, São Paulo, Brazil*

---

## Abstract

In the past decade, due to the experimental observation of many charmonium-like states, there has been a revival of hadron spectroscopy. In particular, the experimental observation of charged charmonium-like,  $Z_c$  states, and bottomonium-like,  $Z_b$  states, represents a challenge since they can not be accommodated within the naive quark model. These charged states are good candidates of either tetraquark or molecular states and their observation motivated a vigorous theoretical activity. This is a rapidly evolving field with enormous amount of new experimental information. In this work, we review the current experimental progress and investigate various theoretical interpretations of these candidates of the multi-quark states. The present review is written from the perspective of the QCD sum rules approach, where we present the main steps of concrete calculations and compare the results with other approaches and with experimental data.

---

---

\*Corresponding author

*Email addresses:* raphael.albuquerque@uerj.br (Raphael M. Albuquerque), dias@if.usp.br (Jorgivan M. Dias), kanchan.khemchandani@unifesp.br (K. P. Khemchandani), amartine@if.usp.br (A. Martínez Torres), navarra@if.usp.br (Fernando S. Navarra), mnielsen@if.usp.br (Marina Nielsen), carina.zanetti@gmail.com (Carina M. Zanetti)

## Contents

<b>1</b>	<b>Introduction</b>	<b>3</b>
<b>2</b>	<b>QCD sum rules technique</b>	<b>6</b>
2.1	Correlation Functions . . . . .	6
2.2	The QCD side . . . . .	7
2.3	The phenomenological side . . . . .	9
2.4	Borel Transform . . . . .	10
2.5	QCD sum rules: Two-point function and Mass . . . . .	10
2.6	QCD Input Parameters . . . . .	11
2.7	QCD sum rules: Three-point function and Decay Width . . . . .	11
2.7.1	QCD or OPE side . . . . .	12
2.7.2	Phenomenological side . . . . .	14
2.7.3	Three-point function sum rule . . . . .	15
2.8	Extrapolation of the form factor and the coupling constant . . . . .	16
2.9	Limitations of the applications of the QCDSR to the exotic states . . . . .	18
<b>3</b>	<b>The X(3872) state</b>	<b>19</b>
3.1	QCDSR calculations for X(3872) . . . . .	21
3.2	QCDSR for pure four-quark structures . . . . .	21
3.2.1	Two-point correlation function . . . . .	21
3.2.2	Three-point correlation function . . . . .	24
3.3	Mixing of two- and four-quarks structure from QCDSR . . . . .	26
3.3.1	Two-point correlation function . . . . .	26
3.3.2	Three-point correlation function: $X(3872) \rightarrow J/\psi(n\pi)$ decay . . . . .	27
3.3.3	$X(3872) \rightarrow \gamma J/\psi$ radiative decay . . . . .	29
3.3.4	$X(3872)$ production in $B$ decays . . . . .	33
3.4	Summary for X(3872) . . . . .	36
<b>4</b>	<b>Vector Charmonium <math>Y</math> States</b>	<b>36</b>
4.1	$Y(4260)$ . . . . .	37
4.1.1	Theoretical explanations for $Y(4260)$ . . . . .	38
4.1.2	QCDSR calculations for the $Y(4260)$ mass . . . . .	38
4.1.3	$Y(4260) \rightarrow J/\psi\pi\pi$ decay width . . . . .	39
4.1.4	$Y(4260)$ production in $B$ decays . . . . .	43
4.2	Remarks on $Y(4220)$ . . . . .	45
4.3	$Y(4360)$ . . . . .	46
4.3.1	Theoretical explanations for $Y(4360)$ . . . . .	46
4.3.2	QCDSR calculations for $Y(4360)$ . . . . .	46
4.4	Remarks on $Y(4390)$ . . . . .	47
4.5	$Y(4660)$ . . . . .	48
4.5.1	Theoretical explanations for $Y(4660)$ . . . . .	48
4.5.2	QCDSR calculations for $Y(4660)$ . . . . .	48
4.6	Summary for the vector $Y$ states . . . . .	50
<b>5</b>	<b>Isvector states with hidden charm</b>	<b>50</b>
5.1	$Z^+(4430)$ . . . . .	51
5.1.1	History of theoretical studies of $Z^+(4430)$ . . . . .	52
5.2	$Z_c^+(3900)$ . . . . .	53
5.2.1	Theoretical explanations for $Z_c^+(3900)$ . . . . .	53
5.2.2	QCDSR calculations for the $Z_c^+(3900)$ width . . . . .	54

5.3	$Z_c^+(4020)$ (former $Z_c^+(4025)$ ) . . . . .	56
5.3.1	Theoretical explanations for $Z_c^+(4020)$ . . . . .	56
5.3.2	QCDSR calculations for $Z_c^+(4020)$ . . . . .	57
5.4	$Z_1^+(4050)$ , $Z_c^+(4055)$ and $Z_2^+(4250)$ . . . . .	60
5.4.1	Theoretical explanations for $Z_1^+(4050)$ , $Z_c^+(4055)$ and $Z_2^+(4250)$ . . . . .	60
5.4.2	QCDSR calculations for $Z_1^+(4050)$ , $Z_c^+(4055)$ and $Z_2^+(4250)$ . . . . .	61
5.5	$Z_c^+(4200)$ . . . . .	62
5.5.1	Theoretical explanations and QCDSR calculations for $Z_c^+(4200)$ . . . . .	62
5.6	$Z_c^-(4100)$ . . . . .	62
5.6.1	Theoretical explanations and QCDSR calculations for $Z_c^-(4100)$ . . . . .	63
5.7	Summary for the isovector $Z$ states . . . . .	63
<b>6</b>	<b>Controversial <math>Y</math> states</b> . . . . .	<b>63</b>
6.1	$Y(3940)$ or $X(3915)$ state . . . . .	63
6.2	$Y(4140)$ state . . . . .	64
6.3	Theoretical interpretations for the $Y(3940)$ and $Y(4140)$ . . . . .	64
6.4	QCDSR calculations for the $Y(3940)$ and $Y(4140)$ . . . . .	65
6.5	The $Y(4140)$ and $X(4160)$ with a tensorial current . . . . .	67
6.6	Summary for the Controversial $Y$ states . . . . .	69
<b>7</b>	<b>Higher Order Perturbative Corrections in Sum Rules</b> . . . . .	<b>69</b>
7.1	NLO Sum Rules . . . . .	70
7.2	QCD Input Parameters at NLO . . . . .	72
7.3	Heavy-Light Molecular States . . . . .	72
7.4	Heavy-Light Tetraquark States . . . . .	74
7.5	Summary for the higher order corrections in QCDSR . . . . .	76
<b>8</b>	<b>Summary</b> . . . . .	<b>76</b>

## 1. Introduction

If asked, most of the physicists today will say that protons and neutrons are made of quarks. Indeed, the constituent quark model is still widely used to represent all known hadrons and it has been valid for more than half century. On the other hand, more sophisticated QCD-inspired models based on quarks and gluons have predicted the existence of more complex structures than simple mesons (quark-antiquark bound states) or baryons (3 quark bound states), which are called exotic states. The idea of unconventional quark structures is quite old and due to decades of investigation, the existence of exotic meson has been recently confirmed.

In the charmonium sector, below the open-charm threshold the  $c\bar{c}$  charmonium states are successfully described using the quark model supplemented with quark potentials. All the predicted states have been observed with the expected properties below this threshold and excellent agreement is achieved between theory and experiment. Indeed, theoretical models and experiments achieved an overall agreement of 2–3 MeV/ $c^2$  precision in the mass measurements of charmonium states. Above the open-charm threshold, however, there are still many predicted states that have not yet been discovered, and, surprisingly, several unexpected states have been observed since 2003. Interesting examples of these so - called (exotic) charmonium-like XYZ states are the axial-vector  $X(3872)$ , the vector states  $Y(4260)$ ,  $Y(4360)$  and  $Y(4660)$  and the charged state  $Z_c(3900)^\pm$ . This latter is a manifestly exotic state. It became evident that charmonium-like states with more than a quark and an antiquark exist and several new models and possible interpretations have been advanced. These interpretations are still open, mostly due to the poor available statistics in the past experiments to investigate them, i.e. to perform a full amplitude analysis.

The number of the exotic charmonium states has increased year by year. Up to now there are more than twenty of these  $X$ ,  $Y$ ,  $Z$  states. In Table 1 we give a list of these charmonium states. These states have been studied using

different kind of models and there are several reviews about these studies [1–20]. An experimental review can be found in [21].

The study of spectroscopy and the decay properties of the heavy flavor mesonic states provides us with useful information about the dynamics of quarks and gluons at the hadronic scale. One interesting question about the QCD dynamics refers to the existence of diquarks. Whether or not quarks form diquark clusters inside a baryon or in multi-quark states, it has implications for the spectrum of the radial excitations. If diquarks are relevant, then the number of possible excitations is smaller. This fact may be verified experimentally. A systematic scan of the states lying in this energy region is now feasible. In the case of some of the X and Y states, we can say that there are still attempts to interpret them as  $c - \bar{c}$ . One can pursue this approach introducing corrections in the potential, such as quark pair creation. This “screened potential” changes the previous results, obtained with the unscreened potential and allows to understand some of the new data in the  $c - \bar{c}$  approach. Departing from the  $c - \bar{c}$  assignment, the next option is a system composed by four quarks, which can be uncorrelated, forming a kind of bag, or can be grouped in diquarks which then form a bound system. These configurations are called tetraquarks. Alternatively, these four quarks can form two mesons which then interact and form a bound state. If the mesons contain only one charm quark or antiquark, this configuration is referred to as a molecule. If one of the mesons is a charmonium, then the configuration is called hadro-charmonium. Another possible configuration is a hybrid charmonium. In this case, apart from the  $c - \bar{c}$  pair, the state contains excitations of the gluon field. In some implementations of the hybrid, the excited gluon field is represented by a “string” or flux tube, which can oscillate in normal modes.

The above mentioned configurations are quite different and are governed by different dynamics. In quarkonia states the quarks have a short range interaction dominated by one gluon exchange and a long range non-perturbative confining interaction, which is often parametrized by a linear attractive potential. In tetraquarks besides these two types of interactions, we may have a diquark-antidiquark interaction, which is not very well known. In molecules and hadro-charmonium the interaction occurs through meson exchange. Finally, in some models inspired by lattice QCD results, there is a flux tube formation between color charges and also string junctions. With these building blocks one can construct very complicated “stringy” combinations of quarks and antiquarks and their interactions follow the rules of string fusion and/or recombination. In principle, the knowledge of the interaction should be enough to determine the spatial configuration of the system. In practice, this is only feasible in simple cases, such as the charmonium in the non-relativistic approach, where having the potential one can solve the Schrödinger equation and determine the wave function. In other approaches the spatial configuration must be guessed and it may play a crucial role in the production and decay of these states.

All recent analyses performed on exotic states show statistics limitation, not allowing a final conclusion. It is definitively necessary to upgrade all the experiments in order to have more statistics. One example of upgrade is the project Belle II. In 2018 the first collisions happened, probably marking the beginning of a new era for the  $e^+e^-$  colliders, which will last at least ten years. With the expected high luminosity, Belle II can improve for sure some of the measurements already performed by Belle, and look for new still undisclosed forms of exotic matter. It will be possible to search for more rare decays, up to now not possible due to the limited statistics. With such high statistics amplitude analysis can be performed and the quantum numbers can be determined.

A comparison of running and future experiments can be found in recent papers and help in understanding the future opportunities in spectroscopy.

A good reason to write a report on the subject is because this is a rapidly evolving field with enormous amount of new experimental information coming from the analysis of BELLE II, BESIII and LHCb accumulated data. In the present review we include and discuss data which were not yet available to the previous reviewers. This astonishing progress on the experimental side has opened up new challenges in the understanding of heavy flavor hadrons and from time to time it is necessary to organize the theoretical and experimental advances in short review papers. This is the goal of this text.

Any theoretical review is biased and naturally emphasizes the approach followed by the authors. We focus on the theoretical developments and more specifically on the works done with QCD sum rules (QCDSR). The present review is written from the perspective of QCD sum rules, where we present the main steps of concrete calculations and compare the results with other approaches and with experimental data. In what follows we will review and comment the work presented in Refs. [86–117].

In the next Section we review the basic concepts of the QCDSR method and, in Sec. 2.9, we discuss some limitations of the application of QCDSR to the exotic states. In Section 3 we describe the progress achieved in the

Table 1: The  $X$ ,  $Y$  and  $Z$  states in the  $c\bar{c}$  region ordered by mass. Masses  $m$  and widths  $\Gamma$  represent the weighted averages from the listed sources, or are taken from [22] when available. The citation given in **red** is for the first observation and the citation given in **blue** is for a non confirmation. The quoted year is the year of the first observation and the given charge conjugation ( $C$ ) of the isovector states is for the neutral state in the multiplet.

State	$m$ (MeV)	$\Gamma$ (MeV)	$J^{PC}$	Process (mode)	experiment	Year
$X(3872)$	$3871.69 \pm 0.17$	$< 1.2$	$1^{++}$	$B \rightarrow K(\pi^+\pi^-J/\psi)$ $p\bar{p} \rightarrow (\pi^+\pi^-J/\psi) (\dots)$ $B \rightarrow K(\omega J/\psi)$ $B \rightarrow K(D^0\bar{D}^0)$ $B \rightarrow K(\gamma J/\psi)$ $B \rightarrow K(\gamma\psi(2S))$ $e^+e^- \rightarrow \pi^+\pi^-J/\psi$ $p\bar{p} \rightarrow (\pi^+\pi^-J/\psi) (\dots)$	<b>Belle</b> [23–25], BaBar [26] CDF [27–29], DØ [30] Belle [31], BaBar [32] Belle [33, 34], BaBar [35] Belle [31], BaBar [36, 37] BaBar [37], LHCb [38] BESIII [39] LHCb [40, 41], CMS [42]	2003
$Z_c(3900)$	$3886.6 \pm 2.4$	$28.2 \pm 2.6$	$1^{+-}$	$Y(4260) \rightarrow (J/\psi \pi^+) \pi^-$ $Y(4260) \rightarrow (D\bar{D}^*)^+ \pi^-$	<b>BESIII</b> [43], Belle [44], CLEO-c [45] BESIII [46]	2013
$Y(3940)$	$3918.4 \pm 1.9$	$20 \pm 5$	$0/2^{++}$	$B \rightarrow K(J/\psi\omega)$ $e^+e^- \rightarrow e^+e^-(\omega J/\psi)$	<b>Belle</b> [47], BaBar [32, 48] Belle [49], BaBar [50]	2004
$X(3940)$	$3942_{-8}^{+9}$	$37_{-17}^{+27}$	$?^{?+}$	$e^+e^- \rightarrow J/\psi (\dots)$ $e^+e^- \rightarrow J/\psi (DD^*)$	<b>Belle</b> [51] Belle [52]	2005
$Y(4008)$	$3891 \pm 42$	$255 \pm 42$	$1^{--}$	$e^+e^- \rightarrow \pi^+\pi^-J/\psi$	<b>Belle</b> [44, 53], <b>BESIII</b> [54]	2007
$Z_c(4020)$	$4024.1 \pm 1.9$	$13 \pm 5$	$?^{?-}$	$e^+e^- \rightarrow \pi^-(\pi^+h_c)$ $Y(4260) \rightarrow \pi^-(D^*\bar{D}^*)^+$	<b>BESIII</b> [55] BESIII [56]	2013
$Z_1(4050)$	$4051_{-43}^{+24}$	$82_{-35}^{+51}$	$?^{?-}$	$B \rightarrow K(\pi^+\chi_{c1}(1P))$	<b>Belle</b> [57], BaBar [58]	2008
$Z_c(4055)$	$4054 \pm 3$	45	$(?^{?-})$	$e^+e^- \rightarrow \pi^-(\pi^+\psi(2S))$	<b>Belle</b> [59]	2014
$Z_c(4100)$	$(4096 \pm_{-32}^{+28})$	$152_{-45}^{+70}$	$0^{++}/1^{+-}$	$B^0 \rightarrow K^+(\pi^-\eta_c(1S))$	LHCb [60]	2018
$Y(4140)$	$4146.8 \pm 2.4$	$22_{-7}^{+8}$	$1^{++}$	$B \rightarrow K(\phi J/\psi)$	CDF [61, 62], D0 [63], LHCb [64], <b>BESIII</b> [65, 66]	2009
$X(4160)$	$4156_{-25}^{+29}$	$139_{-65}^{+113}$	$?^{?+}$	$e^+e^- \rightarrow J/\psi(D^*\bar{D}^*)$	<b>Belle</b> [52]	2007
$Z_c(4200)$	$4196_{-30}^{+35}$	$370_{-110}^{+99}$	$1^{+-}$	$B \rightarrow K(\pi^+J/\psi)$	<b>Belle</b> [67]	2014
$Y(4220)$	$4218_{-4}^{+5}$	$59_{-10}^{+12}$	$1^{--}$	$e^+e^- \rightarrow \chi_{c0} \omega$ $e^+e^- \rightarrow h_c \pi^+\pi^-$ $e^+e^- \rightarrow \psi(2S) \pi^+\pi^-$ $e^+e^- \rightarrow D^0 D^{*-} \pi^+$	<b>BESIII</b> [68] BESIII [69] BESIII [70] BESIII [71]	2014
$Z_2(4250)$	$4248_{-45}^{+185}$	$177_{-72}^{+321}$	$?^{?+}$	$B \rightarrow K(\pi^+\chi_{c1}(1P))$	<b>Belle</b> [57], BaBar [58]	2008
$Y(4260)$	$4230 \pm 8$	$55 \pm 19$	$1^{--}$	$e^+e^- \rightarrow \pi^+\pi^-J/\psi$ $e^+e^- \rightarrow K^+K^-J/\psi$ $e^+e^- \rightarrow \pi^0\pi^0J/\psi$ $e^+e^- \rightarrow Z_c(3900)^\pm \pi^\mp$	BaBar [72, 73], CLEO-c [74], Belle [44, 53], <b>BESIII</b> [54] CLEO-c [75], <b>BESIII</b> [46] CLEO-c [75] Belle [44], <b>BESIII</b> [43]	2005
$X(4350)$	$4350.6_{-5.1}^{+4.6}$	$13.3_{-10.0}^{+18.4}$	$?^{?+}$	$e^+e^- \rightarrow \phi J/\psi$	<b>Belle</b> [76]	2009
$Y(4360)$	$4368 \pm 13$	$96 \pm 7$	$1^{--}$	$e^+e^- \rightarrow \pi^+\pi^-\psi(2S)$ $e^+e^- \rightarrow \pi^+\pi^-J/\psi$	BaBar [77, 78], Belle [59, 79], <b>BESIII</b> [70] BESIII [54]	2007
$Y(4390)$	$4391.5_{-7.8}^{+7.3}$	$139.5_{-20.7}^{+16.3}$	$1^{--}$	$e^+e^- \rightarrow h_c \pi^+\pi^-$	<b>BESIII</b> [69]	2016
$Z(4430)$	$4478_{-18}^{+15}$	$181 \pm 31$	$1^{+-}$	$B \rightarrow K^-(\pi^+\psi(2S))$ $B \rightarrow K^-(\pi^+J/\psi)$	<b>Belle</b> [80–82], BaBar [83], LHCb [84] Belle [67], BaBar [83]	2007
$X(4630)$	$4634_{-11}^{+9}$	$92_{-32}^{+41}$	$1^{--}$	$e^+e^- \rightarrow \Lambda_c^+ \Lambda_c^-$	<b>Belle</b> [85]	2008
$Y(4660)$	$4643 \pm 9$	$72 \pm 11$	$1^{--}$	$e^+e^- \rightarrow \pi^+\pi^-\psi(2S)$ $e^+e^- \rightarrow \Lambda_c^+ \Lambda_c^-$	<b>Belle</b> [59, 79], BaBar [78] BESIII [85]	2007

study of the  $X(3872)$ , which is the best known exotic charmonium state. Section 4 is dedicated to the vector exotic states  $Y$ . In Section 5 we review the electrically charged  $Z$  exotic states. In Section 6 we present an updated discussion of the controversial  $Y$  states, i.e., those which need confirmation. In all the Sections, we give a brief experimental introduction, a short review of the theoretical works on the states and then, in more detail, their interpretation in QCD Sum Rules. Finally, in Section 7 we present the recent theoretical developments in QCDSR involving perturbative  $\alpha_s$  corrections and, in the end, we finish with our concluding remarks in the summary. All the sections are to some extent self-contained. Somewhat inspired by the PDG, this text allows the fast reader to go directly to the particle of his interest and look for recent information.

## 2. QCD sum rules technique

In this section, we discuss in detail one of the most active nonperturbative approach in Quantum Chromodynamics (QCD), which is also an entirely analytical tool for obtaining valuable information about hadronic states, called QCD sum rules (QCDSR) or also known as SVZ sum rules after Shifman, Vainstein and Zakharov, in 1979 [118, 119].

The QCD sum rules approach [118–123] allows us to extract properties of hadronic states from QCD parameters like quark masses, QCD coupling, and QCD condensates. In contrast to some nonperturbative approaches in QCD, for instance, potential models, the QCDSR is an analytic method and fully relativistic [124]. Over the last decade, this approach has been successfully used to describe the new hadronic states in the charmonium and bottomonium spectrum. It was also employed to investigate the exotic structure of some states, recently observed by the LHCb collaboration [125–127], which are candidates to be of Pentaquark nature [18]. It has been largely used in many applications, different to testing the exotic nature of the hadronic matter. In the beginning, it was applied just to investigate mesons and its extension to baryons was done afterwards by Ioffe [128]. There are some textbooks [124, 129] and articles [120, 130–132] in which the initial basic aspects of the method are discussed in many details, as well as the extensions to studies involving the nuclear medium [133].

### 2.1. Correlation Functions

The approach focuses on the correlation functions of local composite operators. A generic two-point correlation function is given by

$$\Pi(q) \equiv i \int d^4x e^{iq \cdot x} \langle 0 | T [j(x) j^\dagger(0)] | 0 \rangle, \quad (1)$$

where  $j(x)$  is the local composite operator,  $\langle \dots \rangle$  is the QCD vacuum expectation value, while  $T$  is the time ordered product between the operators. These operators are build up from quarks and gluons fields in such a way that they carry the quantum numbers of the hadron under investigation. We often refer to such operators as interpolating fields or currents. The interpolating currents for non-exotic states have the following generic expression:

$$j_n(x) = \bar{q}_a(x) \Gamma_n q_a(x), \quad (2)$$

where  $q(x)$  is the spinor representing the quark field,  $a$  stands for the color index and  $\Gamma_n$  is any structure made of Dirac matrices,  $\Gamma_n = 1, \gamma_\mu, \gamma_\mu \gamma_\nu, \gamma_\nu \gamma_5 \dots$ , which allows us to characterize the tensorial structure of the current. For instance,  $\Gamma_0 = 1$  gives us  $j(x) = \bar{q}_a(x) q_a(x)$  and describes a scalar meson with  $J^P = 0^+$ , while  $\Gamma_\mu = \gamma_\mu$  gives  $j_\mu(x) = \bar{q}_a(x) \gamma_\mu q_a(x)$ , that is used to describe a vector meson with  $J^P = 1^-$ . Hence we can choose the scalar, vectorial or tensor character of the interpolator by simply choosing the appropriate gamma matrix  $\Gamma_n$ . The quark content is determined by the flavor of the hadron. For instance, the current  $\bar{c}_a(x) \gamma_\mu c_a(x)$  describes a meson with charm-anti-charm quark content with  $J^P = 1^-$ , and can be used to study, within the QCDSR approach, the  $J/\psi$  meson.

From the Quark-Hadron duality concept [124, 134, 135], which establishes a correspondence between two different descriptions of the correlation functions, we can match a QCD description of a correlation function with a phenomenological one. More specifically, we can take into account the QCD degrees of freedom, quarks and gluon fields, and calculate the correlation function using Wilson's Operator Product Expansion (OPE) [136] in order to separate the physics of short and long-range distances. In this description, the correlator is expressed as the sum of coefficients (called Wilson's coefficients), which are c-numbers, multiplied by the expectation values of composite operators, which give rise to the condensates, for instance, the quark and gluon condensates. It is through those QCD vacuum condensates that the nonperturbative effects are included into the method. By doing this, we are calculating

the QCD side (also called OPE side) of the QCDSR. On the other hand, we can also consider the interpolating fields in the correlation functions representing the hadronic degrees of freedom, in such a way that they are no longer the quarks/gluon operators, but are associated to the creation/annihilation operators for the hadron itself. This description is usually called the Phenomenological side of the QCDSR. Assuming that there is an interval in momentum for which the QCD side and the Phenomenological one are equivalent, we can compare both sides and extract the hadronic parameter we are interested with.

Writing the correlation functions is also the starting point of other nonperturbative QCD approaches like Lattice QCD calculations (in the Euclidean coordinate space) and, in this case, the uncertainties can be systematically improved [133]. In the QCDSR technique we make use of some phenomenological inputs, limiting the accuracy of the method to be around 10% – 20% [124, 137]. This estimate can get worst when we take into account the expectation values of higher dimensional operators on the OPE side, since, as we will discuss later, we have to assume some factorization hypothesis, i.e., we replace the expectation values of higher dimensional operators by the products of the lower dimensional ones. This is one of the main source of uncertainty of the method.

## 2.2. The QCD side

As we are considering the quarks and gluons fields as the building blocks, i.e., the QCD degrees of freedom, we have to deal with the effects of soft gluons and quarks fields populating the QCD vacuum. In other words, we have to take into account the complex structure of the QCD vacuum. This means that the expectation values of the operators associated with those fields are non-zero, giving rise to what we call condensates. One way to deal with this feature of the QCD vacuum is to use the OPE [136].

As mentioned before, the correlation functions can be written as a sum of Wilson's coefficients times the expectation values of the composite operators. The perturbative part is encoded into those coefficients, which are obtained using the perturbative QCD. The information on the complex structure of the QCD vacuum is in the condensates, i. e., the nonperturbative effects due to the QCD vacuum is contained into the expectation values of the composite operators. Therefore, using the OPE we have a clear separation of scales, that is, the short distances effects in the coefficients, and the long-range ones due to the condensates. Therefore, we can write

$$\Pi(q) = i \int d^4x e^{iq \cdot x} \langle 0 | T [j(x) j^\dagger(0)] | 0 \rangle = \sum_d C_d(Q^2) \langle \hat{O}_d \rangle, \quad (3)$$

where  $C_d(Q^2)$  ( $Q^2 = -q^2$ ) is the Wilson's coefficients, and  $\langle \hat{O}_d \rangle$  is the expectation value of the composite local operators. This series is ordered by the dimension of the operator, denoted by the  $d$  index. The lowest-dimension operator with  $d = 0$  is the unit operator associated with the perturbative contribution:  $C_0(Q^2) = \Pi^{per}(Q^2)$ ,  $\hat{O}_0 = 1$ . Since one cannot build gauge invariant composite operators for  $d = 2$  [138], the next term in the expansion of Eq. (3) is for  $d = 3$ . Considering only the lowest dimension operators in the OPE, one obtains:

$$\begin{aligned} \hat{O}_3 &= : \bar{q}(0)q(0) : & \equiv \bar{q}q \\ \hat{O}_4 &= : g_s^2 G_{\alpha\beta}^N(0) G_{\beta\alpha}^N(0) : & \equiv g_s^2 G^2 \\ \hat{O}_5 &= : \bar{q}(0) g_s \sigma^{\alpha\beta} G_{\beta\alpha}(0) q(0) : & \equiv \bar{q}Gq \\ \hat{O}_6^q &= : \bar{q}(0)q(0) \bar{q}(0)q(0) : & \equiv \bar{q}q\bar{q}q \\ \hat{O}_6^G &= : f_{NMK} g_s^3 G_{\alpha\beta}^N(0) G_{\beta\gamma}^M(0) G_{\gamma\alpha}^K(0) : & \equiv g_s^3 G^3 \end{aligned} \quad (4)$$

where the symbol  $::$  represents the normal ordering of the operators,  $q(0)$  is the quark field,  $G_{\alpha\beta}^N(0)$  is the gluon field tensor,  $f_{NMK}$  is the structure constant of the SU(3) group and  $\sigma_{\alpha\beta} = \frac{i}{2} [\gamma_\alpha, \gamma_\beta]$ . The vacuum expectation value (VEV) of these local operators

$$\langle 0 | \hat{O}_n | 0 \rangle, \quad (5)$$

gives the quark condensate  $\langle \bar{q}q \rangle$ , gluon condensate  $\langle g_s^2 G^2 \rangle$ , mixed condensate  $\langle \bar{q}Gq \rangle$ , four-quark condensate  $\langle \bar{q}q\bar{q}q \rangle$  and the triple gluon condensate  $\langle g_s^3 G^3 \rangle$ . In general, the quark condensate and the gluon condensate are enough to reliably investigate non-exotic mesonic systems [7], for instance, the  $J/\psi$  meson [118, 119, 139, 140]. Contrarily, for exotic systems like the ones situated in the charmonium spectrum, the  $X(3872)$  for example, one has to go a step further in the expansion, including the terms of higher dimensions [88].

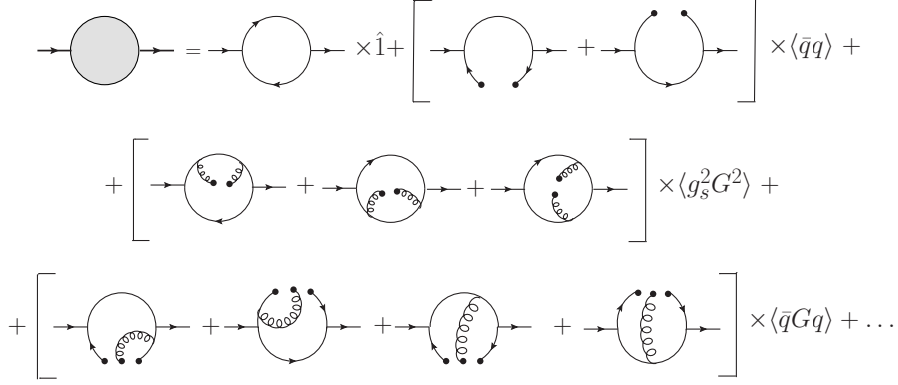


Figure 1: The OPE for the two-point function Eq. (6).

Taking, as an example, the 2-point function for a scalar state, the OPE for this case will be (up to dimension-5):

$$\Pi(Q^2) = C_0(Q^2) 1 + C_3(q^2)\langle \bar{q}q \rangle + C_4(q^2)\langle g_s^2 G^2 \rangle + C_5(q^2)\langle \bar{q}Gq \rangle. \quad (6)$$

The coefficients  $C_0, C_3, C_4, C_5$  multiplying the condensates in Eq. (6), are obtained by calculating the Feynman diagrams, whose topology depends on the particular choice of the interpolating current  $j$ . Examples of such diagrams can be seen in Fig. 1.

The values for the condensates are not determined directly from the experiment and, in general, we extract them from Lattice QCD calculations or, as in the case of quark and gluon condensates, they can be obtained from a QCDSR calculation for a given well-known state. For instance, the gluon condensate was estimated in Ref. [141], where the authors used the QCDSR method to investigate the charmonium system. As a result, they obtained  $\langle g^2 G^2 \rangle = (7.5 \pm 2.0) \times 10^{-2} \text{ GeV}^4$ . The quark condensate can be estimated in terms of the pion mass  $m_\pi$  and its decay constant  $f_\pi$  through the Oakes-Renner relation [142],

$$\langle \bar{q}q \rangle = -\frac{f_\pi^2 m_\pi^2}{(m_u + m_d)}, \quad (7)$$

where  $m_u(m_d)$  is the quark up (down) mass. Using the following values for the pion mass and its decay constant,  $f_\pi = 93.0 \text{ MeV}$  and  $m_\pi = 139.0 \text{ MeV}$  [143], with  $m_u + m_d = 14 \text{ MeV}$ , we have  $\langle \bar{q}q \rangle = -(0.23 \pm 0.03)^3 \text{ GeV}^3$ .

On the other hand, for higher dimensional condensates, as is the case for  $d = 6$  and  $d = 8$ , i. e., four-quark condensate, and eight-dimensional condensate, respectively, we have to assume that they can be factorized and their saturation values are:  $\langle \bar{q}q\bar{q}q \rangle = \langle \bar{q}q \rangle^2$ ,  $\langle \bar{q}q\bar{q}g\sigma.Gq \rangle = \langle \bar{q}q \rangle \langle \bar{q}g\sigma.Gq \rangle$ . In order to give an estimation of their precise values, a more involved analysis has to be done, once it is related to a non-trivial choice of factorization scheme [144]. In general, one introduces a parameter  $\rho$ , that assumes values from 1 up to 2.1, which account for deviations of the factorization hypothesis, with  $\rho = 1$  related to vacuum saturation values and  $\rho = 2.1$  to the violation of the factorization hypothesis assumption [122, 145–147]. This approximation also contributes to the uncertainties of the sum rule calculation.

In conclusion, on the OPE side, we calculate the correlator in terms of the OPE series, and we have to consider the contributions from condensates that are sufficient to guarantee a good OPE convergence. The next step is to write the correlator using the Källén-Lehmann representation or the dispersion relation:

$$\Pi^{OPE}(q^2) = \int_{s_{min}}^{\infty} \frac{\rho^{OPE}(s)}{s - q^2} ds, \quad (8)$$

where

$$\rho^{OPE}(s) = \frac{1}{\pi} \text{Im}[\Pi^{OPE}(s)], \quad (9)$$



is the spectral density function and  $s_{min}$  stands for a kinematical limit in the integral. In the case of interpolating currents with two heavy quarks (charm and bottom),  $s_{min} = 4m_{c(b)}^2$ , with  $m_{c(b)}$  the charm (bottom) quark mass.

### 2.3. The phenomenological side

In this case, the correlation function is evaluated considering the hadron itself as the degree of freedom, i. e., the operators in terms of which the correlation function is defined is now represented by the hadronic state we are interested in. Again, let us consider the two-point function as an example, with the interpolating current  $j$  associated with the operator that creates/annihilates the hadron under investigation. We have

$$\Pi^{phen}(q^2) = i \int d^4x e^{ipx} \langle 0 | T(j(x)j^\dagger(0)) | 0 \rangle. \quad (10)$$

Using the Kallen-Lehmann representation, Eq. (10) is written as

$$\Pi^{phen}(q^2) = \int_0^\infty ds \frac{\rho(s)}{s - q^2 + i\epsilon} + \text{subtraction terms}, \quad (11)$$

where  $\rho(s)$  is the spectral function. It is defined as  $\rho(s) = \sum_n |\langle n | j(0) | 0 \rangle|^2$ , and it means that all intermediate states coupling to the operator  $j$  contribute to the integral in Eq. (11). The spectral representation is a special case of dispersion relations. Within the QCDSR approach, dispersion relations are useful since it encodes the Quark-Hadron duality, which is the underlying concept of the QCDSR method. Therefore, the use of dispersion relations will connect the QCD side with the Phenomenological side, allowing to extract the hadronic observables from the QCD parameters.

In order for the QCDSR technique to be useful, one must parametrize  $\rho(s)$  with a small number of parameters. For this, we recall that in a hadron spectrum, in general, the lowest resonance is often fairly narrow, whereas higher-mass states are broader. Therefore, one can parameterize the spectral density as a single sharp pole representing the lowest resonance of mass  $m_H$ , plus a smooth continuum of resonances representing higher mass states:

$$\rho(s) = \lambda^2 \delta(s - m_H^2) + \rho^{cont}(s). \quad (12)$$

Using this equation into Eq. (11), we get the following expression for the Phenomenological side

$$\Pi^{phen}(q^2) = \frac{\lambda^2}{q^2 - m_H^2} + \int_{s_{min}}^\infty ds \frac{\rho^{cont}(s)}{s - q^2} + \text{subtraction terms}, \quad (13)$$

where  $\lambda$  measures the coupling of the low mass hadron state  $|H\rangle$  to the interpolating current  $j$ , i. e.

$$\langle 0 | j | H \rangle = \lambda. \quad (14)$$

For simplicity, one often assumes that the continuum contribution to the spectral density,  $\rho_{cont}(s)$  in Eq. (12), vanishes below a certain continuum threshold  $s_0$ . Above this threshold, it is assumed to be given by the result obtained with the OPE. Therefore, one uses the ansatz

$$\rho_{cont}(s) = \rho^{OPE}(s) \Theta(s - s_0). \quad (15)$$

Hence, we finally get

$$\Pi^{phen}(q^2) = \frac{\lambda^2}{q^2 - m_H^2} + \int_{s_0}^\infty ds \frac{\rho^{OPE}(s)}{s - q^2} + \text{subtraction terms} \quad (16)$$

As we should discuss later, the second term on the RHS of Eq. (13) is suppressed, when a Borel transform is applied, then we can extract the  $\lambda$  as well as the mass of the low-lying state coupling to the current  $j$ . In the next subsections, we are going to show that we can extract mass of the hadronic state under investigation from the two-point functions. Three-point functions are useful to get the form factors, which provide the coupling we need to know in order to determine the decay widths.

#### 2.4. Borel Transform

According to the Quark-Hadron duality, the sum rule is obtained by equating the correlator evaluated on the OPE side with the one written on the Phenomenological side:

$$\Pi^{OPE}(Q^2) = \Pi^{phen}(Q^2). \quad (17)$$

The validity of Eq. (17) gives us information about the properties of hadrons in terms of the QCD variables. However, such a duality is weakened by: i) the presence of subtraction terms which appear as unknown polynomials in  $Q^2$ ; ii) dominance of excited state contributions in comparison with the lowest hadronic state contribution; and iii) the truncation of the OPE. In order to overcome these problems and to obtain a self-consistent and a reliable match between OPE and Phenomenological sides, the authors in Refs. [118, 119] suggested to perform a Borel transformation on both sides of the sum rule. The Borel transformation (also known as inverse Laplace transformation) is defined as:

$$\Pi(M^2) = \mathcal{B}[\Pi(Q^2)] \equiv \lim_{\substack{Q^2, n \rightarrow \infty \\ Q^2/n = M^2}} \frac{(Q^2)^{n+1}}{(n)!} \left(-\frac{d}{dQ^2}\right)^n \Pi(Q^2), \quad (18)$$

where the parameter  $M^2$  is often called as the Borel mass. Some typical and useful examples of the Borel transformation are:

$$\mathcal{B}[(Q^2)^k] = 0, \quad (19)$$

$$\mathcal{B}\left[\frac{1}{(Q^2)^k}\right] = \frac{(-1)^k}{(k-1)!(M^2)^{k-1}}, \quad (20)$$

$$\mathcal{B}\left[\left(\frac{1}{s+Q^2}\right)^k\right] = \frac{1}{(k-1)!} \left(\frac{1}{M^2}\right)^{k-1} e^{-s/M^2}. \quad (21)$$

Evidently, the Borel transformation kills any eventual subtraction terms in the correlators and suppresses exponentially the continuum contribution, improving the convergence of the dispersion integral. Furthermore, it suppresses factorially the higher-order operators in OPE, which contain inverse powers of  $Q^2$ , justifying the truncation of the OPE and favoring a good OPE convergence.

#### 2.5. QCD sum rules: Two-point function and Mass

After transferring the continuum contribution to the OPE side, and performing a Borel transformation on both sides, the sum rule can be written as

$$\lambda^2 e^{-m_H^2/M^2} = \int_{s_{min}}^{s_0} ds \rho^{OPE}(s) e^{-s/M^2}. \quad (22)$$

By taking the derivative of Eq. (22) with respect to  $1/M^2$  and dividing the result by Eq. (22), we obtain

$$m_H^2 = \frac{\int_{s_{min}}^{s_0} ds s \rho^{OPE}(s) e^{-s/M^2}}{\int_{s_{min}}^{s_0} ds \rho^{OPE}(s) e^{-s/M^2}}. \quad (23)$$

To extract reliable results from Eq. (23), it is necessary to work in a region with a  $M^2$ -stability, a dominance of the lowest hadronic state (or pole dominance) over the continuum contribution, and a good OPE convergence. When it is possible to find a Borel range of  $M^2$  where all above mentioned requirements are fulfilled, then we can define the so-called Borel window. Notice that the Borel mass,  $M^2$ , is intrinsically related to the energy scale of the hadronic system. Therefore, considering higher values for  $M^2$  would correspond to the higher-energy regime where the continuum contribution dominates. In order to avoid this region, one usually sets an upper bound on the Borel mass value,  $M_{max}^2$ , where the pole dominance is guaranteed. A maximum value is determined by imposing the condition that the pole contribution is equal to the continuum contribution. On the other hand, considering smaller values for  $M^2$ ,

implies working in the low-energy regime, where the truncated OPE no longer provides a reasonable information on the lowest hadronic state. The non-perturbative effects become extremely important and higher dimension condensates must be included in the OPE series. Then, one naively expects that there is a minimum value in the Borel mass,  $M_{min}^2$ , which still provides a good OPE convergence. Typically, one defines the  $M_{min}^2$  value where the contribution of the higher dimension condensates in the OPE is smaller than 10% to 25% of the total contribution. This can be controlled by the  $\epsilon_N$ -parameter

$$\epsilon_N \equiv \left| 1 - \frac{\text{OPE}_{N-1}}{\text{OPE}_N} \right| = 0.10 \text{ to } 0.25 . \quad (24)$$

where  $\text{OPE}_N$  is the summation up to the  $N$ -dimension operator in the OPE series. Finally, one expects that the hadron mass has a certain stability in the  $M^2$  parameter inside the Borel window. Then, Borel windows with a large  $M^2$ -instability could indicate that the obtained hadron mass is not reliable, and more improvements must be done for these sum rule calculations. Sometimes, the inclusion of more condensates in the OPE improves such a  $M^2$ -stability. If one can not find a Borel window, then the QCDSR method can not be used to draw any conclusions.

Another important point is the choice of the continuum threshold,  $s_0$ . It is a physical parameter that should be determined from the hadronic spectrum. Using a harmonic-oscillator potential model, it was shown in Ref. [148] that a constant continuum threshold is a very poor approximation. The actual accuracy of the parameters extracted from the sum rules improves considerably when using a Borel dependent continuum threshold. It also allows to estimate realistic systematic errors [149]. However, to be able to fix the form of the Borel dependent continuum threshold, one needs to use the experimental value of the mass of the hadron. Since in our study we want to determine the mass of the state and not to use the experimental value, it is not possible to fix the Borel dependent continuum threshold. For this reason, although aware of the limitations of the values we extract mass from the sum rule, as a first estimate for such states, by using a constant continuum threshold. In many cases, a good approximation for the value of the continuum threshold is the value of the mass of the first excited state squared. In some known cases, like the  $\rho$  and  $J/\psi$  mesons, the first excited state has a mass approximately 0.5 GeV above the ground state mass. As we do not know, in principle, the spectrum of the hadrons we study, the range for the continuum threshold is fixed to be the smallest value which provides a valid Borel window. The optimal choice for  $s_0$  is taken when there is a  $M^2$ -stability inside the Borel window. Therefore, the sum rule calculation that respects these optimal criteria, can reliably extract the mass of hadronic states through Eq. (23).

## 2.6. QCD Input Parameters

We consider here the same values for the quark masses and condensates as used in Refs. [88–94, 150], listed in Table 2.

Table 2: QCD input parameters.

Parameters	Values
$m_b$	$(4.24 \pm 0.05) \text{ GeV}$
$m_c$	$(1.23 \pm 0.05) \text{ GeV}$
$m_s$	$(0.13 \pm 0.03) \text{ GeV}$
$\langle \bar{q}q \rangle$	$-(0.23 \pm 0.01)^3 \text{ GeV}^3$
$\langle \alpha_s^2 G^2 \rangle$	$0.88 \text{ GeV}^4$
$\kappa \equiv \langle \bar{s}s \rangle / \langle \bar{q}q \rangle$	$(0.74 \pm 0.03)$
$m_0^2 \equiv \langle \bar{q}Gq \rangle / \langle \bar{q}q \rangle$	$(0.8 \pm 0.2 \text{ GeV}^2)$

## 2.7. QCD sum rules: Three-point function and Decay Width

The use of three-point or vertex functions in QCDSR technique is related to the decay width, where a coupling constant is involved. Consider, for instance, the hadronic decay process  $H_1(p) \rightarrow H_2(p')H_3(q)$ , in which a given

hadronic state  $H_1(p)$ , with four-momentum  $p$ , decays into two hadrons  $H_2(p')$  and  $H_3(q)$  each with momentum  $p'$ ,  $q$ , respectively. The three-point function associated with this vertex is written as

$$\Pi(p^2, p', q^2) = \int d^4x \int d^4y e^{ip'x} e^{iqy} \langle 0 | T \{ j_{H_3}(x) j_{H_2}(y) j_{H_1}^\dagger(0) \} | 0 \rangle, \quad (25)$$

with  $j_{H_1}$ ,  $j_{H_2}$  and  $j_{H_3}$  the interpolating currents associated with the hadrons  $H_1$ ,  $H_2$  and  $H_3$ , respectively.

The evaluation of Eq. (25) follows the same steps as those used for the two-point case. That is, it can be evaluated using QCD degrees of freedom and, in this case, the OPE is used in order to deal with the complex QCD vacuum structure. The coefficients of this operator expansion are determined by perturbative calculation, while the vacuum expectation value of the operators are parametrized in terms of the condensates. On the other hand, Eq. (25) can also be evaluated using hadronic degrees of freedom. In this case, the three-point function is written in terms of the matrix elements of hadronic states. These matrix elements are, in general, obtained by using some effective field theory approach, where an effective Lagrangian provides the information on the dynamics.

It is worth mentioning that since the analytical structure of the three-point function can be different from the two-point case, the use of a dispersion integral should be treated with care [151–154].

### 2.7.1. QCD or OPE side

Analogously to the two-point function case, the OPE for Eq. (25) can be written as

$$\Pi^{OPE}(p^2, p'^2, Q^2) = \sum_{n=0}^{\infty} C_n(p^2, p'^2, Q^2) \langle \hat{O}_n \rangle, \quad (26)$$

with  $C_n(p^2, p'^2, Q^2)$  being the OPE coefficients. The vacuum expectation values of the local operators are the same ones already defined in Eq. (3) for the two-point case. The coefficients  $C_n(p^2, p'^2, Q^2)$  are obtained by calculating some Feynman diagrams. As an illustration, Fig. 2 shows a typical OPE (for the first lowest dimensions) in which some Feynman diagrams (other permutations are possible) are inside the brackets. The first one in Fig. 2 is associated with the first coefficient on the RHS of Eq. (26), and it gives the coefficient  $C_0$  for the unit operator, reflecting the fact that at zero order, we have contribution only from the perturbative QCD physics domain. The second term in Fig. 2 has dimension  $d = 3$  and is used to determine the coefficient  $C_3$ . The third term in the series in Fig. 2, with dimension  $d = 4$ , determines  $C_4$  that is multiplied to the gluon condensate  $\langle g_s^2 G^2 \rangle$ . The last set of diagrams contributes to the coefficient  $C_5$  multiplying the quark-gluon mixed condensate. According to Ref. [118] these power corrections are more important than higher order perturbative  $\alpha_s$  corrections. This will be discussed in the last section of this manuscript.

Once these diagrams are calculated we arrive at an expression for  $\Pi^{OPE}(p^2, p'^2, q^2)$  that has the generic form:

$$\Pi^{OPE}(p^2, p'^2, q^2) = \sum_i \Gamma_i(p^2, p'^2, q^2) T_i \quad (27)$$

where  $\Gamma_i(p^2, p'^2, q^2)$  are invariant functions of the momenta and  $T_i$  are the tensorial structures, i.e., products of Dirac matrices, the metric tensor and the four momenta, carrying Lorentz indices. The amount of Lorentz indices in those structures depends on the tensorial nature of the current  $j_n$  defined in Eq. (2). The invariant functions  $\Gamma_i(p^2, p'^2, q^2)$  can be written in terms of a double dispersion relation over the virtualities  $p'^2$  and  $p^2$  [155–158]

$$\Gamma_i(p^2, p'^2, q^2) = -\frac{1}{4\pi^2} \int_{s_{min}}^{\infty} ds \int_{u_{min}}^{\infty} du \frac{\rho_i^{OPE}(s, u, q^2)}{(s-p^2)(u-p'^2)} + \dots, \quad (28)$$

where  $\rho_i^{OPE}(s, u, q^2)$  is the double discontinuity that can be calculated using the Cutkosky's rules [159]. The terms not written explicitly, represented by the dots in Eq. (28), are polynomials in  $p'^2$  and  $p^2$ , and they vanish after a double Borel transform is applied to Eq. (28). It is just a Borel transform as in Eq. (18) applied twice, with  $P^2 = -p^2 \rightarrow M^2$  and  $P'^2 = p'^2 \rightarrow M'^2$ . A double transform applied to Eq. (28) leads to

$$\mathcal{B}\{\mathcal{B}[\Gamma_i(P^2, P'^2, Q^2)]\} = -\frac{1}{4\pi^2} \int_{s_{min}}^{\infty} ds \int_{u_{min}}^{\infty} du \rho_i^{OPE}(s, u, Q^2) e^{-s/M^2} e^{-u/M'^2}. \quad (29)$$

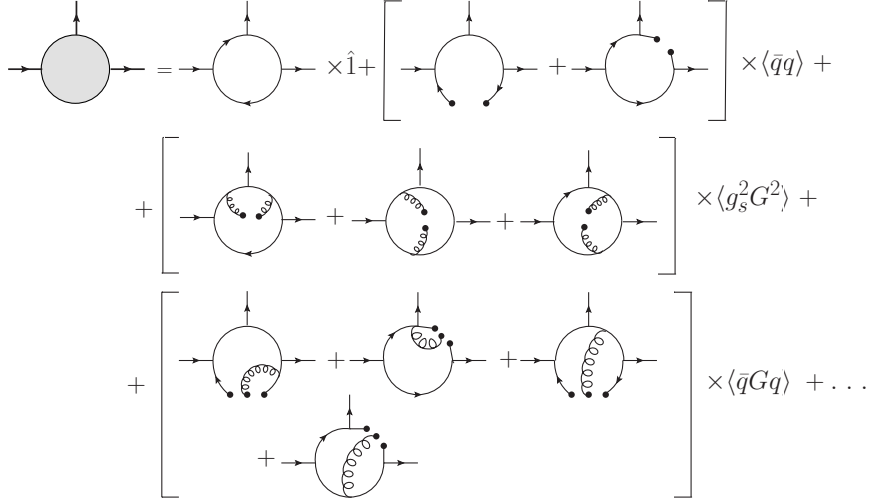


Figure 2: The OPE expansion for the three-point function of non-exotic mesons. Possible permutations are not shown

The Borel parameters,  $M^2$ ,  $M'^2$ , are chosen in such a way that the contribution of the higher states is suppressed at the same time we keep the power corrections under control.

As the interpolating currents are written in the form given by Eq. (2), the three-point function describes the coupling between non-exotic states, i. e., a vertex where a non-exotic meson decays into two other non-exotic mesons [158]. However, most of the new charmonium states have been described as exotic states. In order to describe, within QCDSR approach, those states as exotic four-quark states, the interpolating currents must have an additional pair of quark-anti-quark as compared with Eq. (2):

$$j_{ij} = \epsilon_{abc} \epsilon_{dec} (q_a^T C \Gamma_i q_b) (\bar{q}_d \Gamma_j C \bar{q}_e^T), \quad (30)$$

$$j_{ij} = (\bar{q}_a \Gamma_i q_a) (\bar{q}_b \Gamma_j q_b). \quad (31)$$

These four-quark currents are used to interpret the exotic structures with a tetraquark current, Eq. (30), or with a molecular current, Eq. (31). The new diagrams connected with the coefficients for the OPE in this case are constructed in the same manner as in the previous one. However, the topology changes, i. e. the Feynman diagrams will look like the ones depicted in Fig. 3. This occurs because the additional pair of quark-anti-quark fields on the current definition, gives rise to the “petal” form in the diagrams of Fig. 3.

For most exotic-type current calculations [105, 106, 108, 111, 114, 160], usually, it is sufficient to write the OPE up to dimension five  $d = 5$ . Some of the diagrams of dimension five ( $d = 5$ ) have an interesting feature. When there is a gluon exchange between the petals they are called color-connected. This implies that they are related to an intrinsic tetraquarks structure since the two petals cannot be considered as representing two separated mesons [106, 108, 160, 161].

Before proceeding it is important to stress that the currents in Eqs. (30), (31), and all currents used in this review to describe four-quark states, are local. Therefore, it is not possible to clearly distinguish between a tightly-bound tetraquark structure and a weakly-bound molecular structure. It is just the color combination between the quarks in the currents that is similar to a tetraquark or molecular state. Furthermore, due to Fierz transformation (see for instance Ref. [7]), these currents are related with each other and, in general, it is easy to reproduce the mass of the state for a variety of currents with the same quantum numbers. However, the relation between the currents are suppressed by typical color and Dirac factors and, as a consequence, the coupling between the current and the state can vary largely [99]. Therefore, a current with a large overlap with the physical state can still be used as an indication of the state inner structure.

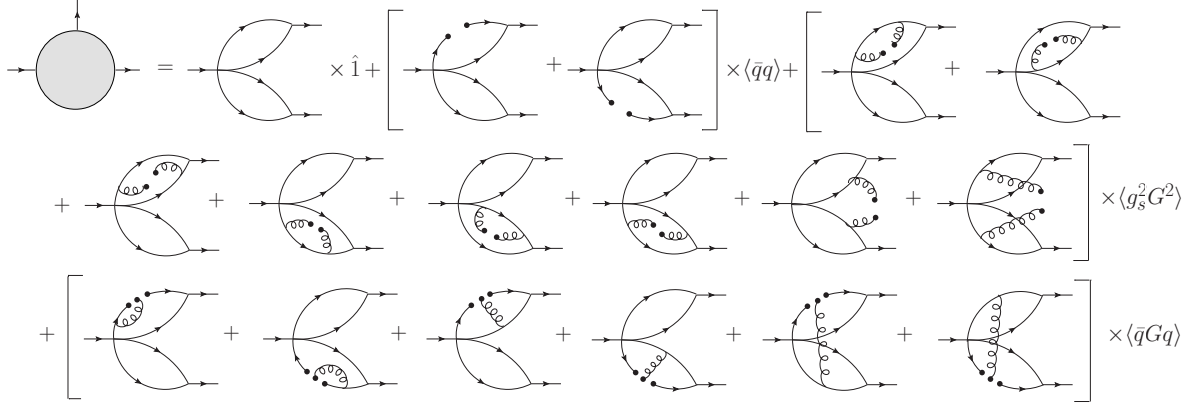


Figure 3: The OPE for the three-point function written in terms of exotic interpolating currents. Possible permutations are not shown.

### 2.7.2. Phenomenological side

The phenomenological side of the three-point function is defined in terms of the hadronic degrees of freedom. This means that one has to consider the current operators as the creation/annihilation of the hadrons in the vertex. The three-point function is evaluated inserting a complete set of intermediate states between these operators. This procedure leads to hadronic matrix elements such as  $\langle 0|j_n(p)|H\rangle$ , that represents the coupling of the hadronic state  $H$  with the current  $j_n$ . These matrix elements are parametrized in terms of hadron parameters. Let us define the parameter  $f_{H_i}$ , associated to each hadron in the vertex, as:

$$\begin{aligned}\langle 0|j_{H_1}(p)|H_1(p)\rangle &= f_{H_1} \\ \langle 0|j_{H_2}(p')|H_2(p')\rangle &= f_{H_2} \\ \langle 0|j_{H_3}(q)|H_3(q)\rangle &= f_{H_3}.\end{aligned}\tag{32}$$

The three-point function can be written as

$$\Pi^{phen}(p^2, p'^2, q^2) = \frac{f_{H_1} f_{H_2} f_{H_3}}{(p^2 - m_{H_1}^2)(p'^2 - m_{H_2}^2)(q^2 - m_{H_3}^2)} \langle H_2(p') H_3(q) | H_1(p) \rangle.\tag{33}$$

The matrix element in Eq. (33):  $\langle H_2(p') H_3(q) | H_1(p) \rangle$ , is associated with the transition  $H_1 \rightarrow H_2 H_3$  and, in general, is obtained from an effective Lagrangian describing the vertex we are interested in. A form factor,  $g_{H_1 H_2 H_3}(q^2)$ , is introduced in Eq. (33) when an effective Lagrangian is used to calculate the matrix element  $\langle H_2(p') H_3(q) | H_1(p) \rangle$ :

$$\langle H_2(p') H_3(q) | H_1(p) \rangle = g_{H_1 H_2 H_3}(q^2) T_i,\tag{34}$$

where  $T_i$  is the tensorial structure discussed previously. These tensor structures will be important in the definition of the sum rules, since the comparison must be done with the same tensorial structure on both sides of the sum rule. In principle all structures are equivalent and should yield the same result. In practice, due to the truncation of the OPE, some differences appear and one structure may be more reliable than others [162]. The Phenomenological side of the sum rule can be written as

$$\Pi^{phen}(p^2, p'^2, q^2) = \sum_i \Gamma_i^{phen}(p^2, p'^2, q^2) T_i,\tag{35}$$

with  $\Gamma_i^{phen}(p^2, p'^2, q^2)$  defined as

$$\Gamma_i^{phen}(p^2, p'^2, q^2) = \frac{f_{H_1} f_{H_2} f_{H_3}}{(p^2 - m_{H_1}^2)(p'^2 - m_{H_2}^2)(q^2 - m_{H_3}^2)} g_{H_1 H_2 H_3}(q^2).\tag{36}$$

In Eqs. (33) and (36) we have written explicitly only the pole contribution to the three-point function. On the other hand, as done on the OPE side, Eq. (36) can also be written in terms of a double dispersion relation, in such a way that the effects of higher states can be taken into account also on the Phenomenological side. Therefore, we write:

$$\Gamma_i^{phen} = -\frac{1}{4\pi^2} \int_{s_{min}}^{\infty} ds \int_{u_{min}}^{\infty} du \frac{\rho_i^{phen}(s, u, Q^2)}{(s-p^2)(u-p'^2)}, \quad (37)$$

where  $\rho_i^{phen}(u, s, Q^2)$  is the double discontinuity of the amplitude  $\Gamma_i(p^2, p'^2, Q^2)$ . In Ref. [158] this spectral density was generically expressed as

$$\begin{aligned} \rho_i^{phen}(s, u, Q^2) = & a\delta(s - m_{H_1}^2)\delta(u - m_{H_2}^2) + b\delta(s - m_{H_1}^2)\theta(u - u_0) \\ & + c\delta(u - m_{H_2}^2)\theta(s - s_0) + \rho^{cont}(s, u, Q^2)\theta(s - s_0)\theta(u - u_0), \end{aligned} \quad (38)$$

where  $s_0, u_0$  are the continuum thresholds associated with the hadrons  $H_1$  and  $H_2$ , respectively. Equation (38) has a simple kinematical interpretation. The first term describes the kinematical situation where the hadrons  $H_1$  and  $H_2$  are on the ground state, while  $H_3$  is off-shell, with arbitrary Euclidian four momentum  $Q^2 = -q^2$ . The second term refers to a situation where  $H_1$  is still on the ground state, but the ground state of the hadron  $H_2$  is absent in the vertex, which contains only its excitations starting at  $u_0$ . The third term is analogous to the second one with the exchange  $H_2 \leftrightarrow H_1$ . Finally, the last term represents the excitations of  $H_1$  and  $H_2$ , which start at  $s_0$  and  $u_0$  respectively. Substituting Eq. (38) into Eq. (37), with the parameter  $a$  (in Eq. (38)) identified as the pole term given in Eq. (36), we obtain

$$\begin{aligned} \Gamma_i^{phen} = & \frac{f_{H_1} f_{H_2} f_{H_3} g_{H_1 H_2 H_3}(q^2)}{(p^2 - m_{H_1}^2)(p'^2 - m_{H_2}^2)(q^2 - m_{H_3}^2)} - \frac{1}{4\pi^2} \left[ \frac{1}{m_{H_1}^2 - p^2} \int_{u_0}^{\infty} du \frac{b(u, q^2)}{(u - p'^2)} \right. \\ & \left. + \frac{1}{m_{H_2}^2 - p'^2} \int_{s_0}^{\infty} ds \frac{c(s, q^2)}{(s - p^2)} \right] + \int_{s_0}^{\infty} ds \int_{u_0}^{\infty} du \frac{\rho_n^{cont}(s, u, Q^2)}{(s - p^2)(u - p'^2)}. \end{aligned} \quad (39)$$

In Eq. (39),  $b(s, q^2)$  and  $c(s, q^2)$  are unknown functions contributing to the pole-continuum transitions [96, 163] of the hadrons  $H_1$  and  $H_2$ , respectively. These functions can be determined adopting the model discussed in Ref. [164].

### 2.7.3. Three-point function sum rule

Analogously to the two-point function case, the three-point function sum rule is obtained by matching the OPE and the Phenomenological sides. In order to do this a given tensorial structure,  $T_i$ , must be present on both sides. Hence, for a given  $T_i$  structure, after doing a Borel transform in both  $P^2 \rightarrow M^2$  and  $P'^2 \rightarrow M'^2$  one has

$$\Gamma_i^{phen}(M^2, M'^2, Q^2) = \Gamma_i^{OPE}(M^2, M'^2, Q^2). \quad (40)$$

Since this review is dedicated to the exotic charmonium states, all of the applications discussed here are related to hadronic states that are described by exotic four-quark interpolating currents. As a consequence, the invariant function,  $\Gamma_i^{OPE}$ , depends only on  $P^2$  and  $Q^2$  or on  $P'^2$  and  $Q^2$  four momenta and, in this case, a double Borel transform eliminates the OPE side. To overcome this problem we first notice that in the calculations involving systems with heavy flavors the approximation  $P^2 \approx P'^2$  is very good [156]. Therefore, taking  $P^2 = P'^2$  we do a single Borel transform to  $P^2 = P'^2 \rightarrow M^2$  on both sides of the sum rules. However, as first noticed by Ioffe and Smilga [163] the pole-continuum transitions are not exponentially suppressed, as compared to the pole contribution, when only one Borel transformation is done in both  $P^2$  and  $P'^2$ . Following Ref. [163] here we introduce an unknown function  $B(Q^2)$  parametrizing the two integrals in the brackets in Eq. (39). Therefore, the sum rule can be written as:

$$\frac{f_{H_1} f_{H_2} f_{H_3} g_{H_1 H_2 H_3}(Q^2)}{(Q^2 + m_{H_3}^2)} \left( \frac{e^{-m_{H_1}^2/M^2} - e^{-m_{H_2}^2/M^2}}{m_{H_2}^2 - m_{H_1}^2} \right) + B(Q^2)e^{-s_0/M^2} = \Gamma^{OPE}(M^2, Q^2). \quad (41)$$

The second term on the LHS of Eq. (41) accounts for the pole-continuum transitions. An expression for the form factor is obtained by taking the derivative of Eq. (41) with respect to  $1/M^2$  and using the result to eliminate  $B(Q^2)$  from the equations.

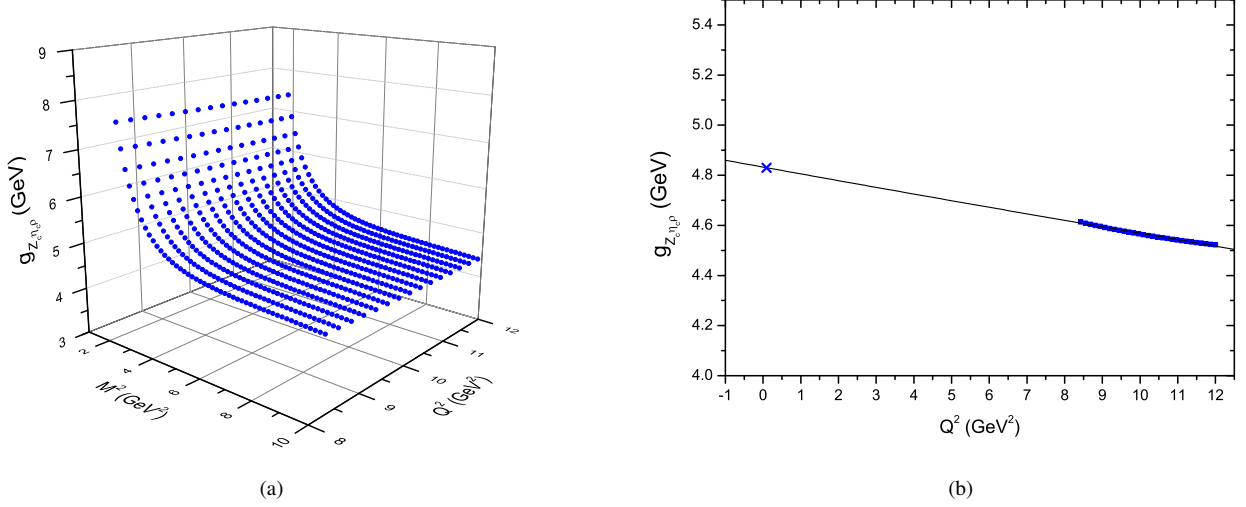


Figure 4: (a) QCDSR results for the form factor  $g_{Z_c \eta_c \rho}(Q^2)$  as a function of  $Q^2$  and  $M^2$ . (b) QCDSR results for  $g_{Z_c \eta_c \rho}(Q^2)$ , as a function of  $Q^2$  for Borel mass values within the interval  $4.0 \leq M^2 \leq 10.0 \text{ GeV}^2$  (squares). The solid line gives the parametrization of the QCDSR results through Eq. (42). The cross gives the value of the coupling constant. Taken from Ref. [106].

### 2.8. Extrapolation of the form factor and the coupling constant

The coupling constant is obtained from the form factor,  $g_{H_1 H_2 H_3}(Q^2)$ , in Eq. (41). In fact, it is defined as the value assumed by the form factor at the hadron pole mass, that is  $g_{H_1 H_2 H_3} = g_{H_1 H_2 H_3}(Q^2 = -m_{H_3}^2)$ . However, we cannot simply consider  $Q^2 = -m_{H_3}^2$  in Eq. (41) since the sum rule is valid only for  $Q^2 > 0$ . Therefore, in order to overcome this problem we use a procedure that allows us to extrapolate the QCDSR results to the time-like region, where the value for the coupling constant can be extracted. To this end we use a function that fits the QCDSR results for the form factor  $g_{H_1 H_2 H_3}(Q^2)$ .

The form factor depends not only on  $Q^2$ , but also on the Borel mass  $M^2$ . The QCDSR results would be independent of this parameter if one could take into account the whole OPE series, without truncating it at some dimension. Since the OPE series is always truncated at some order, we have to look for some interval at  $M^2$  in which the QCDSR results are as independent of the Borel mass as possible. Following this procedure, we are able to guarantee that the QCDSR results depend only on  $Q^2$ . Therefore, we usually plot  $g_{H_1 H_2 H_3}(Q^2)$  as a function of  $Q^2$  and  $M^2$  in order to look for such an interval. As an example, Fig. 4(a) shows the plot of the form factor of the  $Z_c^+(3900) \rightarrow \eta_c \rho^+$  vertex, studied in Ref. [106]. As can be seen, from values within the interval  $4.0 \leq M^2 \leq 10.0 \text{ GeV}^2$ , the form factor  $g_{Z_c \eta_c \rho}$  has almost no  $M^2$  dependence and consequently  $g_{Z_c \eta_c \rho}$  has the same  $Q^2$  dependence for every  $M^2$  value assumed on that interval.

Fig. 4(b) shows  $g_{Z_c \eta_c \rho}$  as a function of  $Q^2$  (represented by the squares) for Borel mass values within the interval  $4.0 \leq M^2 \leq 10.0 \text{ GeV}^2$ . Note that the QCDSR results are evaluated in the interval  $8.5 \leq Q^2 \leq 12.0 \text{ GeV}^2$ . This is the interval in which the results are independent of  $M^2$  and, therefore, we can say that the QCDSR results have a good degree of reliability.

In the  $g_{Z_c \eta_c \rho}$  case, we extrapolate the QCDSR results (given by the squares in Fig. 4(b)) by using an exponential function

$$g_{Z_c \eta_c \rho}(Q^2) = g_1 e^{-g_2 Q^2}, \quad (42)$$

that fits the QCDSR results (the solid line in Fig. 4(b)) for  $g_1 = 4.83 \text{ GeV}$  and  $g_2 = 5.6 \times 10^{-3} \text{ GeV}^2$ . The QCDSR results in Fig. 4(b) were obtained by considering the  $\rho$  meson as being off-shell. The coupling constant  $g_{Z_c \eta_c \rho}$  is then given by  $g_{Z_c \eta_c \rho}(Q^2 = -m_\rho^2)$ , leading to the following result [106]:

$$g_{Z_c \eta_c \rho}(Q^2 = -m_\rho^2) = (4.85 \pm 0.81) \text{ GeV}. \quad (43)$$



The value of the coupling constant extracted from the QCDSR results depends on the choice of the function  $g(Q^2)$ . More concretely, if we would choose another function to fit the QCDSR results, shown in Fig. 4(b), we would get a different value for the coupling constant,  $g_{Z_c\eta_c\rho}$ , in Eq. (43), since two different functions that fit the QCDSR results might have a different behavior at the time-like region. This will give rise to some uncertainty in the extracted value of the coupling constant. In order to illustrate this uncertainty we show, in Fig. 5, the calculation of the  $Y \rightarrow J/\psi\phi$  coupling constant using different parametrizations to extract the coupling constant [114].

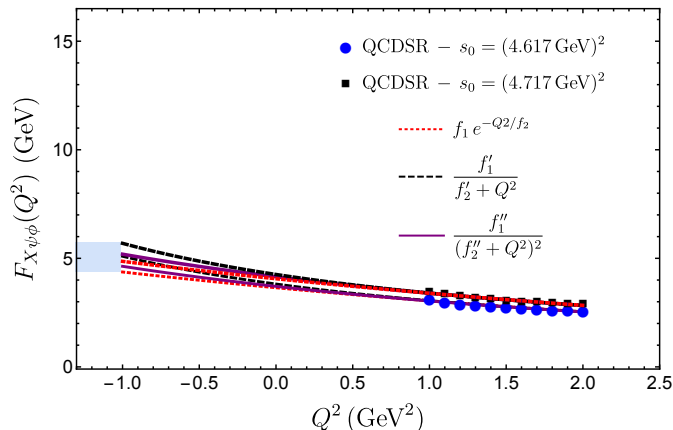


Figure 5: QCDSR results (filled circles) for  $YJ/\psi\phi$  vertex function. The dotted, dashed and solid lines, correspond to the fits using different expressions for the form factor  $F_{Y\psi\phi}$ , as can be seen on the plot. The shaded area near the vertical axis indicates the range of the values for the coupling constant  $F_{Y\psi\phi}$  due to the different choices for the form factor. Taken from Ref. [114].

The QCDSR results in Fig. 5 are represented by the circles and squares. In order to fit these points three different functions, denoted by  $F(Q^2)$ , were used. As it was expected, each one gives a different value for the coupling constant  $F_{Y\psi\phi}$ , as indicated by the shaded area projected into the vertical axis.

In Table 3, we list some few examples of the most common analytical functions used to describe form factors in QCDSR calculations: the monopolar, exponential and Gaussian forms. All of them have in common the fact that, they vanish as  $Q^2 \rightarrow \infty$ .

Table 3: Some examples of analytical functions for the form factors used in QCDSR calculations.

Analytical functions for the form factor	
Monopolar	$\frac{f_1}{f_2 + Q^2}$
Exponential	$f_1 e^{-f_2 Q^2}$
Gaussian	$f_1 e^{-(f_2 + Q^2)^2/f_3}$

In general, as it is discussed in [158], these systematic uncertainties are reduced by performing a double QCDSR analysis. For a given  $H_1 H_2 H_3$  vertex, we take  $H_1$  to be off-shell, calculate the QCDSR points and extrapolate them to the time-like region. At the same time we take  $H_2$  to be off-shell and repeat the procedure. When doing the extrapolations we impose the two form factors to yield the same coupling constant. This matching condition significantly reduces the freedom in the choice of the parameters  $f_1, f_2, \dots$  etc. This procedure is enough to reduce the uncertainties and provides results consistent with the experimental values, as it was the case for the  $D^* D\pi$  and  $J/\psi D^* D^*$  studied in Refs. [165, 166].

Even after the above mentioned improvement one might argue that the choice of the functional form,  $g_{H_1 H_2 H_3}(Q^2)$ , remains arbitrary and this implies a systematic uncertainty. In order to reduce this freedom of choice one may try to

match the QCDSR results with meson loops calculated via effective field theory approach. This idea was advanced in Ref. [167], and can be used to impose constraints that allow us to reduce the freedom of choice of the function parametrizing the QCDSR results in the deep Euclidean region.

As it was shown in Ref. [167], in a certain  $Q^2$  region the  $D^*D\pi$  vertex is described by an effective Lagrangian obeying chiral symmetry. Beyond the tree level one can compute meson loop diagrams. These computations bring up some unknown parameters arising from the renormalization of the loops. Fortunately, these unknown loop parameters can be isolated into some basic constants, and by matching the calculation of the form factor to the QCDSR results, they can be determined, providing a knowledge of the form factor.

This match between chiral and QCDSR results is justified. In the region in which the QCDSR approach does not provide reliable results (at low or negative  $Q^2$  values) the effective field theory approach is valid. On the other hand, for intermediate and higher  $Q^2$  regions the QCDSR is more reliable than the effective theories.

### 2.9. Limitations of the applications of the QCDSR to the exotic states

One of the limitations, as already discussed in Sec. 2.7.1, is due to the use of local currents. One can not distinguish between tetraquarks or molecular states, considered as spatially large objects. The only thing one can say is that if a molecular kind of current couples strongly with the state, this gives us a hint about the color organization of the quarks in the state. In order to consider the size of the states, a possible alternative would be to use non-local currents. To our knowledge, non-local currents have never been used in the QCDSR approach, since quantum corrections to these non-local operators are awful [168]. However, non-local currents for the exotic states, in particular  $Z_c(3900)$  and  $Z(4430)$ , have already been used in a covariant quark model [169]. It is a challenge but it would be important to consider them also in the QCDSR approach.

The lack of  $\alpha_s$  corrections, in most of the previous calculations, can be also a limitation. However, as shown in Sec. 7,  $\alpha_s$  corrections have already been considered in the QCDSR for the exotic states, leading to small corrections to their masses.

Another drawback of the method is the fact that most of the  $X$ ,  $Y$ ,  $Z$  states are found close to the two particle  $S$ -wave thresholds to which they seem to have quite strong couplings. In studies of non-exotic hadrons, the ground state of the spectrum is a zero width state and is well separated from the continuum. In this case, a reasonable Ansatz is adopted for the phenomenological description of the spectral function, which is taken to be a sharp pole separated from a continuum, see Eq.(12). The same Ansatz has been extended to the case of  $X$ ,  $Y$ ,  $Z$  states, assuming that each  $X$ ,  $Y$  or  $Z$  state is the ground state of the related spectrum and that the corresponding higher excited states lie in the high energy region. Such a description can be questioned in the case of exotic hadrons, where two meson thresholds often lie close to their masses and which can couple to them in  $S$ -wave. In fact, such hadron channels may even lie below the mass of the exotic states, contributing to their widths and smearing up a continuum in the background of the spectral function.

There have been several attempts to consider the contribution of such two particle intermediate states to the QCDSR of exotic states [170–173]. In all cases these two-hadron-reducible contributions [170] can be included by adding a term in the phenomenological side of the sum rule. In general, the  $H_1 - H_2$  continuum contribution to the exotic state  $X$ , that couples in  $S$ -wave with these two hadrons, can be included by modifying the phenomenological side of the QCDSR in Eq. (12) as:

$$\rho(s) = \lambda^2 \delta(s - m_X^2) + \rho^{cont}(s) + \rho_{H_1 H_2}(s). \quad (44)$$

To find an expression for  $\rho_{H_1 H_2}(s)$  one needs to introduce a coupling between the current, representing the exotic state, and the two particles (considering here, for simplicity, as spin 0 states):

$$\lambda_{H_1 H_2} = \langle 0 | j_X | H_1 H_2 \rangle. \quad (45)$$

The correlation function of the  $H_1 - H_2$  continuum is then given by [173]:

$$\Pi_{H_1 H_2}(p^2) = i |\lambda_{H_1 H_2}|^2 \int \frac{d^4 q}{(2\pi)^4} \frac{i}{q^2 - m_{H_1}^2} \frac{i}{(p - q)^2 - m_{H_2}^2}, \quad (46)$$

and, therefore,  $\rho_{H_1 H_2}(s)$  is given by

$$\rho_{H_1 H_2}(s) = \frac{1}{\pi} \text{Im}[\Pi_{H_1 H_2}(s)]. \quad (47)$$

The problem in such approach is how to evaluate  $\lambda_{H_1 H_2}$ . It could be evaluated by using the method of current algebra, if the properties of the resonance state are known. It could be evaluated by a new QCDSR, as in Refs. [170–172], with the consequence of introducing more uncertainties in the calculation. In Ref. [173]  $\rho_{\pi\pi}(s)$  was parameterized as:

$$\rho_{\pi\pi}(s) = a s^2 \sqrt{1 - \frac{4m_\pi^2}{s}}, \quad (48)$$

where  $a$  is a new parameter. In Ref. [173] such  $\pi - \pi$  continuum contribution to the QCDSR of the light scalar  $\sigma(600)$  (considered as a tetraquark) was included. The sum rule shows a much better stability of the obtained resonance mass with respect to the continuum threshold parameter  $s_0$ .

In all quoted cases [170–173], the inclusion of the two-hadron-reducible contribution to the QCDSR improves the stability of the results, but it does not change drastically the results for the mass of the exotic state. Therefore one can say that, although an effort should be made to include such contribution to the QCDSR of the  $X$ ,  $Y$ ,  $Z$  states, the results obtained so far can still be trusted.

The presence of two-hadron thresholds near the mass of exotic states can give rise to yet other type of complications. Sometimes the opening of these thresholds can lead to cusp like structures in cross-sections/invariant mass spectra [174, 175]. The cusps usually show up with line shapes different to a Breit-Wigner state, though it may not be straightforward to distinguish between the two. However, it is argued in Ref. [176], that a narrow peak must correspond to a bound state/resonance (pole in the complex plane, in the amplitude). Other difficulty is that sometimes the pole may not be present in the right Riemann sheet and the state may have an alternative interpretation, such as, a virtual state (see the review [20] for more discussions). Such states can also lead to an enhancement in the experimental data. It is, thus, important to investigate if a possible state found in experiments is a genuine state or a threshold effect or a virtual state, etc. Effects, like, cusps, virtual states, etc., cannot be directly identified in QCD sum rules. One would reach a negative result (based on the conditions to be satisfied in order for the results to be reliable) concluding the nonexistence of a state, which would indicate that the enhancement found in experiments may have a different interpretation.

### 3. The $X(3872)$ state

It has been fifteen years since the first observation of the  $X(3872)$  state was reported. It was the first charmonium state that could not be accommodated within the usual quark-antiquark meson model. Ever since then, the study of hadron spectroscopy is continuously being revised, with the observation of several other states with exotic properties in the heavy quark sector. The first observation was reported in 2003 by Belle Collaboration with the measurement of a narrow resonance in the  $B$  meson decay channel  $B^\pm \rightarrow K^\pm X(\rightarrow J/\psi \pi^+ \pi^-)$  [23], and soon it was confirmed by BABAR in the same channel [177], and by D0 and CDF Collaborations in  $p\bar{p}$  collisions [27, 30]. Subsequently, the  $X(3872)$  was observed in many other experiments and in several different channels, leading to a vast amount of experimental data, which are collected and summarized by the PDG [22]. Here, we list some of the main experimental results and their connection with the main theoretical interpretations of  $X(3872)$ .

The current world average mass of the  $X(3872)$  is  $3871.69 \pm 0.17 \text{ MeV}$  and it is a very narrow state, with an upper limit on the decay width of  $\Gamma < 1.2 \text{ MeV}$  at 90% confidential level (CL) [22]. The first interesting aspect one can readily notice is the proximity of the mass of the state to the  $D^0 \bar{D}^{*0}$  threshold,  $3871.81 \pm 0.09 \text{ MeV}$ . The state quantum numbers have been completely determined as  $J^{PC} = 1^{++}$ , corresponding to an axial vector meson [178]. The determination of the charge-conjugation parity was established unambiguously to be  $C = +1$ , due to the observation of the radiative decay  $X \rightarrow \gamma J/\psi$  reported by Belle in Ref. [31]. In Ref. [28], the CDF Collaboration performed an analysis of the angular distributions for the decay channel  $X(3872) \rightarrow J/\psi \pi^+ \pi^-$ ,  $J/\psi \rightarrow \mu^+ \mu^-$  comparing the obtained outcome with the theoretical predictions, and of all possible assignments, only the quantum numbers  $1^{++}$  and  $2^{++}$  were consistent with the data, while the other quantum numbers were excluded with 99.7% CL. Finally, the LHCb Collaboration performed a full amplitude analysis of the angular correlations, in five dimensions, between the

products of the decay mode  $B^\pm \rightarrow K^\pm X(3872)$ , establishing the quantum numbers of the state as  $J^{PC} = 1^{++}$ , definitely ruling out the  $2^{-+}$  possibility [178].

The discussions on the puzzling nature of the  $X(3872)$  started immediately after its observation. A possible candidate, within the quark-antiquark conventional model with proper quantum numbers, would be the  $2^3P_1$  state, also known as  $\chi_{c1}(2P)$  or  $\chi'_{c1}$ . However, the masses obtained for this state, from constituent quark models or lattice QCD, are not compatible with the  $X(3872)$  mass [179–181]. The fact that the  $X(3872)$  could not be accommodated within the conventional quark model and that its mass is very close to the  $D^0\bar{D}^{*0}$  threshold, strongly suggested a possible molecular structure with small binding energy. In fact, the existence of a molecule, with  $1^{++}$  (and also with  $0^{-+}$ ) quantum numbers, near the  $D^0\bar{D}^{*0}$  threshold was predicted by Tornqvist, using the potential model, many years before the discovery of  $X(3872)$  [182].

The measurement of the branching ratio between final states with two and three pions was definitive to establish the unconventional nature of  $X(3872)$ . In Ref. [31], Belle reported the branching ratio for the channels  $X \rightarrow J/\psi\pi^+\pi^-$  and  $J/\psi\pi^+\pi^-\pi^0$ :

$$\frac{\mathcal{B}(X \rightarrow J/\psi\pi^+\pi^-\pi^0)}{\mathcal{B}(X \rightarrow J/\psi\pi^+\pi^-)} = 1.0 \pm 0.4 \pm 0.3. \quad (49)$$

The BaBar Collaboration [32] also observed the decay  $X \rightarrow J/\psi\omega$  at a rate compatible with Eq. (49):

$$\frac{\mathcal{B}(X \rightarrow J/\psi\pi^+\pi^-\pi^0)}{\mathcal{B}(X \rightarrow J/\psi\pi^+\pi^-)} = 0.8 \pm 0.3. \quad (50)$$

The decay mode  $J/\psi\pi^+\pi^-$  occurs via  $\rho J/\psi$ , with isospin  $I = 1$ , and  $J/\psi\pi^+\pi^-\pi^0$  via  $\omega J/\psi$ , with isospin  $I = 0$ , indicating a strong isospin and  $G$  parity violation. The isospin violating modes are strongly suppressed for  $c\bar{c}$  states, while should be a common feature for molecular states [183]. Besides, this result was predicted by Swanson in Ref. [184], considering the  $X(3872)$  as a  $D^0\bar{D}^{*0}$  molecule with a small admixture of  $\rho J/\psi$  and  $\omega J/\psi$  components.

The radiative decays are other important processes that lead to distinguishable results between the charmonium and molecular states, as pointed out by Swanson in Ref. [183]. The Belle Collaboration reported the first observation of the radiative decay channel [31],  $X \rightarrow \gamma J/\psi$ , with a branching ratio of

$$\frac{\Gamma(X \rightarrow \gamma J/\psi)}{\Gamma(X \rightarrow \pi^+\pi^- J/\psi)} = 0.14 \pm 0.05. \quad (51)$$

This result is incompatible with the preferred  $c\bar{c}$  candidate  $\chi_{c1}$ , but it is in agreement with the molecular description for  $X(3872)$  [183, 185]. Although the topic is still not settled, this result has contributed to the general consensus about the unconventional nature of  $X(3872)$ .

Another possibility for the nature of  $X(3872)$  as a four-quark state is a tetraquark structure, as proposed by Maiani *et. al.* [186]. In this model, the state is formed by the binding of a diquark and an antidiquark pair, with a symmetric spin distribution. The mixing of pure isospin states provides the possibility of isospin violating modes.

An additional radiative decay mode,  $X \rightarrow \gamma\psi(2S)$ , was reported by Babar [37], with a large branching ratio in comparison to the  $\gamma J/\psi$  mode:

$$R_{\psi\gamma} = \frac{\mathcal{B}(X \rightarrow \gamma\psi(2S))}{\mathcal{B}(X \rightarrow \gamma J/\psi)} = 3.4 \pm 1.4. \quad (52)$$

The Babar result was confirmed by the LHCb Collaboration [38], where the branching ratio measured was  $R_{\psi\gamma} = 2.46 \pm 0.64 \pm 0.29$ . This ratio varies widely in different theoretical models, and can be used as a distinguishable feature between different models. For example, in Ref. [183], the molecular model gives rise to a suppression of the  $\gamma\psi(2S)$  channel, providing:  $\frac{\Gamma(X \rightarrow \psi(2S)\gamma)}{\Gamma(X \rightarrow \psi\gamma)} \sim 4 \times 10^{-3}$ . In fact, neither pure charmonium or pure molecule can accommodate this experimental result (see [38] and references therein), and the predicted ratio in Eq. (52) favors a different scenario, in which  $X(3872)$  is an admixture of charmonium and four-quark states. The necessity for such type of admixture was anticipated in several studies, see for example Refs. [179, 187–189].

Besides the four-quark and mixed models, there are other theoretical descriptions, like, a cusp [190], a hybrid structure [191, 192], and a glueball, [193] that were also presented as alternative interpretations for the nature of  $X(3872)$ . The debate regarding the puzzling nature of the  $X(3872)$  is still not settled, although the molecule/tetraquark and admixtures of charmonium and molecule scenarios are the most promising ones, being widely studied and tested so far in several theoretical frameworks, including the QCDSR, which is the focus of this review.

### 3.1. QCDSR calculations for $X(3872)$

The  $X(3872)$  state has been studied by various authors using the QCDSR technique. The first QCDSR calculations using a tetraquark current were presented in Refs. [87, 88], where the mass and decay width were obtained. Afterwards, several other QCDSR calculations for the mass of  $X(3872)$  were done, considering different hypothesis for its quark structure: a molecule [94, 194–196], a tetraquark [197, 198], a hybrid [199, 200], and a mixed hybrid-molecule [201, 202]. In particular, in all works considering a four-quark structure, tetraquark or molecule, the mass obtained for  $X(3872)$  is compatible with the experimental one, considering the uncertainties. Thus, from a QCDSR point of view, the mass of tetraquark and molecule structures are indistinguishable and cannot be used as the sole test to determine the state configuration. This finding is not surprising since the currents describing these two structures are related by a Fierz transformation [7]. In Refs. [90, 99], the equivalence between the tetraquark and molecule results for the mass is addressed, asserting the indistinguishability of both results. The only feature that could set apart the structures is that in the molecular configuration a better Borel stability is obtained [90]. Regarding the hybrid structure, from the works quoted above, the mass obtained from a QCDSR calculation for a state with  $J^{PC} = 1^{++}$  is 5.13 GeV, which is much bigger than the experimental mass, while the mixed hybrid-molecule provides compatible results. More recently, the properties of  $X(3872)$  in a dense medium [203] were also studied in the QCDSR framework.

Most of the works quoted above do not address the decay width of the state, which can be crucial to determine the structure of a state. The only work that deals with the decay properties of  $X(3872)$ , considered as a pure four-quark state, was done in Ref. [87]. In Ref. [87] it was shown that the decay width of the tetraquark state is too large in comparison with the experimental decay width of the  $X(3872)$ . A further attempt, using a mixed molecule and charmonium currents, has been successful in explaining the mass, decay and production properties of the  $X(3872)$  [96, 98, 101]. This possibility is also in agreement with the current radiative decay data.

In the remaining of this section, we review briefly the QCDSR studies of the  $X(3872)$  based on a four-quark picture, a tetraquark or a molecular current, to conclude that a pure four-quark state is incompatible with the decay properties of  $X(3872)$ . Next, we present the QCDSR analysis considering an admixture of charmonium and  $D\bar{D}^*$  currents. We show that this kind of current can explain all the data, including those related with the  $X(3872)$  decay processes. We also present the studies of the  $X(3872)$  radiative decay and of the  $X(3872)$  production in  $B$  decays, providing the most complete and consistent QCDSR analysis of the  $X(3872)$  at the present.

### 3.2. QCDSR for pure four-quark structures

In Ref. [88], for the first time a tetraquark structure for  $X(3872)$  was tested in the framework of QCDSR. A diquark-antidiquark current, previously proposed by Maiani *et al.* [186] was used. The current was constructed for the state with quantum numbers  $J^{PC} = 1^{++}$  with a symmetric spin distribution  $[cq]_{S=1}[\bar{c}\bar{q}]_{S=0} + [cq]_{S=0}[\bar{c}\bar{q}]_{S=1}$ , with the corresponding interpolating current given by

$$j_\mu = \frac{i\epsilon_{abc}\epsilon_{dec}}{\sqrt{2}} [(q_a^T C \gamma_5 c_b)(\bar{q}_d \gamma_\mu C \bar{c}_e^T) + (q_a^T C \gamma_\mu c_b)(\bar{q}_d \gamma_5 C \bar{c}_e^T)], \quad (53)$$

where  $a, b, c, \dots$  are color indices,  $C$  is the charge conjugation matrix and  $q$  denotes a  $u$  or  $d$  quark.

#### 3.2.1. Two-point correlation function

The SR for the mass of the state is obtained from the two-point correlation function:

$$\begin{aligned} \Pi_{\mu\nu}(q) &= i \int d^4x e^{iq \cdot x} \langle 0 | T [j_\mu^{(q)}(x) j_\nu^{(q)\dagger}(0)] | 0 \rangle \\ &= -\Pi_1(q^2) \left( g_{\mu\nu} - \frac{q_\mu q_\nu}{q^2} \right) + \Pi_0(q^2) \frac{q_\mu q_\nu}{q^2}, \end{aligned} \quad (54)$$

The non-conservation of the axial-vector current implies that the two functions  $\Pi_1$  and  $\Pi_0$  (with spin 1 and 0, respectively) are independent.

The phenomenological side of the sum rule, computed by inserting intermediate states for  $X$ , is given by

$$\Pi_{\mu\nu}^{phen}(q^2) = \frac{2f_X^2 M_X^8}{M_X^2 - q^2} \left( -g_{\mu\nu} + \frac{q_\mu q_\nu}{M_X^2} \right) \quad (55)$$

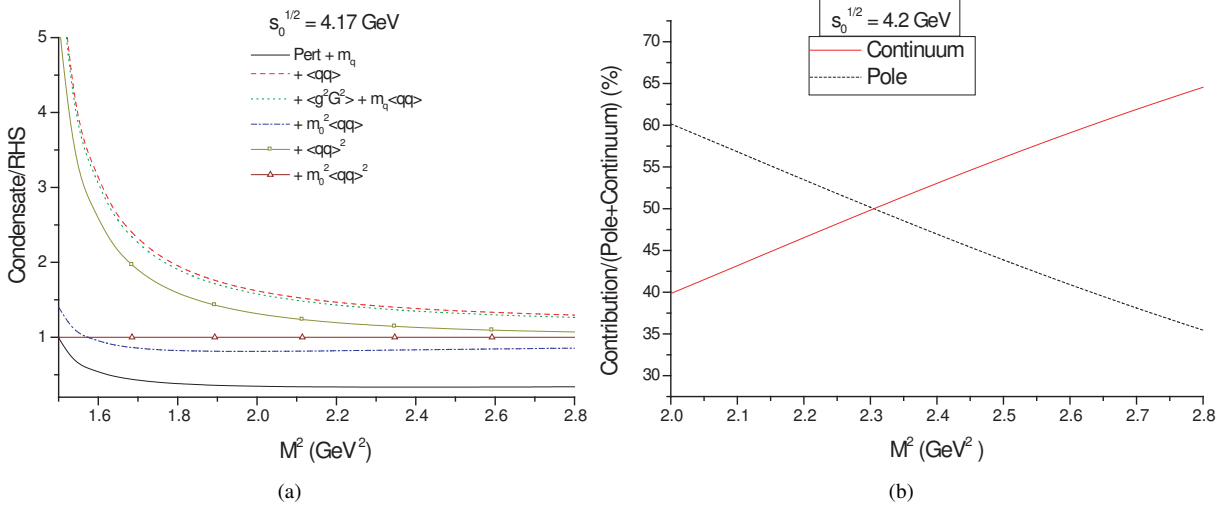


Figure 6: (a) The OPE convergence in the region  $1.6 \leq M^2 \leq 2.8 \text{ GeV}^2$  for  $\sqrt{s_0} = 4.17 \text{ GeV}$ . Starting with the perturbative contribution (plus a very small  $m_q$  contribution). Each subsequent line represents the addition of the contribution associated with the next condensate in the expansion. (b) The dashed line shows the relative pole contribution (i.e., the pole contribution divided by the total, pole plus continuum, contribution) and the solid line shows the relative continuum contribution. Figures taken from Ref. [88].

where the decay constant  $f_X$  is used to parametrize the coupling of the axial-vector meson  $1^{++}$  to the current  $j_\mu$  as

$$\langle 0 | j_\mu | X \rangle = \sqrt{2} f_X M_X^4 \epsilon_\mu. \quad (56)$$

As discussed in Sec. 2.2, in the OPE side, the correlation function  $\Pi_1$  is given by a dispersion relation:

$$\Pi_1^{OPE}(q^2) = \int_{4m_c^2}^{\infty} ds \frac{\rho^{OPE}(s)}{s - q^2} = \frac{1}{\pi} \int_{4m_c^2}^{\infty} ds \frac{\text{Im}[\Pi_1^{OPE}(s)]}{s - q^2}. \quad (57)$$

The matching of both sides of the sum rule is done by applying a Borel transform on both sides. After transferring the continuum contribution to the OPE side, the sum rule up to dimension-eight condensates, is written as

$$2f_X^2 M_X^8 e^{-M_X^2/M^2} = \int_{4m_c^2}^{s_0} ds e^{-s/M^2} \rho(s) + \Pi_1^{\text{mix}(\bar{q}q)}(M^2) \quad (58)$$

with

$$\rho(s) = \rho^{\text{pert}}(s) + \rho^{m_q}(s) + \rho^{\langle \bar{q}q \rangle}(s) + \rho^{\langle G^2 \rangle}(s) + \rho^{\text{mix}}(s) + \rho^{\langle \bar{q}q \rangle^2}(s), \quad (59)$$

and the function  $\Pi_1^{\text{mix}(\bar{q}q)}(M^2)$  is a part of the dimension-eight condensate that does not depend on  $s$ .

The convergence of the OPE and the comparison between the pole and continuum contribution are shown in Figs. 6(a) and 6(b). The lower limit of the Borel window is determined from the convergence of the OPE for higher values of  $M^2$ , and the upper limit from the constraint that the pole contribution must dominate over the continuum contribution. This procedure leads to the following Borel window:  $2.0 \leq M^2 \leq 2.2 \text{ GeV}^2$ .

The mass of the  $X$  state as a function of the Borel mass  $M^2$  is presented in Fig. 7, showing that the sum rule is stable within the Borel mass window. The result for the mass  $M_X$ , taking into account the uncertainties of the parameters and within the range of the Borel mass, is

$$M_X = (3.92 \pm 0.13) \text{ GeV}, \quad (60)$$

a value compatible with the experimental data on  $X(3872)$ .

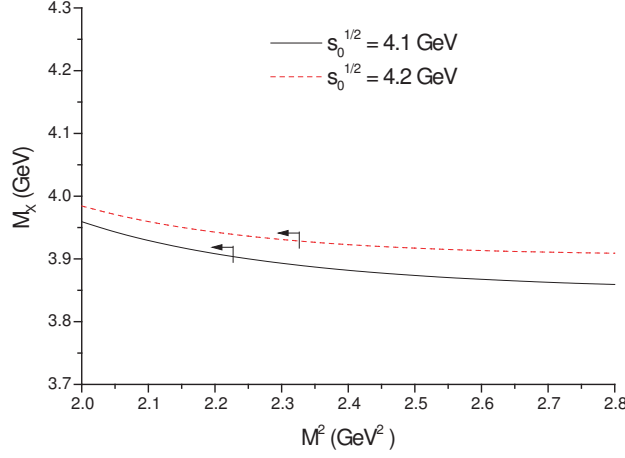


Figure 7: The  $X$  meson mass as a function of the Borel mass  $M^2$  for different values of the continuum threshold:  $\sqrt{s_0} = 4.1$  GeV (solid line) and  $\sqrt{s_0} = 4.2$  GeV (dashed line). The arrows indicate the region allowed for the sum rules: the lower limit (cut below  $2.0$   $\text{GeV}^2$ ) is given by the OPE convergence requirement and the upper limit by the dominance of the QCD pole contribution. Figures taken from Ref. [88].

The above results were obtained using the tetraquark current in Eq. (53), although other four-quark operators with  $1^{++}$  quantum numbers are possible. For example, a different tetraquark current with  $J^{PC} = 1^{++}$  can be constructed by combining the pseudoscalar  $0^-$  and vector  $1^-$  diquarks, instead of the scalar  $0^+$  and isovector  $1^+$  diquarks, as done in Eq. (53). Equivalently, other operators can be constructed with meson type currents. The number of currents increases further if one allows for additional color states; color sextet for the diquark and color octet for the molecular states. An extensive study has been carried out for  $X(3872)$  in Ref. [99]. As shown in Ref. [99, 102], the choice of the current does not matter much for the determination of the mass of the state, provided that one can work with quantities less affected by radiative corrections and where the OPE converges quite well. Besides the current in the  $\bar{3} - 3$  color configuration in Eq. (53), the other currents considered were: a diquark-antidiquark in the color sextet ( $\bar{6} - 6$ ) configuration,

$$j_6^\mu = \frac{i}{\sqrt{2}} [(q_a^T C \gamma_5 \lambda_{ab}^S c_b) (\bar{q}_d \gamma^\mu C \lambda_{de}^S \bar{c}_e^T) + (q_a^T C \gamma^\mu \lambda_{ab}^S c_b) (\bar{q}_d \gamma_5 C \lambda_{de}^S \bar{c}_e^T)], \quad (61)$$

where  $\lambda^S$  stands for the six symmetric Gell-Mann matrices:  $\lambda^S = (\lambda_0, \lambda_1, \lambda_3, \lambda_4, \lambda_6, \lambda_8)$ ; a  $D^* - D$  molecular current,

$$j_\mu^{(mol)}(x) = \frac{1}{\sqrt{2}} \left[ (\bar{q}_a(x) \gamma_5 c_a(x) \bar{c}_b(x) \gamma_\mu q_b(x)) - (\bar{q}_a(x) \gamma_\mu c_a(x) \bar{c}_b(x) \gamma_5 q_b(x)) \right]; \quad (62)$$

and a  $\lambda - J/\psi$ -like molecular current,

$$j_\lambda^\mu = [(\bar{c} \lambda^a \gamma^\mu c) (\gamma \bar{q} \lambda_a \gamma_5 q)], \quad (63)$$

where  $\lambda_a$  is the color matrix.

In particular, it was shown that the three substructure assignments for the  $X$ -meson ( $\bar{3} - 3$  and  $\bar{6} - 6$  tetraquarks and  $D - D^{(*)}$  molecule) lead to (almost) the same mass predictions within the accuracy of the approach. Therefore, a priori, a study of the  $X$ -mass alone cannot reveal its nature and identify if it is mainly composed of these substructures. On the other hand, the analysis of the  $\lambda - J/\psi$ -like molecular current in Eq. (63) showed that a lower mass as compared to the previous configurations can be obtained, with the ratio between the masses obtained with the currents in Eqs. (63) and (53) being  $0.96 \pm 0.03$ .

From the analysis of all these currents, it was found that the distance between the continuum threshold (about 4 GeV) and the resonance mass is relatively small, which indicates that the separation between the resonance and the continuum may be difficult to achieve.

The molecular  $D\bar{D}^*$  current in Eq. (62), together with the tetraquark current, Eq. (53), were also used in Ref. [90] to study the importance of including the width of the state, in a QCDSR calculation. This can be done by replacing the delta function in Eq. (12) by the relativistic Breit-Wigner function:

$$\delta(s - m^2) \rightarrow \frac{1}{\pi} \frac{\Gamma \sqrt{s}}{(s - m^2)^2 + s\Gamma^2}. \quad (64)$$

The mass and width were determined by looking at the stability of the mass results against the varying Borel parameter  $M^2$ , as usual.

Although the effect of the width was not found to be large, it was possible to fit the experimental mass, 3872 MeV, and the width,  $\Gamma < 1.2$  MeV, simultaneously for both currents. However, the molecular current, Eq. (62), gave a better stability as compared with the tetraquark current of Eq. (53).

### 3.2.2. Three-point correlation function

As discussed in the previous subsection, the mass of the  $X(3872)$  can be well reproduced from QCDSR calculations for a variety of four-quark structures. However, it is important to test if these currents can also explain other properties of the state, like, the decay widths.

With such a motivation, in Ref. [87], the tetraquark current of Eq. (53) was tested, within the QCDSR approach, to the calculation the decay width for the isospin violating channels,  $X(3872) \rightarrow J/\psi \pi^+ \pi^-$  and  $X(3872) \rightarrow J/\psi \pi^+ \pi^- \pi^0$ . It was shown in Ref. [87], that the ratio between these decays can be obtained from

$$\frac{\Gamma(X \rightarrow J/\psi \pi^+ \pi^- \pi^0)}{\Gamma(X \rightarrow J/\psi \pi^+ \pi^-)} = 0.118 \left( \frac{g_{X\psi\omega}}{g_{X\psi\rho}} \right)^2, \quad (65)$$

where the coupling constants  $g_{X\psi V}$ , with  $V = \omega, \rho$ , can be evaluated from the study of the vertex  $X\psi V$  in QCDSR, through the three point correlation function:

$$\Pi_{\mu\nu\alpha}^V(p, p', q) = \int d^4x d^4y e^{ip' \cdot x} e^{iq \cdot y} \Pi_{\mu\nu\alpha}^V(x, y), \quad (66)$$

with

$$\Pi_{\mu\nu\alpha}^V(x, y) = \langle 0 | T [j_\mu^\psi(x) j_\nu^V(y) j_\alpha^{X^\dagger}(0)] | 0 \rangle, \quad (67)$$

where  $p = p' + q$ , and the interpolating fields are given by:

$$\begin{aligned} j_\mu^\psi &= \bar{c}_a \gamma_\mu c_a, \\ j_\nu^\rho &= \frac{1}{2} (\bar{u}_a \gamma_\nu u_a - \bar{d}_a \gamma_\nu d_a), \\ j_\nu^\omega &= \frac{1}{6} (\bar{u}_a \gamma_\nu u_a + \bar{d}_a \gamma_\nu d_a). \end{aligned} \quad (68)$$

To be able to reproduce the experimental data, as was shown in Ref. [87], it is necessary to take the current for the  $X$  state as a mixture

$$j_\mu^X = \cos \alpha j_\mu^{(u)} + \sin \alpha j_\mu^{(d)}, \quad (69)$$

where  $j_\mu^{(u)}$  and  $j_\mu^{(d)}$  are tetraquark currents given by Eq. (53) with  $q = u, d$ .

Considering the light quarks as degenerated, we have:

$$\begin{aligned} \Pi_{\mu\nu\alpha}^\rho(x, y) &= \frac{-i}{2\sqrt{2}} (\cos \alpha - \sin \alpha) \Pi_{\mu\nu\alpha}^q(x, y), \\ \Pi_{\mu\nu\alpha}^\omega(x, y) &= \frac{-i}{6\sqrt{2}} (\cos \alpha + \sin \alpha) \Pi_{\mu\nu\alpha}^q(x, y), \end{aligned} \quad (70)$$



On the phenomenological side, the intermediate states of the three mesons are inserted in the vertex, and the following definitions are applied:

$$\begin{aligned}\langle 0|j_\mu^\psi|J/\psi(p')\rangle &= m_\psi f_\psi \epsilon_\mu(p'), \\ \langle 0|j_\nu^V|V(q)\rangle &= m_V f_V \epsilon_\nu(q), \\ \langle X(p)|j_\alpha^X|0\rangle &= \lambda_X \epsilon_\alpha^*(p),\end{aligned}\quad (71)$$

$$\langle J/\psi(p')V(q)|X(p)\rangle = g_{X\psi V} \epsilon^{\sigma\alpha\mu\nu} p_\sigma \epsilon_\alpha(p) \epsilon_\mu^*(p') \epsilon_\nu^*(q), \quad (72)$$

where  $\lambda_X = (\cos \alpha + \sin \alpha) \lambda^q$  (with the coupling between the current and the meson as  $\lambda_q = \sqrt{2} f_X M_X^4$ , from Eq. (56)). The coupling constant  $g_{X\psi V}$  is extracted from the effective Lagrangian that describes the coupling between two vector mesons and one axial vector meson:

$$\mathcal{L} = i g_{X\psi V} \epsilon^{\mu\nu\alpha\sigma} (\partial_\mu X_\nu) \Psi_\alpha V_\sigma. \quad (73)$$

The phenomenological side was, thus, computed in Ref. [87], as

$$\Pi_{\mu\nu\alpha}^{phen}(p, p', q) = \frac{i(\cos \alpha + \sin \alpha) \lambda^q m_\psi f_\psi m_V f_V g_{X\psi V}}{(p^2 - m_X^2)(p'^2 - m_\psi^2)(q^2 - m_V^2)} \times \left( -\epsilon^{\alpha\mu\nu\sigma} (p'_\sigma + q_\sigma) - \epsilon^{\alpha\mu\sigma\gamma} \frac{p'_\sigma q_\gamma q_\nu}{m_V^2} - \epsilon^{\alpha\nu\sigma\gamma} \frac{p'_\sigma q_\gamma p'_\mu}{m_\psi^2} \right) + \dots \quad (74)$$

The OPE side was computed with condensates up to dimension-five, written in terms of a dispersion relation for each Dirac structure  $i$ :

$$\Pi_i^{OPE}(M^2, Q^2) = \int_{4m_c^2}^{\infty} \rho_i^{OPE}(u, Q^2) e^{-u/M^2} du. \quad (75)$$

There are four different Dirac structures contributing to the correlation function. We chose to work with the structures that have more condensates contributing to the OPE. They are:  $\epsilon^{\alpha\mu\nu\sigma} q_\sigma$  and  $\epsilon^{\alpha\nu\sigma\gamma} p'_\sigma q_\gamma p'_\mu$ .

The sum rule for each structure was obtained by matching both sides, and performing a single Borel transformation to  $p^2 = p'^2 \rightarrow M^2$ . Transferring the pure continuum contribution to the OPE side, the general expression for the sum rule for each structure,  $i = 1, 2$ , was obtained:

$$C_i^{XV}(Q^2) \left( e^{-m_\psi^2/M^2} - e^{-m_X^2/M^2} \right) + B_i e^{-s_0/M^2} = -i \frac{Q^2 + m_V^2}{2\sqrt{2}} \Pi_i^{OPE}(M^2, Q^2), \quad (76)$$

where,  $B_i$  takes into account the pole-continuum contribution, as discussed in Sec. 2.7.3, and

$$\begin{aligned}C_1^{XV}(Q^2) &= \frac{f_\psi}{m_\psi} \frac{\lambda_q}{m_X^2 - m_\psi^2} A_{XV}(Q^2) \\ C_2^{XV}(Q^2) &= f_\psi m_\psi \frac{\lambda_q}{m_X^2 - m_\psi^2} A_{XV}(Q^2)\end{aligned}\quad (77)$$

with

$$\begin{aligned}A_{X\rho}(Q^2) &= -m_\rho f_\rho \frac{\cos \alpha + \sin \alpha}{\cos \alpha - \sin \alpha} g_{X\psi\rho}(Q^2) \\ A_{X\omega} &= 3m_\omega f_\omega g_{X\psi\omega}(Q^2).\end{aligned}\quad (78)$$

The OPE side of the sum rule in Eq. (76) determines a unique value for  $C^{XV}$  for each structure, thus, the following ratio between the form factors was found:

$$\frac{g_{X\psi\omega}(Q^2)}{g_{X\psi\rho}(Q^2)} = \frac{m_\rho f_\rho}{3m_\omega f_\omega} \frac{\cos \alpha + \sin \alpha}{\cos \alpha - \sin \alpha}. \quad (79)$$

Using Eq. (79) into Eq. (65) we finally got

$$\frac{\Gamma(X \rightarrow J/\psi \pi^+ \pi^- \pi^0)}{\Gamma(X \rightarrow J/\psi \pi^+ \pi^-)} = 0.153 \left( \frac{\cos \alpha + \sin \alpha}{\cos \alpha - \sin \alpha} \right)^2. \quad (80)$$

The experimental value in Eq. (49) was used to determine the mixing angle:  $\alpha \sim 20^\circ$  [87].

The decay width was finally computed using the coupling constant determined in Ref. [87]:  $g_{X/\psi} = 13.8 \pm 2.0$ , leading to the following result for the partial width:

$$\Gamma(X \rightarrow J/\psi (n\pi)) = (50 \pm 15) \text{ MeV} \quad (81)$$

which is much bigger than the experimental lower limit for the total width  $\Gamma < 1.2 \text{ MeV}$ . In Ref. [96] it was also shown that a similar result is obtained for a molecule. Therefore, a pure four-quark state can not explain both mass and width within the QCDSR framework.

### 3.3. Mixing of two- and four-quarks structure from QCDSR

In the QCDSR studies, the  $X(3872)$  mass is obtained in agreement with the experimental data in both, tetraquark and molecular, pictures. However, the QCDSR results for the decay width were not found to be in agreement with the available data. A new attempt to obtain both, mass and decay width, compatible with experiment was made in Ref. [96], where  $X(3872)$  was considered to be a mixture of two- and four-quarks states. In particular, a mixing between charmonium and molecular  $\bar{D}^*D$  states was done at the level of the currents. This kind of mixture was previously considered, in the QCDSR approach, in Ref. [204] for the light quark sector, and it was also implemented, using QCD factorization, to study the  $X(3872)$  [188]. In order to keep consistency with the available data on the isospin breaking decay modes, Eq.(49), a further mixing was found to be necessary. Therefore,  $X(3872)$  was considered to be a mixing between charmonium,  $(D^{*0}\bar{D}^0 - \bar{D}^{*0}D^0)$  and  $(D^{*+}\bar{D}^- - \bar{D}^{*-}D^+)$  states. In the next subsections we discuss the calculations of the mass, decay widths and the  $B$  meson production channel of  $X(3872)$  in the QCDSR approach.

#### 3.3.1. Two-point correlation function

The interpolating current, in Ref. [96], for the two-quarks and four-quarks mixed states has a two-quark conventional charmonium axial current part:

$$j_\mu^{(2)}(x) = \bar{c}_a(x)\gamma_\mu\gamma_5c_a(x), \quad (82)$$

and a four-quark part given by a  $D^0\bar{D}^{*0}$  molecular current:

$$j_\mu^{(4q)}(x) = \frac{1}{\sqrt{2}} \left[ (\bar{q}_a(x)\gamma_5c_a(x)\bar{c}_b(x)\gamma_\mu q_b(x)) - (\bar{q}_a(x)\gamma_\mu c_a(x)\bar{c}_b(x)\gamma_5 q_b(x)) \right]. \quad (83)$$

Since these two currents have different dimensions, we follow Ref. [204] and to write the two-quark part of the current as:

$$j_\mu^{(2q)} = \frac{1}{6\sqrt{2}} \langle \bar{q}q \rangle j_\mu^{(2)}. \quad (84)$$

The mixing of the two currents was considered as:

$$J_\mu^q(x) = \sin(\theta)j_\mu^{(4q)}(x) + \cos(\theta)j_\mu^{(2q)}(x). \quad (85)$$

The two-point correlation function in Ref. [96] was obtained, as usual, by inserting the corresponding current (Eq. (85)) in the two-point correlation function, to get

$$\Pi_{\mu\nu}(q) = \left( \frac{\langle \bar{q}q \rangle}{6\sqrt{2}} \right)^2 \cos^2(\theta) \Pi_{\mu\nu}^{(2,2)}(q) + \frac{\langle \bar{q}q \rangle}{6\sqrt{2}} (\sin(2\theta)) \Pi_{\mu\nu}^{(2,4)}(q) + \sin^2(\theta) \Pi_{\mu\nu}^{(4,4)}(q), \quad (86)$$

with

$$\Pi_{\mu\nu}^{(i,j)}(q) = i \int d^4x e^{iq \cdot x} \langle 0 | T [ J_\mu^{(i)}(x) J_\nu^{(j)\dagger}(0) ] | 0 \rangle. \quad (87)$$

The phenomenological side was obtained by parametrizing the hadron-current coupling in terms of a single parameter  $\lambda^q$ :

$$\langle 0 | J_\mu^q | X \rangle = \lambda^q \epsilon_\mu, \quad (88)$$

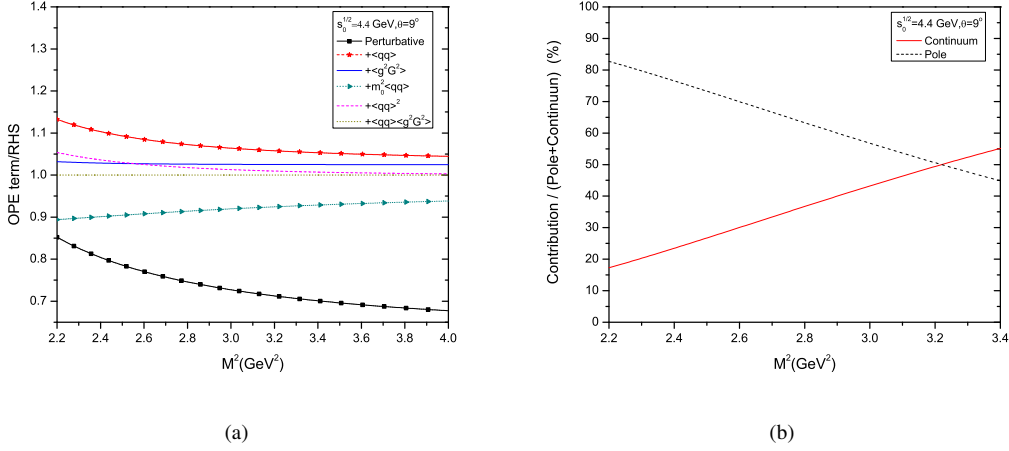


Figure 8: Figures showing the OPE convergence for the correlation function (left) and the pole-continuum dominance (right). Taken from [96]

and by inserting intermediate states in the correlation function, giving

$$\Pi_{\mu\nu}^{phen}(q) = \frac{(\lambda^q)^2}{m_X^2 - q^2} \left( -g_{\mu\nu} + \frac{q_\mu q_\nu}{m_X^2} \right) + \dots, \quad (89)$$

where the chosen Lorentz structure projects out the  $1^{++}$  state. The dots denote higher mass axial-vector resonances.

The QCDSR was obtained by applying the Borel transformation on both sides, and transferring the continuum contribution to the OPE side:

$$(\lambda^q)^2 e^{-m_X^2/M^2} = \left( \frac{\langle \bar{q}q \rangle}{6\sqrt{2}} \right)^2 \cos^2(\theta) \Pi_1^{(2,2)}(M^2) + \frac{\langle \bar{q}q \rangle}{6\sqrt{2}} (\sin(2\theta)) \Pi_1^{(2,4)}(M^2) + \sin^2(\theta) \Pi_1^{(4,4)}(M^2). \quad (90)$$

In Ref. [96] the functions  $\Pi^{i,j}(q)$  were computed in leading order in  $\alpha_s$  up to the dimension-eight condensates. In Figs. 8(a) and 8(b), we show the results for the OPE convergence and for the pole-continuum contributions as obtained in Ref. [96]. These results were obtained using  $\sqrt{s_0} = 4.4$  GeV and  $\theta = 9^\circ$ . From Fig. 8(a) we see that there is a good OPE convergence for values of  $M^2 \geq 2.6$  GeV<sup>2</sup>. The upper limit for the Borel mass is determined from the pole-continuum analysis, fixing the Borel window as:

$$2.6 \text{ GeV}^2 \leq M^2 \leq 3.0 \text{ GeV}^2, \quad (91)$$

The result from the QCDSR for the  $X(3872)$  mass is presented in Fig. 9, showing a good stability within the Borel window. It was found that there is no problem in reproducing the experimental mass of  $X(3872)$  with the mixed current for a large range of the mixing angle  $\theta$ . Considering  $\theta$  in the region  $5^\circ \leq \theta \leq 13^\circ$  one gets [96]:

$$m_X = (3.77 \pm 0.18) \text{ GeV}, \quad (92)$$

which is in good agreement with the experimental data. The value of the meson-current coupling parameter,  $\lambda^q$ , was also obtained:

$$\lambda^q = (3.6 \pm 0.9) \cdot 10^{-3} \text{ GeV}^5. \quad (93)$$

### 3.3.2. Three-point correlation function: $X(3872) \rightarrow J/\psi(n\pi)$ decay

As discussed earlier, to be able to explain the ratio between the decay rates in Eq. (49) one needs to consider also a mixture between the  $D^+D^{*-}$  and  $D^-D^{*+}$  components. Therefore, the most general current is given by

$$j_\mu^X(x) = \cos \alpha J_\mu^u(x) + \sin \alpha J_\mu^d(x), \quad (94)$$

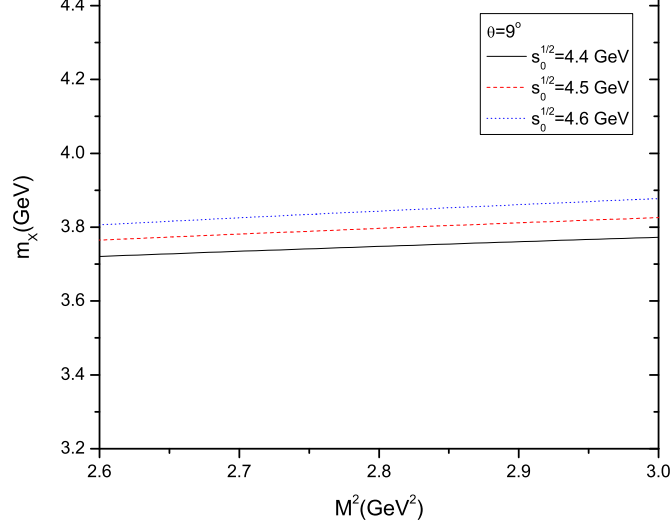


Figure 9: The  $X$  meson mass as a function of the sum rule parameter ( $M^2$ ) within the Borel window range, for different values of the continuum threshold  $s_0$ . Taken from [96].

with  $J_\mu^u(x)$  and  $J_\mu^d(x)$  given by Eq.(85). The interpolating fields for the other mesons in the vertex are given by Eqs. (68). The three point function for the vertex  $X(3872)J/\psi V$  is obtained inserting the currents (Eq. (94) and (68)) into the three-point function of Eq. (227). Taking the quarks  $u$  and  $d$  as degenerated, one arrives at Eqs. (70) multiplied by  $\sin \theta$ , showing that it is only the four-quark part of the current in Eq. (85) that contributes to these decays.

The phenomenological side of the sum rule is given by Eq. (74). As discussed in Sec. 3.2.2, the mixing angle  $\alpha$  is determined in order to reproduce the experimental ratio in Eq. (49):  $\alpha = 20^\circ$ . This is the same result obtained in Refs. [87, 186]. In Ref. [96] the OPE side was evaluated up to dimension five at leading order in  $\alpha_s$ . Taking the limit  $p^2 = p'^2 = -P^2$  and doing a single Borel transform to  $P^2 \rightarrow M^2$ , we get in the structure  $\epsilon^{\alpha\nu\sigma\gamma} p'_\sigma q_\gamma p'_\mu$

$$C(Q^2) \left( e^{-m_\psi^2/M^2} - e^{-m_X^2/M^2} \right) + B e^{-s_0/M^2} = (Q^2 + m_\omega^2) \Pi^{OPE}(M^2, Q^2), \quad (95)$$

where

$$C(Q^2) = \frac{6}{\sin(\theta)} m_\omega f_\omega \frac{f_\psi \lambda^q}{m_\psi (m_X^2 - m_\psi^2)} g_{X\psi\omega}(Q^2), \quad (96)$$

and  $B$  gives the pole-continuum transitions contribution (see Sec. 2.7.3).  $s_0$  and  $u_0$  are the continuum thresholds for  $X$  and  $J/\psi$  respectively.

In Fig. 10(a) we show the function  $C(Q^2)$ , obtained from Eq. (95), as a function of  $M^2$  and  $Q^2$ . As can be seen from this figure, in the region  $3.0 \leq M^2 \leq 3.5 \text{ GeV}^2$   $C(Q^2)$  is a very stable function of  $M^2$ . Therefore, we choose this Borel window to extract  $C(Q^2)$ , as it is shown by the dots in Fig. 10(b). The QCDSR results for  $C(Q^2)$  was fitted using a monopole parametrization:

$$C(Q^2) = \frac{2.5 \times 10^{-2} \text{ GeV}^7}{Q^2 + 38 \text{ GeV}^2}, \quad (97)$$

as shown by the solid line in Fig. 10(b). The form factor  $g_{X\psi\omega}(Q^2)$  can be obtained by using Eqs. (96) and (97). The constant coupling was calculated by extrapolating the form factor at the meson pole  $Q^2 = -m_\omega^2$  as

$$g_{X\psi\omega} = g_{X\psi\omega}(-m_\omega^2) = 5.4 \pm 2.4, \quad (98)$$

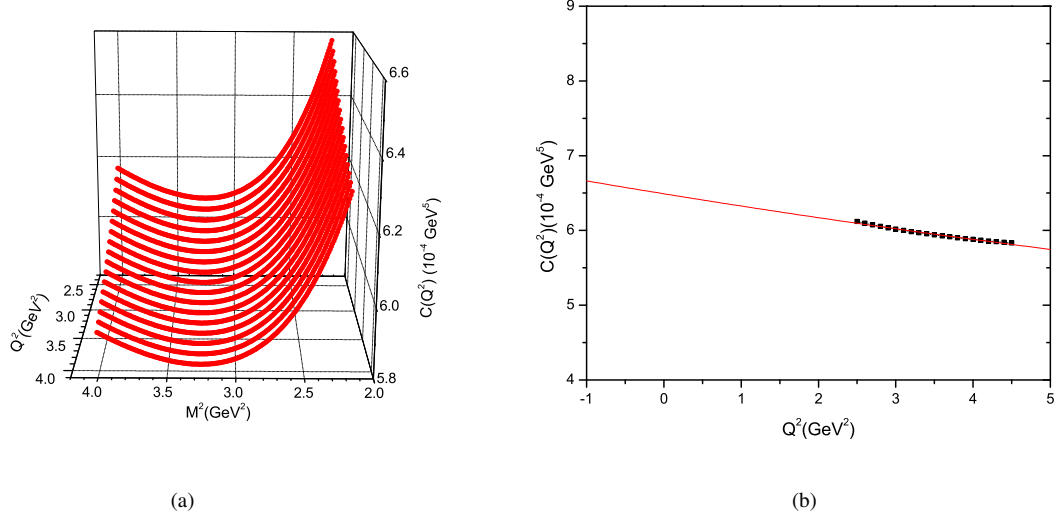


Figure 10: (a) Values of  $C(Q^2)$  obtained by varying both  $Q^2$  and  $M^2$  in Eq. (95). (b) Momentum dependence of  $C(Q^2)$  for  $s_0^{1/2} = 4.4$  GeV. The solid line gives the parametrization of the QCDSR results (dots) through Eq. (97). Taken from [96].

where the value  $5^\circ \leq \theta \leq 13^\circ$  was used for the mixing angle. The decay width was determined to be:

$$\Gamma(X \rightarrow J/\psi \pi^+ \pi^- \pi^0) = (9.3 \pm 6.9) \text{ MeV}, \quad (99)$$

which is in agreement with the experimental upper limit. Since the QCDSR results for the width and the mass grow with the mixing angle  $\theta$ , there is only a small range for the values of this angle that can provide simultaneously good agreement with the experimental values of the mass and the decay width, and this range is  $5^\circ \leq \theta \leq 13^\circ$ .

### 3.3.3. $X(3872) \rightarrow \gamma J/\psi$ radiative decay

Since it is possible to explain both, the mass and the total width of the  $X(3872)$ , using a mixed charmonium-molecular current in a QCDSR calculation, in Ref. [98] the authors used the same current to study the vertex of the radiative decay mode  $X(3872) \rightarrow \gamma J/\psi$ . The calculation was done using the same previously determined mixing angles:  $\alpha = 20^\circ$  and  $\theta = (9 \pm 4)^\circ$  for the mixings in Eqs. (94) and (85) respectively. To study the  $X(3872)$  radiative decay one considers the three-point function:

$$\Pi_{\mu\nu\alpha}(p, p', q) = \int d^4x d^4y e^{ip' \cdot x} e^{iq \cdot y} \langle 0 | T [J_\mu^\psi(x) j_\nu^\gamma(y) j_\alpha^{X^\dagger}(0)] | 0 \rangle, \quad (100)$$

where the  $J/\psi$  current is given in Eq. (68) and the electromagnetic current is given by:

$$j_\nu^\gamma = \sum_{q=u,d,c} e_q \bar{q} \gamma_\nu q, \quad e_{u,c} = +\frac{2}{3}, \quad e_d = -\frac{1}{3}. \quad (101)$$

Parameterizing the coupling of the currents with the states as:

$$\begin{aligned} \langle 0 | j_\mu^\psi | \psi(p') \rangle &= m_\psi f_\psi \epsilon_\mu(p'); \\ \langle X(p) | j_\alpha^X | 0 \rangle &= (\cos \alpha + \sin \alpha) \lambda_q \epsilon_\alpha^*(p), \\ \langle \psi(p') | j_\nu^\gamma(q) | X(p) \rangle &= i \epsilon_\nu^\gamma(q) \mathcal{M}(X(p) \rightarrow \gamma(q) J/\psi(p')), \end{aligned} \quad (102)$$

the phenomenological side is then given by [98]:

$$\begin{aligned} \Pi_{\mu\nu\alpha}^{\text{phen}}(p, p', q) = & \frac{ie(\cos\alpha + \sin\alpha)\lambda_q m_\psi f_\psi}{m_X^2(p^2 - m_X^2)(p'^2 - m_\psi^2)} \left( \epsilon^{\alpha\mu\nu\sigma} q_\sigma p \cdot q A + \epsilon^{\mu\nu\lambda\sigma} p'_\lambda q_\sigma q_\alpha B - \epsilon^{\alpha\nu\lambda\sigma} q_\mu q_\sigma p'_\lambda C \right. \\ & \left. + \epsilon^{\alpha\nu\lambda\sigma} p'_\lambda p'_\mu q_\sigma (C - A) \frac{p \cdot q}{m_\psi^2} - \epsilon^{\mu\nu\lambda\sigma} p'_\lambda q_\sigma (q_\alpha + p'_\alpha) (A + B) \frac{p \cdot q}{m_X^2} \right). \end{aligned} \quad (103)$$

In deriving Eq. (103) we used the decay amplitude,  $\mathcal{M}(X(p) \rightarrow \gamma(q)J/\psi(p'))$ , given in Ref. [205]:

$$\mathcal{M}(X(p) \rightarrow \gamma(q)J/\psi(p')) = e \epsilon^{\kappa\lambda\rho\sigma} \epsilon_X^\alpha(p) \epsilon_\psi^\mu(p') \epsilon_\gamma^\rho(q) \frac{q_\sigma}{m_X^2} (A g_{\mu\lambda} g_{\alpha\kappa} p \cdot q + B g_{\mu\lambda} p_\kappa q_\alpha + C g_{\alpha\kappa} p_\lambda q_\mu). \quad (104)$$

Notice that there are three dimensionless couplings,  $A$ ,  $B$  and  $C$ , to be determined by the QCDSR. There are five independent Lorentz structures in Eq. (103). The authors in Ref. [98] worked with the structures:  $\epsilon^{\alpha\mu\nu\sigma} q_\sigma$ ,  $\epsilon^{\mu\nu\sigma\lambda} p'_\sigma p'_\alpha q_\lambda$  and  $\epsilon^{\alpha\nu\lambda\sigma} p'_\lambda q_\sigma q_\mu$ , to determine the couplings  $A$ ,  $A + B$ , and  $C$  respectively.

The OPE side is defined considering degenerated quarks  $u$  and  $d$ , i.e.,  $m_u = m_d$  and  $\langle \bar{u}u \rangle = \langle \bar{d}d \rangle = \langle \bar{q}q \rangle$ . Using the mixed current, Eq. (94), in Eq. (100), we arrive at:

$$\Pi_{\mu\nu\alpha}(x, y) = \frac{\sin\theta}{3} (2 \cos\alpha - \sin\alpha) \Pi_{\mu\nu\alpha}^{\text{mol}}(x, y) + \frac{\langle \bar{q}q \rangle}{6\sqrt{2}} \cos\theta (\cos\alpha + \sin\alpha) \Pi_{\mu\nu\alpha}^{\text{c}\bar{c}}(x, y). \quad (105)$$

where the charmonium and molecule terms are written as:

$$\Pi_{\mu\nu\alpha}^{\text{c}\bar{c}}(x, y) = \langle 0 | T [ j_\mu^\psi(x) j_\nu^\psi(y) j_\alpha^{(2)\dagger}(0) ] | 0 \rangle, \quad (106)$$

$$\Pi_{\mu\nu\alpha}^{\text{mol}}(x, y) = \langle 0 | T [ j_\mu^\psi(x) j_\nu^\psi(y) j_\alpha^{(4q)\dagger}(0) ] | 0 \rangle, \quad (107)$$

with  $j_\alpha^{(2)}$  and  $j_\alpha^{(4q)}$  given by Eqs. (82) and (83) respectively. In Ref. [98] the OPE side was evaluated in leading order in  $\alpha_s$  up to dimension-five condensates.

Doing a single Borel transform to  $P^2 \rightarrow M^2$ , in the limit  $p^2 = p'^2 = -P^2$ , one gets for each structure  $i$ :

$$G_i(Q^2) \left( e^{-m_\psi^2/M^2} - e^{-m_X^2/M^2} \right) + B_i(Q^2) e^{-s_0/M^2} = \bar{\Pi}_i^{\text{OPE}}(M^2, Q^2), \quad (108)$$

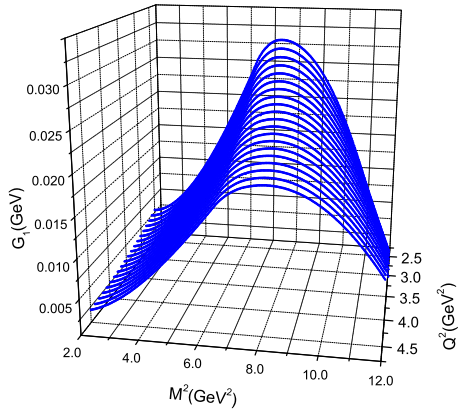
where  $Q^2 = -q^2$  and  $B_i(Q^2)$  is the pole-continuum transitions contribution (see Sec. 2.7.3).  $G_i(Q^2)$  is related to the three form factors:

$$\begin{aligned} G_1(Q^2) &= \frac{3\sqrt{2}\pi^2(\cos\alpha + \sin\alpha)\lambda_q m_\psi f_\psi}{m_X^2(m_X^2 - m_\psi^2)} A(Q^2) \\ G_2(Q^2) &= \frac{3^2 2^4 \sqrt{2}\pi^2(\cos\alpha + \sin\alpha)\lambda_q m_\psi f_\psi (A(Q^2) + B(Q^2))}{\sin\theta(2\cos\alpha - \sin\alpha)m_X^4(m_X^2 - m_\psi^2)} \\ G_3(Q^2) &= \frac{6\sqrt{2}\pi^2\lambda_q m_\psi f_\psi}{\cos\theta m_X^2(m_X^2 - m_\psi^2)} C(Q^2) \end{aligned} \quad (109)$$

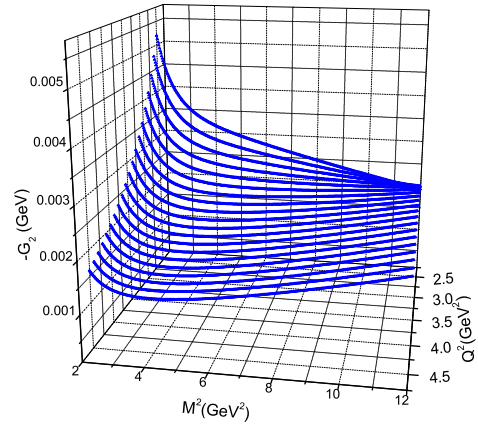
The unknown functions  $G_i$  and  $B_i$  in the LHS of Eq. (108) are determined by fitting both sides of the sum rule. These functions should not depend on the Borel parameter  $M^2$ . Therefore, the Borel region is fixed by imposing that these functions are stable as a function of  $M^2$ . Fig. 11 shows the QCDSR results for the  $G_i$ 's as functions of  $Q^2$  and  $M^2$ . From these figures it is possible to determine the corresponding Borel region for each one of these functions:  $7.0 \text{ GeV}^2 \leq M^2 \leq 8.5 \text{ GeV}^2$  for  $G_1(Q^2)$ ,  $6.5 \text{ GeV}^2 \leq M^2 \leq 7.5 \text{ GeV}^2$  for  $G_2(Q^2)$ , and  $8.0 \text{ GeV}^2 \leq M^2 \leq 9.0 \text{ GeV}^2$  for  $G_3(Q^2)$ . The QCDSR results for the three form factors are shown in Fig. 12.

The  $Q^2$ -dependence for all the three form factors can be fitted by using an exponential parametrization:

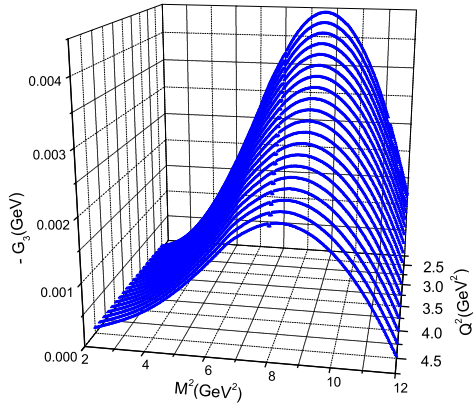
$$G_i(Q^2) = g_i e^{-g_i Q^2}, \quad (110)$$



(a)

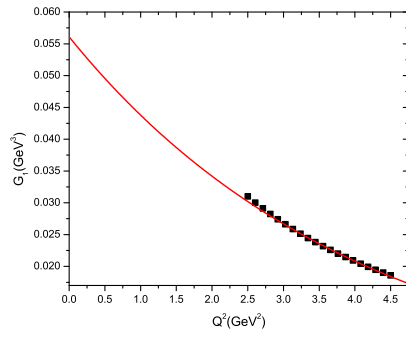


(b)

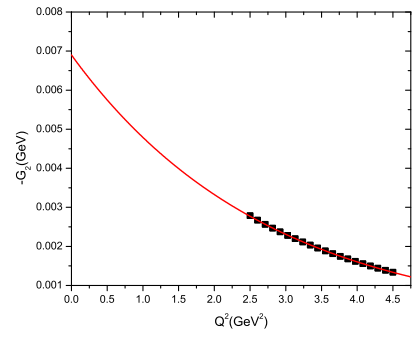


(c)

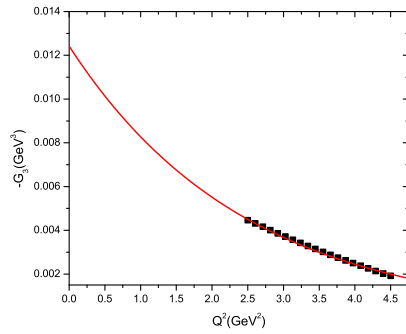
Figure 11: Values of the functions obtained by varying both  $Q^2$  and  $M^2$ : a)  $G_1(Q^2)$ , b)  $G_2(Q^2)$  and c)  $G_3(Q^2)$ . Taken from [98]



(a)



(b)



(c)

Figure 12: Momentum dependence of the functions for  $s_0^{1/2} = 4.4 \text{ GeV}$  and  $u_0^{1/2} = 3.6 \text{ GeV}$ : (a)  $G_1$ , (b)  $G_2$  and (c)  $G_3$ . The solid line gives the parametrization of the QCDSR results (dots) through Eq. (110) and the results in Table 4. Taken from [98].



	$G_1$	$G_2$	$G_3$
$g_1$	$0.056 \text{ GeV}^3$	$-0.0069 \text{ GeV}$	$-0.013 \text{ GeV}^3$
$g_2$	$0.25 \text{ GeV}^{-2}$	$0.365 \text{ GeV}^{-2}$	$0.41 \text{ GeV}^{-2}$

Table 4: Results for the fitting parameters in Eq. (110).

The fitted functions are also shown in Fig. 12 through the solid lines. The fitted parameters are given in the Table 4.

The results from Table 4 can be used to determine the form factors  $A(Q^2)$ ,  $B(Q^2)$  and  $C(Q^2)$  written in terms of the  $G_i(Q^2)$  in Eqs. (109). The coupling constants are obtained from the form factors at  $Q^2 = 0$ . The couplings are:

$$\begin{aligned}
A &= A(Q^2 = 0) = 18.65 \pm 0.94; \\
A + B &= (A + B)(Q^2 = 0) = -0.24 \pm 0.11; \\
C &= C(Q^2 = 0) = -0.843 \pm 0.008.
\end{aligned} \tag{111}$$

The radiative decay width is obtained from these couplings through the expression [98]:

$$\Gamma(X \rightarrow J/\psi \gamma) = \frac{\alpha_e p^{*5}}{3 m_X^4} \left( (A + B)^2 + \frac{m_X^2}{m_\psi^2} (A + C)^2 \right),$$

where  $p^* = (m_X^2 - m_\psi^2)/(2m_X)$  is the momentum of the photon in the rest frame, and  $\alpha_e = \frac{1}{137}$  is the fine structure constant. Using the previous result  $\Gamma(X \rightarrow J/\psi \pi\pi) = (9.3 \pm 6.9) \text{ MeV}$ , we get the ratio

$$\frac{\Gamma(X \rightarrow J/\psi \gamma)}{\Gamma(X \rightarrow J/\psi \pi^+\pi^-)} = 0.19 \pm 0.13, \tag{112}$$

which is in excellent agreement with the experimental result in Eq. (51).

### 3.3.4. $X(3872)$ production in $B$ decays

The next application testing the mixed charmonium-molecule current, was done in Ref. [101], which is related to the production of  $X(3872)$  in  $B$  meson decays, through the channel  $B^\pm \rightarrow K^\pm X(3872)$ . BaBar Collaboration has reported the upper limit for the branching ratio of the  $X(3872)$  production in  $B$  meson decays as [206]:

$$\mathcal{B}(B^\pm \rightarrow K^\pm X(3872)) < 3.2 \times 10^{-4}. \tag{113}$$

The  $B$  meson decay process occurs via weak decay of the  $b$ -quark, with the light quark as the spectator. In effective theory, the Hamiltonian describing the weak interaction at the scale  $\mu = m_b \ll m_W$  can be written in terms of a four-quark interaction vertex with an effective four quark operator  $\mathcal{O}_2 = (\bar{c}\Gamma_\mu c)(\bar{s}\Gamma^\mu b)$ , with a  $V - A$  structure  $\Gamma_\mu = \gamma_\mu(1 - \gamma_5)$ . The interaction can be factorized into two matrix elements, giving the following decay amplitude for the process:

$$\mathcal{M} = i \frac{G_F}{\sqrt{2}} V_{cb} V_{cs}^* \left( C_2 + \frac{C_1}{3} \right) \langle B(p) | J_\mu^W | K(p') \rangle \langle X(q) | J^{\mu(\bar{c}c)} | 0 \rangle, \tag{114}$$

where  $V_{ik}$  are CKM matrix elements,  $C_1(\mu)$  and  $C_2(\mu)$  are short distance Wilson coefficients computed at the renormalization scale  $\mu \sim \mathcal{O}(m_b)$ ,  $p = p' + q$ , and the currents are

$$J_\mu^W = \bar{s}\Gamma_\mu b, \quad J_\mu^{(\bar{c}c)} = \bar{c}\Gamma_\mu c. \tag{115}$$

Here  $X(3872)$ , considered as a mixture of molecule and charmonium currents, interacts through the  $\bar{c}c$  component of the weak current.

The matrix elements in Eq. (114) are parametrized, in Ref. [101], as

$$\langle X(q) | J_\mu^{(\bar{c}c)} | 0 \rangle = \lambda_W \epsilon_\mu(q), \tag{116}$$

$$\langle B(p)|J_\mu^W|K(p')\rangle = f_+(q^2)(p_\mu + p'_\mu) + f_-(q^2)(p_\mu - p'_\mu). \quad (117)$$

The coupling between the current  $J_\mu^{(\bar{c}c)}$  and the  $X(3872)$  is provided by the parameter  $\lambda_W$  in Eq. (166). The form factors,  $f_\pm(q^2)$ , describe the weak transition process  $B \rightarrow K$ .

The decay width for the process  $B^\pm \rightarrow X(3872)K^\pm$  is computed from

$$\Gamma(B \rightarrow XK) = \frac{1}{16\pi m_B^3} \lambda^{1/2}(m_B^2, m_K^2, m_X^2) |\mathcal{M}|^2, \quad (118)$$

where  $\lambda(x, y, z) = x^2 + y^2 + z^2 - 2xy - 2xz - 2yz$ , and the invariant amplitude squared can be obtained from Eq. (114):

$$|\mathcal{M}|^2 = \frac{G_F^2}{2} |V_{cb}V_{cs}|^2 \left( C_2 + \frac{C_1}{3} \right)^2 \lambda(m_B^2, m_K^2, m_X^2) \lambda_W^2 f_+^2(q^2) |_{q^2 \rightarrow -m_X^2}. \quad (119)$$

The unknown parameters, to be determined from the QCDSR approach, are the weak coupling,  $\lambda_W$ , and the value of the form factor  $f_+(q^2)$  at the  $X(3872)$  pole.

The factorization of the amplitude allows the four-quark vertex to be analysed as two separated sub-processes: the creation of  $X(3872)$  and the transition  $B \rightarrow K$ , as in Eqs. (166) and (167). Let us start with the two-point correlator, describing the coupling between the current  $J_\nu^{(\bar{c}c)}$  and  $X(3872)$ :

$$\Pi_{\mu\nu}^{\text{OPE}}(q) = (\cos \alpha + \sin \alpha) \left( \sin \theta \Pi_{\mu\nu}^{4,2}(q) + \frac{\langle \bar{q}q \rangle}{6\sqrt{2}} \cos \theta \Pi_{\mu\nu}^{2,2}(q) \right), \quad (120)$$

where

$$\begin{aligned} \Pi_{\mu\nu}^{4,2}(q) &= i \int d^4y e^{iq \cdot y} \langle 0 | T \{ J_\mu^{4q}(y) J_\nu^{(\bar{c}c)}(0) \} | 0 \rangle \\ \Pi_{\mu\nu}^{2,2}(q) &= i \int d^4y e^{iq \cdot y} \langle 0 | T \{ J_\mu^{2q}(y) J_\nu^{(\bar{c}c)}(0) \} | 0 \rangle. \end{aligned} \quad (121)$$

The contribution from the vector part of the current  $J_\nu^{(\bar{c}c)}$  vanishes after the integration is performed, thus these correlators are equal (except for a minus sign) to the ones calculated previously in Ref. [96] (sub-section 3.3.1) for the two-point correlator of  $X(3872)$ .

On the phenomenological side the correlator is determined inserting the intermediate state of  $X(3872)$ :

$$\begin{aligned} \Pi_{\mu\nu}^{\text{phen}}(q) &= \frac{i}{q^2 - m_X^2} \langle 0 | J_\mu^X | X(q) \rangle \langle X(q) | J_\nu^{(c\bar{c})} | 0 \rangle, \\ &= \frac{i\lambda_X \lambda_W}{Q^2 + m_X^2} \left( g_{\mu\nu} - \frac{q_\mu q_\nu}{m_X^2} \right) \end{aligned} \quad (122)$$

where we have used the definition in Eq. (166) and

$$\langle 0 | J_\mu^X | X(q) \rangle = \lambda_X \epsilon_\mu(q). \quad (123)$$

The parameter defining the coupling between the current  $J_\mu^X$  and the  $X$  meson has been calculated in Ref. [96], and its value is given in Eq. (93).

The QCDSR, in the structure  $g_{\mu\nu}$ , obtained after the Borel transformation is:

$$\lambda_W \lambda_X e^{-\frac{m_X^2}{M^2}} = -(\cos \alpha + \sin \alpha) \left( \sin \theta \Pi^{4,2}(M^2) + \frac{\langle \bar{q}q \rangle}{6\sqrt{2}} \cos \theta \Pi^{2,2}(M^2) \right). \quad (124)$$

This expression is evaluated numerically to obtain the coupling parameter  $\lambda_W$ . To keep consistency through the different analysis, the same parameters are used as before:  $\sqrt{s_0} = 4.4 \text{ GeV}$ ,  $2.6 \text{ GeV}^2 \leq M^2 \leq 3.0 \text{ GeV}^2$ , and the mixing angles  $\theta = (9 \pm 4)^\circ$ , and  $\alpha = 20^\circ$ .

The result for the parameter  $\lambda_W$ , obtained within the given ranges of the Borel mass and the variation in the mixing angle  $\theta$ , is [101]:

$$\lambda_W = (1.29 \pm 0.51) \text{ GeV}^2. \quad (125)$$

The three-point function describing the weak transition  $B \rightarrow K$  is written as:

$$\Pi_\mu(p, p') = \int d^4x d^4y e^{i(p' \cdot x - p \cdot y)} \langle 0 | T \{ J_\mu^W(0) J_K(x) J_B^\dagger(y) \} | 0 \rangle, \quad (126)$$

where the weak current  $J_\mu^W$  is defined in (115) and the interpolating currents of the  $B$  and  $K$  pseudoscalar mesons are:

$$J_K(x) = i \bar{u}_a(x) \gamma_5 s_a(x), \quad J_B = i \bar{u}_a(x) \gamma_5 b_a(x). \quad (127)$$

On the phenomenological side, the insertion of the intermediate  $B$  and  $K$  mesons gives

$$\Pi_\mu^{phen} = - \frac{f_B f_K m_K^2 m_B^2}{m_b(m_s + m_u)} \frac{(f_+(q^2)(p + p')_\mu + f_-(q^2)q_\mu)}{(p^2 - m_B^2)(p'^2 - m_K^2)}, \quad (128)$$

where we have used Eq. (167) and the following definitions:

$$\langle 0 | J_K | K(p') \rangle = f_K \frac{m_K^2}{m_s + m_u}, \quad \langle 0 | J_B | B(p) \rangle = f_B \frac{m_B^2}{m_b}. \quad (129)$$

After a double Borel transform is applied on both sides of the sum rule,  $P^2 \rightarrow M^2$  and  $P'^2 \rightarrow M'^2$ , we get the sum rule in the structure  $(p_\mu + p'_\mu)$ :

$$- \frac{f_B f_K m_K^2 m_B^2 f_+(Q^2)}{m_b(m_s + m_u)} e^{-\frac{m_B^2}{M^2} - \frac{m_K^2}{M'^2}} = \Pi^{OPE}(M^2, M'^2) \quad (130)$$

In Ref. [101] the OPE side was evaluated at leading order in  $\alpha_s$ , considering condensates up to dimension-five and terms linear in the  $s$  quark mass. The following ansatz, relating the Borel masses  $M^2$  and  $M'^2$ , was applied in the numerical analysis:  $M'^2 = \frac{0.64 \text{ GeV}^2}{m_B^2 - m_b^2} M^2$ .

The QCDSR results for the form factor  $f_+$  is plotted in Fig. 13(a) as a function of  $Q^2$  and  $M^2$ , showing a good stability for  $M^2 > 20.0 \text{ GeV}^2$ . The obtained  $Q^2$  dependence of the form factor, in the Borel region  $26 \text{ GeV}^2 \leq M^2 \leq 30 \text{ GeV}^2$  (compatible with the  $B$  mass) is shown in Fig. 13(b).

Using a monopolar parametrization for the form factor,  $f_+(Q^2)$ ;

$$f_+(Q^2) = \frac{(17.55 \pm 0.04) \text{ GeV}^2}{(105.0 \pm 1.76) \text{ GeV}^2 + Q^2}, \quad (131)$$

the QCDSR results in Eq. (130) can be well represented, as shown in Fig. 13(b). Using Eq. (131), the value of the form factor at the  $X(3872)$  pole,  $Q^2 = -m_X^2$ , is given by [101]:

$$f_+(Q^2 = -m_X^2) = 0.195 \pm 0.003. \quad (132)$$

The decay width is determined using the value of the parameter  $\lambda_W$  obtained from the two-point sum rule calculation, Eq. (175), and the value of the form factor,  $f_+$ , in Eq. (170). The branching ratio is obtained by dividing this result by the total width of the  $B$  meson [22]:  $\Gamma_{\text{tot}} = \hbar/\tau_B$ . It gives [101]:

$$\mathcal{B}(B \rightarrow X(3872)K) = (1.00 \pm 0.68) \times 10^{-5}, \quad (133)$$

This value for the branching ratio is smaller but compatible with the experimental upper limit in Eq. (113). Since the factorization hypothesis was employed, this result suggests that non-factorizable contributions, that were not taken into account in Ref. [101], can be significant. Therefore, the result in Eq. (133) should be taken as a lower limit for the branching ratio.

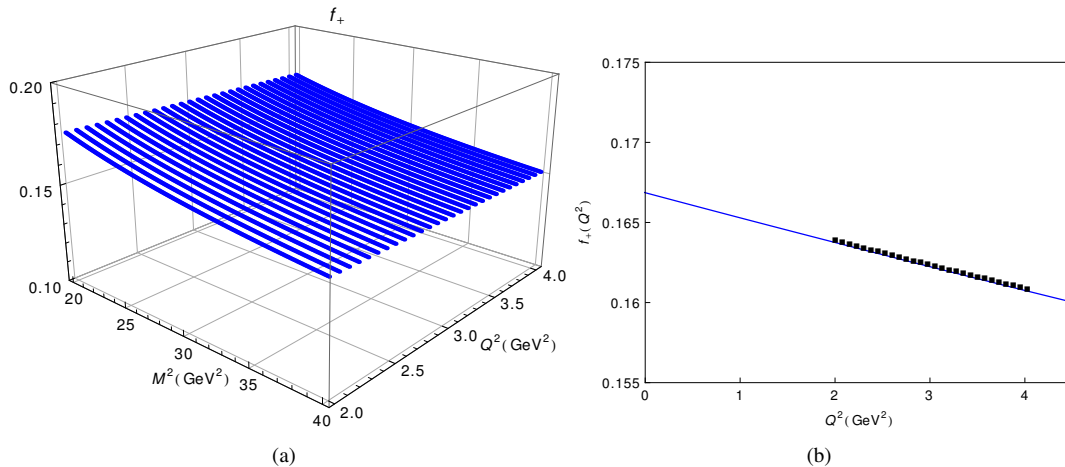


Figure 13: (a) QCDSR results for the form factor  $f_+$  as a function of  $Q^2$  and  $M^2$ . (b) Momentum dependence of  $f_+(Q^2)$ . The solid line gives the parametrization of the QCDSR results (dots) through Eq. (131). Taken from [101].

### 3.4. Summary for $X(3872)$

The mixed charmonium-molecule current proposed in Ref. [96] within the QCDSR framework, provides a consistent description of various properties of  $X(3872)$  state that are neglected in most studies, which are usually concerned only with the mass of the state. This type of mixed state is favored by the  $\gamma\psi(2S)$  decay experimental data, as discussed previously. The consistency of such an approach is guaranteed by applying the same mixing parameters in different analysis. The mixing angles  $\alpha = 20^\circ$  and  $\theta = (9 \pm 4)^\circ$  were fixed in the first study of the mass and decay width of the channel  $X(3872) \rightarrow J/\psi(n\pi)$ , and then applied to study the radiative decay  $X(3872) \rightarrow \gamma J/\psi$  and the production channel  $B \rightarrow K X(3872)$ . Eq. (85) may suggest that the state is dominated by the charmonium component ( $\sim 97\%$ ), as was pointed out in the conclusions of Ref. [96]. However, this is not so straightforward, since the  $c\bar{c}$  component of the current is multiplied by a dimensional parameter and hence the percentage of each component is not provided solely by the mixing angle. Despite being unable to determine the percentages of the charmonium and molecule components, it is possible to establish that both components are mandatory, given that the properties of  $X(3872)$  can not be properly explained with only one of the components.

## 4. Vector Charmonium $Y$ States

Many of the charmonium-like states observed in the Initial State Radiation (ISR) process  $e^+e^- \rightarrow J/\psi \pi^+\pi^-$  by BaBar and Belle collaborations do not fit the quarkonia interpretation, and have stimulated an extensive discussion about exotic hadron configurations. In particular,  $Y(4260)$ , which was reported in Ref. [72] with a mass around  $4.26 \text{ GeV}/c^2$ . This observation was immediately confirmed by CLEO-c [74] and Belle [53], and more recently by the BESIII Collaboration [54]. Historically, the label  $Y$  was used for all states with  $I^G(J^{PC}) = 0^-(1^{--})$  quantum numbers which were produced in  $e^+e^-$  annihilation. In this review we use the same label, though it is different from the recent naming scheme of PDG [22].

The conventional neutral  $1^{--}$  charmonium states in the mass range (3.8 to 5.0 GeV), such as  $\psi(4040)$ ,  $\psi(4160)$ , and  $\psi(4415)$  [22], decay predominantly into open charm final states (e.g.,  $D$  mesons), while the  $Y$  states decay to hidden-charm final states [207]. Furthermore, the observation of the states  $Y(4360)$  and  $Y(4660)$  in  $e^+e^- \rightarrow \psi(2S) \pi^+\pi^-$  [59, 77–79], together with more resonant structures observed in  $e^+e^- \rightarrow \omega \chi_{c0}$  [68] and  $e^+e^- \rightarrow h_c \pi^+\pi^-$  [69], overpopulate the vector charmonium spectrum predicted by potential models [208–210]. These facts indicate that the neutral  $Y$  states may not be conventional charmonium states, and they are good candidates for new types of exotic particles, such as hybrids, tetraquarks, or meson molecules [2, 3, 7, 8, 18, 20, 211].

The list of the most recent experimental results for the  $1^{--}$  family is shown in Table 5. However, one has to be very careful with the information collected from different experimental analysis. One example is the  $Y(4220)$  and  $Y(4260)$

states. Whether they are two different states (as considered in Ref. [22] and quoted in Table 5), or whether, as stated in Ref. [71], the structure around 4260 MeV can be interpreted as a superposition of the two resonances observed in Ref. [54], the so called  $Y(4220)$  and  $Y(4320)$ , is still an open question. In the following we discuss these  $Y$  states.

Table 5: A list of the currently known neutral  $I^G(J^{PC}) = 0^-(1^{--})$  charmonium  $Y$  states. The current naming scheme used by PDG [22] is included in the table. The quoted year is the year of the first observation in each channel.

State	Name in PDG	Decay channel	Experiment	Year	
MeV	$Y(4220)$	$\psi(4230)$	$Y(4220) \rightarrow \chi_{c0} \omega$	BESIII [68]	2015
			$Y(4220) \rightarrow h_c \pi^+ \pi^-$	BESIII [69]	2017
			$Y(4220) \rightarrow \psi(2S) \pi^+ \pi^-$	BESIII [70]	2017
			$Y(4220) \rightarrow D^0 D^{*-} \pi^+$	BESIII [71]	2018
	$Y(4260)$	$\psi(4260)$	$Y(4260) \rightarrow J/\psi \pi^+ \pi^-$	BaBar [72, 73]; CLEO-c [74]; Belle [44, 53]	2005
			$Y(4260) \rightarrow J/\psi \pi^0 \pi^0$	CLEO-c [75]	2006
			$Y(4260) \rightarrow J/\psi K^+ K^-$	CLEO-c [75]; Belle [212, 213]	2006
			$Y(4260) \rightarrow J/\psi f_0(980)$	BaBar [73]	2012
			$Y(4260) \rightarrow Z_c(3900)^\pm \pi^\mp$	Belle [44]; BESIII [43]	2013
			$Y(4260) \rightarrow J/\psi \pi^+ \pi^-$	BESIII [54]	2017
	$Y(4360)$	$\psi(4360)$	$Y(4360) \rightarrow \psi(2S) \pi^+ \pi^-$	Belle [59, 79]; BaBar [77, 78]; BESIII [70]	2007
			$Y(4360) \rightarrow J/\psi \pi^+ \pi^-$	BESIII [54]	2017
$Y(4390)$	$\psi(4390)$	$Y(4390) \rightarrow h_c \pi^+ \pi^-$	BESIII [69]	2017	
		$Y(4390) \rightarrow \psi(2S) \pi^+ \pi^-$	BESIII [70]	2017	
$Y(4660)$	$\psi(4660)$	$Y(4660) \rightarrow \psi(2S) \pi^+ \pi^-$	Belle [59, 79]; BaBar [78]	2007	
		$Y(4660) \rightarrow \Lambda_c^+ \Lambda_c^-$	BESIII [85]	2008	

#### 4.1. $Y(4260)$

The  $Y(4260)$  state is particularly interesting. It was first observed by the BaBar collaboration in the process  $e^+ e^- \rightarrow J/\psi \pi^+ \pi^-$  through ISR [72], and it was confirmed by CLEO-c [74] and Belle [53]. The  $Y(4260)$  was also observed in the  $B^- \rightarrow Y(4260) K^- \rightarrow J/\psi \pi^+ \pi^- K^-$  decay [73], and CLEO-c reported two additional decay channels:  $J/\psi \pi^0 \pi^0$  and  $J/\psi K^+ K^-$  [75]. More recently, the BESIII collaboration has announced new precise measurements of the  $e^+ e^- \rightarrow J/\psi \pi^+ \pi^-$  cross sections [54], reporting not only updated values for the mass and width of the  $Y(4260)$ , but also the presence of a second resonance in the  $J/\psi \pi^+ \pi^-$  mass spectrum. The mass and width of the two observed resonances are, respectively:  $(4222.0 \pm 3.1 \pm 1.4)$  MeV and  $(44.1 \pm 4.3 \pm 2.0)$  MeV for the first one and  $(4320.0 \pm 10.4 \pm 7)$  MeV and  $(101.4^{+25.3}_{-19.7} \pm 10.2)$  MeV for the second one. Although in Ref. [54] it is stated that the mass and width of the two observed resonances are in agreement with the those of  $Y(4260)$  and  $Y(4360)$  respectively, in Ref. [71] it is said that the structure around 4260 MeV can be interpreted as a superposition of the two resonances observed in Ref. [54]. Since this discussion is not yet settled, here we will consider the  $Y(4260)$  as one unique state *i.e.*, the lowest mass state observed in [54].

Since the mass of the  $Y(4260)$  is higher than the  $D^{(*)}\bar{D}^{(*)}$  threshold, if it was a normal  $c\bar{c}$  charmonium state, it would decay mainly to  $D^{(*)}\bar{D}^{(*)}$ . However, the observed  $Y$  state does not match the peaks in  $e^+e^- \rightarrow D^{(*)\pm}D^{(*)\mp}$  cross sections measured by Belle [214] and BaBar [215, 216]. Besides, the  $\psi(3S)$ ,  $\psi(2D)$  and  $\psi(4S)$   $c\bar{c}$  states have been assigned to the well established  $\psi(4040)$ ,  $\psi(4160)$ , and  $\psi(4415)$  mesons respectively, and the prediction from quark models for the  $\psi(3D)$  state is 4.52 GeV. Therefore, the mass of the  $Y(4260)$  is not consistent with any of the  $1^{--} c\bar{c}$  states [3, 4, 7].

#### 4.1.1. Theoretical explanations for $Y(4260)$

There are many theoretical interpretations for the  $Y(4260)$ : tetraquark state [15], hadronic molecule of  $D_1D$  or  $D_0D^*$  [217, 218],  $\chi_{c1}\omega$  [219],  $\chi_{c1}\rho$  [220],  $J/\psi f_0(980)$  [221], a hybrid charmonium state [222], a charm baryonium [223], a cusp [224–226], etc. Within the available experimental information, none of these suggestions can be completely ruled out. However, most of the QCDSR calculations can not explain the mass of the  $Y(4260)$  supposing it to be a tetraquark state [92], or a  $D_1D$  or  $D_0D^*$  hadronic molecule [92], or a  $J/\psi f_0(980)$  molecular state [103]. There is only one exception where the mass of the  $Y(4260)$  can be explained as a tetraquark state in a QCDSR calculation [227].

In the next subsections we will show that it is possible to explain not only the mass, but also the decay width of the  $Y(4260)$ , in a QCDSR calculation, if one uses a mixture of a  $J/\psi$  and a  $[cq\bar{c}\bar{q}]$  tetraquark currents [105], in the same way as discussed in Sec.3.3 for the  $X(3872)$ .

#### 4.1.2. QCDSR calculations for the $Y(4260)$ mass

In Ref. [105] the  $Y(4260)$  was considered as a mixed charmonium-tetraquark state and the QCDSR method was used to study both its mass and decay width. For the charmonium part, the conventional vector current was used:

$$j_\mu^{(2)} = \bar{c}_a(x)\gamma_\mu c_a(x), \quad (134)$$

while the tetraquark part is implemented as [92]:

$$j_\mu^{(4)} = \frac{\epsilon_{abc}\epsilon_{dec}}{\sqrt{2}} \left[ \left( q_a^T(x) C \gamma_5 c_b(x) \right) \left( \bar{q}_d(x) \gamma_\mu \gamma_5 C \bar{c}_e^T(x) \right) + \left( q_a^T(x) C \gamma_5 \gamma_\mu c_b(x) \right) \left( \bar{q}_d(x) \gamma_5 C \bar{c}_e^T(x) \right) \right]. \quad (135)$$

As in Refs. [96, 204], we define the normalized two-quark current as

$$j_\mu^{(2)} = \frac{1}{\sqrt{2}} \langle \bar{q}q \rangle j_\mu^{(2)}, \quad (136)$$

and from these two currents we build the mixed charmonium-tetraquark  $J^{PC} = 1^{--}$  current for the  $Y(4260)$  state:

$$j_\mu(x) = \sin(\theta) j_\mu^{(4)}(x) + \cos(\theta) j_\mu^{(2)}(x). \quad (137)$$

As usual, the phenomenological side is evaluated by inserting, in the two-point correlator, a complete set of intermediate states with  $1^{--}$  quantum numbers. In such a case, the coupling of the vector state  $Y$  to the current in Eq. (137) is parametrized through the coupling parameter  $\lambda_Y$ :

$$\langle 0 | j_\mu(x) | Y \rangle = \lambda_Y \epsilon_\mu, \quad (138)$$

where  $\epsilon_\mu$  is the polarization vector of  $Y(4260)$ . Using Eq. (138), we can write the phenomenological side as

$$\Pi_{\mu\nu}^{phen}(q) = \frac{\lambda_Y^2}{m_Y^2 - q^2} \left( g_{\mu\nu} - \frac{q_\mu q_\nu}{q^2} \right) + \dots \quad (139)$$

where  $m_Y$  is the mass of the  $Y$  state and the dots, in the second term in the RHS of Eq. (139), denotes the higher resonance contributions which will be parametrized, as usual, through the introduction of the continuum threshold parameter  $s_0$  [128]. In the OPE side, we work at leading order in  $\alpha_s$  in the operators and we consider the contributions from the condensates up to dimension eight. Although we consider only a part of the dimension 8 condensates (related to the quark condensate times the mixed condensate), in Ref. [100] it was shown that this is the most important

dimension 8 condensate contribution. Considering the current in Eq. (137), the correlator in the OPE side can be written as

$$\Pi_{\mu\nu}(q) = \frac{1}{2} \langle \bar{q}q \rangle^2 \cos^2 \theta \Pi_{\mu\nu}^{22}(q) + \sin^2 \theta \Pi_{\mu\nu}^{44}(q) + \frac{1}{\sqrt{2}} \langle \bar{q}q \rangle \sin \theta \cos \theta \left[ \Pi_{\mu\nu}^{24}(q) + \Pi_{\mu\nu}^{42}(q) \right], \quad (140)$$

with

$$\Pi_{\mu\nu}^{ij}(q) = i \int d^4x e^{iq \cdot x} \langle 0 | T [j_\mu^i(x) j_\nu^{j\dagger}(0)] | 0 \rangle. \quad (141)$$

In this way,  $\Pi_{\mu\nu}^{22}(q)$  and  $\Pi_{\mu\nu}^{44}(q)$  are the correlation functions of the  $J/\psi$  meson and  $[cq\bar{c}\bar{q}]$  tetraquark state, respectively. After making a Borel transform on both sides of the sum rule, and transferring the continuum contributions to the OPE side, the sum rule, in the  $g_{\mu\nu}$  structure, can be written as:

$$\lambda_Y^2 e^{-m_Y^2/M^2} = \frac{1}{2} \langle \bar{q}q \rangle^2 \cos^2 \theta \Pi^{22}(M^2) + \sin^2 \theta \Pi^{44}(M^2) + \frac{1}{\sqrt{2}} \langle \bar{q}q \rangle \sin \theta \cos \theta \left[ \Pi^{24}(M^2) + \Pi^{42}(M^2) \right]. \quad (142)$$

The expressions for the invariant functions,  $\Pi^{ij}(M^2)$ , in Eq. (142) are given in Ref. [105]. In Fig. 14a, we plot the relative contributions of all the terms in the OPE side. We have used  $\sqrt{s_0} = 4.70$  GeV and  $\theta = 53^\circ$ . For others  $\theta$  values outside the range  $52.5^\circ \leq \theta \leq 53.5^\circ$ , we do not have a good OPE convergence. From this figure we see that the contribution of the dimension-8 condensates is smaller than 15% of the total contribution for values of  $M^2 \geq 2.40$  GeV<sup>2</sup>, indicating a good OPE convergence. Therefore, we fix the lower value of  $M^2$  in the sum rule window as:  $M_{min}^2 = 2.40$  GeV<sup>2</sup>. In Fig. 14b, we show a comparison between the pole and continuum contributions. It is clear that the pole contribution is equal to the continuum contribution for  $M^2 = 2.90$  GeV<sup>2</sup>. Therefore, for  $\sqrt{s_0} = 4.70$  GeV<sup>2</sup> and  $\theta = 53^\circ$  the Borel window is:  $2.40 \leq M^2 \leq 2.90$  GeV<sup>2</sup>. The ground state mass is shown, as a function of  $M^2$ , in Fig. 14c. From this figure we see that there is a very good Borel stability in the determined Borel window, which is represented as crosses in Fig. 14c. Varying the value of the continuum threshold in the range  $\sqrt{s_0} = 4.70 \pm 0.10$  GeV, the mixing angle in the range  $\theta = (53.0 \pm 0.5)^\circ$ , and the other parameters as indicated in Table 2, the mass obtained in Ref. [105] is:

$$m_Y = (4.26 \pm 0.13) \text{ GeV}, \quad (143)$$

which is in excellent agreement with the experimental  $Y(4260)$  mass. Once the mass is determined, its value can be used in Eq. (142) to estimate the meson-current coupling parameter, defined in Eq. (138). Using the same values of  $s_0$ ,  $\theta$  and Borel window one gets [105]:

$$\lambda_Y = (2.00 \pm 0.23) \times 10^{-2} \text{ GeV}^5. \quad (144)$$

#### 4.1.3. $Y(4260) \rightarrow J/\psi \pi \pi$ decay width

To estimate the decay width of the process  $Y(4260) \rightarrow J/\psi \pi^+ \pi^-$ , it was assumed in Ref. [105] that the two pions in the final state come from the  $\sigma$  meson. The coupling constant, associated with the vertex  $YJ/\psi\sigma$ , is evaluated using the three-point correlator

$$\Pi_{\mu\nu}(p, p', q) = \int d^4x d^4y e^{ip' \cdot x} e^{iq \cdot y} \langle 0 | T \{ j_\mu^\psi(x) j_\nu^\sigma(y) j_\nu^{Y\dagger}(0) \} | 0 \rangle. \quad (145)$$

with  $p = p' + q$ . The interpolating fields appearing in Eq. (145) are the currents for  $J/\psi$ ,  $\sigma$  and  $Y(4260)$ , respectively. The currents for  $J/\psi$  and  $Y(4260)$  are defined by Eqs. (134) and (137). For the  $\sigma$  meson, we have

$$j^\sigma = \frac{1}{\sqrt{2}} (\bar{u}_a(x) u_a(x) + \bar{d}_a(x) d_a(x)). \quad (146)$$

In order to evaluate the phenomenological side of the three-point correlator we insert, in Eq. (145), intermediate states for  $Y$ ,  $J/\psi$  and  $\sigma$ . Using the definitions:

$$\begin{aligned} \langle 0 | j_\mu^\psi | J/\psi(p') \rangle &= m_\psi f_\psi \epsilon_\mu(p'), \\ \langle 0 | j^\sigma | \sigma(q) \rangle &= A_\sigma, \\ \langle Y(p) | j_\nu^Y | 0 \rangle &= \lambda_Y \epsilon_\nu^*(p), \end{aligned} \quad (147)$$

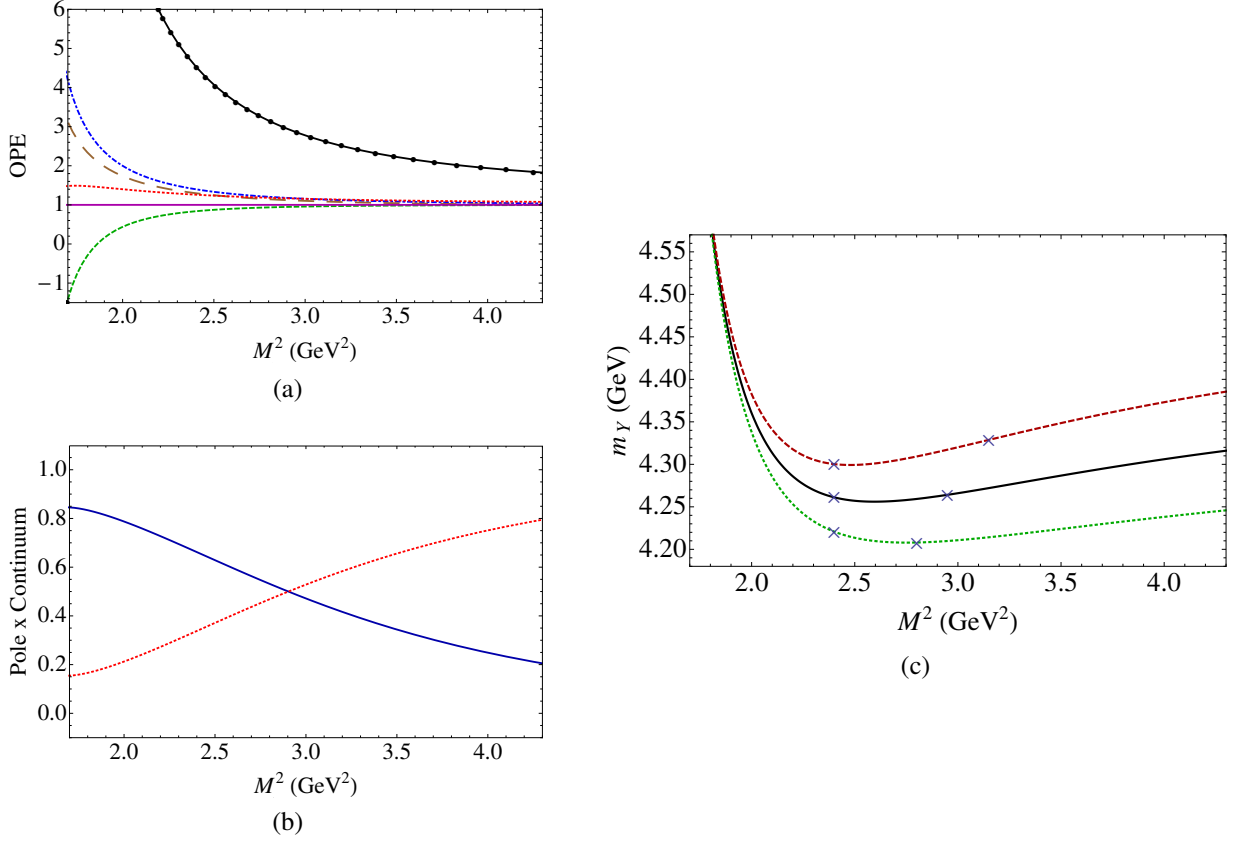


Figure 14: Sum rule calculation for the  $Y(4260)$  state. a) The OPE convergence in the region  $2.0 \leq M_B^2 \leq 6.0$   $\text{GeV}^2$  for  $\sqrt{s_0} = 4.70$   $\text{GeV}$ . We plot the relative contributions, starting with the perturbative contribution (line with circles), and the other lines represent the relative contribution after adding the next term in the expansion:  $+\langle\bar{q}q\rangle$  (dot-dashed line),  $+\langle g_s^2 G^2\rangle$  (long-dashed line),  $+\langle\bar{q}Gq\rangle$  (dotted line),  $+\langle\bar{q}q\rangle^2$  (dashed line) and  $\langle\bar{q}q\rangle\langle\bar{q}Gq\rangle$  (solid line). b) The pole contribution (solid line) and the continuum contribution (dotted line), for  $\sqrt{s_0} = 4.70$   $\text{GeV}$ . c) The mass as a function of the sum rule parameter  $M_B^2$  for  $\sqrt{s_0} = 4.60$   $\text{GeV}$  (dotted line),  $\sqrt{s_0} = 4.70$   $\text{GeV}$  (solid line),  $\sqrt{s_0} = 4.80$   $\text{GeV}$  (long-dashed line). The crosses indicate the valid Borel window. Figures taken from Ref. [105].

we obtain the following relation:

$$\Pi_{\mu\nu}^{phen}(p, p', q) = \frac{\lambda_Y m_\psi f_\psi A_\sigma g_{Y\psi\sigma}(q^2)}{(p^2 - m_Y^2)(p'^2 - m_\psi^2)(q^2 - m_\sigma^2)} \left[ (p' \cdot p) g_{\mu\nu} - p'_\nu q_\mu - p'_\nu p'_\mu \right] + \dots, \quad (148)$$

where the dots stand for the contribution of all possible excited states. The form factor,  $g_{Y\psi\sigma}(q^2)$ , is defined by the generalization of the on-mass-shell matrix element,  $\langle J/\psi \sigma | Y \rangle$ , for an off-shell  $\sigma$  meson [105]:

$$\langle J/\psi \sigma | Y \rangle = g_{Y\psi\sigma}(q^2) (p' \cdot p \epsilon^*(p') \cdot \epsilon(p) - p' \cdot \epsilon(p) p \cdot \epsilon^*(p')). \quad (149)$$

In the OPE side, one works at leading order in  $\alpha_s$ , and considers the condensates up to dimension five. In Ref. [105] the authors have chosen to work with the  $p'_\nu q_\mu$  structure, since it has more terms contributing to the OPE. Taking the limit  $p^2 = p'^2 = -P^2$  and doing the Borel transform such as  $P^2 \rightarrow M^2$ , one gets the following expression for the sum rule in the structure  $p'_\nu q_\mu$ :

$$\frac{\lambda_Y A_\sigma m_\psi f_\psi}{(m_Y^2 - m_\psi^2)} g_{Y\psi\sigma}(Q^2) \left( e^{-m_\psi^2/M^2} - e^{-m_Y^2/M^2} \right) + B(Q^2) e^{-s_0/M^2} = (Q^2 + m_\sigma^2) \Pi^{OPE}(M^2, Q^2) \quad (150)$$



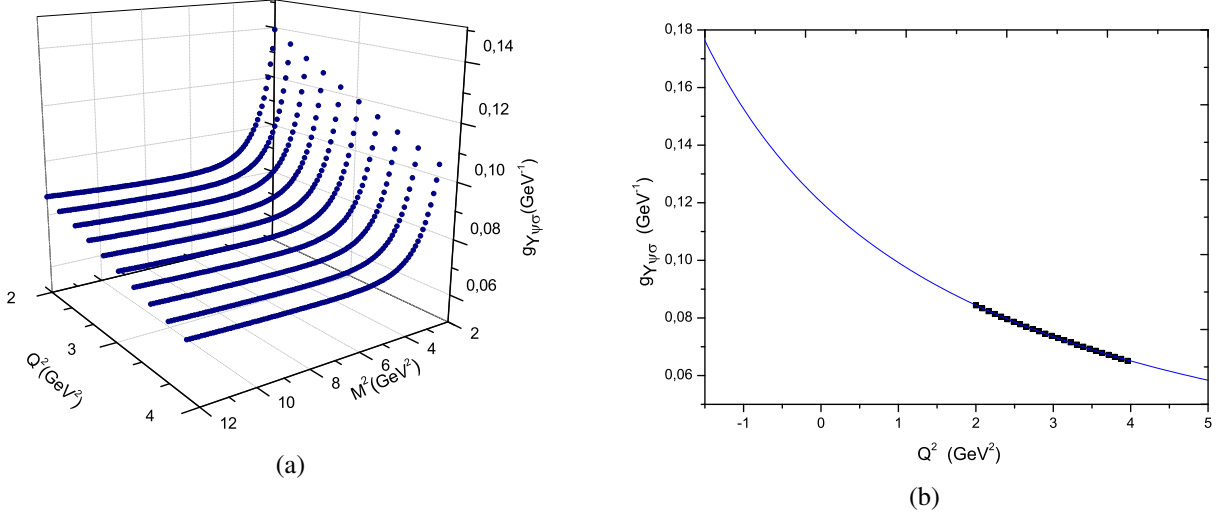


Figure 15: a)  $g_{Y\psi\sigma}(Q^2)$  as a function of both  $Q^2$  and  $M^2$ . b) QCDSR results for  $g_{Y\psi\sigma}(Q^2)$ , as a function of  $Q^2$ , for  $\sqrt{s_0} = 4.76$  GeV and  $M^2 = 8$  GeV<sup>2</sup> (squares). The solid line gives the parametrization of the QCDSR results (see Eq. (152)). Figures taken from Ref. [105].

where  $Q^2 = -q^2$ , and  $B(Q^2)$  gives the contribution to the pole-continuum transitions, as discussed in Sec. 2.7.3. The correlator  $\Pi^{OPE}(M^2, Q^2)$  is given by [105]:

$$\Pi^{OPE}(M^2, Q^2) = \frac{\sin \theta}{3 \cdot 2^4 \sqrt{2} \pi^2} \int_0^1 d\alpha e^{\frac{-m_c^2}{\alpha(1-\alpha)M^2}} \left[ \frac{m_c \langle \bar{q} G q \rangle}{Q^2} \left( \frac{1 - 2\alpha(1-\alpha)}{\alpha(1-\alpha)} \right) - \frac{\langle g_s^2 G^2 \rangle}{2^5 \pi^4} \right]. \quad (151)$$

The  $\sin \theta$  in Eq. (151) indicates that only the tetraquark part of the current in Eq. (137) contributes to the OPE side. In fact, the charmonium part of the current gives only disconnected diagrams that are discarded in the calculations. In Eq. (150), the values of the mass and decay constant of  $J/\psi$  and  $\sigma$  mesons are:  $m_\psi = 3.1$  GeV,  $f_\psi = 0.405$  GeV [22], and  $m_\sigma = 0.478$  GeV [228]. The parameters  $\lambda_Y$  and  $A_\sigma$  represent, respectively, the coupling of the  $Y$  and  $\sigma$  states to the currents defined in Eq. (138) and (147). The value of  $\lambda_Y$  is given in Eq. (144), while  $A_\sigma$  was determined in Ref. [229] and its value is  $A_\sigma = 0.197$  GeV<sup>2</sup>. To obtain  $g_{Y\psi\sigma}(Q^2)$  one uses Eq. (150) and its derivative, with respect to  $M^2$ , to eliminate  $B(Q^2)$  from these equations. In Fig. 15a  $g_{Y\psi\sigma}(Q^2)$  is shown as a function of both  $M^2$  and  $Q^2$ . From Fig. 15a we see that, in the region  $7.0 \leq M^2 \leq 10.0$  GeV<sup>2</sup>, the form factor is very stable as a function of  $M^2$ , for all values of  $Q^2$ . The squares in Fig. 15b show the  $Q^2$  dependence of  $g_{Y\psi\sigma}(Q^2)$ , obtained for  $M^2 = 8.0$  GeV<sup>2</sup>. For other values of the Borel mass, in the range  $7.0 \leq M^2 \leq 10.0$  GeV<sup>2</sup>, the results are equivalent. It is possible to fit the QCDSR results for  $g_{Y\psi\sigma}(Q^2)$  using a monopole form:

$$g_{Y\psi\sigma}(Q^2) = \frac{g_1}{g_2 + Q^2}, \quad (152)$$

with

$$g_1 = (0.58 \pm 0.04) \text{ GeV}; \quad g_2 = (4.71 \pm 0.06) \text{ GeV}^2, \quad (153)$$

as shown by the solid line in Fig. 15b. The coupling constant,  $g_{Y\psi\sigma}$ , is given by using  $Q^2 = -m_\sigma^2$  in Eq. (152). Then one gets [105]:

$$g_{Y\psi\sigma} = g_{Y\psi\sigma}(-m_\sigma^2) = (0.13 \pm 0.01) \text{ GeV}^{-1}. \quad (154)$$

The error in the coupling constant given above comes from variations in  $s_0$  in the range  $4.6 \leq s_0 \leq 4.8$  GeV<sup>2</sup>, and in the mixing angle  $52.5^\circ \leq \theta \leq 53.5^\circ$ .

The decay width for the process  $Y(4260) \rightarrow J/\psi \sigma \rightarrow J/\psi \pi \pi$  in the narrow width approximation is given by [105]:

$$\frac{d\Gamma}{ds}(Y \rightarrow J/\psi \pi \pi) = \frac{|\mathcal{M}|^2}{8\pi m_Y^2} \left( \frac{m_Y^2 - m_\psi^2 + s}{2m_Y^2} \right) \left( \frac{\Gamma_\sigma(s) m_\sigma}{2m_Y \pi} \right) \frac{\sqrt{\lambda(m_Y^2, m_\psi^2, s)}}{(s - m_\sigma^2)^2 + (m_\sigma \Gamma_\sigma(s))^2}, \quad (155)$$

where  $\lambda(a, b, c) = a^2 + b^2 + c^2 - 2ab - 2ac - 2bc$ , and  $\Gamma_\sigma(s)$  is the  $s$ -dependent width of an off-shell  $\sigma$  meson [228]:

$$\Gamma_\sigma(s) = \Gamma_{0\sigma} \sqrt{\frac{\lambda(s, m_\pi^2, m_\pi^2)}{\lambda(m_Y^2, m_\pi^2, m_\pi^2)}} \frac{m_Y^2}{s}. \quad (156)$$

Notice that  $\Gamma_{0\sigma}$  in Eq. (156) is the experimental value for the decay of the  $\sigma$  meson into two pions. Its value is  $\Gamma_{0\sigma} = (0.324 \pm 0.042 \pm 0.021)$  GeV [228]. The squared invariant amplitude can be obtained from the matrix element in Eq. (149):

$$|\mathcal{M}|^2 = g_{Y\psi\sigma}^2(s) f(m_Y, m_\psi, s), \quad (157)$$

where  $g_{Y\psi\sigma}(s)$  is the form factor in the vertex  $YJ/\psi\sigma$ , given in Eq. (152) using  $s = -Q^2$ , and

$$f(m_Y, m_\psi, s) = \frac{1}{3} \left( m_Y^2 m_\psi^2 + \frac{1}{2} (m_Y^2 + m_\psi^2 - s)^2 \right). \quad (158)$$

Therefore, the decay width for the process  $Y(4260) \rightarrow J/\psi\pi\pi$  is given by

$$\Gamma = \frac{m_\sigma}{32\pi^2 m_Y^5} \int_{(2m_\pi)^2}^{(m_Y - m_\psi)^2} ds g_{Y\psi\sigma}^2(s) \Gamma_\sigma(s) (m_Y^2 - m_\psi^2 + s) \sqrt{\lambda(m_Y^2, m_\psi^2, s)} \left( \frac{f(m_Y, m_\psi, s)}{(s - m_\sigma^2)^2 + (m_\sigma \Gamma_\sigma(s))^2} \right). \quad (159)$$

Taking variations in  $s_0$  and  $\theta$  in the same intervals given above, we obtain, from Eqs. (154)-(159), the following value for the decay width [105]:

$$\Gamma_\sigma(Y \rightarrow J/\psi \pi\pi) = (1.0 \pm 0.2) \text{ MeV}. \quad (160)$$

The decay channel  $Y(4260) \rightarrow J/\psi \pi\pi$  can also occur through the formation of  $f_0(980)$  in the intermediate state. Therefore, we have to determine also the coupling constant associated with the vertex  $Y \rightarrow J/\psi f_0(980)$ . For this purpose, we consider the  $f_0(980)$  meson as a quark-antiquark state with a mixture of strange and light components. In this case, the interpolating current for  $f_0(980)$  is given by

$$j^{f_0} = \cos(\alpha) \bar{s}s + \frac{1}{\sqrt{2}} \sin(\alpha) (\bar{u}u + \bar{d}d). \quad (161)$$

Using Eq. (159) with the  $f_0(980)$  meson parameters instead of the ones for  $\sigma$ , *i.e.*, [22]:  $m_{f_0} = (990 \pm 20)$  MeV,  $\Gamma_{0f_0} = (40 - 100)$  MeV and taking the variations  $4.6 \leq \sqrt{s_0} \leq 4.8$  GeV and  $52.3^\circ \leq \theta \leq 53.5^\circ$ , we obtain:

$$\Gamma_{f_0}(Y \rightarrow J/\psi \pi\pi) = (3.1 \pm 0.2) \text{ MeV} \quad (162)$$

leading to the following decay width into this channel:

$$\Gamma(Y \rightarrow J/\psi \pi\pi) = (4.1 \pm 0.6) \text{ MeV}, \quad (163)$$

which is consistent with the lower bound given in Ref. [8]:  $\Gamma(Y \rightarrow J/\psi \pi\pi) > 508$  keV at 90% CL.

Assuming that the two pions in the final state of the decay  $Y \rightarrow J/\psi \pi\pi$  come only from the  $\sigma$  and  $f_0(980)$  scalar mesons intermediate states, we obtain a value for the width  $\Gamma_{Y \rightarrow J/\psi \pi\pi} \approx (4.1 \pm 0.6)$  MeV, which is much smaller than the total experimental width:  $\Gamma_{exp} \approx (55 \pm 19)$  MeV [22]. This can be interpreted as an indication that the main decay channel of the  $Y(4260)$  should be into two  $D$  mesons. The possibility that the main decay mode of the  $Y(4260)$  is into two  $D$  mesons corroborates the interpretation that the  $Y(4260)$  consists of two resonances, as suggested in Ref. [71]. If the main component of the  $Y(4260)$  is the lower mass resonance, that is called  $Y(4220)$ , this component indeed decays into  $\pi^+ D^0 D^{*-}$  [71]. Therefore, we conclude that it is possible to explain the  $Y(4260)$  state as a mixed charmonium-tetraquark state.

#### 4.1.4. $Y(4260)$ production in $B$ decays

The same mixed current between the  $J/\psi$  charmonium and a tetraquark state, proposed in Ref. [105], was used in Ref. [112] to estimate the  $Y(4260)$  production in the process  $B^- \rightarrow Y(4260) K^-$ . The experimental upper limit on the branching fraction for such a production from  $B$  meson decay has been reported by the BaBar Collaboration [230], with 95% C.L.:

$$\mathcal{B}_Y < 2.9 \times 10^{-5} \quad (164)$$

where  $\mathcal{B}_Y \equiv \mathcal{B}(B^- \rightarrow K^- Y(4260), Y(4260) \rightarrow J/\psi \pi^+ \pi^-)$ .

The process  $B \rightarrow Y(4260) K$  occurs via weak decay of the  $b$  quark, while the  $u$  quark is a spectator. The  $Y(4260)$  state, as a mixed state of tetraquark and charmonium, interacts via the  $\bar{c}c$  component of the weak current. As discussed in Sec. 3.3.4, in an effective theory the Hamiltonian describing the weak interaction can be written in terms of a four-quark interaction vertex with an effective four quark operator  $\mathcal{O}_2 = (\bar{c}\Gamma_\mu c)(\bar{s}\Gamma^\mu b)$ , with a  $V-A$  structure  $\Gamma_\mu = \gamma_\mu(1-\gamma_5)$ . The interaction can be factorized into two matrix elements, giving the following decay amplitude for the process:

$$\mathcal{M} = i \frac{G_F}{\sqrt{2}} V_{cb} V_{cs}^* \left( C_2 + \frac{C_1}{3} \right) \langle B(p) | J_\mu^W | K(p') \rangle \langle Y(q) | J^{\mu(\bar{c}c)} | 0 \rangle, \quad (165)$$

where  $p = p' + q$  and  $J_\mu^W, J^{\mu(\bar{c}c)}$  are given in Eq. (115). Following Ref. [101], the matrix elements in Eq. (165) are parametrized as:

$$\langle Y(q) | J_\mu^{\bar{c}c} | 0 \rangle = \lambda_W \epsilon_\mu^*(q), \quad (166)$$

and

$$\langle B(p) | J_\mu^W | K(p') \rangle = f_+(q^2)(p_\mu + p'_\mu) + f_-(q^2)(p_\mu - p'_\mu). \quad (167)$$

The parameter  $\lambda_W$  in Eq. (166) gives the coupling between the current  $J_\mu^{\bar{c}c}$  and the  $Y$  state. The form factors  $f_\pm(q^2)$  describe the weak transition  $B \rightarrow K$ . Hence we can see that the factorization of the matrix element describes the decay as two separated sub-processes. The decay width for the process  $B^- \rightarrow Y(4260)K^-$  is given by

$$\Gamma(B \rightarrow YK) = \frac{|\mathcal{M}|^2}{16\pi m_B^3} \sqrt{\lambda(m_B^2, m_K^2, m_Y^2)}, \quad (168)$$

with  $\lambda(x, y, z) = x^2 + y^2 + z^2 - 2xy - 2xz - 2yz$ . The squared invariant amplitude can be obtained from Eq. (165), using Eqs. (166) and (167):

$$|\mathcal{M}|^2 = \frac{G_F^2}{2m_Y^2} |V_{cb} V_{cs}|^2 \left( C_2 + \frac{C_1}{3} \right)^2 \lambda(m_B^2, m_K^2, m_Y^2) \lambda_W^2 f_+^2. \quad (169)$$

The form factor  $f_+(Q^2)$  was determined in Sec. 3.3.4 and is given by Eq. (131):

$$f_+(Q^2) = \frac{(17.55 \pm 0.04) \text{ GeV}^2}{(105.0 \pm 1.8) \text{ GeV}^2 + Q^2}.$$

For the decay width calculation, we need the value of the form factor at  $Q^2 = -m_Y^2$ , where  $m_Y$  is the mass of the  $Y(4260)$  meson. Using  $m_Y = (4251 \pm 9) \text{ MeV}$  [22] we get:

$$f_+(Q^2 = -m_Y^2) = 0.206 \pm 0.004. \quad (170)$$

The parameter  $\lambda_W$  can also be determined using the QCDSR approach for the two-point correlator as done in Sec. 3.3.4

$$\Pi_{\mu\nu}(q) = i \int d^4y e^{iq \cdot y} \langle 0 | T [J_\mu^Y(y) J_\nu^{\bar{c}c}(0)] | 0 \rangle, \quad (171)$$

where the current  $J_\nu^{\bar{c}c}$  is defined in Eq. (115). For the  $Y(4260)$  state we consider the mixed charmonium-tetraquark current given in Eq. (137). The mixing angle,  $\theta$ , was determined in Ref. [105] to be:  $\theta = (53.0 \pm 0.5)^\circ$ .

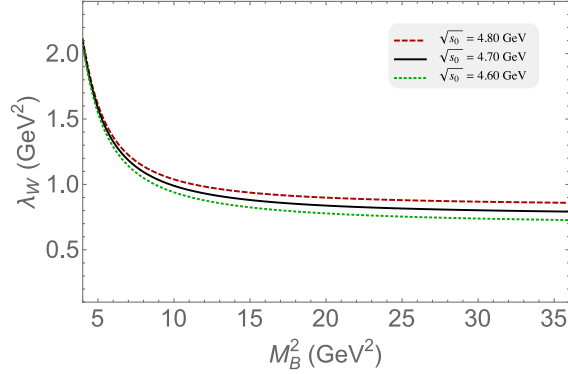


Figure 16: The coupling parameter  $\lambda_W$  as a function of  $M^2$  for different values of the continuum threshold. Figure taken from Ref. [112].

The phenomenological side of the SR is obtained by considering intermediate  $Y$  states:

$$\Pi_{\mu\nu}^{phen}(q) = \frac{i}{q^2 - m_Y^2} \langle 0 | J_\mu^Y | Y(q) \rangle \langle Y(q) | J_\nu^{(\bar{c}c)} | 0 \rangle = \frac{i\lambda_Y\lambda_W}{Q^2 + m_Y^2} \left( g_{\mu\nu} - \frac{q_\mu q_\nu}{m_Y^2} \right) \quad (172)$$

where the definition in Eq. (166) was used and

$$\langle 0 | J_\mu^Y | Y(q) \rangle = \lambda_Y \epsilon_\mu(q). \quad (173)$$

The parameter  $\lambda_Y$ , that defines the coupling between the current  $J_\mu^Y$  and the  $Y$  meson, was determined in Sec. 4.1.2:  $\lambda_Y = (2.00 \pm 0.23) \times 10^{-2} \text{ GeV}^5$ .

After performing the Borel transform in both sides of the sum rule one gets from the  $g_{\mu\nu}$  structure:

$$\lambda_W \lambda_Y e^{-m_Y^2/M^2} = \frac{1}{\sqrt{2}} \sin \theta \Pi^{4,2}(M^2) + \frac{1}{\sqrt{2}} \langle \bar{q}q \rangle \cos \theta \Pi^{2,2}(M^2) \quad (174)$$

where the invariant functions,  $\Pi^{2,2}(M^2)$  and  $\Pi^{4,2}(M^2)$ , are given in Ref. [112]. The calculation of the coupling parameter  $\lambda_W$  was done using the same values for the masses and QCD condensates as in Ref. [105], values which are listed in Table 2. To be consistent with the calculation of  $\lambda_Y$  we also use the same region in the threshold parameter  $s_0$  as in Ref. [105]:  $\sqrt{s_0} = (4.70 \pm 0.10) \text{ GeV}$ . As one can see in Fig. 16, the region of  $M^2$ -stability is given by  $(8.0 \leq M^2 \leq 25.0) \text{ GeV}^2$ . Taking into account the variation in the Borel mass parameter, in the continuum threshold, in the quark condensate, in the coupling constant  $\lambda_Y$  and in the mixing angle  $\theta$ , the result for the  $\lambda_W$  parameter is:

$$\lambda_W = (0.90 \pm 0.32) \text{ GeV}^2. \quad (175)$$

The decay width in Eq. (168) can be evaluated using the values of  $f_+(-M_Y^2)$  and  $\lambda_W$ , determined in Eqs. (170) and (175) respectively. The branching ratio is evaluated dividing the result by the total width of the  $B$  meson,  $\Gamma_{\text{tot}} = 4.280 \times 10^{-4} \text{ eV}$  [112]:

$$\mathcal{B}(B \rightarrow Y(4260)K) = (1.34 \pm 0.47) \times 10^{-6}, \quad (176)$$

where we have used the CKM parameters  $V_{cs} = 1.023$ ,  $V_{cb} = 40.6 \times 10^{-3}$  [22], and the Wilson coefficients  $C_1(\mu) = 1.082$ ,  $C_2(\mu) = -0.185$ , computed at  $\mu = m_b$  and  $\bar{\Lambda}_{\text{MS}} = 225 \text{ MeV}$  [231].

In order to compare the branching ratio in Eq. (176) with the branching fraction obtained experimentally in Eq. (164), we use the results found in Ref. [105]:

$$\mathcal{B}(Y(4260) \rightarrow J/\psi \pi^+ \pi^-) = (4.3 \pm 0.9) \times 10^{-2}, \quad (177)$$

and then, considering the uncertainties, we estimate  $\mathcal{B}_Y > 3.0 \times 10^{-8}$ . However, it is important to notice that the authors in Ref. [105] have considered that the two pions in the final state come only from the intermediate  $\sigma$  and  $f_0(980)$  states,

which could indicate that the result in Eq. (177) might be underestimated. In this sense, considering that the main decay channel observed for the  $Y(4260)$  state is into  $J/\psi \pi^+ \pi^-$ , we would naively expect that the branching ratio into this channel could be  $\mathcal{B}(Y(4260) \rightarrow J/\psi \pi^+ \pi^-) \sim 1.0$ , which leads to the result,  $\mathcal{B}_Y < 1.8 \times 10^{-6}$ . Therefore, we obtain an interval for the branching fraction

$$3.0 \times 10^{-8} < \mathcal{B}_Y < 1.8 \times 10^{-6}, \quad (178)$$

which is in agreement with the experimental upper limit reported by Babar Collaboration given in Eq. (164). In general the experimental evaluation of the branching fraction takes into account additional factors related to the number of reconstructed events for the final state ( $J/\psi \pi^+ \pi^- K$ ), for the reference process ( $B \rightarrow Y(4260) K$ ), and for the respective reconstruction efficiencies. However, since such information has not been provided in Ref. [230], these factors were neglected in the calculation of the branching fraction  $\mathcal{B}_Y$ . Therefore, the comparison of the result in Eq. (178) with the experimental result could be affected by these differences.

Remember that the above result was obtained by considering the mixing angle in Eq. (137) in the range  $\theta = (53.0 \pm 0.5)^\circ$ . Since there is no new free parameter analysis presented above, the result shown here strengthens the interpretation of  $Y(4260)$  as a mixture between a  $J/\psi$  charmonium and a tetraquark state.

As discussed in Ref. [101], it is not simple to determine the charmonium and the tetraquark contribution to the state described by the current in Eq. (137). From Eq. (137) one can see that, besides the  $\sin \theta$ , the  $c\bar{c}$  component of the current is multiplied by a dimensional parameter, the quark condensate, in order to have the same dimension as the tetraquark part of the current. Therefore, it is not clear that only the angle in Eq. (137) determines the percentage of each component. One possible way to evaluate the importance of each part of the current is to analyze what one would get for the production rate with each component, *i.e.*, using  $\theta = 0$  and  $90^\circ$  in Eq. (137). Doing this we get respectively for the pure tetraquark and pure charmonium:

$$\mathcal{B}(B \rightarrow Y_{\text{tetra}} K) = (1.25 \pm 0.23) \times 10^{-6}, \quad (179)$$

$$\mathcal{B}(B \rightarrow Y_{c\bar{c}} K) = (1.14 \pm 0.20) \times 10^{-5}. \quad (180)$$

Comparing the results for the pure states with the one for the mixed state in Eq. (176), we can see that the branching ratio for the pure tetraquark is one order of magnitude smaller, while for the pure charmonium it is larger. From these results we see that the  $c\bar{c}$  part of the state plays a very important role in the determination of the branching ratio. On the other hand, in the decay  $Y \rightarrow J/\psi \pi^+ \pi^-$ , the width obtained in our approach for a pure  $c\bar{c}$  state is [105]:

$$\Gamma(Y_{c\bar{c}} \rightarrow J/\psi \pi \pi) = 0, \quad (181)$$

and, therefore, the tetraquark part of the state is the only one that contributes to this decay, playing an essential role in the determination of this decay width. Therefore, although we can not determine the percentages of the  $c\bar{c}$  and the tetraquark components in the  $Y(4260)$ , we may say that both components are extremely important, and that, in our approach, it is not possible to explain all the experimental data about the  $Y(4260)$  with only one component.

#### 4.2. Remarks on $Y(4220)$

As discussed above, recently, the BESIII Collaboration has announced the precise measurement of the production cross section for  $e^+ e^- \rightarrow J/\psi \pi^+ \pi^-$  [54]. The results show two resonances with masses around 4220 MeV and 4320 MeV. The mass of the lower resonance is consistent with the prediction of the  $D\bar{D}_1(2420)$  molecular model [232] and is also consistent with the  $Y(4260)$  mass [54]. Furthermore, a  $Y(4220)$  resonance has also been reported by the BESIII collaboration in the cross-section measurements of  $e^+ e^- \rightarrow \omega \chi_{c0}$  [68],  $e^+ e^- \rightarrow h_c \pi^+ \pi^-$  [69],  $e^+ e^- \rightarrow \psi(2S) \pi^+ \pi^-$  [70], and  $e^+ e^- \rightarrow \pi^+ D^0 D^{*-}$  [71]. It is important to notice that the cross section of  $e^+ e^- \rightarrow \pi^+ D^0 D^{*-}$  was first measured by the Belle Collaboration using ISR events [233], with no evidence for the presence of charmonium-like states in this channel. On the other hand, the results found by the BESIII Collaboration in Ref. [71] can be the first experimental evidence for open-charm production associated with the  $Y$  states. The authors in Ref. [68] argue that the parameters found for the  $Y(4220)$  are inconsistent with those obtained for the  $Y(4260)$  state. However the authors in Ref. [54] found the parameters for the state with mass around 4220 MeV consistent with those for the  $Y(4260)$ .

In the previous sections we have evaluated a sum rule with a mixed charmonium-tetraquark current to describe the  $Y(4260)$  state. However, the uncertainty in the mass found in Eq. (143) shows that our result is also compatible with the  $Y(4220)$  mass. Indeed, the quantum numbers are the same for the  $Y(4220)$  and  $Y(4260)$  states. As noted in

Ref. [71], the measured cross section of  $e^+e^- \rightarrow \pi^+D^0D^{*-}$  at the  $Y(4220)$  peak is higher than the sum of the known hidden-charm channels. Since no other open-charm production associated with this  $Y$  state has yet been reported, the  $\pi^+D^0D^{*-}$  final state might be the dominant decay mode of the  $Y(4220)$ . In principle, this conclusion is compatible with the results found for the mixed charmonium-tetraquark current, which says that the main decay channel could be into  $D$  mesons. Therefore, the charmonium-tetraquark current given in Eq. (137) can be used to describe either the  $Y(4220)$  state or the  $Y(4260)$  state, which points in the direction that there is only one state in this mass region. More experiments are needed to settle the question if there are two, as considered in the PDG [22], or just one state, as considered in Ref. [20], in the 4220 ~ 4260 MeV mass region.

### 4.3. $Y(4360)$

Repeating the same kind of analysis that led to the observation of the  $Y(4260)$  state, the BaBar collaboration has used ISR events to study the channel  $e^+e^- \rightarrow \psi(2S)\pi^+\pi^-$  in the c.m. energy range 3.95 to 5.95 GeV. Initially, they found a broad peak at a mass around 4.34 GeV [77]. Soon after, the Belle collaboration not only confirmed the presence of such a state, but also observed another resonant state in the  $\psi(2S)\pi^+\pi^-$  mass spectrum at around 4.67 GeV [79]. More recently, the BaBar collaboration has announced improvements to their analysis and confirmed the experimental findings from the Belle collaboration of a structure near 4.65 GeV [78]. Both states were named as  $Y(4360)$  and  $Y(4660)$ , respectively. In order to investigate more precisely the properties of these two states, and for a better understanding of their nature, Belle revisited the process  $e^+e^- \rightarrow \psi(2S)\pi^+\pi^-$  using the ISR technique with a larger data sample [59]. The results improved the experimental measurements of the  $Y(4360)$  state [59]:

$$M_{Y(4360)} = (4347 \pm 6 \pm 3) \text{ MeV} \quad \text{and} \quad \Gamma_{Y(4360)} = (103 \pm 9 \pm 5) \text{ MeV}$$

Recent experiments carried out by the BESIII collaboration confirmed once more the existence of such a state and, for the first time, announced its observation in the  $J/\psi\pi\pi$  mass spectrum [54].

More recently the BESIII collaboration measured the  $e^+e^- \rightarrow \psi(2S)\pi^+\pi^-$  cross section between 4.0 to 4.6 GeV and found two resonances with mass around 4210 MeV and 4380 MeV [70]. However, instead of identifying the higher mass resonance with the  $Y(4360)$ , they stated that it could be the same state as that observed by the BESIII collaboration in the process  $e^+e^- \rightarrow \pi^+\pi^-h_c$  [69], the so-called  $Y(4390)$ . If such identification is confirmed, this measurement could be the first non confirmation for the existence of the  $Y(4360)$  state.

#### 4.3.1. Theoretical explanations for $Y(4360)$

Some interpretations for this state can be found in Refs. [7, 8, 211]. The absence of open charm decay channels (into  $D$  mesons) does not favor the conventional  $c\bar{c}$  explanation for the  $Y(4360)$  state. Although it does not seem to fit the charmonium spectrum [22], the authors in Refs. [234, 235] propose to accommodate it as a conventional  $c\bar{c}$  state, in particular as a  $3^3D_1$  state. Some possible interpretations are radial excitation of the  $Y(4260)$  state [236], charmed baryonium [237], vector hybrid charmonium [238], radial excitation of  $D^*D_1$  molecule [239] and  $[cq\bar{c}\bar{q}]$  tetraquark state [92].

#### 4.3.2. $QCDSR$ calculations for $Y(4360)$

For this study one considers the lowest dimension tetraquark current, with  $J^{PC} = 1^{--}$ , and symmetric spin distribution  $[cq]_{S=0}[\bar{c}\bar{q}]_{S=1} + [c\bar{q}]_{S=1}[\bar{c}q]_{S=0}$  [92]:

$$j_\mu = \frac{\epsilon_{abc}\epsilon_{dec}}{\sqrt{2}} \left[ (q_a^T C \gamma_5 c_b)(\bar{q}_d \gamma_\mu \gamma_5 C \bar{c}_e^T) + (q_a^T C \gamma_5 \gamma_\mu c_b)(\bar{q}_d \gamma_5 C \bar{c}_e^T) \right]. \quad (182)$$

It is interesting to notice that the structure of the current relates the spin of the charm quark with the spin of the light quarks. The sum rule calculations are done in Ref. [92] and the results are shown in Fig. 17. From Fig. 17a, we see that a good OPE convergence is obtained for  $M^2 \geq 3.2 \text{ GeV}^2$ . Again the upper limit for  $M^2$  is obtained by imposing that the pole contribution should be bigger than the continuum contribution. In Fig. 17b, we show the relative continuum (solid line) and pole (dashed line) contributions, using  $\sqrt{s_0} = 4.9 \text{ GeV}$ , from where we clearly see that the pole contribution is bigger than the continuum contribution for  $M^2 \leq 3.5 \text{ GeV}^2$ . Thus we obtain a certain stability for the

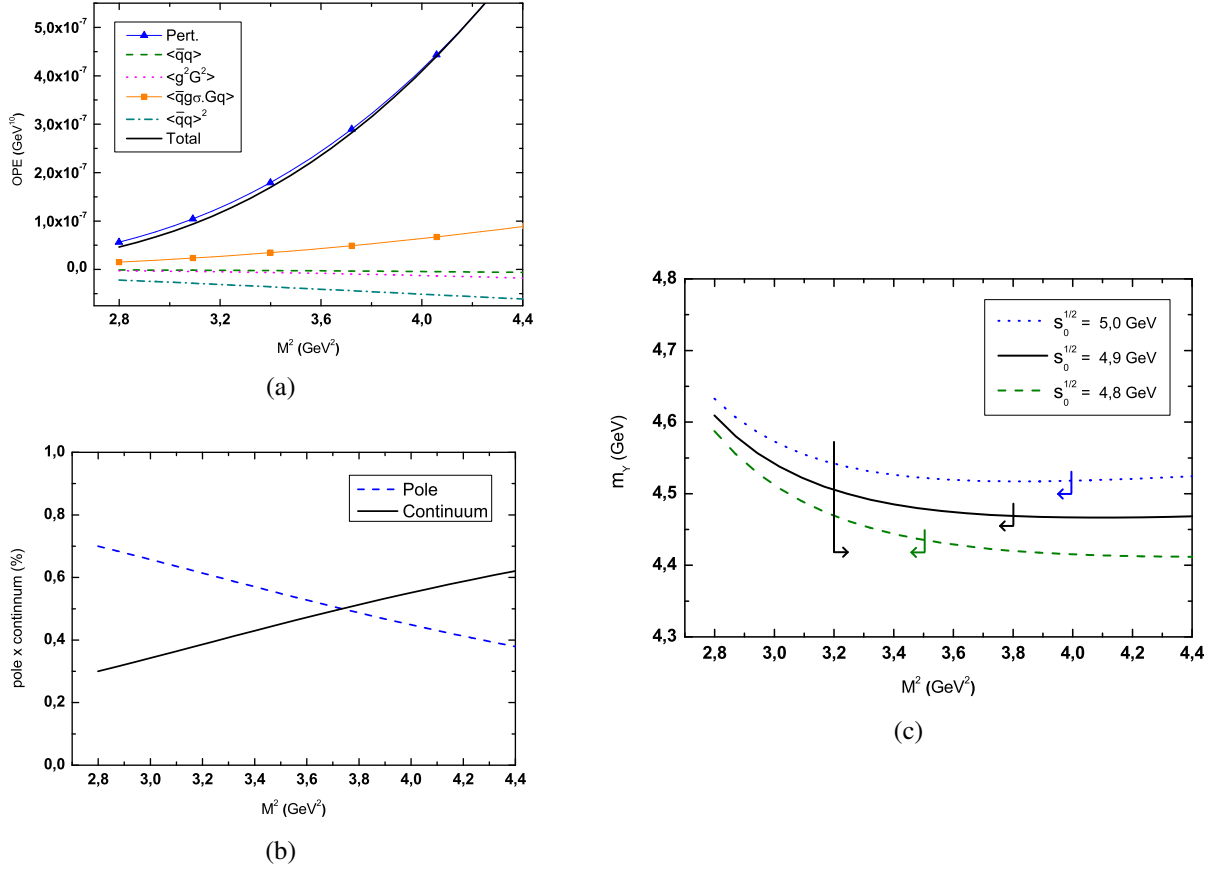


Figure 17: Sum rule calculation for the  $Y(4360)$  state. a) The OPE convergence in the region  $2.8 \leq M^2 \leq 4.4$   $\text{GeV}^2$  for  $\sqrt{s_0} = 4.9$   $\text{GeV}$ . We plot the OPE contributions starting with perturbative (line with triangles), quark condensate  $\langle \bar{q}q \rangle$  (dashed line), gluon condensate  $\langle g^2 G^2 \rangle$  (dotted line), mix condensate  $\langle \bar{q}Gq \rangle$  (line with squares), four-quark condensate  $\langle \bar{q}q \rangle^2$  (dot-dashed line) and eighth condensate  $\langle \bar{q}q \rangle \langle \bar{q}Gq \rangle$  (solid line). b) The pole contribution (dashed line) and the continuum contribution (solid line), for the  $\sqrt{s_0} = 4.90$   $\text{GeV}$ . c) The mass as a function of the sum rule parameter  $M^2$  for  $\sqrt{s_0} = 4.8$   $\text{GeV}$  (dashed line),  $\sqrt{s_0} = 4.9$   $\text{GeV}$  (solid line),  $\sqrt{s_0} = 5.0$   $\text{GeV}$  (dotted line). The arrows indicate the valid Borel Window. Figures taken from [92].

$m_Y$  mass, in the allowed sum rule window, as can be seen in Fig. 17c. Taking into account the variations on  $M^2$ ,  $s_0$ ,  $\langle \bar{q}q \rangle$  and  $m_c$  we get [92]:

$$m_Y = (4.49 \pm 0.11) \text{ GeV}, \quad (183)$$

which is bigger than the  $Y(4360)$  mass, but consistent with it considering the uncertainty. Therefore, from a sum rule point of view we can describe the  $Y(4360)$  state as a  $[cq\bar{c}\bar{q}]$  tetraquark state. However, it would be better to explore other possibilities for the  $Y(4360)$  structure, before reaching a definite conclusion about its nature.

#### 4.4. Remarks on $Y(4390)$

Besides the observation of the  $Y(4220)$  state, the BESIII Collaboration has also reported another peak resonance with a mass around 4390 MeV, in the processes  $e^+e^- \rightarrow h_c \pi^+\pi^-$  [69] and  $e^+e^- \rightarrow \psi(2S) \pi^+\pi^-$  [70]. The mass of the  $Y(4390)$  state is about 45 MeV greater than that of the  $Y(4360)$  state. As pointed out by the BESIII Collaboration, the open-charm decay channel for the  $Y(4390)$  needs more experimental evidence since the resonance parameters for this enhancement are strongly dependent on the model assumptions [71].

The experimental confirmation of the  $Y(4390)$  is very important, since the tetraquark current in Eq. (182) could be used to explain such a state. Notice that the obtained mass in Eq. (183) is closer to the  $Y(4390)$  mass than to the

$Y(4360)$  mass. However, results from QCDSR calculations are not so precise to discriminate between these two states. Therefore, we need more information from future experiments to determine if there are two, or only one state with mass in the region (4350 – 4390) MeV. If there are really two states, with more experimental information we could be able to understand which of them,  $Y(4360)$  or  $Y(4390)$ , can be better explained as a  $[cq\bar{c}\bar{q}]$  tetraquark state, with  $J^{PC} = 1^{--}$ , and symmetric spin distribution.

#### 4.5. $Y(4660)$

The most recent experimental data for the  $Y(4660)$  state was reported by BaBar and Belle collaborations [59, 78]. This state was observed in the channel  $e^+e^- \rightarrow \psi(2S)\pi^+\pi^-$  with a mass and width given by:

$$M_{Y(4660)} = (4652 \pm 10 \pm 8) \text{ MeV} \quad \text{and} \quad \Gamma_{Y(4660)} = (68 \pm 11 \pm 1) \text{ MeV}.$$

A critical information for understanding the structure of the  $Y(4660)$  state is whether the pion pair comes from a resonance state. Both collaborations state that most of the di-pion candidates are consistent with a  $f_0(980)$  decay.

##### 4.5.1. Theoretical explanations for $Y(4660)$

From the di-pion invariant mass spectra shown in Ref. [79] there is some indication that only the  $Y(4660)$  has a well-defined intermediate state consistent with  $f_0(980)$ . Due to this fact and the proximity of the mass of the  $\psi(2S)f_0(980)$  system with the mass of the  $Y(4660)$  state, in Ref. [240], the  $Y(4660)$  was considered as an  $\psi(2S)f_0(980)$  bound state. The  $Y(4660)$  was also suggested to be a baryonium state [236, 237], a conventional  $5^3S_1 c\bar{c}$  state [234], a hadro-charmonium [241] and tetraquark state [92, 242–244]. We still have no evidence for open charm decay channels for this state, which does not favor the conventional  $c\bar{c}$  explanation for the  $Y(4660)$  state.

##### 4.5.2. QCDSR calculations for $Y(4660)$

In Ref. [92] the  $Y(4660)$  was considered as a  $[cs\bar{c}\bar{s}]$  tetraquark state, with  $J^{PC} = 1^{--}$ , and symmetric spin distribution  $[cs]_{S=0}[\bar{c}\bar{s}]_{S=1} + [cs]_{S=1}[\bar{c}\bar{s}]_{S=0}$ . The lowest dimension tetraquark current is given by:

$$j_\mu = \frac{\epsilon_{abc}\epsilon_{dec}}{\sqrt{2}} \left[ (s_a^T C \gamma_5 c_b) (\bar{s}_d \gamma_\mu \gamma_5 C \bar{c}_e^T) + (s_a^T C \gamma_5 \gamma_\mu c_b) (\bar{s}_d \gamma_5 C \bar{c}_e^T) \right]. \quad (184)$$

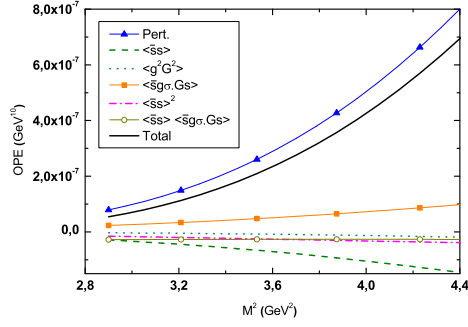
The QCDSR analysis for this state is the same as the one done for  $Y(4360)$ , with the only difference being the substitution of the light quark condensates by those related to the strange quark for the  $Y(4660)$ . The quark content in Eq. (184) is consistent with the di-pion invariant mass spectrum [79]. The sum rule is evaluated in the Borel range  $2.8 \leq M^2 \leq 4.6 \text{ GeV}^2$ , and with  $s_0$  in the range  $5.0 \leq \sqrt{s_0} \leq 5.2 \text{ GeV}$ . From Fig. 18a, we see that there is a quite good OPE convergence for  $M^2 \geq 3.2 \text{ GeV}^2$ . Therefore, we fix  $M_{min}^2 = 3.2 \text{ GeV}^2$ . This figure also shows that the dimension-eight condensate contribution is very small. In Fig. 18b, we show the comparison between the pole and continuum contributions for  $\sqrt{s_0} = 5.1 \text{ GeV}$ , and we see that for  $M^2 \leq 4.05 \text{ GeV}^2$ , the pole contribution is bigger than the continuum contribution. Therefore, we fix  $M^2 = 4.05 \text{ GeV}^2$  as the upper limit of the Borel window for  $\sqrt{s_0} = 5.1 \text{ GeV}$ . In Fig. 18c, we show the  $m_Y$  mass, for different values of  $s_0$ , as a function of  $M^2$ , with the upper and lower Borel window limits indicated by the arrows. From this figure we see that there is a very good Borel stability for  $m_Y$ . Taking into account the variations on  $M^2$ ,  $s_0$ ,  $\langle \bar{s}s \rangle$ ,  $m_s$  and  $m_c$  in the regions mentioned above, we get [92]:

$$m_Y = (4.65 \pm 0.10) \text{ GeV} \quad (185)$$

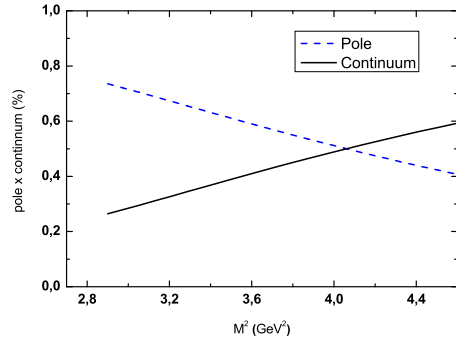
which is in excellent agreement with the mass of the  $Y(4660)$  state. Therefore we conclude that the  $Y(4660)$  can be described by a diquark-antidiquark  $[cs\bar{c}\bar{s}]$  tetraquark state with a spin configuration given by scalar and vector diquarks. This quark content is consistent with the di-pion invariant mass spectra shown in Ref. [79], which shows that there is some indication that the  $Y(4660)$  has a well-defined di-pion intermediate state consistent with the formation of  $f_0(980)$ .

Another possible interpretation for the  $Y(4660)$  could be as a  $\psi(2S)f_0(980)$  bound state. The decay channel into  $\psi(2S)\pi^+\pi^-$  favors such a molecular interpretation. However, it is very difficult to work with excited states in a QCDSR

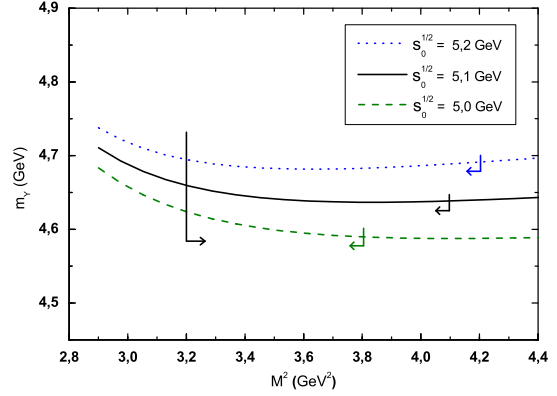




(a)



(b)



(c)

Figure 18: Sum rule calculation for the  $Y(4660)$  state. a) The OPE convergence in the region  $2.8 \leq M^2 \leq 4.5 \text{ GeV}^2$  for  $\sqrt{s_0} = 5.1 \text{ GeV}$ . We plot the OPE contributions starting with perturbative (line with triangles), quark condensate  $\langle \bar{q}q \rangle$  (dashed line), gluon condensate  $\langle g^2 G^2 \rangle$  (dotted line), mix condensate  $\langle \bar{q}Gq \rangle$  (line with squares), four-quark condensate  $\langle \bar{q}q \rangle^2$  (dot-dashed line) and eighth condensate  $\langle \bar{q}q \rangle \langle \bar{q}Gq \rangle$  (solid line), for the  $\sqrt{s_0} = 5.1 \text{ GeV}$ . b) The pole contribution (dashed line) and the continuum contribution (solid line), for the  $\sqrt{s_0} = 5.1 \text{ GeV}$ . c) The mass as a function of the sum rule parameter  $M^2$  for  $\sqrt{s_0} = 5.0 \text{ GeV}$  (dashed line),  $\sqrt{s_0} = 5.1 \text{ GeV}$  (solid line),  $\sqrt{s_0} = 5.2 \text{ GeV}$  (dotted line). The arrows indicate the valid Borel Window. Figures taken from Ref. [92].

calculation. For this reason, in Ref. [103] the following current, which couples to a  $J/\psi f_0(980)$  molecular state with quantum numbers  $J^{PC} = 1^{--}$ , was considered:

$$j_\mu = (\bar{c}_i \gamma_\mu c_i) (\bar{s}_j s_j). \quad (186)$$

Although there are conjectures that the  $f_0(980)$  itself could be a tetraquark state [245], in Ref. [246] it was shown that it is difficult to explain the light scalars as tetraquark states from a QCDSR calculation. Therefore, in Ref. [103] a simple quark-antiquark current describing the  $f_0(980)$  meson was used. The value used for the continuum threshold is in the range:  $5.0 \leq \sqrt{s_0} \leq 5.2 \text{ GeV}$ .

With this current it is also possible to get a good OPE convergence and to determine a Borel window with good Borel stability for the mass of the state, as can be seen in Ref. [103]. Varying the value of the continuum threshold in the range  $\sqrt{s_0} = 5.1 \pm 0.1 \text{ GeV}$ , and the other parameters as indicated in Table 2, one gets [103]:

$$m_Y = (4.67 \pm 0.09) \text{ GeV}. \quad (187)$$

This result is in an excellent agreement with the mass of the  $Y(4660)$  state. The obtained mass is far above the  $J/\psi f_0(980)$  threshold and, therefore, such a state cannot be interpreted as a  $J/\psi f_0(980)$  bound state. It is important to

remember that the current in Eq (186) is written in terms of the currents that couples to the  $J/\psi$  and  $f_0(980)$  mesons, but it also couples with all excited states with the  $J/\psi$  and  $f_0(980)$  quantum numbers. From the QCDSR analysis presented here we can only guarantee that the mass in Eq. (187) is the mass of the ground state of all the states described by the current in Eq (186), but not that their constituents, described by the  $\bar{c}_i \gamma_\mu c_i$  and  $\bar{s}_j s_j$  currents, are the ground states of these currents: the  $J/\psi$  and  $f_0(980)$  mesons.

Therefore, it is possible that the mass obtained in Eq (187) describes a  $\psi(2S) f_0(980)$  molecular state, since the  $\psi(2S) f_0(980)$  threshold is at 4.66 GeV, compatible with a loosely bound state. The interpretation of the  $Y(4660)$  as a  $\psi(2S) f_0(980)$  molecular state was first proposed in Ref. [240] and is also in agreement with the  $Y(4660)$  main decay channel:  $Y(4660) \rightarrow \psi(2S) \pi^+ \pi^-$ . It is also important to mention that this result indicates that, from a QCDSR point of view, there is no  $J/\psi f_0(980)$  bound state.

It is straightforward to extend the study presented in the above section to the non-strange case. To do that one only has to replace  $\langle \bar{s}s \rangle \rightarrow \langle \bar{q}q \rangle$  and to use  $m_s = 0$  in the spectral density expressions given in Ref. [103]. In Ref. [103] it was shown that the OPE convergence is worse in this case as compared to the  $J/\psi f_0(980)$  case. This is due to the fact that the dimension-3 and dimension-5 condensates do not contribute to the sum rule. Varying the continuum threshold in the range  $5.0 \leq \sqrt{s_0} \leq 5.2$  GeV, and the other QCD parameters in Table 2 one gets [103]:

$$m_Y = (4.63 \pm 0.10) \text{ GeV} . \quad (188)$$

The result found for the  $J/\psi \sigma(600)$  molecular current is also in agreement with the results obtained with the  $J/\psi f_0(980)$  current. This kind of findings is not uncommon in QCDSR calculations for multiquark states [88]. Again, since the masses obtained are largely above the  $J/\psi \sigma(600)$  threshold, we conclude that there is no  $J/\psi \sigma(600)$  bound state. In this case, since the mass obtained is also above the  $\psi(2S) \sigma(600)$  threshold we can not interpret the  $Y(4660)$  as a  $\psi(2S) \sigma(600)$  molecular state, despite the fact that the obtained mass is in agreement with the  $Y(4660)$  mass.

#### 4.6. Summary for the vector $Y$ states

The mixed charmonium-molecule current proposed in Ref. [105] within the QCDSR framework, provides a consistent description of various properties of the  $Y(4260)$  state. Fixing the mixing angle fixed as  $\theta = (53.0 \pm 0.5)^\circ$  it was possible to describe not only the mass of the  $Y(4260)$ , but also its decay width into  $J/\psi \pi^+ \pi^-$ , and the branching fraction for its production in the  $B$  meson decay channel  $B \rightarrow KY(4260)$ . The presented results for  $Y(4260)$  are also consistent for a state with a smaller mass around 4220 MeV. Therefore, if future experiments confirm the hypothesis presented in Ref. [71], that the  $Y(4260)$  is in fact a superposition of two states with masses around (4220) MeV and (4320) MeV, the  $Y(4220)$  resonance could be explained as such mixed state.

The  $Y(4360)$  state can be explained as a normal  $[cq\bar{c}\bar{q}]$  tetraquark, although the obtained mass is slightly bigger than the  $Y(4360)$  mass. Therefore, if the state recently observed by the BESIII collaboration in the process  $e^+ e^- \rightarrow \pi^+ \pi^- h_c$  [69], the  $Y(4390)$  state, is confirmed, the proposed tetraquark current could describe such state.

In the case of the  $Y(4660)$  it was show that it is possible to describe this state with a tetraquark current  $[cs\bar{c}\bar{s}]$  with a spin configuration given by scalar and vector diquarks, or with a molecular current,  $(\bar{c}_i \gamma_\mu c_i) (\bar{s}_j s_j)$ , representing a  $\psi(2S) f_0(980)$  bound state.

### 5. Isovector states with hidden charm

The recent years might be recalled in the future as a period of revolution in the field of hadron physics since several manifestly exotic states have been discovered. Among them, mesons labelled as “Z” may be considered as specially interesting, since they have a charmonium like mass but are electrically charged at the same time. A description of such properties unavoidably requires (at least) four valence quarks in the wave function. The first among the series of Z’s discovered was  $Z^\pm(4430)$ . After this discovery, several other charged states with hidden charm (and their neutral partners) have been reported to exist. We list these states in Table. ??, denoting all of them by  $Z_c$  or simply  $Z$ , although the names are different in the latest naming scheme of the Particle Data Group (PDG) [22]. Within this scheme, the label  $Z_c$  is used to represent isovector states with hidden charm and with well defined quantum numbers among which the parity ( $P$ ) and  $C$ -parity ( $C$ ) is  $+-$ . The label  $X$  is used for states with not yet defined quantum numbers. We shall use  $Z$  ( $Z_c$ ), throughout this review, to refer to isovector states with hidden charm, independently of their quantum numbers.

Table 6: A list of the currently known isovector mesons with a hidden charm content. The current naming scheme, used by PDG [22], is included in the table. The quoted year is the year of the first observation in each channel and the quoted charge conjugation,  $C$ , is for the neutral state in the multiplet.

State	name in PDG	$I^G(J^{PC})$	Decay channel	Experiment	Year
$Z_c(3900)$	$Z_c(3900)$	$1^+(1^{+-})$	$Z_c^+(3900) \rightarrow \pi^+ J/\psi$	BESIII [43], Belle [44], CLEO-c [45]]	2013
			$Z_c^+(3900) \rightarrow D\bar{D}^{*+}$	BESIII [46]	2013
$Z_c(4020)$	$X(4020)$	$1^+(?^{2-})$	$Z_c^+(4020) \rightarrow \pi^+ h_c$	BESIII [55]	2013
			$Z_c^+(4020) \rightarrow (D^*\bar{D}^*)^+$	BESIII [56]	2013
$Z_1^+(4050)$	$X(4050)$	$1^-(?^{2+})$	$Z_1^+(4050) \rightarrow \pi^+ \chi_{c1}$	Belle [57]	2008
$Z_c(4055)$	$X(4055)$	$1^+(?^{2-})$	$Z_c^+(4055) \rightarrow \pi^+ \psi(2S)$	Belle [59]	2014
$Z_c(4100)$	—	$1^-(0^{++})$ or $(1^{-+})$	$Z_c^-(4100) \rightarrow \pi^- \eta_c(1S)$	LHCb [60]	2018
$Z_c(4200)$	$Z_c(4200)$	$1^+(1^{+-})$	$Z_c^+(4200) \rightarrow \pi^+ J/\psi$	Belle [67]	2014
$Z_2(4250)$	$X(4250)$	$1^-(?^{2+})$	$Z_2^+(4250) \rightarrow \pi^+ \chi_{c1}$	Belle [57]	2008
$Z(4430)$	$Z_c(4430)$	$1^+(1^{+-})$	$Z^+(4430) \rightarrow \pi^+ \psi(2S)$	Belle [80–82], LHCb [84]	2007
			$Z^+(4430) \rightarrow \pi^+ J/\psi$	Belle [67]	2014

### 5.1. $Z^+(4430)$

The real turning point in the discussion regarding the structure of the new charmonium states was the observation announced by the Belle Collaboration of a charged state decaying into  $\psi'\pi^+$ , produced in  $B^+ \rightarrow K\psi'\pi^+$  [80]. After its discovery, the subsequent progress on the experimental studies of  $Z^+(4430)$  was astonishing. Soon after the Belle observation, the Babar Collaboration searched for the  $Z^-(4430)$  signature in four decay modes and concluded that there was no significant evidence for the presence of a relevant signal in any of these processes [83]. However, using the same data sample as in ref. [80], Belle performed a full Dalitz plot analysis and confirmed the observation of the  $Z^+(4430)$  signal with a  $6.4\sigma$  statistical significance [81]. It was only after four years of this disagreement that the controversy came to an end. First the Belle Collaboration confirmed the  $Z^+(4430)$  observation and determined the preferred assignment of the quantum numbers to be  $J^P = 1^+$  [82], and soon after that, the LHCb Collaboration confirmed both, the  $Z^+(4430)$  observation and the preferred assignment of the quantum numbers [84]. The LHCb Collaboration also did the first attempt to demonstrate the resonant behavior of the  $Z^+(4430)$  state. They have performed a fit in which the Breit-Wigner amplitude was replaced by a combination of independent complex amplitudes at six equally spaced points in the  $m_{\psi(2S)\pi}$  range covering the  $Z^+(4430)$  peak region [84]. The resulting Argand diagram is consistent with a rapid phase transition at the peak of the amplitude, just as expected for a resonance. Therefore, the confirmation of the observation of  $Z^+(4430)$  by the LHCb Collaboration with the demonstration of its resonant behavior can be considered as the first experimental proof of the existence of the exotic states. Finally, Belle also searched for this state in the  $J/\psi\pi^+$  channel and a  $4\sigma$  signal consistent with  $Z^+(4430)$  was found [67]. Comparing the measured product of branching fractions [82],

$$\mathcal{B}(B^0 \rightarrow K^+ Z^-(4300)) \times \mathcal{B}(Z^-(4430) \rightarrow \psi(2S)\pi^-) = (6.0_{-2.0-1.4}^{+1.7+2.5}) \times 10^{-5}. \quad (189)$$

and [67]

$$\mathcal{B}(\bar{B}^0 \rightarrow K^- Z^+(4300)) \times \mathcal{B}(Z^+(4430) \rightarrow J/\psi\pi^+) = (5.4_{-1.0-0.6}^{+4.0+1.1}) \times 10^{-6}, \quad (190)$$

the ratio between the two observed decay channels is estimated to be [169]:

$$\frac{\mathcal{B}(Z^\pm(4430) \rightarrow \psi(2S)\pi^\pm)}{\mathcal{B}(Z^\pm(4430) \rightarrow J/\psi\pi^\pm)} = 11.1_{-8.6}^{+18}. \quad (191)$$

The averaged mass and width of this state are  $M = (4478 \pm 17) \text{ MeV}$  and  $\Gamma = (180 \pm 31) \text{ MeV}$  [22].

### 5.1.1. History of theoretical studies of $Z^+(4430)$

Before the quantum numbers of  $Z^+(4430)$  were determined, due to the proximity of its mass with the  $\bar{D}^*D_1$  threshold, Rosner [247] suggested that it was an  $S$ -wave threshold effect, Bugg considered it to be a cusp in the  $\bar{D}^*D_1$  channel [248], while in Ref. [241] it was considered as a hadro-charmonium. Other authors considered it to be a natural candidate for a loosely bound  $S$ -wave  $\bar{D}^*D_1$  molecular state with quantum numbers  $J^P = 0^-$  [89, 93, 249–253]. There exists also a quenched lattice QCD calculation which found attractive interaction in the  $\bar{D}^*D_1$  system in the  $J^P = 0^-$  channel [254]. The authors of ref. [254] also find positive scattering length. Based on these findings, they conclude that although the interaction between the two charmed mesons is attractive in this channel, it is unlikely that they can form a genuine bound state right below the threshold.

The first theoretical proposition for the correct quantum numbers of  $Z^+(4430)$  was made by Maiani, Polosa and Riquer in Ref. [255], where this state was interpreted as the first radial excitation of the tetraquark supermultiplet to which  $X(3872)$  belongs [186]. In Ref. [186] it was conjectured that  $X(3872)$  must have a charged partner  $X^+$  with  $J^{PC} = 1^{+-}$  with a similar mass. In Ref. [255] it was pointed out that since the mass difference

$$M_{Z^+(4430)} - M_{X^+(3872)} \sim 560 \text{ MeV} \quad (192)$$

is close to the mass difference  $M_{\Psi(2S)} - M_{\Psi(1S)} = 590 \text{ MeV}$ , the  $Z^+(4430)$  may well be the first radial excitation of  $X^+$ . Later, after the discovered of the  $Z_c^+(3900)$  state, Maiani *et al.* identified it as the predicted  $X^+$  [256], and  $Z^+(4430)$  as the first radial excitation of  $Z_c^+(3900)$  [257]. In Refs. [169, 242, 258–262]  $Z^+(4430)$  was also interpreted as the first radial excitation ( $2S$ ) of a charged diquark-antidiquark  $[cu][\bar{c}\bar{d}]$  tetraquark state. However, in Ref. [263], using a color flux-tube model with a four-body confinement potential, the authors could not explain  $Z^+(4430)$  as a tetraquark state.

After Belle and LHCb established the quantum numbers of  $Z^+(4430)$  to be  $J^P = 1^+$ , it was clear that the  $S$ -wave  $\bar{D}^*D_1$  molecular state assignment of  $Z^+(4430)$  is not possible. Following the latter findings, in Ref. [264] the authors proposed three possible molecular configurations for  $Z^+(4430)$ : a  $P$ -wave excitation of the  $D_1\bar{D}^*$  or  $D_2\bar{D}^*$  molecule; an  $S$ -wave molecule composed of a  $D$  or  $D^*$  meson and a  $D$ -wave vector  $D$  meson; (3) a cousin of the molecular state of  $Z_c(3900)$  composed of a  $D$  or  $D^*$  meson and their radial excitations. In Refs. [265, 266]  $Z^+(4430)$  is interpreted as a  $D\bar{D}^*(2S)$  state, and the authors of Ref. [266] showed that the ratio measured by Belle [67] in Eq. (191) can be explained by considering  $Z^+(4430)$  as a  $D\bar{D}^*(2S)$  molecular state. The ratio in Eq. (191) can also be explained by considering  $Z^+(4430)$  as the first radial excitation ( $2S$ ) of a tetraquark state [262].

From the above discussions we can conclude that the two possible explanations for the  $Z^+(4430)$  structure are: 1) the first radial excitation ( $2S$ ) of the charged diquark-antidiquark  $[cu][\bar{c}\bar{d}]$   $Z_c^+(3900)$  tetraquark state; 2) a  $D\bar{D}^*(2S)$  molecular state. It is very interesting to notice that in the Supersymmetric Light Front Holographic QCD [267–271]  $Z_c^+(3900)$  and  $Z^+(4430)$  are also identified as tetraquark states, but as, respectively, the first and second radial excitation of the state  $\chi_{c1}(3510)$ , considered as the tetraquark superpartner of the  $\Xi_{cc}$  baryon [272], as can be seen in Fig. 19.

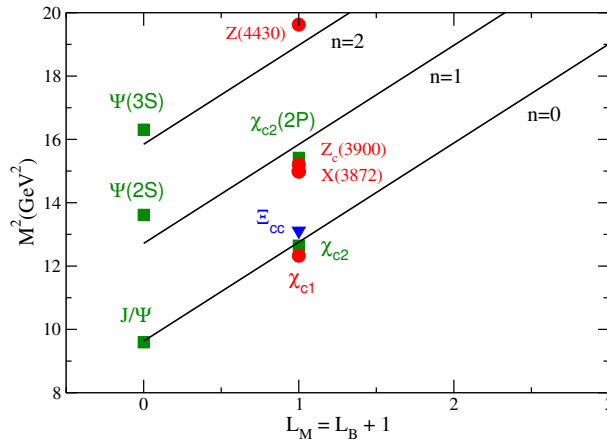


Figure 19: Double charm mesons (shown as green squares) baryons (shown as blue triangles) and tetraquarks (shown as red circles) with different values of angular momentum  $L$  and radial excitation  $n$ . The solid lines are the trajectories fit from [272]. Hadron masses are taken from PDG [22].

## 5.2. $Z_c^+(3900)$

In 2013, the BESIII Collaboration announced the observation of a charged charmonium-like state, called  $Z_c(3900)$ , in the  $J/\psi\pi^\pm$  invariant mass distribution of the  $e^+e^- \rightarrow Y(4260) \rightarrow J/\psi\pi^+\pi^-$  process [43]. This structure, was also observed, at the same time, by the Belle collaboration [44] and was confirmed by the authors of Ref. [45] using the CLEO-c data. From these three experiments, assuming the orbital angular momentum between  $J/\psi$  and  $\pi$  to be zero, the quantum number of  $Z_c(3900)$  was argued to be  $I^G J^P = 1^+ 1^+$ . The confirmation of the spin and parity of  $Z_c^+(3900)$  as  $J^P = 1^+$  was done in Ref. [273] with a statistical significance larger than  $7\sigma$ . In Ref. [45] an evidence of the existence of the neutral state  $Z_c(3900)^0$  decaying into  $\pi^0 J/\psi$  was also brought forward and in Ref. [274]  $Z_c(3900)^0$  was observed by BESIII in the  $e^+e^- \rightarrow \pi^0 Z_c(3900)^0 \rightarrow \pi^0 \pi^0 J/\psi$  process. The mass and decay width of  $Z_c(3900)$  from all these different experiments are consistent with each other. The averaged mass and width are:  $M = (3886.6 \pm 2.4)$  MeV and  $\Gamma = (28.2 \pm 2.6)$  MeV [22].

Soon after the  $Z_c^+(3900)$  observation, the BESIII Collaboration announced the finding of three other charged states:  $Z_c(3885)$  [46, 275],  $Z_c(4020)$  [55] and  $Z_c(4025)$  [56]. All these structures were observed in the process  $e^+e^- \rightarrow Y(4260) \rightarrow \pi^- Z_c^+$ .

The  $Z_c^+(3885)$  state was found in the process  $e^+e^- \rightarrow Y(4260) \rightarrow (D\bar{D}^*)^\pm \pi^\mp$  with mass  $M = (3881.7 \pm 1.6 \pm 1.6)$  MeV and width  $\Gamma = (26.5 \pm 1.7 \pm 2.1)$  MeV [275]. Since its measured mass was slightly lower than that of  $Z_c(3900)$  measured in the  $J/\psi\pi$  channel by BESIII:  $M = (3899.0 \pm 3.6 \pm 4.9)$  MeV [43] and by Belle:  $M = (3894.5 \pm 6.6 \pm 4.5)$  MeV [44], BESIII called it  $Z_c^+(3885)$ . However, the measured mass and width of  $Z_c(3885)$  are consistent with those of the  $Z_c(3900)$  state obtained by Xiao *et al.*:  $M = (3886 \pm 4 \pm 2)$  MeV [45]. BESIII also reported the finding of a neutral state  $Z_c(3885)^0$  in the  $e^+e^- \rightarrow (D\bar{D}^*)^0 \pi^0$  process [276]. The analysis on the angular distribution of the  $\pi Z_c(3885)$  system performed by BESIII supports the  $J^P = 1^+$  assignment [46]. With the same spin-parity and similar mass and width,  $Z_c(3900)$  and  $Z_c(3885)$  are probably the same state and they are considered as the same state in PDG [22]. Under this assumption, the ratio of the partial decay width of these two decay modes is [19]

$$\frac{\Gamma(Z_c(3900) \rightarrow D\bar{D}^*)}{\Gamma(Z_c(3900) \rightarrow J/\psi\pi)} = 7.7 \pm 1.3 \pm 2.8. \quad (193)$$

### 5.2.1. Theoretical explanations for $Z_c^+(3900)$

As discussed in the case of  $Z^+(4430)$ , the two possible explanations for the  $Z_c^+(3900)$  structure are: a charged diquark-antidiquark  $[cu][\bar{c}\bar{d}]$  state, or a  $D\bar{D}^*$  molecular state. Concerning the molecular configuration, there are many calculations that could not accommodate  $Z_c^+(3900)$  as a  $J^P = 1^+ D\bar{D}^*$  molecule [277, 278] including lattice QCD calculations [279–281]. However, in Refs. [195, 282–292] the authors did find a  $D\bar{D}^*$  molecular state compatible with  $Z_c^+(3900)$ . There are also some QCDSR calculations for the  $Z_c^+(3900)$ , done using molecular type of interpolating currents, for which the obtained mass agrees with the experimental values within errors [195, 293–295]. However, it is important to remember that, although the interpolating current is of molecular type, the current is local and, therefore, the four quarks in the current have the same space-time position as in the case of tetraquark currents [99]. In the case of tetraquark configuration, many calculations, using different approaches, found a positive signal [106, 198, 256, 296, 297].

In all calculations, which found a positive signal, the mass of the  $Z_c(3900)$  is relatively easily reproduced. However, the  $Z_c(3900)$  decay width represents a challenge to theorists. While its mass is very close to the  $X(3872)$  mass, it has a much larger decay width. Indeed, while the  $Z_c(3900)$  decay width is in the range 30 MeV, the  $X(3872)$  width is smaller than 1.2 MeV. This difference can be attributed to the fact that  $X(3872)$  may contain a significant  $[c\bar{c}]$  component [96], which is absent in  $Z_c(3900)$ . As pointed out in Ref. [218], this would also explain why  $Z_c$  has not been observed in  $B$  decays.

According to the experimental observations,  $Z_c^+(3900)$  decays into  $J/\psi\pi^+$  with a relatively large decay width. If  $Z_c$  is a real  $D^* - \bar{D}$  molecular state, its decay into  $J/\psi\pi^+$  must involve the exchange of charmed mesons. When the distance between  $D^*$  and the  $\bar{D}$  is large, as expected for a  $D^* - \bar{D}$  molecular state, it becomes more difficult to exchange mesons, since the exchange of heavy mesons is a short range process. In Ref. [298] it was shown that, in order to reproduce the measured  $Z_c(3900)$  width, the effective radius must be  $\langle r_{eff} \rangle \simeq 0.4$  fm. This size scale is small and represents a challenge to the molecular picture. In Ref. [285], the  $Z_c^+(3900)$  was also treated as a charged  $D^* - \bar{D}$  molecule in which the interaction between the charm mesons is described by a pionless effective field theory. Introducing electromagnetic interactions through the minimal substitution in this theory, the authors explored its

electromagnetic structure, arriving at the conclusion that its charge radius is of the order of  $\langle r^2 \rangle \simeq 0.11 \text{ fm}^2$ . Taking this radius as a measure of the spatial size of the state, we conclude that it is more compact than  $J/\psi$ , for which  $\langle r^2 \rangle \simeq 0.16 \text{ fm}^2$ . In Ref. [106] the combined results of Refs. [298] and [285] were taken as an indication that  $Z_c$  is a compact object, which may be better understood as a quark cluster, such as a tetraquark.

### 5.2.2. QCDSR calculations for the $Z_c^+(3900)$ width

In Ref. [106]  $Z_c^+(3900)$  was interpreted as the isospin 1 partner of  $X(3872)$ , as in Ref. [256]. The quantum numbers for the neutral state in the isospin multiplet are  $I^G(J^{PC}) = 1^+(1^{+-})$  and, therefore, the interpolating field for  $Z_c^+(3900)$ , considered as a tetraquark state, is given by:

$$j_\alpha = \frac{i\epsilon_{abc}\epsilon_{dec}}{\sqrt{2}} [(u_a^T C \gamma_5 c_b)(\bar{d}_d \gamma_\alpha C \bar{c}_e^T) - (u_a^T C \gamma_\alpha c_b)(\bar{d}_d \gamma_5 C \bar{c}_e^T)], \quad (194)$$

where  $a, b, c, \dots$  are color indices, and  $C$  is the charge conjugation matrix. Considering SU(2) symmetry, the mass obtained in QCDSR for the  $Z_c$  state is exactly the same as that obtained for  $X(3872)$  [88, 99]. As discussed above, QCDSR calculations for the  $Z_c$  state using a  $\bar{D}D^*$  molecular type interpolating current lead to similar results for the mass of the state [195, 293–295]. These calculations only confirm the results presented in Refs. [88, 99].

The evaluation of the  $Z_c^+(3900) \rightarrow J/\psi \pi^+$  decay width in the QCDSR approach is based on the three-point function:

$$\Pi_{\mu\nu\alpha}(p, p', q) = \int d^4x d^4y e^{ip' \cdot x} e^{iq \cdot y} \Pi_{\mu\nu\alpha}(x, y), \quad (195)$$

with  $\Pi_{\mu\nu\alpha}(x, y) = \langle 0 | T [j_\mu^\psi(x) j_{5\nu}^\pi(y) j_\alpha^\dagger(0)] | 0 \rangle$ , where  $p = p' + q$  and  $j_\mu^\psi, j_{5\nu}^\pi$  are the interpolating fields for  $J/\psi$  and  $\pi$  respectively.

The phenomenological side of the sum rule is obtained by inserting intermediate states for  $Z_c, J/\psi$  and  $\pi$  into Eq.(227). One arrives at [106]:

$$\Pi_{\mu\nu\alpha}^{(phen)}(p, p', q) = \frac{\lambda_{Z_c} m_\psi f_\psi F_\pi g_{Z_c \psi \pi}(q^2) q_\nu}{(p^2 - m_{Z_c}^2)(p'^2 - m_\psi^2)(q^2 - m_\pi^2)} \left( -g_{\mu\lambda} + \frac{p'_\mu p'_\lambda}{m_\psi^2} \right) \left( -g_\alpha^\lambda + \frac{p_\alpha p^\lambda}{m_{Z_c}^2} \right) + \dots, \quad (196)$$

where the dots stand for the contribution of all possible excited states. The form factor,  $g_{Z_c \psi \pi}(q^2)$ , is defined as the generalization of the on-mass-shell matrix element,  $\langle J/\psi \pi | Z_c \rangle$ , for an off-shell pion:

$$\langle J/\psi(p') \pi(q) | Z_c(p) \rangle = g_{Z_c \psi \pi}(q^2) \epsilon_\lambda^*(p') \epsilon^\lambda(p), \quad (197)$$

where  $\epsilon_\alpha(p), \epsilon_\mu(p')$  are the polarization vectors of the  $Z_c$  and  $J/\psi$  mesons respectively.

In Ref. [106] the coupling constant,  $g_{Z_c \psi \pi}$ , was evaluated directly by considering a sum rule at the pion-pole [158], valid only at  $Q^2 = 0$ , as suggested in [120] for the pion-nucleon coupling constant. It consists of neglecting the pion mass in the denominator of Eq. (196) and working at  $q^2 = 0$ . In the OPE side only terms proportional to  $1/q^2$  will contribute to the sum rule. Therefore, up to dimension five the only diagrams that contribute are the quark condensate and the mixed condensate. Besides, only the diagrams with non-trivial color structure, which are called color-connected (CC) diagrams, as shown in Fig. 20, were considered on the OPE side. Possible permutations (not shown) of the diagram in Fig. 20 also contribute.

The diagram in Fig. 20 contributes only to the structures  $q_\nu g_{\mu\alpha}$  and  $q_\nu p'_\mu p'_\alpha$  appearing on the phenomenological side. On the OPE side we choose to work with the  $q_\nu p'_\mu p'_\alpha$  structure, since structures with more momenta are supposed to give better results. We obtain:

$$\Pi^{(OPE)} = \frac{\langle \bar{q} g \sigma \cdot G q \rangle}{12 \sqrt{2} \pi^2} \frac{1}{q^2} \int_0^1 d\alpha \frac{\alpha(1-\alpha)}{m_c^2 - \alpha(1-\alpha)p'^2}. \quad (198)$$

Making a single Borel transformation to both  $P^2 = P'^2 \rightarrow M^2$ , we finally get the sum rule:

$$A \left( e^{-m_\psi^2/M^2} - e^{-m_{Z_c}^2/M^2} \right) + B e^{-s_0/M^2} = \frac{\langle \bar{q} g \sigma \cdot G q \rangle}{12 \sqrt{2} \pi^2} \int_0^1 d\alpha e^{-\frac{m_c^2}{\alpha(1-\alpha)M^2}}, \quad (199)$$

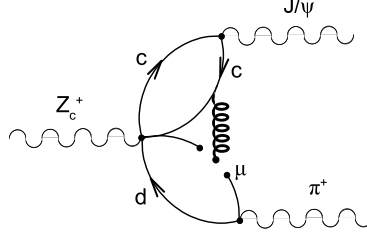


Figure 20: CC diagram which contributes to the OPE side of the sum rule. From Ref. [106].

where  $s_0$  is the continuum threshold parameter for  $Z_c$ ,

$$A = \frac{g_{Z_c\psi\pi}\lambda_{Z_c}f_\psi F_\pi(m_{Z_c}^2 + m_\psi^2)}{2m_{Z_c}^2 m_\psi(m_{Z_c}^2 - m_\psi^2)}, \quad (200)$$

and the parameter  $B$  is introduced to take into account pole-continuum transitions (see Sec. 2.7.3). To determine the coupling constant  $g_{Z_c\psi\pi}$  we fit the QCDSR results with the analytical expression on the left-hand side (LHS) of Eq.(199), and find:  $A = 1.46 \times 10^{-4} \text{ GeV}^5$  and  $B = -8.44 \times 10^{-4} \text{ GeV}^5$ . Using the definition of  $A$  in Eq.(200), the value obtained for the coupling constant is [106]

$$g_{Z_c\psi\pi} = (3.89 \pm 0.56) \text{ GeV}, \quad (201)$$

which is in excellent agreement with the estimate made in [256], based on dimensional arguments. The corresponding decay width is [106]:

$$\Gamma(Z_c^+(3900) \rightarrow J/\psi\pi^+) = (29.1 \pm 8.2) \text{ MeV}. \quad (202)$$

In Ref. [106] the three-point QCDSR was also used to evaluate the coupling constants at the vertices  $Z_c^+(3900)\eta_c\rho^+$ ,  $Z_c^+(3900)D^+\bar{D}^{*0}$  and  $Z_c^+(3900)\bar{D}^0D^{*+}$ . In all cases only CC diagrams were considered.

To illustrate let us consider the  $Z_c^+(3900)\eta_c\rho^+$  case. In this case the phenomenological side is

$$\Pi_{\mu\alpha}^{(phen)}(p, p', q) = \frac{-i\lambda_{Z_c}m_\rho f_\rho f_{\eta_c} m_{\eta_c}^2 g_{Z_c\eta_c\rho}(q^2)}{2m_c(p^2 - m_{Z_c}^2)(p'^2 - m_{\eta_c}^2)(q^2 - m_\rho^2)} \left( -g_{\mu\lambda} + \frac{q_\mu q_\lambda}{m_\rho^2} \right) \left( -g_\alpha^\lambda + \frac{p_\alpha p'^\lambda}{m_{Z_c}^2} \right) + \dots \quad (203)$$

On the OPE side, for the  $p'_\alpha q_\mu$  structure we have:

$$\Pi^{(OPE)} = \frac{-im_c \langle \bar{q}g\sigma Gq \rangle}{48\sqrt{2}\pi^2} \frac{1}{q^2} \int_0^1 d\alpha \frac{1}{m_c^2 - \alpha(1-\alpha)p'^2}. \quad (204)$$

Isolating the  $q_\alpha p'_\mu$  structure in Eq. (203) and making a single Borel transformation on both  $P^2 = P'^2 \rightarrow M^2$ , we finally get the sum rule:

$$C \left( e^{-m_{\eta_c}^2/M^2} - e^{-m_{Z_c}^2/M^2} \right) + D e^{-s_0/M^2} = \frac{Q^2 + m_\rho^2}{Q^2} \frac{m_c \langle \bar{q}g\sigma Gq \rangle}{48\sqrt{2}\pi^2} \int_0^1 d\alpha \frac{e^{-\frac{m_c^2}{\alpha(1-\alpha)M^2}}}{\alpha(1-\alpha)}, \quad (205)$$

with  $Q^2 = -q^2$  and

$$C = \frac{g_{Z_c\eta_c\rho}(Q^2)\lambda_{Z_c}m_\rho f_\rho f_{\eta_c} m_{\eta_c}^2}{2m_c m_{Z_c}^2 (m_{Z_c}^2 - m_{\eta_c}^2)}. \quad (206)$$

One can use Eq. (205) and its derivative with respect to  $M^2$  to eliminate  $D$  from Eq. (205) and to isolate  $g_{Z_c\eta_c\rho}(Q^2)$ . In Sec. 2.8 the QCDSR results for the  $g_{Z_c\eta_c\rho}(Q^2)$  form factor are illustrated together with the extrapolation procedure

used to extract the coupling constant. The QCDSR results are shown in Figs. 4(a) and 4(b). The squares in Fig. 4(b) show the  $Q^2$  dependence of  $g_{Z_c\eta_c\rho}(Q^2)$ , obtained for  $M^2 = 5.0 \text{ GeV}^2$ . For other values of the Borel mass, in the range  $4.0 \leq M^2 \leq 10.0 \text{ GeV}^2$ , the results are equivalent. Using the parametrization in Eq. (42), also shown in Fig. 4(b) as a line, the coupling constant is obtained as [106]:

$$g_{Z_c\eta_c\rho} = (4.85 \pm 0.81) \text{ GeV}. \quad (207)$$

The couplings, with the respective decay widths, for all studied decays in [106] are given in Table 7. A total width of  $\Gamma = (63.0 \pm 18.1) \text{ MeV}$  was found for the  $Z_c(3900)$ , in good agreement with the two experimental values:  $\Gamma = (46 \pm 22) \text{ MeV}$  from BESIII [43], and  $\Gamma = (63 \pm 35) \text{ MeV}$  from BELLE [44].

Table 7: Coupling constants and decay widths in different channels

Vertex	coupling constant (GeV)	decay width (MeV)
$Z_c^+(3900)J/\psi\pi^+$	$3.89 \pm 0.56$	$29.1 \pm 8.2$
$Z_c^+(3900)\eta_c\rho^+$	$4.85 \pm 0.81$	$27.5 \pm 8.5$
$Z_c^+(3900)D^+\bar{D}^{*0}$	$2.5 \pm 0.3$	$3.2 \pm 0.7$
$Z_c^+(3900)\bar{D}^0D^{*+}$	$2.5 \pm 0.3$	$3.2 \pm 0.7$

From the results in Table 7 it is possible to evaluate the ratio

$$\frac{\Gamma(Z_c(3900) \rightarrow D\bar{D}^*)}{\Gamma(Z_c(3900) \rightarrow \pi J/\psi)} = 0.22 \pm 0.12, \quad (208)$$

which is not compatible with the result in Eq. (193). In Ref. [297], also with a QCDSR calculation, it was obtained that just the decays  $Z_c^+(3900)J/\psi\pi^+$  and  $Z_c^+(3900)\eta_c\rho^+$  lead to a total  $Z_c$  decay width of  $\Gamma = (65.7 \pm 10.3) \text{ MeV}$ . This means that the ratio in Eq. (208) would be even smaller than the quoted one. From the results presented in Ref. [256], using the diquark model, one arrives at

$$\frac{\Gamma(Z_c(3900) \rightarrow D\bar{D}^*)}{\Gamma(Z_c(3900) \rightarrow \pi J/\psi)} \sim 0.14. \quad (209)$$

Therefore, from these results one should conclude that the states  $Z_c(3885)$  [46] and  $Z_c(3900)$  [43] are not the same.

### 5.3. $Z_c^+(4020)$ (former $Z_c^+(4025)$ )

The charged  $Z_c^+(4025)$  state was first discovered by the BESIII collaboration [55] in the  $\pi^\pm h_c(1P)$  invariant mass distribution of the process  $e^+e^- \rightarrow \pi^+\pi^-h_c(1P)$ , and it was also observed by the same collaboration [56] as a peak in the  $(D^*\bar{D}^*)^\pm$  invariant mass distribution from the reaction  $e^+e^- \rightarrow (D^*\bar{D}^*)^\pm\pi^\mp$ . The BESIII collaboration also found a signal for a neutral  $Z_c^0(4020)$  in the corresponding  $\pi^0 h_c(1P)$  and  $(D^*\bar{D}^*)^0$  invariant masses of the reactions  $e^+e^- \rightarrow \pi^0\pi^0 h_c(1P)$ ,  $(D^*\bar{D}^*)^0\pi^0$  [299, 300]. Production rates and mass values support putting together the manifestation of these charged and neutral states as an evidence for the existence of an isospin 1 particle with mass  $(4024.1 \pm 1.9) \text{ MeV}$  and width  $(13 \pm 5) \text{ MeV}$ , which nowadays is named as  $X(4020)$ . With the exception of parity, the quantum numbers of this isospin 1 state have not been determined, but all the above mentioned experimental analysis assume  $s$ -wave production and thus the quantum number assignment  $I^G(J^{PC}) = 1^+(1^{+-})$ .

#### 5.3.1. Theoretical explanations for $Z_c^+(4020)$

The proximity of the mass of  $Z_c(4020)$  to the  $D^*\bar{D}^*$  threshold motivated the association of a molecule-like structure to it. In such a case, it should be possible to determine the origin of  $Z_c(4020)$  purely from the dynamics of the open charm vector mesons. The idea of forming molecular  $D^*\bar{D}^*$  resonances close to the threshold is not new and was foreseen in Refs. [182, 301–304] much before the experimental findings in Refs. [55, 56, 299, 300].

The same motivation, that is, the proximity of the  $(D^*\bar{D}^*)^\pm$  threshold (4017 MeV) to the resonance mass, has encouraged the search of a state arising from the dynamics involved in the  $D^*\bar{D}^*$  system and coupled channels within



other formalisms too. Within the context of effective field theories, in Ref. [305], using arguments of heavy quark symmetry and solving the Lippmann-Schwinger equation for the  $D^*\bar{D}^*$  system, a (virtual) state with mass in the range 3950-4017 MeV is found with isospin 1 and  $J^{PC} = 1^{+-}$ . In Ref. [306], using effective field theories based on the local hidden symmetry, it was found that a  $I^G(J^{PC}) = 1^-(2^{++})$  state arises from the coupled channel dynamics involved in the  $D^*\bar{D}^*$ ,  $J/\psi\rho$  coupled system with a mass around 3920 MeV. This calculation was updated in Ref. [307] and the binding energy was reduced, finding the state with a mass around 3990 MeV and width around 160 MeV.

Using the model of Refs. [306, 307], in Ref. [110], the cross section for the  $e^+e^- \rightarrow (D^*\bar{D}^*)^\pm\pi^\mp$  reaction was calculated and it was shown that the experimental result is compatible with a  $J^P = 1^+$  state with mass around 4025 MeV and small width,  $\sim 30$  MeV, and, thus, in line with the result in Ref. [56]. But it was also found to be consistent with the existence of a  $J^P = 2^+$  state below the  $D^*\bar{D}^*$  threshold with mass around 3990 MeV and width of 160 MeV, as found in Ref. [307]. Note that even if the state found in Refs. [306, 307] is below the  $D^*\bar{D}^*$  threshold, because of its large width, when considering the phase space for the  $e^+e^- \rightarrow (D^*\bar{D}^*)^\pm\pi^\mp$  process, a narrow peak will be produced slightly above the threshold in the  $D^*\bar{D}^*$  invariant mass distribution of the reaction (for more details see Ref. [?]). In this sense, the signal observed in Ref. [56] could be due to the presence of a state below the  $D^*\bar{D}^*$  threshold. There are some facts in favor of such an interpretation. For example, if, as assumed in Ref. [56], the signal found in the  $D^*\bar{D}^*$  invariant mass distribution of  $e^+e^- \rightarrow (D^*\bar{D}^*)^\pm\pi^\mp$  would correspond to a  $J^P = 1^+$  state produced in  $s$ -wave, such a state could easily decay to  $J/\psi\pi$ , implying that a clear signal around 4025 MeV (which in this case is quite far from the  $J/\psi\pi$  threshold) should be seen in the  $J/\psi\pi$  invariant mass distribution of the reaction  $e^+e^- \rightarrow \pi^+\pi^-J/\psi$ . This reaction was precisely studied by the BESIII collaboration [43] and they found a  $Z_c$  state around 3900 MeV, but no signal for  $Z_c(4025)$  was found.

Additionally, if  $Z_c(4025)$  should be interpreted as a state generated from the  $D^*\bar{D}^*$  interaction it should be expected to be below the threshold and not above: the dominant contribution to the wave function of the  $Z_c$  state would come from the  $D^*\bar{D}^*$  component. In effective field theories, the lowest order amplitude describing the  $D^*\bar{D}^*$  interaction has a weak energy dependence, and as shown in Ref. [308], in a single channel system with an energy-independent amplitude, when used as kernel in the Bethe-Salpeter equation to determine the scattering  $T$ -matrix, a state below the threshold, and not above, is produced. In this sense, if a  $Z_c$  state could be generated from the  $D^*\bar{D}^*$  system, it is expected to be below the  $D^*\bar{D}^*$  threshold. This fact, together with the results of Refs. [110, 306, 307] could hint to a possible misinterpretation of the signal observed in Ref. [?].

In Refs. [263, 296], a study of tetraquark states, within a diquark-antidiquark configuration, was performed in the context of a color flux tube with a multibody confinement potential and it was found that the nearest state to  $Z_c^+(4025)$  obtained with the model was the one with quantum numbers  $J^P = 2^+$ . However, several works support the  $1^{+-}$  quantum numbers too. Using a framework of non-relativistic quark model and Cornell-type potentials, a  $Q\bar{q}-\bar{Q}q$  molecular-like four quark state with  $J^{PC} = 1^{+-}$  and mass around 4036 MeV was found [259], among others with a similar mass but other quantum numbers, and identified with  $Z_c(4025)$ .

Alternative explanations for the experimental findings have also been brought forward. In Refs. [174, 309] a simple model inspired by effective field theories is used to show that the signal observed in the experiments could be an artifact arising from a coupled channel cusp effect. Studies based on a finite volume seem not to support the existence of a  $Z_c$  state arising from the  $D^*\bar{D}^*$  interaction [280, 310], considering interpolating currents with  $I^G(J^{PC}) = 1^+(1^{+-})$ . Though it is unclear if these findings imply the absence of  $Z_c$ 's with  $I^G(J^{PC}) = 1^+(1^{+-})$  or if they are due to the limitations of the simulations (for example, the use of unphysical masses for the quarks  $u$  and  $d$ ).

### 5.3.2. QCDSR calculations for $Z_c^+(4020)$

To study the  $Z_c^+(4020)$  within the scheme of the QCD sum rules, the authors in Ref. [109] considered the current:

$$j_{\mu\nu}(x) = [\bar{c}_a(x)\gamma_\mu u_a(x)] [\bar{d}_b(x)\gamma_\nu c_b(x)]. \quad (210)$$

With this current, which does not have a defined spin-parity, one can construct the two-point correlation function

$$\Pi_{\mu\nu\alpha\beta}(q^2) = i \int d^4x e^{iqx} \langle 0 | T [j_{\mu\nu}(x) j_{\alpha\beta}^\dagger(0)] | 0 \rangle, \quad (211)$$

from which it is necessary to extract the contributions to different well defined spin-parity combinations, in order to interpret the results. Considering an effective field theory point of view, bound states of two mesons are expected

to be formed, most likely, when the constituent mesons interact at low energies. At such energies, the interactions can be well described by taking the lowest relative angular momentum in the system, in other words by considering interactions in the  $s$ -partial wave. In such a picture, the  $D^* \bar{D}^*$  system can have total spin 0, 1 or 2. In the QCD sum rules approach, as described in the previous sections, the correlation function is written in terms of quark propagators and is calculated within the OPE. To do such calculations for a defined total spin 0, 1 or 2, we need to project Eq. (211) on a particular spin, which can be done using the spin projectors given in Ref. [107]. These projectors were obtained in Ref. citeTorr es:2013saa to study the  $D^* \rho$  system, inspired by a study of the same system within an effective field approach done in Ref. [311]. They are:

$$\begin{aligned}\mathcal{P}^{(0)} &= \frac{1}{3} \Delta^{\mu\nu} \Delta^{\alpha\beta}, \\ \mathcal{P}^{(1)} &= \frac{1}{2} \left( \Delta^{\mu\alpha} \Delta^{\nu\beta} - \Delta^{\mu\beta} \Delta^{\nu\alpha} \right), \\ \mathcal{P}^{(2)} &= \frac{1}{2} \left( \Delta^{\mu\alpha} \Delta^{\nu\beta} + \Delta^{\mu\beta} \Delta^{\nu\alpha} \right) - \frac{1}{3} \Delta^{\mu\nu} \Delta^{\alpha\beta},\end{aligned}\tag{212}$$

where  $\Delta_{\mu\nu}$  is defined in terms of the metric tensor,  $g^{\mu\nu}$ , and the four momentum  $q$  of the correlation function as

$$\Delta_{\mu\nu} \equiv -g_{\mu\nu} + \frac{q_\mu q_\nu}{q^2}.\tag{213}$$

The spin projected spectral density was calculated by going in the OPE series up to dimension six in Ref. [109]:

$$\rho_{\text{OPE}}^S = \rho_{\text{pert}}^S + \rho_{\langle \bar{q}q \rangle}^S + \rho_{\langle g^2 G^2 \rangle}^S + \rho_{\langle \bar{q}g\sigma Gq \rangle}^S + \rho_{\langle \bar{q}q \rangle^2}^S + \rho_{\langle g^3 G^3 \rangle}^S,\tag{214}$$

where the superscript  $S$  denotes the spin of the states in the spectrum. The spectral density on the phenomenological side is written as a sum of a narrow, sharp state and a smooth continuum

$$\rho_{\text{phenom}}^S(s) = \lambda_S^2 \delta(s - m_S^2) + \rho_{\text{cont}}^S(s),\tag{215}$$

where  $s = q^2$  is the squared four-momentum flowing in the correlation function,  $\lambda_S$  is the coupling of the current to the state we are looking for and  $m_S$  denotes its mass. As explained in the previous sections, the continuum is assumed to be separated from the ground state by about 500 MeV, although this separation energy is considered as an unknown parameter and is varied in the calculations to estimate errors in the results. As the standard procedure, a Borel transform of both the OPE and phenomenological sides is taken, which introduces a dependence of the results on the Borel mass. The criteria to establish a range of Borel mass, within which the results are considered to be reliable, are: (1) to ensure the dominance of the first term of Eq. (215), called as the pole term, over the continuum contribution, in agreement with the ansatz chosen for the phenomenological description of the spectral density and (2) to have a converging OPE series. It can be seen from the left panel of Fig. 21, for a fixed value of  $\sqrt{s_0} = 4.55$  GeV, that the pole term dominates for all the three spin configurations until the squared Borel Mass value of about 2.9 GeV<sup>2</sup>. The right panel of the same figure shows that the contribution of the penultimate term reduces from  $\sim 25\%$  to  $\sim 20\%$  in the range of Borel mass  $2.56 \text{ GeV}^2 \leq M^2 \leq 2.9 \text{ GeV}^2$ . This range can be considered as a Borel window within which the results are reliable and thus we can look at the mass values obtained in this range for the three cases of spin. As can be seen from Fig. 22, the mass value is reasonably stable and it ranges from 3.87-3.91 GeV. In Ref. [109] the authors have varied  $\sqrt{s_0}$  by  $\pm 0.5$  GeV and have better estimated the errors by taking into account the uncertainties involved in the values of other parameters, such as the condensates, the quark mass, etc.. The obtained values for the masses of the states with spin 0, 1 and 2, are respectively,

$$\begin{aligned}M^{S=0} &= (3943 \pm 104) \text{ MeV}, \\ M^{S=1} &= (3950 \pm 105) \text{ MeV}, \\ M^{S=2} &= (3946 \pm 104) \text{ MeV}.\end{aligned}\tag{216}$$

In Ref. [109], three states with different spin but with almost similar mass are found, all with a  $D^* \bar{D}^*$  molecular nature. The fact that the  $s$ -wave interaction must dominate in the formation of a molecular state implies that all these states

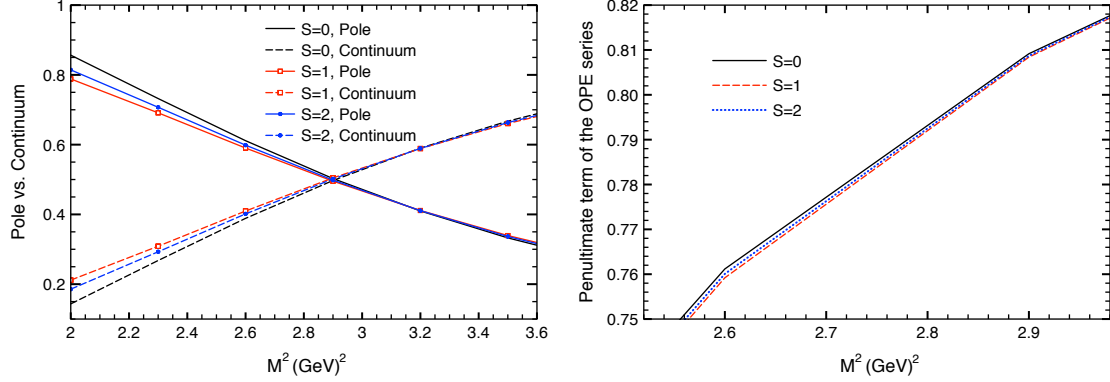


Figure 21: Figures depicting the pole dominance on the phenomenological side and the convergence of the OPE series for the correlation function of Eq. (211).

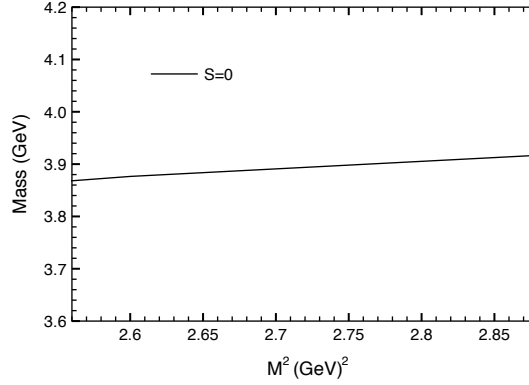


Figure 22: Mass of a state with spin-parity  $0^+$  as a function of Borel mass, varying in the reliable range of the validity of results.

have a positive parity. With the discovery of the neutral member of the isospin 1 triplet, in the  $D^{*0}\bar{D}^{*0}$  system, it is also possible to define the  $C$ - and  $G$ -parity of the a state with spin 0, 1, and 2 formed in such a system. The spin 0 and 2 states formed in the  $D^*\bar{D}^*$  should have positive  $C$ -parity and negative  $G$ -parity, while the state with spin 1 has negative  $C$ -parity and positive  $G$ -parity. As discussed in [109], the formation of a  $0^+$  state in the  $D^*\bar{D}^*$  system, in the process  $e^+e^- \rightarrow (D^*\bar{D}^*)^{\pm,0}\pi^{\mp,0}$  is not possible, due to the conservation of parity and angular momentum. However, both  $I^G(J^{PC}) = 1^+(1^{+-})$  and  $1^-(2^{++})$  can be assigned to  $Z_c(4020)$ . As can be seen from Table ??, the particle data group assigns a positive  $G$ -parity and negative  $C$ -parity to this state, which seems to be motivated by the assumption of spin 1 for the state  $Z_c(4020)$ . From Ref. [109], either of the possible quantum numbers  $1^+(1^{+-})$  or  $1^-(2^{++})$  can be associated to  $Z_c(4020)$ .

The central values of the results, given in Eq. (216), are in line with the findings of Refs. [110, 306, 307], although the mass values can be above the threshold when including error bars.

Other interpretations for the internal structure of this state, like a tetraquark nature, have also been suggested. Using QCD sum rules, in Ref. [312], a diquark-antidiquark structure was studied, giving rise to two possible spin-parity assignments for the state,  $J^{PC} = 1^{+-}$  or  $2^{++}$ . Using the same technique, in Ref. [313], considering  $J^P = 1^-$  and  $2^+$  tetraquark currents, it was found that the mass obtained with the  $2^+$  current was consistent with the experimental data of  $Z_c^+(4025)$ , while the mass determined with the  $1^-$  current was not compatible within the error-bars, suggesting then, a  $2^+$  assignment for the state.

The possibility of this  $Z_c$  state being a  $D^*\bar{D}^*$  molecule kind has also been investigated within QCD sum rules, in Ref. [314], using a color octet-octet axial-vector current and values for the mass and width were found to be

compatible with the experimental data, supporting the association of quantum numbers  $J^{PC} = 1^{+-}$  to  $Z_c(4020)$ . In Ref. [315] a  $J^P = 1^+$  molecular current was used and the mass extracted was  $(4.04 \pm 0.24)$  GeV. A similar conclusion was found in Ref. [316] with a different current and with calculations done up to leading order in  $\alpha_s$ . In Ref. [293], charmonium-like molecular interpolating currents with quantum numbers  $J^{PC} = 1^{+-}$  were constructed including both color singlet-singlet and color octet-octet structures and the authors arrived to the conclusion that  $Z_c(4025)$  could be a  $D^*\bar{D}^*$  or a  $D_1\bar{D}_1$  molecular state.

Evidence for a state with spin-parity  $0^{++}$ , and a mass around 4000 MeV, also comes from other formalisms; within the constituent quark model, in Ref. [317] a tetraquark with mass 4005.7 MeV and quantum numbers  $I(J^{PC}) = 1(0^{++})$  was found with a mass similar to  $Z_c(4025)$ . This result is in agreement with the  $0^{++}$  state found in [109] (as summarized in Eq. 216).

There exist other studies based on QCDSR, which find states with different spins, but almost same mass, as in [109]. Such is the case of Ref. [318], where using vector  $\times$  vector interpolating currents, the formation of  $J^{PC} = 0^{++}, 1^{+-}, 2^{++}$  molecular states was studied and the existence of three states was found, one for each spin, with basically the same mass, within the uncertainties, with a central value of 4.01-4.04 GeV.

#### 5.4. $Z_1^+(4050)$ , $Z_c^+(4055)$ and $Z_2^+(4250)$

In the energy region around 4050 MeV, two states with basically the same mass have been claimed,  $Z_1(4050)$  and  $Z_c(4055)$ , nowadays named as  $X(4050)$  and  $X(4055)$ . In spite of their similar masses, the quantum numbers assignments seem to differ, with the former being a state with positive  $C$ -parity, isospin 1 and negative  $G$ -parity, while the latter has isospin 1 but opposite  $C$ - and  $G$ -parities. The other quantum numbers are unknown.

The experimental evidence for  $Z_1(4050)$  is controversial, as in case of the state  $Z_2(4250)$  (or  $X(4250)$  in Ref. [22] notation): they were observed by the Belle collaboration [57] in the  $\pi^+\chi_{c1}(1P)$  invariant mass distribution of the reaction  $\bar{B}^0 \rightarrow K^-\pi^+\chi_{c1}(1P)$ . The fit to the data performed in Ref. [57] indicates that the consideration of two resonances is preferred by  $13.2\sigma$ , and that the inclusion of two resonances is preferable to the consideration of one by  $5.7\sigma$ . These fits were done assuming  $J = 0$  and 1 and the lowest possible orbital angular momentum for the system, but the  $\chi^2$  result of the fit is not significantly altered by changing  $J$ . However, the BaBar collaboration [58] could reproduce the data on the  $\pi^+\chi_{c1}(1P)$  invariant mass distributions of the processes  $\bar{B}^0 \rightarrow K^-\pi^+\chi_{c1}(1P)$  and  $B^+ \rightarrow K_S^0\pi^+\chi_{c1}(1P)$  with the  $Z$  resonance contribution consistent with zero.

In case of  $Z_c(4055)$ , the Belle collaboration claimed its existence based on an excess of events in the  $\pi^\pm\psi(2S)$  invariant mass of the process  $Y(4360) \rightarrow \pi^+\pi^-\psi(2S)$  with a  $3.5\sigma$  significance [59].

##### 5.4.1. Theoretical explanations for $Z_1^+(4050)$ , $Z_c^+(4055)$ and $Z_2^+(4250)$

The possibility of  $Z_1(4050)$  and  $Z_2(4250)$  being tetraquarks has been studied with different models. In Ref. [259], using a Cornell potential the four-quark configuration of  $Z_1(4050)$  as a cluster of  $Q\bar{q}$  and  $\bar{Q}q$  with some residual color forces that bind the two clusters is investigated and the existence of a state with mass 4046 MeV is found with quantum numbers  $J^{PC} = 2^{+-}$  together with a state with mass 4054 MeV and quantum number  $3^{++}$ . Both results are associated with  $Z_1(4050)$ . In Ref. [263], using a color flux-tube model, the authors arrived to the conclusion that  $Z_1(4050)$  has a tetraquark  $[cu][\bar{c}\bar{d}]$  nature, with a compact three-dimensional spatial configurations, with spin-parity  $J^P = 1^-$ , while  $Z_2(4250)$  can be interpreted as a  $[cu][\bar{c}\bar{d}]$  tetraquark with  $J^P = 1^+$ . No tetraquark candidate was found in Ref. [242] for  $Z_1(4050)$  by using a relativistic quark model. On the other hand,  $Z_2(4250)$  could be interpreted as a tetraquark [242].

In Ref. [319], possible molecular states composed by a pair of heavy mesons, as  $D^*$  and  $\bar{D}^*$ , were studied by means of a meson exchange potential obtained from an effective Lagrangian based on the chiral and heavy quark symmetries. The authors of Ref. [319] found two states, one with  $J^P = 0^+$  and other with  $J^P = 1^+$ , which could correspond to  $Z_1(4050)$ . However, as the authors mention, the values of the cut-off used seem too large (4 GeV for the  $0^+$  state and 10 GeV for the  $1^+$  state) and it is too naive to exclude, in such a situation, other components in the wave function of such a state. By using a chiral SU(3) quark model, the authors of Ref. [320] reached the conclusion that  $Z_1(4050)$  is unlikely to be an  $s$ -wave isospin 1  $D^*\bar{D}^*$  molecule. In Ref. [217], using heavy meson chiral perturbation and an effective meson exchange potential, the authors found that the consideration of  $Z_2(4250)$  as a  $D_1\bar{D}$  molecule with quantum numbers  $I^G(J^P) = 1^-(1^-)$  is disfavored, since it requires a cut-off in their model of around  $\Lambda \sim 3$  GeV.

#### 5.4.2. QCDSR calculations for $Z_1^+(4050)$ , $Z_c^+(4055)$ and $Z_2^+(4250)$

Within the context of QCD sum rules, the tetraquark and molecular pictures have also been investigated. In Ref. [312] it was concluded that the association of  $Z_1(4050)$  and  $Z_2(4250)$  with a  $J^{PC} = 0^{++}$  diquark-antidiquark tetraquark was disfavored. In Ref. [321], by considering a superposition of  $C\gamma_5 - C\gamma_5$  and  $C - C$  currents a state with mass  $(4.36 \pm 0.18)$  GeV was found and associated with  $Z_2(4250)$ . In Ref. [293], the authors constructed charmonium-like molecular interpolating currents with quantum numbers  $J^{PC} = 1^{+-}$  and found that  $Z_1(4050)$  could be described by a  $D^*\bar{D}^*$  or a  $D_1\bar{D}_1$  molecular current, and  $Z_2(4250)$  with a  $D\bar{D}^*$  molecular current. In Ref. [91] the  $I^G(J^P) = 1^-(0^+)$  current

$$(\bar{d}\gamma_\mu c)(\bar{c}\gamma^\mu u) \quad (217)$$

was used to study the  $D^*\bar{D}^*$  system and the  $I^G(J^P) = 1^-(1^-)$  current

$$\frac{i}{\sqrt{2}}[(\bar{d}\gamma_\mu\gamma_5 c)(\bar{c}\gamma_5 u) + (\bar{d}\gamma_5 c)(\bar{c}\gamma_\mu\gamma_5 u)] \quad (218)$$

was used to investigate the  $D_1\bar{D}$  system. In the case of the  $D^*\bar{D}^*$  system, a state with a mass around 130 MeV above the threshold and 100 MeV above the nominal mass of  $Z_1(4050)$  was found, while for the  $D_1\bar{D}$  system a state with a mass around 100 MeV below the threshold and 60 MeV below the mass of  $Z_2(4250)$  was obtained. In the former case, it was concluded that the signal found could be probably a virtual state which is not related to  $Z_1(4050)$ , while in the latter, the mass found is consistent with both  $Z_1(4050)$  and  $Z_2(4250)$  and thus no definite conclusions could be drawn.

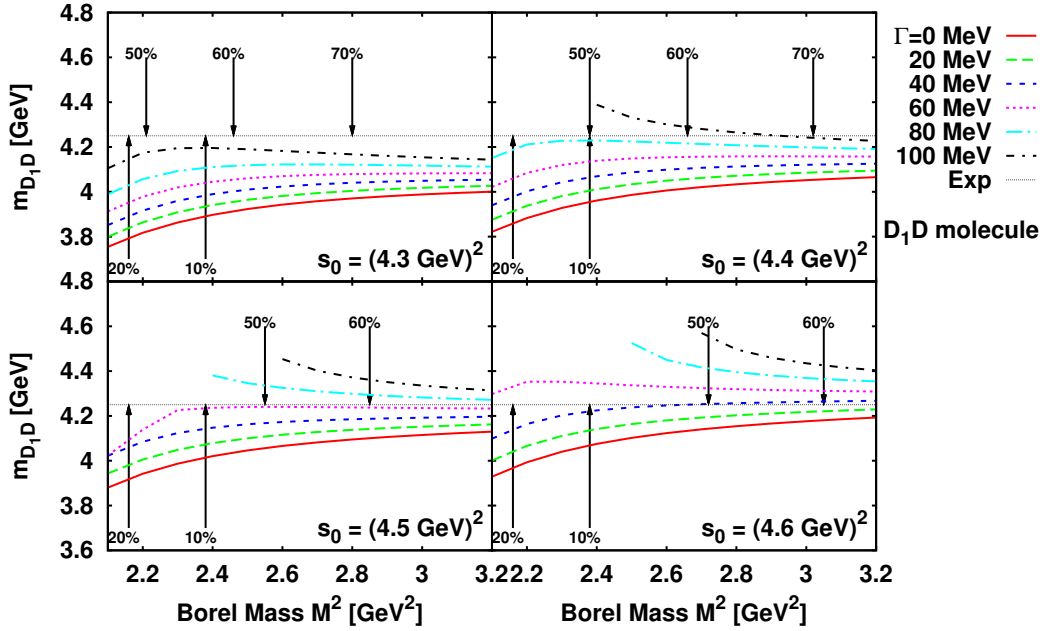


Figure 23: Results for the  $D_1D$  molecule from Ref. [90]. Each panel shows a different choice of the continuum threshold. Upward and downward arrows indicate the region of the Borel window  $M_{\min}^2$  and  $M_{\max}^2$ , respectively. Associated numbers in % denote the dimension eight condensate contribution for upward arrows and continuum contribution for downward ones. Taken from [90].

These conclusions were reached by ignoring the width of the  $Z$  states in the spectral density of the phenomenological side of the sum rule. In view of this, in Ref. [90] the same authors incorporated the width in the phenomenological spectral density and studied its effect on the mass, finding that using the current in Eq. (218), it is possible to obtain a mass  $m_{D_1D} = 4.25$  GeV with a width  $40 \leq \Gamma \leq 60$  MeV, in agreement with the mass and width of  $Z_2(4250)$ , as can be seen in Fig. 23.

Therefore, the authors of Ref. [90] conclude that it is possible to describe the  $Z_2^+(4250)$  resonance structure with a

$D_1\bar{D}$  molecular current with  $I^G J^P = 1^- 1^-$  quantum numbers, and that the  $D^*\bar{D}^*$  current is probably not related with the  $Z_1^+(4050)$  resonance-like structure.

### 5.5. $Z_c^+(4200)$

The existence of  $Z_c(4200)$  is based on the study of the  $\psi\pi^+$  mass spectrum, obtained in the decay process  $\bar{B}^0 \rightarrow J/\psi K^- \pi^+$ , by the Belle Collaboration [67]. The  $\chi^2$ -fit to the experimental data with the spin-parity assignment of  $1^+$  for the  $Z_c(4200)$  state leads to the highest statistical significance ( $8.2\sigma$ ) [67]. The same data set also shows a signal for the better known  $Z_c(4430)$ . The mass and width for  $Z_c(4200)$  are found to be  $4196_{-70}^{+31+17}$  MeV and  $370_{-70}^{+70+70}$  MeV, respectively, in Ref. [67]. The inclusion of a  $Z_c$  state with mass around 4200 MeV, apart from  $Z_c(4430)$ , in the experimental data on  $B^0 \rightarrow J/\psi K^- \pi^+$ , was also considered by the LHCb collaboration [84] and the quality of the fit was found to improve with the consideration of two  $Z_c$  states rather than  $Z_c(4430)$  alone. Although the mass and width of the state near 4200 MeV found by the LHCb collaboration,  $4239 \pm 18_{-10}^{+45}$  MeV and  $220 \pm 47_{-74}^{+108}$  MeV, are compatible with those determined in Ref. [67], the preferred spin-parity was found to be different,  $0^-$ . The LHCb collaboration, though, does not claim the observation of any state with mass around 4200. The particle data group, thus, lists its spin-parity to be  $1^+$ . In a recent article [322], the D0 collaboration confirms finding a resonant structure above 4 GeV which is similar to the one found in Ref. [67]. An analysis of the decay  $\Lambda_b^0 \rightarrow J/\psi p \pi^-$  was made by the LHCb collaboration and it was found that the inclusion of either the two exotic pentaquarks,  $P_c^+$ , or that of  $Z_c(4200)$ , was important to describe the data [127].

#### 5.5.1. Theoretical explanations and QCDSR calculations for $Z_c^+(4200)$

From a theoretical point of view, a tetraquark nature of  $Z_c(4200)$  has been studied within different model calculations. For example, the authors of Ref. [323] find a  $[cu][\bar{c}\bar{d}]$  state, with quantum numbers  $n(^{2S+1}L_J) = 1(^3D_1)$  and spin-parity  $1^+$  and associate it with  $Z_c(4200)$ , in a model treating quark-quark interactions through one gluon exchange, one boson exchange and  $\sigma$  exchange. Evidence for  $Z_c(4200)$  has also been found in a light-front holographic QCD model with a generic dilaton profile [324]. Using a formalism based on color magnetic interactions, in Ref. [325],  $Z_c(4200)$  is described as an axial vector tetraquark state.

More information is available from other works. A study of the cross sections of the process  $p\bar{p} \rightarrow Z_c^0(4200)\pi^0$  has been done in Ref. [326] and it has been suggested that proton-antiproton annihilation is an ideal process to investigate the neutral  $Z_c(4200)$ . Further, an estimate of the upper limit of the partial width  $\Gamma(Z_c(4200) \rightarrow J/\psi\pi)$  has been done in Ref. [327] to be  $\sim 37$  MeV. Based on a tetraquark nature of  $Z_c(4200)$  with  $J^{PC} = 1^{+-}$ , it is also argued in Ref. [328] that the decay  $Z_c(4200) \rightarrow h_c\pi$  should be suppressed.

Within QCD sum rules, using the current

$$J_\mu(x) = \frac{\bar{u}i\gamma_5\lambda^a c(x)\bar{c}(x)\gamma_\mu\lambda^a d(x) + \bar{u}\gamma_\mu\lambda^a c(x)\bar{c}(x)i\gamma_5\lambda^a d(x)}{\sqrt{2}}, \quad (219)$$

$Z_c(4200)$  is described as an octet-octet type axial vector molecule-like state [314]. The decay widths of  $Z_c(4200) \rightarrow J/\psi\pi^+$ ,  $\eta_c\rho^+ D^+\bar{D}^{*0}$ ,  $\bar{D}^0 D^{*+}$  were obtained in Ref. [329], respectively, as  $87.3 \pm 47.1$  MeV,  $334.4 \pm 119.8$  MeV and  $6.6 \pm 6.4$  MeV, using the following current for  $Z_c(4200)$

$$J_\nu = u_a^T C \gamma_5 c_b (\bar{d}_a \gamma_\nu C \bar{c}_b^T + \bar{d}_b \gamma_\nu C \bar{c}_a^T) - u_a^T C \gamma_\nu c_b (\bar{d}_a \gamma_5 C \bar{c}_b^T + \bar{d}_b \gamma_5 C \bar{c}_a^T). \quad (220)$$

The obtained total width is consistent with the experimental value  $\Gamma = (370 \pm 70_{-132}^{+70})$  MeV [67].

Another study, based on QCD sum rules, has been done in Ref. [293], where a  $D\bar{D}^*$  current has been suggested for  $Z_c(4200)$ . However, this suggestion is not consistent with the usual interpretations where the  $D\bar{D}^*$  current is associated with the  $X(3872)$  state.

### 5.6. $Z_c^-(4100)$

The  $Z_c^-(4100)$  state is the newest acquisition to the list of charged exotic charmonium states. The evidence for the existence of  $Z_c(4100)$  was reported by the LHCb Collaboration [60] and is based on the study of the  $\eta_c(1S)\pi^-$  mass spectrum, obtained from the decay process  $B^0 \rightarrow \eta_c(1S)K^+\pi^-$ . The reported significance of this exotic resonance is more than three standard deviations. Its mass and width are  $M = (4096 \pm 20_{-22}^{+18})$  MeV and  $\Gamma = (152 \pm 58_{-35}^{+60})$  MeV

respectively, and the spin-parity assignments  $J^P = 0^+$  and  $1^-$  are both consistent with data [60]. Since  $Z_c^-(4100)$  decays into  $\eta_c(1S)\pi^-$  its  $G$ -parity is  $-$ . Therefore, the possible quantum numbers for its neutral partner are  $I^G(J^{PC}) = 1^-(0^{++})$  or  $1^-(1^{+-})$ . While  $J^{PC} = 0^{++}$  are quantum numbers that can be also associated with quark-antiquark states,  $J^{PC} = 1^{--}$  is not consistent with the constituent quark model for a quark-antiquark system and it is considered exotic. Up to now only one state is known with such quantum numbers:  $\pi_1(1600)$  [22].

### 5.6.1. Theoretical explanations and QCDSR calculations for $Z_c^-(4100)$

In Ref. [60] it was suggested that this state could be the  $J^P = 0^+$  tetraquark predicted by the diquark model in [186]. However, the predicted masses for the  $0^{++}$  tetraquark states were 3723 MeV and 3823 MeV, well below the observed mass [186]. Up to now there are only a few theoretical calculations for  $Z_c^-(4100)$ . In Ref. [330] the authors used a simple chromomagnetic model to study the mass splitting among tetraquark states, including  $Z_c^-(4100)$ . The model is based on the description that the mass splitting among hadron states, with the same quark content, are mainly due to the chromomagnetic interaction term in the one-gluon-exchange potential. Based on these findings the authors concluded that  $Z_c^-(4100)$  seems to be a  $0^{++}$  ( $cq)(\bar{c}\bar{q})$  tetraquark state. In Ref. [331] it was argued that  $Z_c^-(4100)$  is (dominantly) a hadrocharmonium with the  $\eta_c$  embedded in a light  $t$ -quark excitation, with quantum numbers of the pion, in the same way that  $Z_c(4200)$  is a similar four-quark state containing  $J/\psi$  instead of  $\eta_c$ . In this approach the natural quantum numbers for  $Z_c^-(4100)$  would be  $0^+$ . In Ref. [332] the  $Z_c^-(4100)$  can either be interpreted as a  $P$ -wave resonance state arising from the  $D^*\bar{D}^*$  interaction, or be caused by final state interaction effects. In Ref. [333] the author conjecture that the  $Z_c^-(4100)$  observed in the  $\eta_c\pi^-$  decay channel is the charge conjugate of the  $Z_c^+(4050)$  observed in the  $\chi_{c1}\pi^+$  decay channel.

In Ref. [227] the author used a  $P$ -wave diquark-antidiquark  $J^{PC} = 1^{--}$  interpolating field, in a QCDSR calculation, to study the mass of possible  $J^{PC} = 1^{--}$  tetraquark charmonium states. The obtained mass disfavors the assignment of  $Z_c^-(4100)$  as a vector tetraquark state. Besides, as pointed out above,  $J^{PC} = 1^{--}$  quantum numbers are not allowed for  $Z_c^-(4100)$ . A QCDSR calculation for a  $J^{PC} = 1^{+-}$  four-quark state, using a molecular  $D^*D_0^*$  current, was done in Ref. [97]. The obtained mass was  $m_{D^*D_0^*} = (4.92 \pm 0.08)$  GeV [97]. In another QCDSR calculation, using a tetraquark current with  $J^{PC} = 1^{+-}$ , the obtained mass was around 4.6 GeV [197]. In both cases the obtained masses are not consistent with the  $Z_c^-(4100)$  observed mass. On the other hand a mass  $m_{X,0^{++}} = (3.81 \pm 0.19)$  GeV was obtained in a QCDSR calculation for a scalar  $0^{++}$  tetraquark state! [? ], in excellent agreement with the mass obtained using a spin 0 projection of a  $\bar{D}^*D^*$  interpolating current as shown in Fig. 22 and given in Eq. (216):  $M^{S=0} = (3.94 \pm 0.10)$  MeV [109], and with a  $0^{++}$   $\bar{D}_0^*D_0^*$  interpolating current in a N2LO QCDSR calculation:  $m_{X,0^{++}} = (3.95 \pm 0.22)$  GeV [115]. Therefore, the theoretical calculations seem to indicate that the  $0^{++}$  quantum numbers are more compatible with the observed mass.

### 5.7. Summary for the isovector $Z$ states

The discovery of several manifestly exotic states, the  $Z^+$  states, may be considered as one of the most exciting findings of the last years. The description of such states unavoidably requires (at least) four valence quarks in the wave function. For the first of them,  $Z^+(4430)$ , there is now basically a consensus that it is the first radial excitation of  $Z_c^+(3900)$ . This interpretation favors a diquark-antidiquark tetraquark assignment for the  $Z_c^+(3900)$ . Using a four-quark current in the QCDSR approach, one can explain not only the mass, but also the decay width of  $Z_c^+(3900)$ . The ratio in Eq. (193) still remains to be explained. Regarding the state  $Z_c^+(4020)$ , it is possible to explain its mass either as a  $J^{PC} = 1^{+-}$  or a  $J^{PC} = 2^{++}$  state, from a  $D^*\bar{D}^*$  current. More experimental information is needed to confirm the existence of the states  $Z_1^+(4050)$  and  $Z_2^+(4250)$ , as well as the new state just observed by LHCb,  $Z_c^-(4100)$ .

## 6. Controversial $Y$ states

### 6.1. $Y(3940)$ or $X(3915)$ state

The  $Y(3940)$  was first observed by the Belle Collaboration in the decay  $B \rightarrow KY(3940) \rightarrow K\omega J/\psi$  [47]. It was later confirmed by BaBar in two channels  $B^+ \rightarrow K^+\omega J/\psi$  and  $B^0 \rightarrow K^0\omega J/\psi$  [32, 48]. The measured mass from these two Collaborations are:  $(3943 \pm 11)$  MeV from Belle and  $(3919.1^{+3.8}_{-3.4} \pm 2)$  MeV from BaBar, which gives an average mass of  $(3929 \pm 7)$  MeV and the total width  $(31^{+10}_{-8} \pm 5)$  MeV. This state has positive  $C$  and  $G$  parities and its possible spin-parity is  $J^P = 0^+$  or  $2^+$ . A similar state was observed also by Belle Collaboration [49] in  $\gamma\gamma \rightarrow \omega J/\psi$

process. The measured mass and decay width are  $M = (3915 \pm 3 \pm 2)$  MeV and  $\Gamma = (17 \pm 10 \pm 3)$  MeV, respectively and the state was called  $X(3915)$ . It also carries positive  $C$  and  $G$  parities. From the  $\gamma\gamma$  fusion process, the possible spin-parity for the  $X(3915)$  is also  $J^P = 0^+$  or  $2^+$ . The BaBar Collaboration confirmed the existence of the  $X(3915)$  decaying into  $\omega J/\psi$  in  $\gamma\gamma \rightarrow \omega J/\psi$  process, with the mass  $(3919.4 \pm 2.2 \pm 1.6)$  MeV and width  $(13 \pm 6 \pm 3)$  MeV [50]. Their analysis favored the  $J^P = 0^+$  assignment.

Due to the recent smaller mass observed by the BaBar Collaboration for the  $Y(3940)$  [32], in PDG [22] both states are considered as the same and are called  $X(3915)$ . In this review we keep the original name  $Y(3940)$ . The decay  $Y \rightarrow J/\psi\omega$  is OZI suppressed for a charmonium state and hence the  $Y(3940)$  is a candidate to be an exotic, a hybrid, a molecular or a tetraquark state.

## 6.2. $Y(4140)$ state

The first observation of the  $Y(4140)$  structure was reported by the CDF Collaboration in the exclusive  $B^+ \rightarrow J/\psi\phi K^+$  decays, in 2009 [61]. A prominent peak was observed in the  $J/\psi\phi$  mass spectrum with mass  $M = 4143.4_{-3.0}^{+2.9}$  (stat)  $\pm 0.6$  (syst), and decay width  $\Gamma = 15.3_{-6.1}^{+10.4}$  (stat)  $\pm 2.5$  (syst). In 2010, however, the Belle Collaboration performed an analysis of the data for events on the two-photon process and, as a result, no signal of the  $Y(4140)$  state was found [76]. Soon after, in 2011, the LHCb Collaboration corroborated Belle's data, also reporting negative results in the search for the  $Y$  structure [334]. Later on, the CMS Collaboration confirmed the observation of the  $Y(4140)$  and another state, called  $Y(4274)$ , in exclusive  $B^+ \rightarrow J/\psi\phi K^+$  decays [335]. Recently, the LHCb Collaboration performed a full amplitude analysis of  $B^+ \rightarrow J/\psi\phi k^+$  decays [64, 336] and claimed that four structures were required to fit the data, and the  $Y(4140)$  was one of them. However, according to the LHCb results, the  $Y(4140)$  is most likely a  $J^{PC} = 1^{++}$  state and has a width  $\Gamma \approx 83 \pm 24 \pm_{-14}^{+21}$ , which is significantly larger than the one reported by the former experiments. Finally, the BESIII Collaboration searched for  $Y(4140)$  via  $e^+ e^- \rightarrow \gamma\phi J/\psi$  at  $\sqrt{s} = 4.23, 4.26, 4.36,$  and  $4.60$  GeV, but no significant  $Y(4140)$  signal is observed in any of the data samples [65, 66].

In spite of these controversial experimental results, over the last decade there have been many experimental studies of the  $J/\psi\phi$  mass spectrum, and we expect the  $Y(4140)$  to be confirmed in the future analysis.

## 6.3. Theoretical interpretations for the $Y(3940)$ and $Y(4140)$

On the theoretical side, many efforts to understand the  $Y(3940)$  and  $Y(4140)$  nature have been made. The  $Y(4140)$  is the first state to be observed decaying into two heavy mesons containing both  $c\bar{c}$  and  $s\bar{s}$  content. Since it is far above the open charm threshold, it would be expected to decay into open charm states with a large decay width. However, this feature is not observed by the experimental collaborations. In addition, since both  $J/\psi$  and  $\phi$  mesons have  $J^{PC} = 1^{--}$  quantum numbers, the states observed in the  $J/\psi\phi$  mass spectra must have positive  $C$ -parity such that the exotic  $1^{++}$  quantum numbers are accessible. This set of quantum numbers is not allowed for any conventional charmonium state. Thus, these features put the  $Y(4140)$  into the list of candidates that require exotic quark configurations to be understood.

In Ref. [337] the exotic  $1^{++}$  quantum numbers were assigned to  $Y(4140)$  assuming it to be a hybrid charmonium state, although it was argued that the  $D_s^* \bar{D}_s^*$  molecular interpretation could also be applied to the  $Y$  state.

A conventional charmonium interpretation was adopted in Ref. [338], where the  $Y(4140)$  was assumed to be the second radial excitation of the  $P$ -wave charmonium  $\chi_{cJ}' (J = 0, 1)$ . With this assumption, the hidden charm decay mode of  $Y$  was estimated in terms of the rescattering mechanism and, as a result, the value obtained was much smaller than the one reported by the CDF Collaboration in Ref. [61]. This result indicates that the conventional charmonium picture cannot be ascribed to the  $Y$  structure.

A tetraquark model was used in Ref. [339]. However, this model provides a decay width around 100 MeV for the  $Y$  with  $J^{PC} = 0^{++}$ . According to the experimental results, this interpretation cannot be supported since the decay width measured for the  $Y(4140)$  is around 11-20 MeV. On the other hand, the  $J^{PC} = 1^{++}$  quantum numbers seem to be favored by the tetraquark model since the decay width estimated, in this case, provides a result smaller than the one obtained assigning  $J^{PC} = 0^{++}$  for  $Y$ .

Since the  $Y(3940)$  and  $Y(4140)$  masses are close to  $D^* \bar{D}^*$  and  $D_s^* \bar{D}_s^*$  thresholds respectively, it seems natural to adopt a molecular picture to understand their features. In fact, in Ref. [340] the authors have investigated these meson molecules through a meson-exchange model and claimed that the  $Y(3940)$  must be the molecular,  $D^* \bar{D}^*$ , partner of the  $Y(4140)$ , a  $D_s^* \bar{D}_s^*$  molecule. This interpretation has been tested in several approaches, such as phenomenological Lagrangians [341] and vector-meson dominance models [342].



On the other hand, within the QCDSR approach such quark configuration can be described, and an estimate for the  $Y(4140)$  mass can be done for a current with  $J^{PC} = 0^{++}$ . In addition, a tensorial  $2^{++}$  state can also be studied with QCDSR with the help of spin projectors, which will be discussed later. In the following subsection we start to discuss the results obtained for  $Y(3940)$  and  $Y(4140)$  using the  $D^*\bar{D}^*$  and  $D_s^*\bar{D}_s^*$  multi-quark configurations with  $0^{++}$  quantum numbers, in the QCDSR approach.

#### 6.4. QCDSR calculations for the $Y(3940)$ and $Y(4140)$

Considering  $Y(4140)$  as a  $D_s^*\bar{D}_s^*$  structure with  $I^G(J^{PC}) = 0^+(0^{++})$ , a suitable interpolating current describing such state, considered in Ref. [95], is given by

$$j_{D_s^*\bar{D}_s^*} = (\bar{s}_a \gamma_\mu c_a)(\bar{c}_a \gamma^\mu s_b). \quad (221)$$

The authors considered contributions from the condensates up to dimension eight on the OPE side. The QCDSR analysis done showed a good Borel stability for  $M^2$  values in the interval  $2.3 \leq M^2 \leq 3.0 \text{ GeV}^2$ , with  $4.4 \leq \sqrt{s_0} \leq 4.7 \text{ GeV}$ . The effects related to the violation of the factorization hypothesis were also included in the error estimates. The result obtained for the mass was

$$m_{D_s^*\bar{D}_s^*} = (4.14 \pm 0.09) \text{ GeV}, \quad (222)$$

in good agreement with the experimental mass of the narrow structure  $Y(4140)$ .

A similar analysis based on the QCDSR technique was done in Ref. [343] in which the author also adopted a  $D_s^*\bar{D}_s^*$  molecular interpolating current with  $0^{++}$ . However, the result found in this latter work was different, around 290 MeV higher than the one obtained in Eq. (222), and equal to

$$m_{D_s^*\bar{D}_s^*} = (4.43 \pm 0.16) \text{ GeV}. \quad (223)$$

In order to get this result, in Ref. [343] the condensates up to dimension eight were also included in the OPE. But, in this case, the convergence seems to be too slow in comparison to the one in Ref. [95]. In fact, the minimum for the Borel mass in the former work is  $2.6 \text{ GeV}^2$  against  $2.3 \text{ GeV}^2$  in the latter one. In addition, the Borel window in the work of Ref. [343] is smaller, implying a smaller  $M^2$  region of stability.

From the QCDSR calculations done in Ref. [95], it is possible to get a sum rule for a  $D^*\bar{D}^*$  structure, by simply replacing the strange/anti-strange quark fields by the corresponding up/anti-up and down/anti-down quark in the interpolating current definition in Eq. (221). In this case, the interpolating current for  $D^*\bar{D}^*$  is

$$j_{D^*\bar{D}^*} = (\bar{q}_a \gamma_\mu c_a)(\bar{c}_a \gamma^\mu q_b). \quad (224)$$

It was expected that the structure described by this current could be used to explain the  $Y(3940)$  state as suggested in Ref. [340]. The mass obtained in [95] for such a structure is consistent, considering the errors, with the result in Eq. (216) and also consistent with the result in Eq. (222). The degeneracy between the QCDSR results for these two currents in Eqs. (224) and (221) is not surprising. In fact, from the point of view of a standard mass sum rule, like the one used here, the difference in studying the  $D^*\bar{D}^*$  or the  $D_s^*\bar{D}_s^*$  system arises from the fact that the latter one involves diagrams with strange quarks instead of the light ones. In the  $D^*\bar{D}^*$  case, the mass of the light quarks ( $u$  and  $d$ ) is taken to be negligible, thus, the corrections to the free propagator are related to condensates involving light quarks and gluons, while in the  $D_s^*\bar{D}_s^*$  case we have corrections associated with strange quark condensates, gluon condensates and the mass of the  $s$  quark. Since, as can be seen from Table 2, the value for the light quark condensate is larger than the one of the strange quark, this difference is compensated by the  $m_s$  corrections for the case of the  $D_s^*\bar{D}_s^*$  system.

In Ref. [253] a mass of 3.9 GeV was obtained from the application of the QCDSR approach to the  $D^*\bar{D}^*$  current. In this case, the OPE was calculated up to dimension six, and the OPE convergence was found to be slower. It can be shown that the OPE convergence could be improved if the contributions from the condensates up to dimension eight would be included. Furthermore, the QCDSR analysis of Ref. [253] does not present any pole dominance, which means that a reliable Borel window cannot be established, compromising the results for the mass.

Although in Ref. [340] it has been argued that the  $D_s^*\bar{D}_s^*$  and  $D^*\bar{D}^*$  molecules could be assigned to the  $Y(4140)$  and  $Y(3940)$ , respectively, within QCDSR both currents provide similar masses. On the other hand, a molecular-charmonium interpretation for the  $Y(3940)$  is also possible. Indeed, in Ref. [111], a mixed  $(\chi_{c0})-(D^*\bar{D}^*)$  current, with

$J^{PC} = 0^{++}$ :

$$j = -\cos\theta \frac{\langle \bar{q}q \rangle}{\sqrt{2}} j_{\chi_{c0}} + \sin\theta j_{D^*D^*}, \quad (225)$$

was used to study the  $Y(3940)$  state. The current in Eq. (225) is similar to the ones used in Secs.3.3 and 4.1.2 to study the states  $X(3872)$  and  $Y(4260)$  respectively, with  $\theta$  being the mixing angle. The molecular  $D^*\bar{D}^*$  current is given in Eq. (224) and the  $\chi_{c0}$  current is:  $j_{\chi_{c0}} = \bar{c}_k c_k$ .

Fixing the mixing angle in the range  $\theta = (76.0 \pm 5.0)^\circ$ , the mass obtained in [111] for the mixed state is:

$$M_Y = (3.95 \pm 0.11) \text{ GeV}, \quad (226)$$

which is in agreement, within the errors, with the experimental mass for the  $Y(3940)$  state observed by the Belle Collaboration:  $(3943 \pm 11) \text{ MeV}$ [47], and by BaBar:  $(3919.1^{+3.8}_{-3.4} \pm 2)$  [32].

Since it is possible to explain the mass of the  $Y(3940)$  with the mixed current, in Ref. [111] the decay width  $Y(3940) \rightarrow J/\psi \omega$  was also considered. The three-point function for the vertex  $YJ/\psi \omega$  is defined as:

$$\Pi_{\mu\nu}(p, p', q) = \int d^4x d^4y e^{ip' \cdot x} e^{iq \cdot y} \langle 0 | T \{ J_\mu^\psi(x) J_\nu^\omega(y) j^\dagger(0) | 0 \rangle, \quad (227)$$

where the mixed  $(\chi_{c0})-(D^*\bar{D}^*)$  current, given in Eq. (225), was considered, and

$$J_\mu^\psi = (\bar{c}_a \gamma_\mu c_a), \quad J_\nu^\omega = \frac{1}{6} (\bar{u}_a \gamma_\nu u_a + \bar{d}_a \gamma_\nu d_a). \quad (228)$$

The OPE side of the correlation function was evaluated at the leading order in  $\alpha_s$ , considering condensates up to dimension 7, in the  $q_\mu p'_\nu$  structure [111]. After extrapolating the form factor to the  $\omega$  pole, following the procedure discussed in Sec. 2.8 the coupling constant, using the same mixing angle  $\theta = (76.0 \pm 5.0)^\circ$ , was obtained as,  $g_{Y\psi\omega} = (0.58 \pm 0.14) \text{ GeV}^{-1}$ ,

The decay width for the process  $Y(3940) \rightarrow J/\psi \omega$  is given by

$$\Gamma_{Y(3940) \rightarrow J/\psi \omega} = \frac{g_{Y\psi\omega}^2}{3} \frac{p(M_Y, M_\omega, M_\psi)}{8\pi M_Y^2} \left( M_\psi^2 M_\omega^2 + \frac{1}{2} (M_Y^2 - M_\psi^2 - M_\omega^2)^2 \right), \quad (229)$$

where

$$p(a, b, c) \equiv \frac{\sqrt{a^4 + b^4 + c^4 - 2a^2b^2 - 2a^2c^2 - 2b^2c^2}}{2a}. \quad (230)$$

Inserting the value obtained for the coupling constant in Eq.(229) one gets [111]:

$$\Gamma_{Y(3940) \rightarrow J/\psi \omega} = (1.7 \pm 0.6) \text{ MeV}. \quad (231)$$

This result is consistent with the experimental width of the state and the lower limit for the process  $Y \rightarrow J/\psi \omega$  [47, 48]. It is also of the same order as other available theoretical evaluations [341, 342].

As we have seen, many efforts have been done in order to understand the quark configuration of the  $Y(3940)$  and  $Y(4140)$  structures as well as their  $J^{PC}$  quantum numbers. From the theoretical side, many models such as the conventional charmonium, hybrid, tetraquark, meson molecule and mixed states have been employed to investigate these systems.

As mentioned before, the new LHCb analysis on the  $J/\psi\phi$  data brought surprises to the spectrum around 4.1 GeV since other structures were seen in this channel. According to the LHCb results, in order to fit the data, the  $Y(4140)$  is required to have a large decay width. This new value is close, within the error bars, to the one reported for the  $Y(4140)$  state, measured by the Belle Collaboration [52] in the  $D^*\bar{D}^*$  mass spectra in the process  $e^+e^- \rightarrow J/\psi D^*\bar{D}^*$ . The mass and width obtained for this state are  $M = 4156 \pm 29 \text{ MeV}$  and  $\Gamma = 139^{+113}_{-65} \text{ MeV}$ , respectively [52]. Its quantum numbers, such as, spin, isospin, and parity are not known yet. The decay of  $X(4160)$  to  $D^*\bar{D}^*$ , in a  $D_s^*\bar{D}_s^*$  molecular model, could be understood in terms of triangular loop diagrams involving a strange meson. In this perspective, the

$X(4160)$  state could be a  $D_s^* \bar{D}_s^*$  molecule-like structure. In fact, a dynamically generated state that could be assigned to  $X(4160)$  was found in many coupled channel investigations [306, 342, 344]. If we compare its mass and width with the corresponding ones known for  $Y(4140)$ , and also have in mind that both are close to the  $D_s^* \bar{D}_s^*$  threshold, a question arises: are they the same state?

With the aim to shed light on this discussion, in Ref. [114], a more general QCDSR analysis was done, considering a tensorial current that allows exploring spin contributions other than the  $0^{++}$ , considered by the QCDSR works discussed above. We are going to discuss the details of this analysis in the next subsection.

### 6.5. The $Y(4140)$ and $X(4160)$ with a tensorial current

The simplest vector times vector type interpolating current coupling to the  $D_s^{*+} D_s^{*-}$  meson-meson system, used in Ref. [114], is given by

$$j_{\mu\nu}(x) = (\bar{c}_a \gamma_\mu s_a) (\bar{s}_b \gamma_\nu c_b). \quad (232)$$

As discussed in Sec. 5.3.2, since the current in Eq. (232) is tensorial, it provides contributions for spin 0, 1, and 2 particles. From calculations in the QCDSR approach for both, mass and decay width, the contributions from different spins can be studied separately by projecting a particular spin using the projectors defined in Eqs. (212), which separate the  $J^P = 0^+, 1^+, 2^+$  contributions to the correlation function. If a state of isospin  $I$ , and spin  $S$  is formed as a consequence of the interaction between a  $\bar{D}_s^*$  and a  $D_s^*$  meson with angular momentum  $L$ , the parity  $P$ , charge conjugation  $C$ , and  $G$ -parity, associated with a particular state can be determined through:  $P = (-1)^L$ ,  $C = (-1)^{L+S}$ , and  $G = (-1)^{L+S+I}$ . In the case considered here, since  $I = 0$  and  $L = 0$ , the possible states must have positive parity and  $C = G = (-1)^S$ . This means that the states with quantum numbers  $I^G(J^{PC}) = 0^+(0^{++})$ ,  $0^-(1^{+-})$ ,  $0^+(2^{++})$ .

In Ref. [114] a QCDSR calculation, based on the current in Eq. (232), was done considering contributions from the QCD condensates up to dimension eight, for each spin projection. As a result, three states were found with isospin 0, nearly degenerate, with masses around 4.1 GeV:

$$M_0 = (4.114 \pm 0.130) \text{ GeV}, \quad (233)$$

$$M_1 = (4.120 \pm 0.127) \text{ GeV}, \quad (234)$$

$$M_2 = (4.117 \pm 0.123) \text{ GeV}. \quad (235)$$

This result suggests the presence of a  $I^G(J^{PC}) = 0^{++}$ , a  $0^-(1^{+-})$  and a  $0^+(2^{++})$  states with masses given by the values in Eqs. (233), (234) and (235), respectively.

It is worth mentioning that the  $\bar{D}^* D^*$  system, described in Sec. 5.3.2, revealed the possibility of having spin 0, 1, and 2 states with masses around  $3950 \pm 100$  MeV (see Eq. (216)) with isospin 0 and 1. Comparing the masses obtained in the study of the  $\bar{D}^* D^*$  (isoscalar) current [109] with Eqs. (233), (234), (235), we clearly see that, within the errors, the two results are compatible. Within the QCDSR technique the reason for this degeneracy can be understood recalling that the additional  $m_s$  contributions on the OPE side of the  $D_s^* \bar{D}_s^*$  sum rule, for each spin case, are compensated by the smaller value of the strange quark condensate as compared with the light quark condensate. Therefore, one ends up with no significant difference in the sum rules results for both,  $D_s^* \bar{D}_s^*$  and  $D^* \bar{D}^*$  currents. Furthermore, this degeneracy can also be interpreted as a manifestation of heavy quark symmetry. In fact, although the strange quarks are heavier than the light quarks when compared a  $D^* \bar{D}^*$  state with a  $D_s^* \bar{D}_s^*$  state, there are two charm quarks in both systems. Since the charm quarks are much heavier than both, strange and light quarks, their presence overshadows the mass difference between light and strange quarks. This can be compared to the use of heavy quark symmetry in the calculations based on effective field theories, where  $D^* \bar{D}^*$  and  $D_s^* \bar{D}_s^*$  are considered as coupled channels. The results obtained in these calculations [345] seem to be very similar to the ones discussed in this subsection.

Even arguing that this degeneracy can be understood as a manifestation of heavy quark symmetry or by the QCDSR point of view, an intriguing question still remains: are the states found in Ref. [109] the same as the ones in Ref. [114]? There are two possibilities. One is that the states found in the QCDSR studies can couple to both currents, since they have the same quantum numbers. Therefore, they can be the same states and hence, we conclude that there are only three states in the mass interval 3.8-4.2 GeV, with  $0^{++}$ ,  $1^{+-}$  and  $2^{++}$  quantum numbers. Another possibility is that both QCDSR studies describe different states, due to their quark content and, in this case, we have six different states in the mass region 3.8-4.2 GeV. In either case, just the mass analysis is not enough to discriminate between

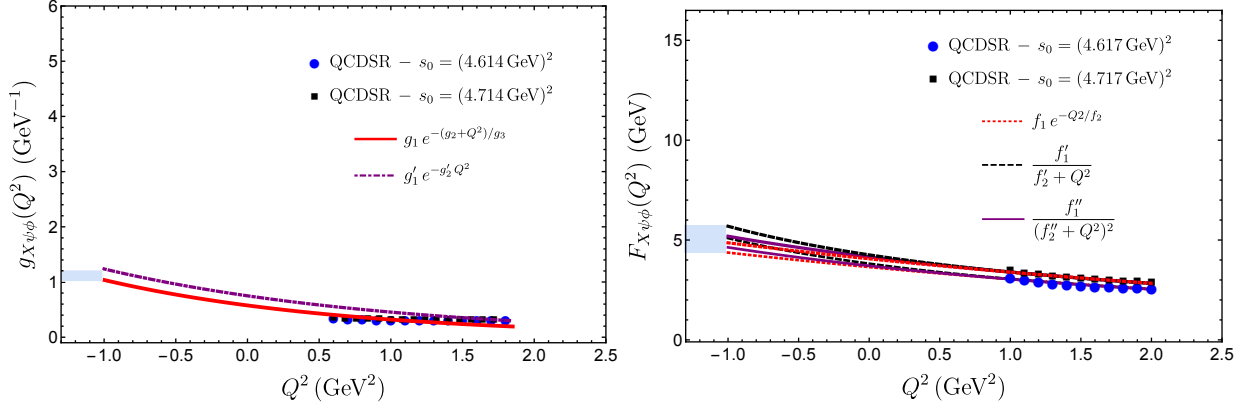


Figure 24: Solutions for the form factors for spin 0 (left panel) and spin 2 (right panel) cases for a fixed  $M^2$ . The shaded region in the figures represents the range of the values for the corresponding coupling constants due to the different choices for the parametrization of the form factor. Taken from [114].

them. Since the  $D^*\bar{D}^*$  states cannot decay into  $J/\psi\phi$  because this channel is Okubo-Zweig-Iizuka (OZI) suppressed, a QCDSR calculation of the decay width is useful to distinguish the states coupling to  $D^*\bar{D}^*$  and  $D_s^*\bar{D}_s^*$ .

The decay width sum rule analysis was done in Ref. [114] for each spin projection of the  $D_s^*\bar{D}_s^*$  current in Eq. (232). The three-point function of the  $XJ/\psi\phi$  vertex, with  $X$  denoting each spin component of the  $D_s^*\bar{D}_s^*$  current, is given by:

$$\Pi_{\mu\nu\alpha\beta}(p^2) = \int d^4x d^4y e^{ip'\cdot x} e^{iq\cdot y} \langle 0 | T \{ j_\mu^\psi(x) j_\nu^\phi(y) j_{\alpha\beta}^{\dagger X}(0) \} | 0 \rangle. \quad (236)$$

Since a state with  $J^{PC} = 1^{+-}$  cannot decay into  $J/\psi\phi$ , only the scalar and tensorial components of the  $j_{\alpha\beta}$  current were considered. The interpolating currents used for  $\omega$  and  $J/\psi$  are given in Eq. (228) and the  $\phi$  meson current is:  $j_\nu^\phi = \bar{s}_b \gamma_\nu s_b$ .

The three-point function QCDSR was evaluated in Ref. [114] at leading order in  $\alpha_s$ , considering contributions from condensates up to dimension five. The details of the calculations can be found in [114]. In Fig. 24 the solutions for both  $0^{++}$  and  $2^{++}$  cases are shown, with the corresponding form factors used to extrapolate the QCDSR results to the time-like region, as discussed in Sec. 2.8. The resulting coupling constants found for spin 0 and 2 cases denoted by  $g_{X\psi\phi}^{S=0}$  and  $F_{X\psi\phi}^{S=2}$ , are [114]:

$$\begin{aligned} g_{X\psi\phi}^{S=0}(-m_\phi^2) &\approx 1.115 \pm 0.085 \text{ GeV}^{-1}, \\ F_{X\psi\phi}^{S=2}(-m_\phi^2) &\approx 5.0 \pm 0.6 \text{ GeV}. \end{aligned} \quad (237)$$

The decay width is given by:

$$\Gamma = \frac{1}{8\pi} \frac{p(m_X^2, m_\psi^2, m_\phi^2)}{m_X^2} \frac{1}{2S_X + 1} \sum_{\text{pol}} |\mathcal{M}|^2, \quad (238)$$

where  $p(m_X^2, m_\psi^2, m_\phi^2)$  is the center of mass momentum,  $S_X$  is the spin of  $X$  state. The matrix elements for the  $0^{++}$  and  $2^{++}$  cases are given by

$$\sum_{\text{pol}} |\mathcal{M}|^2 = (g_{X\psi\phi}^{S=0})^2 \left[ m_\psi^2 m_\phi^2 + \frac{1}{2} (m_X^2 - m_\psi^2 - m_\phi^2)^2 \right], \quad (239)$$

and

$$\begin{aligned} \sum_{\text{pol}} |\mathcal{M}|^2 &= \frac{(F_{X\psi\phi}^{S=2})^2}{24m_X^4 m_\psi^2 m_\phi^2} \left\{ m_X^8 + 6m_X^6 (m_\psi^2 + m_\phi^2) - 14m_X^4 (m_\psi^4 + m_\phi^4 - 6m_\psi^2 m_\phi^2) \right. \\ &\quad \left. + 6m_X^2 (m_\phi^2 - m_\psi^2)^2 (m_\psi^2 + m_\phi^2) + (m_\phi^2 - m_\psi^2)^4 \right\}. \end{aligned} \quad (240)$$

Taking into account the error associated with the mass found within QCD sum rules for the spin 0 and 2 states, given by Eqs. (233) and (235), the obtained values of the decay width are [114]:

$$\Gamma_{S=0} \approx (34 \pm 14) \text{ MeV} \quad (241)$$

for the spin 0 state, and

$$\Gamma_{S=2} \approx (20 \pm 7) \text{ MeV}, \quad (242)$$

for the spin 2 state.

According to the above results, both  $0^{++}$  and  $2^{++}$  can be associated with the  $X(4160)$  state. In Ref. [306] the authors have studied the  $D_s^* \bar{D}_s^*$  system using effective field theories, and have concluded that the interaction between  $D_s^*$  and  $\bar{D}_s^*$  mesons generates a state with mass 4170 MeV and full width equal to 130 MeV, which is compatible with the corresponding experimental values for the  $X(4160)$  state. From the couplings provided in Ref. [306], it is possible to estimate the partial decay width of the  $2^{++}$  state to be 20-30 MeV. Thus, the result for the decay width associated with the  $2^{++}$  state found in Ref. [114] within QCDSR, given in Eq. (242) is compatible with the one obtained in Ref. [306].

The findings in Ref. [114] presented above suggest that the  $D_s^* \bar{D}_s^*$  molecular current with  $2^{++}$  is most likely the charmonium-like state  $X(4160)$ , and not the  $Y(4140)$ . It is worth pointing out that although the  $1^{++}$  quantum numbers for  $Y(4140)$  are favored by the LHCb analysis [64, 336], the set of  $0^{++}$  and  $2^{++}$  cannot be excluded since fits to the data have a good statistical significance. This is what the results of Ref. [114] seem to indicate, i. e., that more than one resonance may contribute around 4.1 GeV in the data of Ref. [64, 336]. Recently, this conclusion was reinforced by the study conducted in Ref. [346]. So far no fit to the data of Ref. [64, 336] with more than one resonance around 4.1 GeV has been done. According to the reasoning made in Ref. [346] the peak seen by LHCb in the  $J/\psi\phi$  spectrum can be fitted using more than one resonance in the 4.1 GeV region. More concretely, the authors claim that in the LHCb data there is a lack of information related to the  $X(4160)$  contribution that, if included in the analysis, would provide a narrow width for  $Y(4140)$ .

### 6.6. Summary for the Controversial $Y$ states

From the QCDSR studies presented in this section it is possible to explain not only the mass, but also the decay width of the  $Y(3940)$  (or  $X(3915)$ ) considered as a mixed  $(\chi_{c0})-(D^* \bar{D}^*)$  state, with a mixing angle:  $\theta = (76.0 \pm 5.0)^\circ$ .

Regarding the  $Y(4140)$ , considering the observations and non-confirmations of its existence, from the experimental point of view it is very important to make an effort to determine if the state  $Y(4140)$  really exists. Supposing it exists, with a QCDSR calculation it is possible to explain its mass either as a  $D^* \bar{D}^*$  or a  $D_s^* \bar{D}_s^*$ , with quantum numbers  $J^{PC} = 0^{++}$  or  $2^{++}$ . However, the analysis done for the decay width presented above suggest that the  $D_s^* \bar{D}_s^*$  molecular current with  $2^{++}$  is more likely related with the charmonium-like state  $X(4160)$ , than to the  $Y(4140)$  one.

## 7. Higher Order Perturbative Corrections in Sum Rules

In previous sections, all the works done with the QCDSR method take into account approximations at Leading Order (LO) of perturbative QCD and include non-perturbative condensates in the OPE, to study the masses and coupling constants of the  $XYZ$ -states. In the literature we have many successful examples of using this approach at LO to explain the properties of such states. A natural improvement of such a method would be including, whenever possible, up to Next-to-Leading Order (NLO) corrections in perturbative QCD and estimate their relevance for the available LO sum rule calculations.

In this section, we explain how to include up to order  $\alpha_s^2$  (N2LO) perturbative corrections in the chiral limit and, adding to these, the SU(3) NLO corrections to the heavy-light exotic (molecules and tetraquarks) correlators. In doing so, we assume the factorization of the four-quark operator into a convolution of two-quark operators, built from bilinear quark currents. The contributions of the unknown order  $\alpha_s^3$  (N3LO) correction are estimated from a geometric growth of the perturbative series [347] and are added as a source of systematic uncertainties in the truncation of the perturbative series. For a complete description on these NLO techniques in QCDSR, see [115, 116] and references therein.

### 7.1. NLO Sum Rules

The conventional use of QCDSR obviously suffers from the ill-defined heavy quark mass definition used at LO. The favored numerical input values for the charm quark mass,  $m_c(m_c) \approx (1.23 - 1.26)$  GeV, used in the current literature correspond numerically to the one of the running masses. However, there is no reason to discard values like  $m_c \approx 1.5$  GeV of the on-shell (pole) quark masses, which are more natural because the spectral functions have been evaluated using the on-shell heavy quark propagator. For this reason, the perturbative expression of the spectral function obtained using on-shell renormalization must be transformed into the  $\overline{MS}$ -scheme by using the relation between the  $\overline{MS}$  running mass,  $\overline{m}_c(\mu)$ , and the on-shell mass (pole),  $M_c$ , to order  $\alpha_s^2$  [348–355]:

$$M_c = \overline{m}_c(\mu) \left[ 1 + \frac{4}{3} a_s + (16.2163 - 1.0414 n_l) a_s^2 + \ln \left( \frac{\mu}{M_c} \right)^2 (a_s + (8.8472 - 0.3611 n_l) a_s^2) + \ln^2 \left( \frac{\mu}{M_c} \right)^2 (1.7917 - 0.0833 n_l) a_s^2 + \dots \right], \quad (243)$$

for  $n_l$  light flavors where  $\mu$  is the arbitrary subtraction point and  $a_s \equiv \alpha_s/\pi$ .

To extract the perturbative  $\alpha_s^n$  corrections to the correlator of a four-quark current, and due to the technical complexity of the calculations, we shall assume that these radiative corrections are dominated by the ones from the factorized diagrams shown in Figs. 25a,b, while we neglect the ones from non-factorized diagrams in Figs. 25c-f. This fact has been proven explicitly in Refs. [356, 357], in the case of the  $\overline{B}^0 B^0$  systems (very similar correlator as the ones discussed in the following), where the non-factorized  $\alpha_s$  corrections do not exceed 10% of the total  $\alpha_s$  contributions. As can be seen in Refs. [115, 116], the effect of factorization in a sum rule calculation at LO is about 2.2% for the decay constant, and 0.5% for the mass which is quite tiny. However, to avoid this (small) effect, we shall work in the following with the full non-factorized perturbative  $\oplus$  condensates of the LO expressions. For the NLO expressions, we work with the spectral function as a convolution of the ones associated to quark bilinear current, as illustrated by the Feynman diagrams in Fig. 25. In this way, we use the low-energy representation of the effective spectral function, as suggested in Ref. [358], to obtain the expression:

$$\frac{1}{\pi} \text{Im} \Pi^{(1)}(s) = \theta(s - 4M_c^2) \left( \frac{s}{4\pi} \right)^2 \int_{M_c^2}^{(\sqrt{s}-M_c)^2} ds_1 \frac{1}{\pi} \text{Im} \Pi^{(1)}(s_1) \int_{M_c^2}^{(\sqrt{s}-\sqrt{s_1})^2} ds_2 \frac{1}{\pi} \text{Im} \Pi^{(0)}(s_2) \cdot \lambda^{3/2}, \quad (244)$$

for the  $J = 1$  states, and

$$\frac{1}{\pi} \text{Im} \Pi_A^{(0)}(s) = \theta(s - 4M_Q^2) \left( \frac{s}{4\pi} \right)^2 \int_{M_c^2}^{(\sqrt{s}-M_c)^2} ds_1 \frac{1}{\pi} \text{Im} \Pi^{(0)}(s_1) \int_{M_c^2}^{(\sqrt{s}-\sqrt{s_1})^2} ds_2 \frac{1}{\pi} \text{Im} \Pi^{(0)}(s_2) \cdot \lambda^{1/2} \left( \frac{s_1}{s} + \frac{s_2}{s} - 1 \right)^2, \quad (245)$$

$$\frac{1}{\pi} \text{Im} \Pi_B^{(0)}(s) = \theta(s - 4M_Q^2) \left( \frac{s}{4\pi} \right)^2 \int_{M_c^2}^{(\sqrt{s}-M_c)^2} ds_1 \frac{1}{\pi} \text{Im} \Pi^{(1)}(s_1) \int_{M_c^2}^{(\sqrt{s}-\sqrt{s_1})^2} ds_2 \frac{1}{\pi} \text{Im} \Pi^{(1)}(s_2) \cdot \lambda^{1/2} \left[ \left( \frac{s_1}{s} + \frac{s_2}{s} - 1 \right)^2 + \frac{8s_1 s_2}{s^2} \right], \quad (246)$$

for the  $J = 0$  states. We use the definition

$$\lambda \equiv \left( 1 - \frac{(\sqrt{s_1} - \sqrt{s_2})^2}{s} \right) \left( 1 - \frac{(\sqrt{s_1} + \sqrt{s_2})^2}{s} \right), \quad (247)$$

which is the phase space factor. The invariant spectral function,  $\text{Im} \Pi^{(1)}(s)$ , is associated to the bilinear  $\bar{c}\gamma_\mu q$  vector or  $\bar{c}\gamma_\mu\gamma_5 q$  axial-vector current, while  $\text{Im} \Pi^{(0)}(s)$  is associated to the  $\bar{c}q$  scalar or  $\bar{c}\gamma_5 q$  pseudoscalar current. Notice that, in the limit where the light quark mass  $m_q \rightarrow 0$ , the perturbative expressions of the vector (scalar) and axial-vector (pseudoscalar) spectral functions are the same. These representations allow us to evaluate the perturbative  $\alpha_s^n$ -corrections of the spectral functions of heavy-light bilinear currents, since we can use the expressions that are already

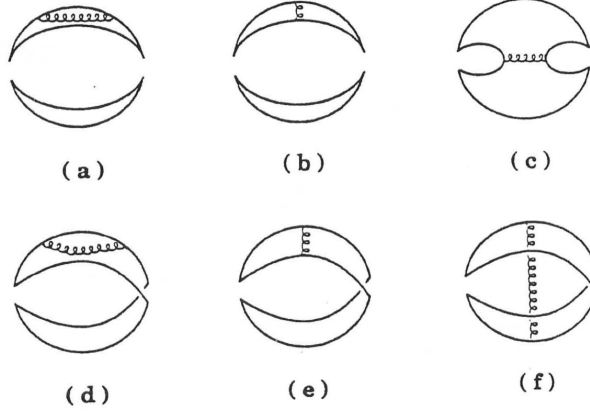


Figure 25: (a) Factorized contributions to the four-quark correlator at NLO of perturbative contribution; (b) Non-factorized diagrams at NLO of perturbative contribution. Taken from [358].

known to order  $\alpha_s$  (NLO) from Ref. [359]. N2LO corrections are known in the chiral limit,  $m_q = 0$ , from Ref. [360, 361]. We use the NLO SU(3) breaking perturbative corrections obtained in [362] from the two-point function formed by bilinear currents. From the above representation, the anomalous dimensions of the molecular correlators come from the (pseudo)scalar current. Therefore, the corresponding renormalization group invariant interpolating current reads to NLO as:

$$\bar{\mathcal{O}}_{mol}^{(0)}(\mu) = a_s(\mu)^{4/\beta_1} \mathcal{O}_{mol}^{(0)}, \quad \bar{\mathcal{O}}_{mol}^{(1)}(\mu) = a_s(\mu)^{2/\beta_1} \mathcal{O}_{mol}^{(1)}, \quad (248)$$

where  $\beta_1 = -(1/2)(11 - 2n_f/3)$  is the first coefficient of the QCD  $\beta$ -function for  $n_f$  flavors, and  $a_s \equiv (\alpha_s/\pi)$ . The spin-0 currents built from two (axial)-vector currents have no anomalous dimension. We have introduced the super-index (1) for denoting the vector and axial-vector spin-1 channels.

Another aspect of including higher order perturbative corrections is related with the  $1/q^2$  corrections due to a tachyonic gluon mass discussed in [363, 364]. However, such corrections will not be included here because they are dual to the sum of the large order perturbative series [347]. Therefore, we shall consider the inclusion of the N3LO terms, estimated from the geometric growth of the QCD perturbative series [347], as a source of the errors. The estimate of these errors is given in Refs. [115, 116]. We are still using the ansatz of pole plus continuum, in Eq. (249), for parametrizing the spectral function (generic notation):

$$\frac{1}{\pi} \text{Im} \Pi(s) \simeq f_H^2 M_H^8 \delta(s - M_H^2) + \text{“QCD continuum”} \theta(s - s_0), \quad (249)$$

where  $f_H$  is the hadronic decay constant defined as:

$$\langle 0 | \mathcal{O}^{(0)} | H \rangle = f_H^{(0)} M_H^4, \quad \langle 0 | \mathcal{O}_\mu^{(1)} | H \rangle = f_H^{(1)} M_H^5 \epsilon_\mu, \quad (250)$$

respectively, for spin 0 and 1 hadronic states, with  $\epsilon^\mu$  being the vector polarization. The higher state contributions are given by the “QCD continuum” coming from the discontinuity of the QCD diagrams and starting from a constant threshold  $s_0$ . Finite width corrections to this simple model have been studied in, e.g., [90, 365, 366] and have been found to be negligible.

Noting that, due to Eq. (248), the bilinear (pseudo)scalar currents, in Table 9, acquires an anomalous dimension due to its normalization, thus the decay constants run to order  $\alpha_s^2$  as:

$$f_{mol}^{(0)}(\mu) = \hat{f}_{mol}^{(0)} (-\beta_1 a_s)^{4/\beta_1} / r_m^2, \quad f_{mol}^{(1)}(\mu) = \hat{f}_{mol}^{(1)} (-\beta_1 a_s)^{2/\beta_1} / r_m, \quad (251)$$

where the QCD corrections ( $r_m$ ) numerically read to N2LO as [121, 353]:

$$r_m(n_f = 4) = 1 + 1.014 a_s + 1.389 a_s^2. \quad (252)$$

In Eq. (251) we have introduced the renormalization group invariant coupling  $\hat{f}_{mol}$  and the first coefficient of the QCD  $\beta$ -function for  $n_f$  flavors,  $a_s \equiv \alpha_s/\pi$ . Notice that the coupling of the (pseudo)scalar molecule built from two (axial)-vector currents has no anomalous dimension and does not run.

As usual in a QCDSR calculation, to obtain the hadronic masses we use the expression:

$$M_H^2 \simeq \frac{\int_{4m_c^2}^{s_0} ds s e^{-s/M^2} \text{Im} \Pi(s, \mu)}{\int_{4m_c^2}^{s_0} ds e^{-s/M^2} \text{Im} \Pi(s, \mu)}, \quad (253)$$

where  $\mu$  is the subtraction point which appears in the approximate QCD series when radiative corrections are included. Since our studies are concentrated on charmonium-like states, the lower limit integral in Eq. (253) is given by the square of constituent quark masses of these hadrons.

In this section, we shall add to the previous well-known  $M^2$ - and  $s_0$ -stability criteria, discussed in Sec. 2.5, the one associated with the requirement of stability versus the arbitrary subtraction constant  $\mu$ . The  $\mu$ -stability procedure has been applied recently in Refs. [367–370]. It gives a much better meaning of the choice of  $\mu$ -value at which the observable is extracted. The errors in the determination of the results have been reduced due to a better control of the  $\mu$  region of variation.

### 7.2. QCD Input Parameters at NLO

The QCD parameters appearing in the following analysis will be the charm quark mass  $m_c$ , the strange quark mass  $m_s$  (we shall neglect the light quark masses  $m_{u,d}$ ), the light quark condensates  $\langle \bar{q}q \rangle$  ( $q \equiv u, d, s$ ), the gluon condensates  $\langle g_s^2 G^2 \rangle$  and  $\langle g_s^3 G^3 \rangle$ , the mixed quark condensate  $\langle \bar{q}Gq \rangle$  and the four-quark condensate  $\rho \alpha_s \langle \bar{q}q \rangle^2$ , where  $\rho \simeq 3 - 4$  indicates the deviation from the four-quark vacuum saturation. Their values are given in Tables 2 and 8. We shall work with the running light quark condensates which, in leading order in  $\alpha_s$ , is given by:

$$\langle \bar{q}q \rangle(M_\tau) = -\langle \bar{q}q \rangle (-\beta_1 a_s(M_\tau))^{2/\beta_1}, \quad \langle \bar{q}Gq \rangle(M_\tau) = -m_0^2 \langle \bar{q}q \rangle (-\beta_1 a_s(M_\tau))^{1/3\beta_1}, \quad (254)$$

and the running strange quark mass to NLO (for the number of flavours  $n_f = 3$ ):

$$\bar{m}_s(M_\tau) = \hat{m}_s (-\beta_1 a_s(M_\tau))^{-2/\beta_1} (1 + 0.8951 a_s(M_\tau)), \quad (255)$$

where  $\langle \bar{q}q \rangle$  (given in Table 2) and  $\hat{m}_s$  are the spontaneous RGI light quark condensate and strange quark mass [371]. For the heavy quarks, we shall use the running mass and the corresponding value of  $\alpha_s$  evaluated at the scale  $\mu$ , whose value used here corresponds to the optimal one obtained in Ref. [115].

For the  $\langle \alpha_s G^2 \rangle$  condensate, we have enlarged the original error by a factor about 3 in order to have a conservative result for recovering the original SVZ estimate and the alternative extraction in Ref. [372, 373] from charmonium sum rules. However, a direct naive comparison of this range of values obtained within short QCD series (few terms) with the one from lattice calculations [374] obtained within a long QCD series [375] can be misleading. We shall see later on that the effects of the gluon and four-quark condensates on the values of the decay constants and masses are relatively small even though they play an important role in the stability analysis.

### 7.3. Heavy-Light Molecular States

For describing these molecular states, we consider the usual lowest dimension local interpolating currents where each bilinear current has the quantum number and quark content of the open-charm mesons:

$$D(0^-), D_0^*(0^+), D^*(1^-), D_1(1^+) \quad (256)$$

and their respective extension to the strange sector:

$$D_s(0^-), D_{s0}^*(0^+), D_s^*(1^-), D_{s1}(1^+). \quad (257)$$



Table 8: QCD input parameters used in sum rules at NLO.

Parameters	Values	Ref.
$\alpha_s(M_\tau)$	$0.325 \pm 0.008$	[146, 376, 377]
$\hat{m}_s$	$(0.114 \pm 0.006) \text{ GeV}$	[121, 146, 352, 368, 378–380]
$\bar{m}_c(m_c)$	$(1261 \pm 12) \text{ MeV}$	average [22, 141, 372, 373, 381, 382]
$\langle \alpha_s G^2 \rangle$	$(7 \pm 3) \times 10^{-2} \text{ GeV}^4$	[141, 145, 146, 150, 381–388]
$\langle g_s^3 G^3 \rangle$	$(8.2 \pm 2.0) \text{ GeV}^2 \times \langle \alpha_s G^2 \rangle$	[141, 381, 382]
$\rho \alpha_s \langle \bar{q}q \rangle^2$	$(5.8 \pm 1.8) \times 10^{-4} \text{ GeV}^6$	[145, 146, 389, 390]

For simplicity, we do not consider colored and more general combinations of interpolating operators discussed e.g in Ref. [106, 293], as well as the higher dimension ones involving derivatives. This choice justifies the approximate use (up to order  $1/N_c$ ) of the factorization of the four-quark currents as a convolution of two bilinear quark-antiquark currents when estimating higher order perturbative corrections. These states and the corresponding interpolating currents, for the states studied in this review, are given in Table 9. A more general study can be found in Refs. [115, 116].

Next, we show the techniques and strategies for evaluating the mass and decay constants of the  $\bar{D}D$  molecular state. Essentially, the sum rule analysis for the other interpolating currents are very similar. Therefore, we only quote the results for the remaining states. We start with the mass,  $M_{DD}$ , obtained with the  $\bar{D}D$  molecular current, at LO approximation. We show in Fig.26 the results in terms of the Borel mass variable  $\tau = 1/M^2$  at different values of continuum threshold  $s_0$ . Then we implement the higher order perturbative corrections to this sum rule and the results are shown in Fig. 27a at N2LO.

We consider as an optimal choice the mean value of the coupling and mass obtained at the minimum or inflection point for the common range of  $s_0$ -values corresponding to the starting of the  $\tau$ -stability and the one where  $s_0$ -stability is reached. In these stability regions, the requirement that the pole contribution is larger than the one of the continuum is automatically satisfied (see e.g. [7]). Therefore, from the Fig. 27a at N2LO, we obtain the range for the continuum threshold as  $s_0 \simeq (27.5 \pm 4.5) \text{ GeV}^2$ , for  $1/M^2 = (0.30 \pm 0.05) \text{ GeV}^{-2}$ . Another interesting point discussed in Refs. [115, 116] is about the running versus the pole quark mass definitions in QCDSR at LO. It was pointed out that the effect of the definitions (running and pole) of the heavy quark mass should be added as errors in the LO analysis.

As we can see in Fig. 27b, using  $s_0 = 32 \text{ GeV}^2$ , the convergence of the perturbative series is obtained for an optimal choice:  $\mu = (4.5 \pm 0.5) \text{ GeV}$ . We observe that from NLO to N2LO the mass of the state decreases by about only 0.1 %, as another indication of the good convergence of the perturbative series. Using the fact that the final result must be independent of the arbitrary parameter  $\mu$  (plateau / inflection point for the coupling and minimum for the

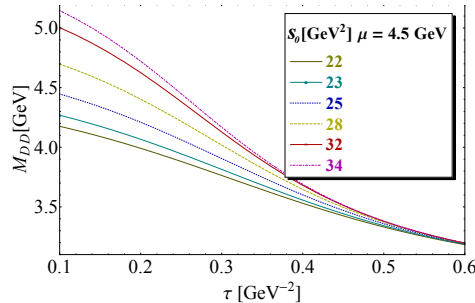


Figure 26:  $M_{DD}$  at LO as function of  $1/M^2$  for different values of  $s_0$ , for  $\mu = 4.5 \text{ GeV}$  and for the QCD parameters in Table 8. Figure taken from [115].

Table 9: Interpolating currents with a definite  $C$ -parity describing the  $\bar{D}D$ - and  $\bar{D}_s D_s$ -like molecular states for  $J^{PC} = 0^{++}, 1^{++}$  and  $1^{--}$ .  $q \equiv u, d, s$ .

$J^{PC}$	States	Molecule Currents $\equiv \mathcal{O}_{mol}(x)$
$0^{++}$	$\bar{D}D, \bar{D}_s D_s$	$(\bar{q}\gamma_5 c)(\bar{c}\gamma_5 q)$
	$\bar{D}^* D^*, \bar{D}_s^* D_s^*$	$(\bar{q}\gamma_\mu c)(\bar{c}\gamma^\mu q)$
	$\bar{D}_0^* D_0^*, \bar{D}_{s0}^* D_{s0}^*$	$(\bar{q}c)(\bar{c}q)$
	$\bar{D}_1 D_1, \bar{D}_{s1} D_{s1}$	$(\bar{q}\gamma_\mu \gamma_5 c)(\bar{c}\gamma^\mu \gamma_5 q)$
$1^{++}$	$\bar{D}^* D, \bar{D}_s^* D_s$	$\frac{i}{\sqrt{2}} [(\bar{c}\gamma_\mu q)(\bar{q}\gamma_5 c) - (\bar{q}\gamma_\mu c)(\bar{c}\gamma_5 q)]$
	$\bar{D}_0^* D_1, \bar{D}_{s0}^* D_{s1}$	$\frac{1}{\sqrt{2}} [(\bar{q}c)(\bar{c}\gamma_\mu \gamma_5 q) + (\bar{c}q)(\bar{q}\gamma_\mu \gamma_5 c)]$
$1^{--}$	$\bar{D}_0^* D^*, \bar{D}_{s0}^* D_s^*$	$\frac{1}{\sqrt{2}} [(\bar{q}c)(\bar{c}\gamma_\mu q) + (\bar{c}q)(\bar{q}\gamma_\mu c)]$
	$\bar{D}D_1, \bar{D}_s D_{s1}$	$\frac{i}{\sqrt{2}} [(\bar{c}\gamma_\mu \gamma_5 q)(\bar{q}\gamma_5 c) - (\bar{q}\gamma_\mu \gamma_5 c)(\bar{c}\gamma_5 q)]$

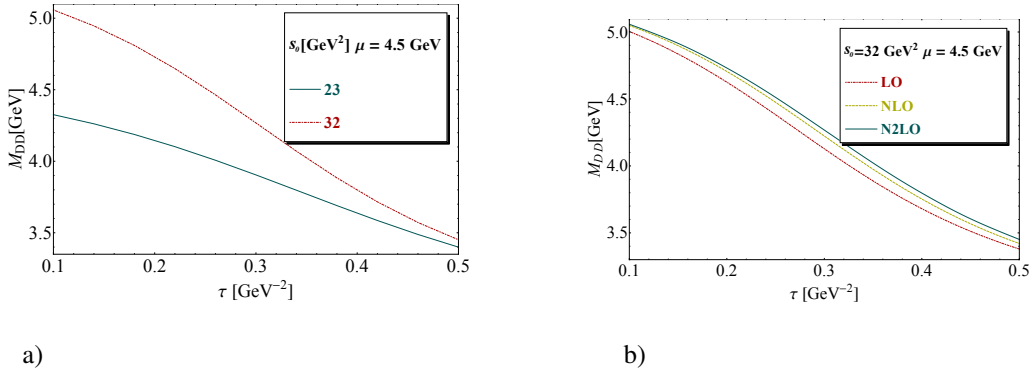


Figure 27: a)  $M_{DD}$  at N2LO as function of  $\tau = 1/M^2$  for different values of  $s_0$ , for  $\mu = 4.5$  GeV and for the QCD parameters in Table 8; b) The same as a) but for a given value of  $s_0 = 32$  GeV<sup>2</sup>, and for different truncation of the perturbative series. Figures taken from [115].

mass), we consider as an optimal result the one at  $\mu \simeq 4.5$  GeV, where we deduce the result at N2LO,

$$M_{DD} = (3898 \pm 36) \text{ MeV}, \quad \text{and} \quad f_{DD} = (170 \pm 15), \text{ keV} \quad (258)$$

which is included in Table 10. Notice that the mass obtained for the  $\bar{D}D$  molecular state is above the  $\bar{D}D$ -threshold ( $\sim 3729$  MeV) and, for this reason, such a molecule would not be consistent with a bound state. Therefore, from a QCDSR point of view, we can not use the  $\bar{D}D$  molecular state to describe any new  $XYZ$  states observed so far.

We proceed with our investigation for other molecular currents in Table 9, where we apply the same analysis for extracting the optimal values for the masses and couplings at N2LO approximation. Then we check if the molecular currents could describe some of these  $XYZ$  states. The final results are summarized in Table 10.

#### 7.4. Heavy-Light Tetraquark States

The tetraquark states were first introduced in Ref. [391] for interpreting the complex spectra of light scalar mesons. Recent analysis based on  $1/N_c$  expansion has shown that the tetraquark states should be narrow [392–394], which do not then favor the tetraquark interpretation of the light scalar meson  $f_0(500)$ . In the following, we also study the

Table 10: The masses and couplings of the  $\bar{D}D$ - and  $\bar{D}_s D_s$ -like Molecular states from QCDSR within stability criteria at N2LO of perturbative series. The value of the continuum threshold,  $s_0$ , is also included for completeness.

States $J^{PC}$	$\sqrt{s_0}$ (GeV)	Mass (MeV)	Coupling (keV)	States $J^{PC}$	$\sqrt{s_0}$ (GeV)	Mass (MeV)	Coupling (keV)
<b>0<sup>++</sup></b>				<b>0<sup>++</sup></b>			
$\bar{D}D$	4.7 ~ 5.7	3898 ± 36	170 ± 15	$\bar{D}_s D_s$	5.0 ~ 6.9	4169 ± 48	167 ± 18
$\bar{D}^* D^*$	4.7 ~ 5.7	3903 ± 179	302 ± 47	$\bar{D}_s^* D_s^*$	5.0 ~ 6.9	4196 ± 200	284 ± 34
$\bar{D}_0^* D_0^*$	4.7 ~ 5.7	3954 ± 224	114 ± 18	$\bar{D}_{s_0}^* D_{s_0}^*$	5.5 ~ 7.0	4225 ± 132	102 ± 14
$\bar{D}_1 D_1$	4.7 ~ 5.7	3784 ± 56	274 ± 37	$\bar{D}_{s_1} D_{s_1}$	5.3 ~ 6.9	4124 ± 61	229 ± 31
<b>1<sup>±±</sup></b>				<b>1<sup>±±</sup></b>			
$\bar{D}^* D$	4.7 ~ 5.7	3903 ± 62	161 ± 17	$\bar{D}_s^* D_s$	5.0 ~ 6.9	4188 ± 67	156 ± 17
$\bar{D}_0^* D_1$	6.5 ~ 6.9	3854 ± 182	112 ± 17	$\bar{D}_{s_0}^* D_{s_1}$	5.5 ~ 6.9	4275 ± 206	110 ± 18
<b>1<sup>--</sup></b>				<b>1<sup>--</sup></b>			
$\bar{D}_0^* D^*$	6.5 ~ 6.9	5748 ± 101	261 ± 17	$\bar{D}_{s_0}^* D_s^*$	6.0 ~ 7.5	5571 ± 180	216 ± 11
$\bar{D}D_1$	6.5 ~ 6.9	5544 ± 162	231 ± 21	$\bar{D}_s D_{s_1}$	6.2 ~ 7.5	5272 ± 120	213 ± 13

Table 11: Interpolating currents with a definite  $P$ -parity describing the tetraquark states.  $q \equiv u, d, s$ .

$J^P$	States	Tetraquark Currents $\equiv \mathcal{O}_{4q}(x)$
<b>0<sup>+</sup></b>	$S_c, S_{cs}$	$\epsilon_{abc}\epsilon_{dec} \left[ (q_a^T C \gamma_5 c_b)(\bar{q}_d \gamma_5 C \bar{c}_e^T) + k(q_a^T C c_b)(\bar{q}_d C \bar{c}_e^T) \right]$
<b>1<sup>+</sup></b>	$A_c, A_{cs}$	$\epsilon_{abc}\epsilon_{dec} \left[ (q_a^T C \gamma_5 c_b)(\bar{q}_d \gamma_\mu C \bar{c}_e^T) + k(q_a^T C c_b)(\bar{q}_d \gamma_\mu \gamma_5 C \bar{c}_e^T) \right]$
<b>1<sup>-</sup></b>	$V_c, V_{cs}$	$\epsilon_{abc}\epsilon_{dec} \left[ (q_a^T C \gamma_5 c_b)(\bar{q}_d \gamma_\mu \gamma_5 C \bar{c}_e^T) + k(q_a^T C c_b)(\bar{q}_d \gamma_\mu C \bar{c}_e^T) \right]$

tetraquark currents to investigate possible hadronic structures to describe the  $XYZ$  states in the charmonia spectra. The tetraquark states  $[cq\bar{c}\bar{q}]$  will be described by the interpolating currents given in Table 11. A more general study can be found in Refs. [115, 116]. We use the following naming scheme for the scalar, pseudoscalar, axial-vector and vector states for the tetraquark currents:

$$S_c(0^+), A_c(1^-), V_c(1^+) \quad (259)$$

and their respective extension to the strange sector:

$$S_{cs}(0^+), A_{cs}(1^+), V_{cs}(1^-) . \quad (260)$$

The analysis of the masses and couplings of tetraquark states is very similar to the one of the molecules and present analogous features: presence of minima or/and inflection points, good convergence of the perturbative series and the OPE. The results for the tetraquark states are summarized in Table 12 and for a complete discussion see Refs. [115, 116].

Just to show an example of the results on the use of the sum rules for the tetraquarks, we state the mass and

coupling of the scalar  $S_c(0^+)$  tetraquark state. At N2LO, the corresponding set of parameters are:

$$\tau \simeq (0.35 \pm 0.05) \text{ GeV}^{-2}, \quad s_0 \simeq (27.5 \pm 4.5) \text{ GeV}^2 \quad \text{and} \quad \mu \simeq 4.5 \text{ GeV}, \quad (261)$$

and taking into account the uncertainties, as indicated in Table 8, we get:

$$M_{S_c} = 3898 \pm 54 \text{ MeV} \quad \text{and} \quad f_{S_c} = 191 \pm 20 \text{ keV} . \quad (262)$$

This value for the mass is compatible with the  $Y(3940)$  mass and we could naively describe it as a non-strange scalar tetraquark state. It is important to notice that this mass value, calculated at N2LO approximation, has almost the same magnitude as the one calculated at LO, and the difference is in order of  $\sim 0.1\%$ . This weak impact on the results from LO to N2LO is verified for the other tetraquark states too (see Refs. [115, 116]).

Table 12: The masses and couplings of the  $[\bar{c}\bar{q}cq]$  and  $[\bar{c}\bar{s}cs]$  tetraquark states from QCDSR within stability criteria at N2LO of perturbative series.

States ( $J^P$ )	$\sqrt{s_0}$ (Gev)	Mass (MeV)	Coupling (MeV)	States ( $J^P$ )	$\sqrt{s_0}$ (Gev)	Mass (MeV)	Coupling (MeV)
$S_c(0^+)$	4.7 ~ 5.7	$3898 \pm 54$	$191 \pm 20$	$S_{cs}(0^+)$	5.2 ~ 6.7	$4233 \pm 61$	$187 \pm 19$
$A_c(1^+)$	4.7 ~ 5.7	$3888 \pm 130$	$184 \pm 30$	$A_{cs}(1^+)$	5.3 ~ 6.7	$4209 \pm 112$	$160 \pm 17$
$P_c(0^-)$	6.0 ~ 6.4	$5750 \pm 127$	$310 \pm 13$	$P_{cs}(0^-)$	6.2 ~ 7.5	$5524 \pm 176$	$267 \pm 30$
$V_c(1^-)$	6.0 ~ 6.4	$5793 \pm 122$	$296 \pm 19$	$V_{cs}(1^-)$	6.2 ~ 7.5	$5539 \pm 234$	$258 \pm 33$

### 7.5. Summary for the higher order corrections in QCDSR

The N2LO predictions for the masses differ only slightly from the LO ones when the value of the running mass is used for the latter. However, the magnitude of the meson couplings is strongly affected by the radiative corrections in some channels, which consequently may modify the existing estimates of the meson hadronic widths based on vertex functions. The  $0^{++}$   $\bar{D}D$ -like molecular states are almost degenerated with the  $1^{++}$  states. They have masses around 3900 MeV, which is consistent, within the errors, with the mass of the  $Y(3940)$  state. It is also consistent with the scalar  $S_c(0^+)$  tetraquark state.

As mentioned in the introduction, there are several  $1^{++}$  observed states. In addition to the well-established  $X(3872)$ , we have  $X(4140)$  and  $X(4274)$ . From the results presented here it is possible to describe the mass of the  $X(3872)$  as a  $\bar{D}^*D$  molecule or a  $A_c$  tetraquark state, which is consistent with the results presented in Sec. 3. For the remaining  $1^{++}$  states,  $X(4140)$  and  $X(4274)$ , one could interpret them as a  $\bar{D}_s^*D_s$  molecule and a  $A_{cs}$  tetraquark state, respectively. From a QCDSR calculation at N2LO, and considering the relevant uncertainties, there are some molecule and/or tetraquark states which could be consistent with some of the observed charged states. The  $\bar{D}^*D(1^{+-})$  and  $\bar{D}_0^*D_1(1^{+-})$  molecules would be good candidates to explain the  $Z_c^+(3900)$ . In particular, the  $\bar{D}_0^*D_1(1^{+-})$  molecule could also be compatible with the  $Z_c^+(4020)$ . The  $Z_c^+(4200)$  state might be identified as a charmed-strange axial  $A_{cs}$  tetraquark state and the  $\bar{D}_0^*D_0^*(0^{++})$  molecule could be naively associated with the recently observed charged state  $Z_c^-(4100)$ .

## 8. Summary

In this review we have discussed the exotic charmonium states, observed by BaBar, Belle, CDF, DØ, LHCb and BESIII Collaborations, from the perspective of QCD sum rules. We have computed the masses of several  $X$ ,  $Y$  and  $Z$  states and, as it was seen case by case, the method of QCDSR, in spite of its limitations, contributes a great deal to the understanding of the structure of these new states. In some cases a tetraquark current gives a better agreement with the observed mass and in some other cases the agreement is better with a molecular current. However, as a general result, the two kinds of currents, molecular or tetraquark, lead to almost the same result for the mass of the state.

Besides, since the used currents are local, a molecular current does not represent a true molecule. It is just the color combination between the quarks that is similar to a molecular state. For the non-charged states, QCDSR results favor a mixing between two and four-quark currents.

The limitations in statements made with QCDSR estimates come mostly from uncertainties in the method. However these statements can be made progressively more precise as we know more experimental information about the state in question. One good example is the  $X(3872)$ , from which, besides the mass, several decay modes were measured. Combining all the available information and using QCDSR to calculate the observed decay widths, we were able to say that the  $X(3872)$  is a mixed state, where the most important component is a  $c\bar{c}$  pair, which is mixed with a small four-quark component, out of which a large fraction is composed by neutral combinations of  $D$ -like and  $D^*$ -like two-quark states with only a tiny fraction of charged  $D$ -like and  $D^*$ -like states. This conclusion is very specific and precise and it is more elaborated than the other results presented addressing only the masses of the new charmonia. This improvement was a consequence of studying simultaneously the mass and the decay width. This type of combined calculation should be extended to all states.

One of the drawbacks of previous QCDSR calculations was the absence of  $\alpha_s$  corrections. In a series of recent works it was shown that these corrections are tiny. Another problem is the use of the factorization hypothesis, according to which  $\langle \bar{q}q\bar{q}q \rangle = \rho \langle \bar{q}q \rangle^2$ , where  $\rho \simeq 1$ . Also here, there has been some progress on the theoretical side showing the violation of this hypothesis, its origin and the best value of  $\rho$ .

The next generation of experimental data from  $e^+e^-$  colliders will increase a lot the statistics and will yield invariant mass spectra with high precision. Consequently, what was previously seen as a single bump, a single state, will reveal itself as a series of different peaks at different masses. The beginning of this “unfolding” has already been observed in the case of the  $Y(4360)$  and more recently in the case of the  $Y(4260)$ . For QCDSR this is challenging and asks for improvement of the pole-continuum model of the spectral function. Efforts along this direction should become a priority in the work of our community.

New data on hadronic production of exotic charmonium are also expected to appear at the LHC. In central collisions exotic charmonium production is essentially a high energy process, calculable either with perturbative QCD [395, 396] or with effective theories [397]. On the other hand in ultraperipheral collisions these states are produced by photon-photon fusion [398, 399] and the cross section is proportional to the 2-photon decay width of the states. Here again QCDSR is relevant since this decay receives large non-perturbative contributions. The decay width of some states has been calculated but there is room for improvement and also other states to be considered.

The above mentioned uncertainties put some limits on the predictive power of QCDSR. In QCDSR, as in quark model calculations [400], one may find more states than those really observed. On the other hand, exactly because of this feature, QCDSR calculations have “veto power”, i.e.: *If it is not true in QCDSR it is not true in QCD*. This veto power has been already used to say that the existence of tetraquarks made only of light quarks is disfavored [246].

We close this review with some conclusions from the results presented in the previous sections. They are contained in Table 13 where we present a summary of the most plausible interpretations for some of the states presented in Table 1. It is important to remember that a molecular or tetraquark structure assignment in Table 13 is just the indication of the current used in the calculations, and that they are equivalent, from a QCDSR perspective.

Table 13 represents the final result of a comprehensive effort and a careful analysis of several theoretical possibilities in the light of existing data. It is an encouraging example of what QCDSR can do. This Table contains a short summary of what we have learned about the new charmonium states in the recent past. In particular, similar to the  $X(3872)$  state, mixed charmonium-tetraquark currents give a better description for all neutral exotic states, like the  $Y(3940)$  (or  $X(3915)$ ),  $Y(4140)$  and the  $Y(4260)$ .

The discovery of several manifestly exotic states, the  $Z^+$  states, may be considered as one of the most exciting findings of the last years. The description of such states unavoidably requires (at least) four valence quarks in the wave function.

**Acknowledgements:** The authors would like to thank M. E. Bracco, S. H. Lee, R.D. Matheus, K. Morita, S. Narison J.-M. Richard, R. Rodrigues da Silva with whom they have collaborated in one or more of the works described in this review. The authors are indebted to the Brazilian funding agency CNPq.

Table 13: Structure and quantum numbers from QCDSR studies. In the case of isovector states, the quoted charge conjugation,  $C$ , is for the neutral state in the multiplet.

state	structure	$J^{PC}$
$X(3872)$	mixed $\chi_{c1} - D\bar{D}^*$	$1^{++}$
$Z_c(3900)$	$D\bar{D}^*$	$1^{+-}$
$Y(3940)$	mixed $\chi_{c0} - D^*\bar{D}^*$	$0^{++}$
$Z_c(4020)$	$D^*\bar{D}^*$	$1^{+-}$ or $2^{++}$
$Z_c(4100)$	$D_0^*\bar{D}_0^*$	$0^{++}$
$Y(4140)$	mixed $D^*\bar{D}^* - D_s^*\bar{D}_s^*$	$0^{++}$
$X(4160)$	$D_s^*\bar{D}_s^*$	$2^{++}$
$Z_c(4200)$	$[cs][\bar{c}\bar{s}]$	$1^+$
$Z_2(4250)$	$D\bar{D}_1$	$1^-$
$Y(4260)$	mixed $J/\psi - [cq][\bar{c}\bar{q}]$	$1^{--}$
$Y(4360)$	$[cq][\bar{c}\bar{q}]$	$1^{--}$
$Y(4660)$	$[cs][\bar{c}\bar{s}]$	$1^{--}$

## References

- [1] R. L. Jaffe, Exotica, Phys. Rept. 409 (2005) 1–45. arXiv:hep-ph/0409065, doi:10.1016/j.physrep.2004.11.005.
- [2] E. S. Swanson, The New heavy mesons: A Status report, Phys. Rept. 429 (2006) 243–305. arXiv:hep-ph/0601110, doi:10.1016/j.physrep.2006.04.003.
- [3] S.-L. Zhu, New hadron states, Int. J. Mod. Phys. E17 (2008) 283–322. arXiv:hep-ph/0703225, doi:10.1142/S0218301308009446.
- [4] E. Klempt, A. Zaitsev, Glueballs, Hybrids, Multiquarks. Experimental facts versus QCD inspired concepts, Phys. Rept. 454 (2007) 1–202. arXiv:0708.4016, doi:10.1016/j.physrep.2007.07.006.
- [5] M. B. Voloshin, Charmonium, Prog. Part. Nucl. Phys. 61 (2008) 455–511. arXiv:0711.4556, doi:10.1016/j.pnnp.2008.02.001.
- [6] S. Godfrey, S. L. Olsen, The Exotic XYZ Charmonium-like Mesons, Ann. Rev. Nucl. Part. Sci. 58 (2008) 51–73. arXiv:0801.3867, doi:10.1146/annurev.nucl.58.110707.171145.
- [7] M. Nielsen, F. S. Navarra, S. H. Lee, New Charmonium States in QCD Sum Rules: A Concise Review, Phys. Rept. 497 (2010) 41–83. arXiv:0911.1958, doi:10.1016/j.physrep.2010.07.005.
- [8] N. Brambilla, et al., Heavy quarkonium: progress, puzzles, and opportunities, Eur. Phys. J. C71 (2011) 1534. arXiv:1010.5827, doi:10.1140/epjc/s10052-010-1534-9.
- [9] V. P. Druzhinin, S. I. Eidelman, S. I. Serednyakov, E. P. Solodov, Hadron Production via e+e- Collisions with Initial State Radiation, Rev. Mod. Phys. 83 (2011) 1545. arXiv:1105.4975, doi:10.1103/RevModPhys.83.1545.
- [10] N. Li, Z.-F. Sun, J. He, X. Liu, Z.-G. Luo, S.-L. Zhu, Few-Body Systems Composed of Heavy Quarks, Few Body Syst. 54 (2013) 807–812. arXiv:1208.6347, doi:10.1007/s00601-012-0564-2.
- [11] X. Liu, An overview of XYZ new particles, Chin. Sci. Bull. 59 (2014) 3815–3830. arXiv:1312.7408, doi:10.1007/s11434-014-0407-2.
- [12] N. Brambilla, et al., QCD and Strongly Coupled Gauge Theories: Challenges and Perspectives, Eur. Phys. J. C74 (10) (2014) 2981. arXiv:1404.3723, doi:10.1140/epjc/s10052-014-2981-5.
- [13] S. L. Olsen, A New Hadron Spectroscopy, Front. Phys.(Beijing) 10 (2) (2015) 121–154. arXiv:1411.7738, doi:10.1007/S11467-014-0449-6.
- [14] M. Nielsen, F. S. Navarra, Charged Exotic Charmonium States, Mod. Phys. Lett. A29 (2014) 1430005. arXiv:1401.2913, doi:10.1142/S0217732314300055.
- [15] A. Esposito, A. L. Guerrieri, F. Piccinini, A. Pilloni, A. D. Polosa, Four-Quark Hadrons: an Updated Review, Int. J. Mod. Phys. A30 (2015) 1530002. arXiv:1411.5997, doi:10.1142/S0217751X15300021.
- [16] R. A. Briceno, et al., Issues and Opportunities in Exotic Hadrons, Chin. Phys. C40 (4) (2016) 042001. arXiv:1511.06779, doi:10.1088/1674-1137/40/4/042001.
- [17] A. Hosaka, T. Iijima, K. Miyabayashi, Y. Sakai, S. Yasui, Exotic hadrons with heavy flavors: X, Y, Z, and related states, PTEP 2016 (6) (2016) 062C01. arXiv:1603.09229, doi:10.1093/ptep/ptw045.
- [18] H.-X. Chen, W. Chen, X. Liu, S.-L. Zhu, The hidden-charm pentaquark and tetraquark states, Phys. Rept. 639 (2016) 1–121. arXiv:1601.02092, doi:10.1016/j.physrep.2016.05.004.
- [19] A. Esposito, A. Pilloni, A. D. Polosa, Multiquark Resonances, Phys. Rept. 668 (2016) 1–97. arXiv:1611.07920, doi:10.1016/j.physrep.2016.11.002.
- [20] F.-K. Guo, C. Hanhart, U.-G. Meiner, Q. Wang, Q. Zhao, B.-S. Zou, Hadronic molecules, Rev. Mod. Phys. 90 (1) (2018) 015004. arXiv:1705.00141, doi:10.1103/RevModPhys.90.015004.
- [21] C.-Z. Yuan, The XYZ states revisited, Int. J. Mod. Phys. A33 (21) (2018) 1830018. arXiv:1808.01570, doi:10.1142/S0217751X18300181.
- [22] M. Tanabashi, et al., Review of Particle Physics, Phys. Rev. D98 (3) (2018) 030001. doi:10.1103/PhysRevD.98.030001.
- [23] S. K. Choi, et al., Observation of a narrow charmonium-like state in exclusive  $B^\pm \rightarrow K^\pm \pi^+ \pi^- J/\psi$  decays, Phys. Rev. Lett. 91 (2003) 262001. arXiv:hep-ex/0309032, doi:10.1103/PhysRevLett.91.262001.
- [24] I. Adachi, et al., Study of  $X(3872)$  in  $B$  meson decays, in: Proceedings, 34th International Conference on High Energy Physics (ICHEP

2008); Philadelphia, Pennsylvania, July 30-August 5, 2008, 2008. arXiv:0809.1224.

URL <http://inspirehep.net/record/795806/files/arXiv:0809.1224.pdf>

- [25] S. K. Choi, et al., Bounds on the width, mass difference and other properties of  $X(3872) \rightarrow \pi^+\pi^-J/\psi$  decays, Phys. Rev. D84 (2011) 052004. arXiv:1107.0163, doi:10.1103/PhysRevD.84.052004.
- [26] B. Aubert, et al., A Study of  $B \rightarrow X(3872)K$ , with  $X_{3872} \rightarrow J/\psi\pi^+\pi^-$ , Phys. Rev. D77 (2008) 111101. arXiv:0803.2838, doi:10.1103/PhysRevD.77.111101.
- [27] D. Acosta, et al., Observation of the narrow state  $X(3872) \rightarrow J/\psi\pi^+\pi^-$  in  $p\bar{p}$  collisions at  $\sqrt{s} = 1.96$  TeV, Phys. Rev. Lett. 93 (2004) 072001. arXiv:hep-ex/0312021, doi:10.1103/PhysRevLett.93.072001.
- [28] A. Abulencia, et al., Analysis of the quantum Numbers  $J^{PC}$  of the  $X(3872)$ , Phys. Rev. Lett. 98 (2007) 132002. arXiv:hep-ex/0612053, doi:10.1103/PhysRevLett.98.132002.
- [29] T. Aaltonen, et al., Precision Measurement of the  $X(3872)$  Mass in  $J/\psi\pi^+\pi^-$  Decays, Phys. Rev. Lett. 103 (2009) 152001. arXiv:0906.5218, doi:10.1103/PhysRevLett.103.152001.
- [30] V. M. Abazov, et al., Observation and properties of the  $X(3872)$  decaying to  $J/\psi\pi^+\pi^-$  in  $p\bar{p}$  collisions at  $\sqrt{s} = 1.96$  TeV, Phys. Rev. Lett. 93 (2004) 162002. arXiv:hep-ex/0405004, doi:10.1103/PhysRevLett.93.162002.
- [31] K. Abe, et al., Evidence for  $X(3872) \rightarrow \gamma J/\psi$  and the sub-threshold decay  $X(3872) \rightarrow \omega J/\psi$ , in: Lepton and photon interactions at high energies. Proceedings, 22nd International Symposium, LP 2005, Uppsala, Sweden, June 30-July 5, 2005, 2005. arXiv:hep-ex/0505037.
- [32] P. del Amo Sanchez, et al., Evidence for the decay  $X(3872) \rightarrow J/\psi\omega$ , Phys. Rev. D82 (2010) 011101. arXiv:1005.5190, doi:10.1103/PhysRevD.82.011101.
- [33] G. Gokhroo, et al., Observation of a Near-threshold  $D0$  anti- $D0$   $\pi0$  Enhancement in  $B \rightarrow D0$  anti- $D0$   $\pi0$  K Decay, Phys. Rev. Lett. 97 (2006) 162002. arXiv:hep-ex/0606055, doi:10.1103/PhysRevLett.97.162002.
- [34] T. Aushev, et al., Study of the  $B \rightarrow X(3872)(D^*0$  anti- $D0)$  K decay, Phys. Rev. D81 (2010) 031103. arXiv:0810.0358, doi:10.1103/PhysRevD.81.031103.
- [35] B. Aubert, et al., Study of Resonances in Exclusive B Decays to anti- $D^*$   $D^*$  K, Phys. Rev. D77 (2008) 011102. arXiv:0708.1565, doi:10.1103/PhysRevD.77.011102.
- [36] B. Aubert, et al., Search for  $B^+ \rightarrow X(3872)K^+$ ,  $X_{3872} \rightarrow J/\psi\gamma$ , Phys. Rev. D74 (2006) 071101. arXiv:hep-ex/0607050, doi:10.1103/PhysRevD.74.071101.
- [37] B. Aubert, et al., Evidence for  $X(3872) \rightarrow \psi_{2S}\gamma$  in  $B^{\pm} \rightarrow X_{3872}K^{\pm}$  decays, and a study of  $B \rightarrow c\bar{c}\gamma K$ , Phys. Rev. Lett. 102 (2009) 132001. arXiv:0809.0042, doi:10.1103/PhysRevLett.102.132001.
- [38] R. Aaij, et al., Evidence for the decay  $X(3872) \rightarrow \psi(2S)\gamma$ , Nucl. Phys. B886 (2014) 665–680. arXiv:1404.0275, doi:10.1016/j.nuclphysb.2014.06.011.
- [39] M. Ablikim, et al., Observation of  $e^+e^-X(3872)$  at BESIII, Phys. Rev. Lett. 112 (9) (2014) 092001. arXiv:1310.4101, doi:10.1103/PhysRevLett.112.092001.
- [40] R. Aaij, et al., Observation of  $X(3872)$  production in  $pp$  collisions at  $\sqrt{s} = 7$  TeV, Eur. Phys. J. C72 (2012) 1972. arXiv:1112.5310, doi:10.1140/epjc/s10052-012-1972-7.
- [41] R. Aaij, et al., Determination of the  $X(3872)$  meson quantum Numbers, Phys. Rev. Lett. 110 (2013) 222001. arXiv:1302.6269, doi:10.1103/PhysRevLett.110.222001.
- [42] S. Chatrchyan, et al., Measurement of the  $X(3872)$  production cross section via decays to  $J/\psi$   $\pi$   $\pi$  in  $pp$  collisions at  $\sqrt{s} = 7$  TeV, JHEP 04 (2013) 154. arXiv:1302.3968, doi:10.1007/JHEP04(2013)154.
- [43] M. Ablikim, et al., Observation of a Charged Charmoniumlike Structure in  $e^+e^- \rightarrow \pi^+\pi^-J/\psi$  at  $\sqrt{s} = 4.26$  GeV, Phys. Rev. Lett. 110 (2013) 252001. arXiv:1303.5949, doi:10.1103/PhysRevLett.110.252001.
- [44] Z. Q. Liu, et al., Study of  $e^+e^- \rightarrow \pi^+\pi^-J/\psi$  and Observation of a Charged Charmoniumlike State at Belle, Phys. Rev. Lett. 110 (2013) 252002. arXiv:1304.0121, doi:10.1103/PhysRevLett.110.252002.
- [45] T. Xiao, S. Dobbs, A. Tomaradze, K. K. Seth, Observation of the Charged Hadron  $Z_c^{\pm}(3900)$  and Evidence for the Neutral  $Z_c^0(3900)$  in  $e^+e^- \rightarrow \pi\pi J/\psi$  at  $\sqrt{s} = 4170$  MeV, Phys. Lett. B727 (2013) 366–370. arXiv:1304.3036, doi:10.1016/j.physletb.2013.10.041.
- [46] M. Ablikim, et al., Observation of a charged ( $D\bar{D}^*$ ) $^{\pm}$  mass peak in  $e^+e^- \rightarrow \pi D\bar{D}^*$  at  $\sqrt{s} = 4.26$  GeV, Phys. Rev. Lett. 112 (2) (2014) 022001. arXiv:1310.1163, doi:10.1103/PhysRevLett.112.022001.
- [47] K. Abe, et al., Observation of a near-threshold omega  $J/\psi$  mass enhancement in exclusive  $B \rightarrow K$  omega  $J/\psi$  decays, Phys. Rev. Lett. 94 (2005) 182002. arXiv:hep-ex/0408126, doi:10.1103/PhysRevLett.94.182002.
- [48] B. Aubert, et al., Observation of  $Y(3940) \rightarrow J/\psi\omega$  in  $B \rightarrow J/\psi\omega K$  at BABAR, Phys. Rev. Lett. 101 (2008) 082001. arXiv:0711.2047, doi:10.1103/PhysRevLett.101.082001.
- [49] S. Uehara, et al., Observation of a charmonium-like enhancement in the  $\gamma\gamma \rightarrow \omega J/\psi$  process, Phys. Rev. Lett. 104 (2010) 092001. arXiv:0912.4451, doi:10.1103/PhysRevLett.104.092001.
- [50] J. P. Lees, et al., Search for resonances decaying to  $\eta_c\pi^+\pi^-$  in two-photon interactions, Phys. Rev. D86 (2012) 092005. arXiv:1206.2008, doi:10.1103/PhysRevD.86.092005.
- [51] K. Abe, et al., Observation of a new charmonium state in double charmonium production in  $e^+e^-$  annihilation at  $s^{**}(1/2) = 10.6$ -GeV, Phys. Rev. Lett. 98 (2007) 082001. arXiv:hep-ex/0507019, doi:10.1103/PhysRevLett.98.082001.
- [52] P. Pakhlov, et al., Production of New Charmoniumlike States in  $e^+e^- \rightarrow J/\psi D^*(*)$  anti- $D^*(*)$  at  $s^{**}(1/2) = 10$ . GeV, Phys. Rev. Lett. 100 (2008) 202001. arXiv:0708.3812, doi:10.1103/PhysRevLett.100.202001.
- [53] C. Z. Yuan, et al., Measurement of  $e^+e^- \rightarrow \pi^+\pi^-J/\psi$  cross-section via initial state radiation at Belle, Phys. Rev. Lett. 99 (2007) 182004. arXiv:0707.2541, doi:10.1103/PhysRevLett.99.182004.
- [54] M. Ablikim, et al., Precise measurement of the  $e^+e^- \rightarrow \pi^+\pi^-J/\psi$  cross section at center-of-mass energies from 3.77 to 4.60 GeV, Phys. Rev. Lett. 118 (9) (2017) 092001. arXiv:1611.01317, doi:10.1103/PhysRevLett.118.092001.
- [55] M. Ablikim, et al., Observation of a Charged Charmoniumlike Structure  $Z_c(4020)$  and Search for the  $Z_c(3900)$  in  $e^+e^- \rightarrow \pi^+\pi^-h_c$ , Phys. Rev. Lett. 111 (24) (2013) 242001. arXiv:1309.1896, doi:10.1103/PhysRevLett.111.242001.
- [56] M. Ablikim, et al., Observation of a charged charmoniumlike structure in  $e^+e^- \rightarrow (D^*\bar{D}^*)^{\pm}\pi^{\mp}$  at  $\sqrt{s} = 4.26$ GeV, Phys. Rev. Lett. 112 (13)

- (2014) 132001. arXiv:1308.2760, doi:10.1103/PhysRevLett.112.132001.
- [57] R. Mizuk, et al., Observation of two resonance-like structures in the  $\pi^+ \chi_{c1}$  mass distribution in exclusive anti- $B^0 \rightarrow K^- \pi^+ \chi_{c1}$  decays, Phys. Rev. D78 (2008) 072004. arXiv:0806.4098, doi:10.1103/PhysRevD.78.072004.
- [58] J. P. Lees, et al., Search for the  $Z_1(4050)^+$  and  $Z_2(4250)^+$  states in  $\bar{B}^0 \rightarrow \chi_{c1} K^- \pi^+$  and  $B^+ \rightarrow \chi_{c1} K_S^0 \pi^+$ , Phys. Rev. D85 (2012) 052003. arXiv:1111.5919, doi:10.1103/PhysRevD.85.052003.
- [59] X. L. Wang, et al., Measurement of  $e^+e^- \rightarrow \pi^+ \pi^- \psi(2S)$  via Initial State Radiation at Belle, Phys. Rev. D91 (2015) 112007. arXiv:1410.7641, doi:10.1103/PhysRevD.91.112007.
- [60] R. Aaij, et al., Evidence for an  $\eta_c(1S)\pi^-$  resonance in  $B^0 \rightarrow \eta_c(1S)K^+\pi^-$  decays, Submitted to: Eur. Phys. J.arXiv:1809.07416.
- [61] T. Aaltonen, et al., Evidence for a Narrow Near-Threshold Structure in the  $J/\psi\phi$  Mass Spectrum in  $B^+ \rightarrow J/\psi\phi K^+$  Decays, Phys. Rev. Lett. 102 (2009) 242002. arXiv:0903.2229, doi:10.1103/PhysRevLett.102.242002.
- [62] T. Aaltonen, et al., Observation of the  $Y(4140)$  structure in the  $J/\psi\phi$  mass spectrum in  $B^{\pm} \rightarrow J/\psi\phi K^{\pm}$  decays, Mod. Phys. Lett. A32 (26) (2017) 1750139. arXiv:1101.6058, doi:10.1142/S0217732317501395.
- [63] V. M. Abazov, et al., Search for the  $X(4140)$  state in  $B^+ \rightarrow J_{\psi, \phi} K^+$  decays with the D0 Detector, Phys. Rev. D89 (1) (2014) 012004. arXiv:1309.6580, doi:10.1103/PhysRevD.89.012004.
- [64] R. Aaij, et al., Observation of  $J/\psi\phi$  structures consistent with exotic states from amplitude analysis of  $B^+ \rightarrow J/\psi\phi K^+$  decays, Phys. Rev. Lett. 118 (2) (2017) 022003. arXiv:1606.07895, doi:10.1103/PhysRevLett.118.022003.
- [65] M. Ablikim, et al., Search for the  $Y(4140)$  via  $e^+e^- J/\psi$  at  $\sqrt{s}=4.23, 4.26$  and  $4.36$  GeV, Phys. Rev. D91 (3) (2015) 032002. arXiv:1412.1867, doi:10.1103/PhysRevD.91.032002.
- [66] M. Ablikim, et al., Observation of  $e^+e^- \rightarrow \phi\chi_{c1}$  and  $\phi\chi_{c2}$  at  $\sqrt{s}=4.600$  GeV, Phys. Rev. D97 (3) (2018) 032008. arXiv:1712.09240, doi:10.1103/PhysRevD.97.032008.
- [67] K. Chilikin, et al., Observation of a new charged charmoniumlike state in  $\bar{B}^0 \rightarrow J/\psi K^- \pi^+$  decays, Phys. Rev. D90 (11) (2014) 112009. arXiv:1408.6457, doi:10.1103/PhysRevD.90.112009.
- [68] M. Ablikim, et al., Study of  $e^+e^- \rightarrow \omega\chi_{cJ}$  at center-of-mass energies from 4.21 to 4.42 GeV, Phys. Rev. Lett. 114 (9) (2015) 092003. arXiv:1410.6538, doi:10.1103/PhysRevLett.114.092003.
- [69] M. Ablikim, et al., Evidence of Two Resonant Structures in  $e^+e^- \rightarrow \pi^+ \pi^- h_c$ , Phys. Rev. Lett. 118 (9) (2017) 092002. arXiv:1610.07044, doi:10.1103/PhysRevLett.118.092002.
- [70] M. Ablikim, et al., Measurement of  $e^+e^- \rightarrow \pi^+ \pi^- \psi(3686)$  from 4.008 to 4.600 GeV and observation of a charged structure in the  $\pi^{\pm}\psi(3686)$  mass spectrum, Phys. Rev. D96 (3) (2017) 032004. arXiv:1703.08787, doi:10.1103/PhysRevD.96.032004.
- [71] M. Ablikim, et al., Evidence of a resonant structure in the  $e^+e^- \rightarrow \pi^+ D^0 D^{*-}$  cross section between 4.05 and 4.60 GeV arXiv:1808.02847.
- [72] B. Aubert, et al., Observation of a broad structure in the  $\pi^+ \pi^- J/\psi$  mass spectrum around 4.26-GeV/ $c^2$ , Phys. Rev. Lett. 95 (2005) 142001. arXiv:hep-ex/0506081, doi:10.1103/PhysRevLett.95.142001.
- [73] J. P. Lees, et al., Study of the reaction  $e^+e^- \rightarrow J/\psi\pi^+\pi^-$  via initial-state radiation at BaBar, Phys. Rev. D86 (2012) 051102. arXiv:1204.2158, doi:10.1103/PhysRevD.86.051102.
- [74] Q. He, et al., Confirmation of the  $Y(4260)$  resonance production in ISR, Phys. Rev. D74 (2006) 091104. arXiv:hep-ex/0611021, doi:10.1103/PhysRevD.74.091104.
- [75] T. E. Coan, et al., Charmonium decays of  $Y(4260)$ ,  $\psi(4160)$  and  $\psi(4040)$ , Phys. Rev. Lett. 96 (2006) 162003. arXiv:hep-ex/0602034, doi:10.1103/PhysRevLett.96.162003.
- [76] C. P. Shen, et al., Evidence for a new resonance and search for the  $Y(4140)$  in the  $\gamma\gamma \rightarrow \phi J/\psi$  process, Phys. Rev. Lett. 104 (2010) 112004. arXiv:0912.2383, doi:10.1103/PhysRevLett.104.112004.
- [77] B. Aubert, et al., Evidence of a broad structure at an invariant mass of 4.32- GeV/ $c^2$  in the reaction  $e^+e^- \rightarrow \pi^+ \pi^- \psi_{2S}$  measured at BaBar, Phys. Rev. Lett. 98 (2007) 212001. arXiv:hep-ex/0610057, doi:10.1103/PhysRevLett.98.212001.
- [78] J. P. Lees, et al., Study of the reaction  $e^+e^- \rightarrow \psi(2S)\pi^+\pi^-$  via initial-state radiation at BaBar, Phys. Rev. D89 (11) (2014) 111103. arXiv:1211.6271, doi:10.1103/PhysRevD.89.111103.
- [79] X. L. Wang, et al., Observation of Two Resonant Structures in  $e^+e^-$  to  $\pi^+ \pi^- \psi(2S)$  via Initial State Radiation at Belle, Phys. Rev. Lett. 99 (2007) 142002. arXiv:0707.3699, doi:10.1103/PhysRevLett.99.142002.
- [80] S. K. Choi, et al., Observation of a resonance-like structure in the  $\pi^+ \pi^- \psi'$  mass distribution in exclusive  $B \rightarrow K\pi^{\pm}\psi'$  decays, Phys. Rev. Lett. 100 (2008) 142001. arXiv:0708.1790, doi:10.1103/PhysRevLett.100.142001.
- [81] R. Mizuk, et al., Dalitz analysis of  $B \rightarrow K\pi^+\psi'$  decays and the  $Z(4430)^+$ , Phys. Rev. D80 (2009) 031104. arXiv:0905.2869, doi:10.1103/PhysRevD.80.031104.
- [82] K. Chilikin, et al., Experimental constraints on the spin and parity of the  $Z(4430)^+$ , Phys. Rev. D88 (7) (2013) 074026. arXiv:1306.4894, doi:10.1103/PhysRevD.88.074026.
- [83] B. Aubert, et al., Search for the  $Z(4430)^-$  at BABAR, Phys. Rev. D79 (2009) 112001. arXiv:0811.0564, doi:10.1103/PhysRevD.79.112001.
- [84] R. Aaij, et al., Observation of the resonant character of the  $Z(4430)^-$  state, Phys. Rev. Lett. 112 (22) (2014) 222002. arXiv:1404.1903, doi:10.1103/PhysRevLett.112.222002.
- [85] G. Pakhlova, et al., Observation of a near-threshold enhancement in the  $e^+e^- \rightarrow \Lambda_c^+ \Lambda_c^-$  cross section using initial-state radiation, Phys. Rev. Lett. 101 (2008) 172001. arXiv:0807.4458, doi:10.1103/PhysRevLett.101.172001.
- [86] R. D. Matheus, F. S. Navarra, M. Nielsen, R. R. da Silva, Comparative study of pentaquark interpolating currents, Phys. Lett. B602 (2004) 185–196. arXiv:hep-ph/0406246, doi:10.1016/j.physletb.2004.09.072.
- [87] F. S. Navarra, M. Nielsen,  $X(3872) \rightarrow J/\psi \pi^+ \pi^-$  and  $X(3872) \rightarrow J/\psi \pi^+ \pi^- \pi^0$  decay widths from QCD sum rules, Phys. Lett. B639 (2006) 272–277. arXiv:hep-ph/0605038, doi:10.1016/j.physletb.2006.06.054.
- [88] R. D. Matheus, S. Narison, M. Nielsen, J. M. Richard, Can the  $X(3872)$  be a  $1^{++}$  four-quark state?, Phys. Rev. D75 (2007) 014005. arXiv:hep-ph/0608297, doi:10.1103/PhysRevD.75.014005.
- [89] S. H. Lee, A. Mihara, F. S. Navarra, M. Nielsen, QCD sum rules study of the meson  $Z(4430)$ , Phys. Lett. B661 (2008) 28–32. arXiv:0710.1029, doi:10.1016/j.physletb.2008.01.062.
- [90] S. H. Lee, K. Morita, M. Nielsen, Width of exotics from QCD sum rules: Tetraquarks or molecules?, Phys. Rev. D78 (2008) 076001.



- arXiv:0808.3168, doi:10.1103/PhysRevD.78.076001.
- [91] S. H. Lee, K. Morita, M. Nielsen, Can the  $\pi^+ \chi(c1)$  resonance structures be  $D^*$  anti- $D^*$  and  $D(1)$  anti- $D$  molecules?, Nucl. Phys. A815 (2009) 29–39. arXiv:0808.0690, doi:10.1016/j.nuclphysa.2008.10.012.
- [92] R. M. Albuquerque, M. Nielsen, QCD sum rules study of the  $J(PC) = 1^-$  charmonium  $Y$  mesons, Nucl. Phys. A815 (2009) 53–66, [Erratum: Nucl. Phys. A857,48(2011)]. arXiv:0804.4817, doi:10.1016/j.nuclphysa.2011.04.001, 10.1016/j.nuclphysa.2008.10.015.
- [93] M. E. Bracco, S. H. Lee, M. Nielsen, R. Rodrigues da Silva, The Meson  $Z^+(4430)$  as a tetraquark state, Phys. Lett. B671 (2009) 240–244. arXiv:0807.3275, doi:10.1016/j.physletb.2008.12.021.
- [94] S. H. Lee, M. Nielsen, U. Wiedner,  $D(s)D^*$  molecule as an axial meson, J. Korean Phys. Soc. 55 (2009) 424. arXiv:0803.1168, doi:10.3938/jkps.55.424.
- [95] R. M. Albuquerque, M. E. Bracco, M. Nielsen, A QCD sum rule calculation for the  $Y(4140)$  narrow structure, Phys. Lett. B678 (2009) 186–190. arXiv:0903.5540, doi:10.1016/j.physletb.2009.06.022.
- [96] R. D. Matheus, F. S. Navarra, M. Nielsen, C. M. Zanetti, QCD Sum Rules for the  $X(3872)$  as a mixed molecule-charmonium state, Phys. Rev. D80 (2009) 056002. arXiv:0907.2683, doi:10.1103/PhysRevD.80.056002.
- [97] R. M. Albuquerque, J. M. Dias, M. Nielsen, Can the  $X(4350)$  narrow structure be a  $1^{+-}$  exotic state?, Phys. Lett. B690 (2010) 141–144. arXiv:1001.3092, doi:10.1016/j.physletb.2010.05.024.
- [98] M. Nielsen, C. M. Zanetti, Radiative decay of the  $X(3872)$  as a mixed molecule-charmonium state in QCD Sum Rules, Phys. Rev. D82 (2010) 116002. arXiv:1006.0467, doi:10.1103/PhysRevD.82.116002.
- [99] S. Narison, F. S. Navarra, M. Nielsen, On the nature of the  $X(3872)$  from QCD, Phys. Rev. D83 (2011) 016004. arXiv:1006.4802, doi:10.1103/PhysRevD.83.016004.
- [100] S. I. Finazzo, M. Nielsen, X. Liu, QCD sum rule calculation for the charmonium-like structures in the  $J/\psi\phi$  and  $J/\psi\omega$  invariant mass spectra, Phys. Lett. B701 (2011) 101–106. arXiv:1102.2347, doi:10.1016/j.physletb.2011.05.042.
- [101] C. M. Zanetti, M. Nielsen, R. D. Matheus, QCD Sum Rules for the production of the  $X(3872)$  as a mixed molecule-charmonium state in B meson decay, Phys. Lett. B702 (2011) 359–363. arXiv:1105.1343, doi:10.1016/j.physletb.2011.07.018.
- [102] J. M. Dias, S. Narison, F. S. Navarra, M. Nielsen, J. M. Richard, Relation between  $T_{cc,bb}$  and  $X_{c,b}$  from QCD, Phys. Lett. B703 (2011) 274–280. arXiv:1105.5630, doi:10.1016/j.physletb.2011.07.082.
- [103] R. M. Albuquerque, M. Nielsen, R. Rodrigues da Silva, Exotic  $1^{--}$  States in QCD Sum Rules, Phys. Rev. D84 (2011) 116004. arXiv:1110.2113, doi:10.1103/PhysRevD.84.116004.
- [104] Z.-F. Sun, X. Liu, M. Nielsen, S.-L. Zhu, Hadronic molecules with both open charm and bottom, Phys. Rev. D85 (2012) 094008. arXiv:1203.1090, doi:10.1103/PhysRevD.85.094008.
- [105] J. M. Dias, R. M. Albuquerque, M. Nielsen, C. M. Zanetti,  $Y(4260)$  as a mixed charmonium-tetraquark state, Phys. Rev. D86 (2012) 116012. arXiv:1209.6592, doi:10.1103/PhysRevD.86.116012.
- [106] J. M. Dias, F. S. Navarra, M. Nielsen, C. M. Zanetti,  $Z_c^+(3900)$  decay width in QCD sum rules, Phys. Rev. D88 (1) (2013) 016004. arXiv:1304.6433, doi:10.1103/PhysRevD.88.016004.
- [107] A. Martínez Torres, K. P. Khemchandani, M. Nielsen, F. S. Navarra, E. Oset, Exploring the  $D^*\rho$  system within QCD sum rules, Phys. Rev. D88 (7) (2013) 074033. arXiv:1307.1724, doi:10.1103/PhysRevD.88.074033.
- [108] J. M. Dias, X. Liu, M. Nielsen, Prediction for the decay width of a charged state near the  $D_s\bar{D}^*/D_s^*\bar{D}$  threshold, Phys. Rev. D88 (9) (2013) 096014. arXiv:1307.7100, doi:10.1103/PhysRevD.88.096014.
- [109] K. P. Khemchandani, A. Martínez Torres, M. Nielsen, F. S. Navarra, Relating  $D^*\bar{D}^*$  currents with  $J^\pi = 0^+, 1^+$  and  $2^+$  to  $Z_c$  states, Phys. Rev. D89 (1) (2014) 014029. arXiv:1310.0862, doi:10.1103/PhysRevD.89.014029.
- [110] A. Martínez Torres, K. P. Khemchandani, F. S. Navarra, M. Nielsen, E. Oset, Reanalysis of the  $e^+e^- \rightarrow (D^*\bar{D}^*)\pi^\pm$  reaction and the claim for the  $Z_c(4025)$  resonance, Phys. Rev. D89 (1) (2014) 014025. arXiv:1310.1119, doi:10.1103/PhysRevD.89.014025.
- [111] R. M. Albuquerque, J. M. Dias, M. Nielsen, C. M. Zanetti,  $Y(3940)$  as a Mixed Charmonium-Molecule State, Phys. Rev. D89 (7) (2014) 076007. arXiv:1311.6411, doi:10.1103/PhysRevD.89.076007.
- [112] R. M. Albuquerque, M. Nielsen, C. M. Zanetti, Production of the  $Y(4260)$  state in B meson decay, Phys. Lett. B747 (2015) 83–87. arXiv:1502.00119, doi:10.1016/j.physletb.2015.05.022.
- [113] R. M. Albuquerque, R. D. Matheus, The  $J/\Psi\Phi$  decay channel of the  $Y(4140)$  molecular state, Nucl. Part. Phys. Proc. 258-259 (2015) 148–151. doi:10.1016/j.nuclphysbps.2015.01.032.
- [114] A. Martínez Torres, K. P. Khemchandani, J. M. Dias, F. S. Navarra, M. Nielsen, Understanding close-lying exotic charmonia states within QCD sum rules, Nucl. Phys. A966 (2017) 135–157. arXiv:1606.07505, doi:10.1016/j.nuclphysa.2017.06.022.
- [115] R. Albuquerque, S. Narison, F. Fanomezana, A. Rabemananjara, D. Rabetiarivony, G. Randriamanatrika, XYZ-like Spectra from Laplace Sum Rule at N2LO in the Chiral Limit, Int. J. Mod. Phys. A31 (36) (2016) 1650196. arXiv:1609.03351, doi:10.1142/S0217751X16501967.
- [116] R. Albuquerque, S. Narison, D. Rabetiarivony, G. Randriamanatrika, XYZ-SU3 Breakings from Laplace Sum Rules at Higher Orders, Int. J. Mod. Phys. A33 (16) (2018) 1850082. arXiv:1709.09023, doi:10.1142/S0217751X18500823.
- [117] R. M. Albuquerque, F. Fanomezana, S. Narison, A. Rabemananjara, D. Rabetiarivony, G. Randriamanatrika,  $0^+$  and  $1^+$  heavy-light exotic mesons at N2LO in the chiral limit, in: 20th High-Energy Physics International Conference in Quantum Chromodynamics (QCD 17) Montpellier, France, July 3-7, 2017, 2018. arXiv:1801.09110. URL <http://inspirehep.net/record/1650836/files/arXiv:1801.09110.pdf>
- [118] M. A. Shifman, A. I. Vainshtein, V. I. Zakharov, QCD and Resonance Physics. Theoretical Foundations, Nucl. Phys. B147 (1979) 385–447. doi:10.1016/0550-3213(79)90022-1.
- [119] M. A. Shifman, A. I. Vainshtein, V. I. Zakharov, QCD and Resonance Physics: Applications, Nucl. Phys. B147 (1979) 448–518. doi:10.1016/0550-3213(79)90023-3.
- [120] L. J. Reinders, H. Rubinstein, S. Yazaki, Hadron Properties from QCD Sum Rules, Phys. Rept. 127 (1985) 1. doi:10.1016/0370-1573(85)90065-1.
- [121] S. Narison, QCD as a Theory of Hadrons, Vol. 17, Cambridge University Press, 2007. URL <http://www.cambridge.org/zw/academic/subjects/physics/particle-physics-and-nuclear-physics/qcd-theory-hadrons-parton>

- [122] S. Narison, QCD spectral sum rules, World Sci. Lect. Notes Phys. 26 (1989) 1–527.
- [123] S. Narison, Techniques of Dimensional Renormalization and Applications to the Two Point Functions of QCD and QED, Phys. Rept. 84 (1982) 263–399. doi:10.1016/0370-1573(82)90023-0.
- [124] S. Narison, Withdrawn: QCD as a theory of hadrons from partons to confinement arXiv:hep-ph/0205006.
- [125] R. Aaij, et al., Observation of  $J/\psi p$  Resonances Consistent with Pentaquark States in  $\Lambda_b^0 \rightarrow J/\psi K^- p$  Decays, Phys. Rev. Lett. 115 (2015) 072001. arXiv:1507.03414, doi:10.1103/PhysRevLett.115.072001.
- [126] R. Aaij, et al., Model-independent evidence for  $J/\psi p$  contributions to  $\Lambda_b^0 \rightarrow J/\psi p K^-$  decays, Phys. Rev. Lett. 117 (8) (2016) 082002. arXiv:1604.05708, doi:10.1103/PhysRevLett.117.082002.
- [127] R. Aaij, et al., Evidence for exotic hadron contributions to  $\Lambda_b^0 \rightarrow J/\psi p \pi^-$  decays, Phys. Rev. Lett. 117 (8) (2016) 082003, [Addendum: Phys. Rev. Lett. 118, 119901 (2017)]. arXiv:1606.06999, doi:10.1103/PhysRevLett.118.119901, 10.1103/PhysRevLett.117.082003, 10.1103/PhysRevLett.117.109902.
- [128] B. L. Ioffe, Calculation of Baryon Masses in Quantum Chromodynamics, Nucl. Phys. B188 (1981) 317–341, [Erratum: Nucl. Phys. B191, 591 (1981)]. doi:10.1016/0550-3213(81)90315-1, 10.1016/0550-3213(81)90259-5.
- [129] M. Shifman, B. Ioffe (Eds.), At the frontier of particle physics. Handbook of QCD. Vol. 1-3, World Scientific, Singapore, Singapore, 2001. doi:10.1142/4544.
- [130] A. V. Radyushkin, Introduction into QCD sum rule approach, in: Strong interactions at low and intermediate energies. Proceedings, 13th Annual Hampton University Graduate Studies, HUGS'98, Newport News, USA, May 26-June 12, 1998, 1998. arXiv:hep-ph/0101227.
- [131] V. A. Novikov, L. B. Okun, M. A. Shifman, A. I. Vainshtein, M. B. Voloshin, V. I. Zakharov, Charmonium and Gluons: Basic Experimental Facts and Theoretical Introduction, Phys. Rept. 41 (1978) 1–133. doi:10.1016/0370-1573(78)90120-5.
- [132] M. A. Shifman, Snapshots of hadrons or the story of how the vacuum medium determines the properties of the classical mesons which are produced, live and die in the QCD vacuum, Prog. Theor. Phys. Suppl. 131 (1998) 1–71, [111(1998)]. arXiv:hep-ph/9802214, doi:10.1143/PTPS.131.1.
- [133] T. D. Cohen, R. J. Furnstahl, D. K. Griegel, X.-m. Jin, QCD sum rules and applications to nuclear physics, Prog. Part. Nucl. Phys. 35 (1995) 221–298, [221(1994)]. arXiv:hep-ph/9503315, doi:10.1016/0146-6410(95)00043-I.
- [134] M. A. Shifman, Quark hadron duality, in: At the frontier of particle physics. Handbook of QCD. Vol. 1-3, World Scientific, World Scientific, Singapore, 2001, pp. 1447–1494, [3,1447(2000)]. arXiv:hep-ph/0009131.
- [135] M. Shifman, Lectures on quark hadron duality, Czech. J. Phys. 52 (2002) B102–B135. doi:10.1007/s10582-002-0080-6.
- [136] K. G. Wilson, Nonlagrangian models of current algebra, Phys. Rev. 179 (1969) 1499–1512. doi:10.1103/PhysRev.179.1499.
- [137] D. B. Leinweber, QCD sum rules for skeptics, Annals Phys. 254 (1997) 328–396. arXiv:nucl-th/9510051, doi:10.1006/aphy.1996.5641.
- [138] C. A. Dominguez, Introduction to QCD sum rules, Mod. Phys. Lett. A28 (2013) 1360002. arXiv:1305.7047, doi:10.1142/S021773231360002X.
- [139] L. J. Reinders, H. R. Rubinstein, S. Yazaki, QCD CONTRIBUTIONS TO VACUUM POLARIZATION, Phys. Lett. 94B (1980) 203–206. doi:10.1016/0370-2693(80)90859-X.
- [140] L. J. Reinders, H. R. Rubinstein, S. Yazaki, QCD Sum Rules for Heavy Quark Systems, Nucl. Phys. B186 (1981) 109–146. doi:10.1016/0550-3213(81)90095-X.
- [141] S. Narison, Gluon condensates and c, b quark masses from quarkonia ratios of moments, Phys. Lett. B693 (2010) 559–566, [Erratum: Phys. Lett. B705, 544 (2011)]. arXiv:1004.5333, doi:10.1016/j.physletb.2011.09.116, 10.1016/j.physletb.2010.09.007.
- [142] M. Gell-Mann, R. J. Oakes, B. Renner, Behavior of current divergences under  $SU(3) \times SU(3)$ , Phys. Rev. 175 (1968) 2195–2199. doi:10.1103/PhysRev.175.2195.
- [143] M. Tanabashi, et al., Review of Particle Physics, Phys. Rev. D98 (3) (2018) 030001. doi:10.1103/PhysRevD.98.030001.
- [144] E. Bagan, J. I. Latorre, P. Pascual, R. Tarrach, Heavy Quark Expansion, Factorization and Eight-dimensional Gluon Condensates, Nucl. Phys. B254 (1985) 555–568. doi:10.1016/0550-3213(85)90233-0.
- [145] G. Launer, S. Narison, R. Tarrach, Nonperturbative QCD Vacuum From  $e^+e^- \rightarrow I = 1$  Hadron Data, Z. Phys. C26 (1984) 433–439. doi:10.1007/BF01452571.
- [146] S. Narison, Power corrections to  $\alpha(s)(M(\tau))$ — $V(u)$ — and  $\alpha(m(s))$ , Phys. Lett. B673 (2009) 30–36. arXiv:0901.3823, doi:10.1016/j.physletb.2009.01.062.
- [147] F. L. Braghin, F. S. Navarra, Factorization breaking of four-quark condensates in the NambuJona-Lasinio model, Phys. Rev. D91 (7) (2015) 074008. arXiv:1404.4094, doi:10.1103/PhysRevD.91.074008.
- [148] P. Pascual, R. Tarrach, QCD: RENORMALIZATION FOR THE PRACTITIONER, Lect. Notes Phys. 194 (1984) 1–277.
- [149] W. Lucha, D. Melikhov, S. Simula, Systematic uncertainties of hadron parameters obtained with QCD sum rules, Phys. Rev. D76 (2007) 036002. arXiv:0705.0470, doi:10.1103/PhysRevD.76.036002.
- [150] S. Narison, V-A hadronic tau decays: A Laboratory for the QCD vacuum, Phys. Lett. B624 (2005) 223–232. arXiv:hep-ph/0412152, doi:10.1016/j.physletb.2005.08.007.
- [151] G. Kallen, A. S. Wightman, The Analytic Properties of the Vacuum Expectation Value of a Product of Three Scalar Local Fields, Vol. 1, 1958.
- [152] G. Kallen, H. Wilhelmsson, Generalized singular functions, Vol. 1, 1959.
- [153] A. Martin, The Rigorous analyticity unitarity program and its successes, Lect. Notes Phys. 558 (2000) 127–135, [127(1999)]. arXiv:hep-ph/9906393.
- [154] R. Zwicky, A brief Introduction to Dispersion Relations and Analyticity, in: Proceedings, Quantum Field Theory at the Limits: from Strong Fields to Heavy Quarks (HQ 2016): Dubna, Russia, July 18-30, 2016, 2017, pp. 93–120. arXiv:1610.06090, doi:10.3204/DESY-PROC-2016-04/Zwicky.
- [155] B. L. Ioffe, A. V. Smilga, Meson Widths and Form-Factors at Intermediate Momentum Transfer in Nonperturbative QCD, Nucl. Phys. B216 (1983) 373–407. doi:10.1016/0550-3213(83)90291-2.
- [156] L. J. Reinders, QCD Sum Rules: An Introduction and Some Applications, Acta Phys. Polon. B15 (1984) 329.
- [157] V. A. Nesterenko, A. V. Radyushkin, Sum Rules and Pion Form-Factor in QCD, Phys. Lett. 115B (1982) 410. doi:10.1016/0370-

2693(82)90528-7.

- [158] M. E. Bracco, M. Chiapparini, M. Navarra, F. S. and Nielsen, Charm couplings and form factors in QCD sum rules, *Prog. Part. Nucl. Phys.* 67 (2012) 1019–1052. arXiv:1104.2864, doi:10.1016/j.pnnp.2012.03.002.
- [159] R. E. Cutkosky, Singularities and discontinuities of Feynman amplitudes, *J. Math. Phys.* 1 (1960) 429–433. doi:10.1063/1.1703676.
- [160] J. M. Dias, K. P. Khemchandani, A. Martínez Torres, M. Nielsen, C. M. Zanetti, A QCD sum rule calculation of the  $X^\pm(5568) \rightarrow B_s^0 \pi^\pm$  decay width, *Phys. Lett. B* 758 (2016) 235–238. arXiv:1603.02249, doi:10.1016/j.physletb.2016.05.015.
- [161] F. O. Duraes, S. H. Lee, F. S. Navarra, M. Nielsen,  $J/\psi$  dissociation by pions in QCD, *Phys. Lett. B* 564 (2003) 97–103. arXiv:nucl-th/0210075, doi:10.1016/S0370-2693(03)00709-3.
- [162] M. E. Bracco, F. S. Navarra, M. Nielsen,  $g_{N\bar{K}\Lambda}$  and  $g_{N\bar{K}\Sigma}$  from QCD sum rules in the  $\gamma_5 \sigma_{\mu\nu}$  structure, *Phys. Lett. B* 454 (1999) 346–352. arXiv:nucl-th/9902007, doi:10.1016/S0370-2693(99)00354-8.
- [163] B. L. Ioffe, A. V. Smilga, Nucleon Magnetic Moments and Magnetic Properties of Vacuum in QCD, *Nucl. Phys. B* 232 (1984) 109–142. doi:10.1016/0550-3213(84)90364-X.
- [164] M. Eidemuller, F. S. Navarra, R. Nielsen, M. and Rodrigues da Silva, Pentaquark decay width in QCD sum rules, *Phys. Rev. D* 72 (2005) 034003. arXiv:hep-ph/0503193, doi:10.1103/PhysRevD.72.034003.
- [165] F. S. Navarra, M. Nielsen, M. E. Bracco,  $D^* D$  pi form-factor revisited, *Phys. Rev. D* 65 (2002) 037502. arXiv:hep-ph/0109188, doi:10.1103/PhysRevD.65.037502.
- [166] M. E. Bracco, M. Chiapparini, F. S. Navarra, M. Nielsen,  $J/\psi$   $D^* D^*$  vertex from QCD sum rules, *Phys. Lett. B* 605 (2005) 326–334. arXiv:hep-ph/0410071, doi:10.1016/j.physletb.2004.11.024.
- [167] F. O. Duraes, F. S. Navarra, M. Nielsen, M. R. Robilotta, Meson loops and the  $g(D^* D \pi)$  coupling, *Braz. J. Phys.* 36 (2006) 1232–1237. arXiv:hep-ph/0403064, doi:10.1590/S0103-97332006000700021.
- [168] H. G. Dosch, Nonperturbative methods in quantum chromodynamics, *Prog. Part. Nucl. Phys.* 33 (1994) 121–200. doi:10.1016/0146-6410(94)90044-2.
- [169] F. Goerke, T. Gutsche, M. A. Ivanov, J. G. Korner, V. E. Lyubovitskij, P. Santorelli, Four-quark structure of  $Z_c(3900)$ ,  $Z(4430)$  and  $X_b(5568)$  states, *Phys. Rev. D* 94 (9) (2016) 094017. arXiv:1608.04656, doi:10.1103/PhysRevD.94.094017.
- [170] Y. Kondo, O. Morimatsu, T. Nishikawa, Two-hadron-irreducible QCD sum rule for pentaquark baryon, *Phys. Lett. B* 611 (2005) 93–101. arXiv:hep-ph/0404285, doi:10.1016/j.physletb.2005.01.070.
- [171] S. H. Lee, H. Kim, Y. Kwon, Parity of  $\Theta^+(1540)$  from QCD sum rules, *Phys. Lett. B* 609 (2005) 252–258. arXiv:hep-ph/0411104, doi:10.1016/j.physletb.2005.01.029.
- [172] H.-J. Lee, N. I. Kochelev, On the pi pi contribution to the QCD sum rules for the light tetraquark, *Phys. Rev. D* 78 (2008) 076005. arXiv:hep-ph/0702225, doi:10.1103/PhysRevD.78.076005.
- [173] H.-X. Chen, A. Hosaka, H. Toki, S.-L. Zhu, Light Scalar Meson  $\sigma(600)$  in QCD Sum Rule with Continuum, *Phys. Rev. D* 81 (2010) 114034. arXiv:0912.5138, doi:10.1103/PhysRevD.81.114034.
- [174] E. S. Swanson,  $Z_b$  and  $Z_c$  Exotic States as Coupled Channel Cusps, *Phys. Rev. D* 91 (3) (2015) 034009. arXiv:1409.3291, doi:10.1103/PhysRevD.91.034009.
- [175] D. V. Bugg, An Explanation of Belle states  $Z_b(10610)$  and  $Z_b(10650)$ , *EPL* 96 (1) (2011) 11002. arXiv:1105.5492, doi:10.1209/0295-5075/96/11002.
- [176] F.-K. Guo, C. Hanhart, Q. Wang, Q. Zhao, Could the near-threshold  $XYZ$  states be simply kinematic effects?, *Phys. Rev. D* 91 (5) (2015) 051504. arXiv:1411.5584, doi:10.1103/PhysRevD.91.051504.
- [177] B. Aubert, et al., Study of the  $B \rightarrow J/\psi K^- \pi^+ \pi^-$  decay and measurement of the  $B \rightarrow X(3872) K^-$  branching fraction, *Phys. Rev. D* 71 (2005) 071103. arXiv:hep-ex/0406022, doi:10.1103/PhysRevD.71.071103.
- [178] R. Aaij, et al., Quantum Numbers of the  $X(3872)$  state and orbital angular momentum in its  $\rho^0 J/\psi$  decay, *Phys. Rev. D* 92 (1) (2015) 011102. arXiv:1504.06339, doi:10.1103/PhysRevD.92.011102.
- [179] T. Barnes, S. Godfrey, Charmonium options for the  $X(3872)$ , *Phys. Rev. D* 69 (2004) 054008. arXiv:hep-ph/0311162, doi:10.1103/PhysRevD.69.054008.
- [180] T. Barnes, S. Godfrey, E. S. Swanson, Higher charmonia, *Phys. Rev. D* 72 (2005) 054026. arXiv:hep-ph/0505002, doi:10.1103/PhysRevD.72.054026.
- [181] M. Okamoto, et al., Charmonium spectrum from quenched anisotropic lattice QCD, *Phys. Rev. D* 65 (2002) 094508. arXiv:hep-lat/0112020, doi:10.1103/PhysRevD.65.094508.
- [182] N. A. Tornqvist, From the deuteron to deusons, an analysis of deuteron - like meson meson bound states, *Z. Phys. C* 61 (1994) 525–537. arXiv:hep-ph/9310247, doi:10.1007/BF01413192.
- [183] E. S. Swanson, Diagnostic decays of the  $X(3872)$ , *Phys. Lett. B* 598 (2004) 197–202. arXiv:hep-ph/0406080, doi:10.1016/j.physletb.2004.07.059.
- [184] E. S. Swanson, Short range structure in the  $X(3872)$ , *Phys. Lett. B* 588 (2004) 189–195. arXiv:hep-ph/0311229, doi:10.1016/j.physletb.2004.03.033.
- [185] F. Aceti, R. Molina, E. Oset, The  $X(3872) \rightarrow J/\psi \gamma$  decay in the  $D\bar{D}^*$  molecular picture, *Phys. Rev. D* 86 (2012) 113007. arXiv:1207.2832, doi:10.1103/PhysRevD.86.113007.
- [186] L. Maiani, F. Piccinini, A. D. Polosa, V. Riquer, Diquark-antidiquarks with hidden or open charm and the nature of  $X(3872)$ , *Phys. Rev. D* 71 (2005) 014028. arXiv:hep-ph/0412098, doi:10.1103/PhysRevD.71.014028.
- [187] E. J. Eichten, K. Lane, C. Quigg, New states above charm threshold, *Phys. Rev. D* 73 (2006) 014014, [Erratum: *Phys. Rev. D* 73, 079903 (2006)]. arXiv:hep-ph/0511179, doi:10.1103/PhysRevD.73.014014, 10.1103/PhysRevD.73.079903.
- [188] M. Suzuki, The  $X(3872)$  boson: Molecule or charmonium, *Phys. Rev. D* 72 (2005) 114013. arXiv:hep-ph/0508258, doi:10.1103/PhysRevD.72.114013.
- [189] C. Meng, Y.-J. Gao, K.-T. Chao,  $B_{c1}(1P,2P)K$  decays in QCD factorization and  $X(3872)$ , *Phys. Rev. D* 87 (7) (2013) 074035. arXiv:hep-ph/0506222, doi:10.1103/PhysRevD.87.074035.
- [190] D. V. Bugg, Reinterpreting several narrow ‘resonances’ as threshold cusps, *Phys. Lett. B* 598 (2004) 8–14. arXiv:hep-ph/0406293,

- doi:10.1016/j.physletb.2004.07.047.
- [191] B. A. Li, Is  $X(3872)$  a possible candidate of hybrid meson, Phys. Lett. B605 (2005) 306–310. arXiv:hep-ph/0410264, doi:10.1016/j.physletb.2004.11.062.
- [192] F. E. Close, S. Godfrey, Charmonium hybrid production in exclusive B meson decays, Phys. Lett. B574 (2003) 210–216. arXiv:hep-ph/0305285, doi:10.1016/j.physletb.2003.09.011.
- [193] K. K. Seth, An Alternative Interpretation of  $X(3872)$ , Phys. Lett. B612 (2005) 1–4. arXiv:hep-ph/0411122, doi:10.1016/j.physletb.2005.02.057.
- [194] J.-R. Zhang, M.-Q. Huang, Q anti-santi-Q-(prime)s molecular states in QCD sum rules, Commun. Theor. Phys. 54 (2010) 1075–1090. arXiv:0905.4672, doi:10.1088/0253-6102/54/6/22.
- [195] Z.-G. Wang, T. Huang, Possible assignments of the  $X(3872)$ ,  $Z_c(3900)$  and  $Z_b(10610)$  as axial-vector molecular states, Eur. Phys. J. C74 (5) (2014) 2891. arXiv:1312.7489, doi:10.1140/epjc/s10052-014-2891-6.
- [196] H. Mutuk, Y. Sara, H. Gms, A. Ozpineci,  $X(3872)$  and Its Heavy Quark Spin Symmetry Partners in QCD Sum Rules, Eur. Phys. J. C78 (11) (2018) 904. arXiv:1807.04091, doi:10.1140/epjc/s10052-018-6382-z.
- [197] W. Chen, S.-L. Zhu, The Vector and Axial-Vector Charmonium-like States, Phys. Rev. D83 (2011) 034010. arXiv:1010.3397, doi:10.1103/PhysRevD.83.034010.
- [198] Z.-G. Wang, T. Huang, Analysis of the  $X(3872)$ ,  $Z_c(3900)$  and  $Z_c(3885)$  as axial-vector tetraquark states with QCD sum rules, Phys. Rev. D89 (5) (2014) 054019. arXiv:1310.2422, doi:10.1103/PhysRevD.89.054019.
- [199] D. Harnett, R. T. Kleiv, T. G. Steele, H.-y. Jin, Axial Vector  $J^{PC} = 1^{++}$  Charmonium and Bottomonium Hybrid Mass Predictions with QCD Sum-Rules, J. Phys. G39 (2012) 125003. arXiv:1206.6776, doi:10.1088/0954-3899/39/12/125003.
- [200] W. Chen, R. T. Kleiv, T. G. Steele, B. Bulthuis, D. Harnett, J. Ho, T. Richards, S.-L. Zhu, Mass Spectrum of Heavy Quarkonium Hybrids, JHEP 09 (2013) 019. arXiv:1304.4522, doi:10.1007/JHEP09(2013)019.
- [201] W. Chen, H.-y. Jin, R. T. Kleiv, T. G. Steele, M. Wang, Q. Xu, QCD sum-rule interpretation of  $X(3872)$  with  $J^{PC} = 1^{++}$  mixtures of hybrid charmonium and  $\bar{D}D^*$  molecular currents, Phys. Rev. D88 (4) (2013) 045027. arXiv:1305.0244, doi:10.1103/PhysRevD.88.045027.
- [202] A. Palameta, D. Harnett, T. G. Steele, Meson-Hybrid Mixing in  $J^{PC} = 1^{++}$  Heavy Quarkonium from QCD Sum-Rules, Phys. Rev. D98 (7) (2018) 074014. arXiv:1805.04230, doi:10.1103/PhysRevD.98.074014.
- [203] K. Azizi, N. Er,  $X(3872)$ : propagating in a dense medium, Nucl. Phys. B936 (2018) 151–168. arXiv:1710.02806, doi:10.1016/j.nuclphysb.2018.09.014.
- [204] J. Sugiyama, T. Nakamura, N. Ishii, T. Nishikawa, M. Oka, Mixings of 4-quark components in light non-singlet scalar mesons in QCD sum rules, Phys. Rev. D76 (2007) 114010. arXiv:0707.2533, doi:10.1103/PhysRevD.76.114010.
- [205] Y.-b. Dong, A. Faessler, T. Gutsche, V. E. Lyubovitskij, Estimate for the  $X(3872) \rightarrow \gamma J/\psi$  decay width, Phys. Rev. D77 (2008) 094013. arXiv:0802.3610, doi:10.1103/PhysRevD.77.094013.
- [206] B. Aubert, et al., Measurements of the absolute branching fractions of  $B^\pm \rightarrow K^\pm X(c\bar{c})$ , Phys. Rev. Lett. 96 (2006) 052002. arXiv:hep-ex/0510070, doi:10.1103/PhysRevLett.96.052002.
- [207] X. H. Mo, G. Li, C. Z. Yuan, K. L. He, H. M. Hu, J. H. Hu, P. Wang, Z. Y. Wang, Determining the upper limit of  $\Gamma(ee)$  for the  $Y(4260)$ , Phys. Lett. B640 (2006) 182–187. arXiv:hep-ex/0603024, doi:10.1016/j.physletb.2006.07.060.
- [208] E. Eichten, K. Gottfried, T. Kinoshita, K. D. Lane, T.-M. Yan, Charmonium: The Model, Phys. Rev. D17 (1978) 3090, [Erratum: Phys. Rev. D21.313(1980)]. doi:10.1103/PhysRevD.17.3090, 10.1103/physrevd.21.313.2.
- [209] E. Eichten, K. Gottfried, T. Kinoshita, K. D. Lane, T.-M. Yan, Charmonium: Comparison with Experiment, Phys. Rev. D21 (1980) 203. doi:10.1103/PhysRevD.21.203.
- [210] S. Godfrey, N. Isgur, Mesons in a Relativized Quark Model with Chromodynamics, Phys. Rev. D32 (1985) 189–231. doi:10.1103/PhysRevD.32.189.
- [211] S. L. Olsen, Hadronic Spectrum - Multiquark States, Nucl. Phys. A827 (2009) 53C–60C, [,53(2009)]. arXiv:0901.2371, doi:10.1016/j.nuclphysa.2009.05.018.
- [212] C. Z. Yuan, et al., Observation of  $e^+e^- \rightarrow K^+K^-J/\psi$  via initial state radiation at Belle, Phys. Rev. D77 (2008) 011105. arXiv:0709.2565, doi:10.1103/PhysRevD.77.011105.
- [213] C. P. Shen, et al., Updated cross section measurement of  $e^+e^- \rightarrow K^+K^-J/\psi$  and  $K_S^0K_S^0J/\psi$  via initial state radiation at Belle, Phys. Rev. D89 (7) (2014) 072015. arXiv:1402.6578, doi:10.1103/PhysRevD.89.072015.
- [214] K. Abe, et al., Measurement of the near-threshold  $e^+e^- \rightarrow D^{*+}D^{*0}$  cross section using initial-state radiation, Phys. Rev. Lett. 98 (2007) 092001. arXiv:hep-ex/0608018, doi:10.1103/PhysRevLett.98.092001.
- [215] B. Aubert, et al., Exclusive Initial-State-Radiation Production of the D anti-D,  $D^*$  anti- $D^*$ , and  $D^*$  anti- $D^*$  Systems, Phys. Rev. D79 (2009) 092001. arXiv:0903.1597, doi:10.1103/PhysRevD.79.092001.
- [216] G. Pakhlova, et al., Measurement of the near-threshold  $e^+e^- \rightarrow D$  anti-D cross section using initial-state radiation, Phys. Rev. D77 (2008) 011103. arXiv:0708.0082, doi:10.1103/PhysRevD.77.011103.
- [217] G.-J. Ding, Are  $Y(4260)$  and  $Z+(2)$  are  $D(1)$  D or  $D(0)$   $D^*$  Hadronic Molecules?, Phys. Rev. D79 (2009) 014001. arXiv:0809.4818, doi:10.1103/PhysRevD.79.014001.
- [218] Q. Wang, C. Hanhart, Q. Zhao, Decoding the riddle of  $Y(4260)$  and  $Z_c(3900)$ , Phys. Rev. Lett. 111 (13) (2013) 132003. arXiv:1303.6355, doi:10.1103/PhysRevLett.111.132003.
- [219] C. Z. Yuan, P. Wang, X. H. Mo, The  $Y(4260)$  as an omega chi(c1) molecular state, Phys. Lett. B634 (2006) 399–402. arXiv:hep-ph/0511107, doi:10.1016/j.physletb.2006.01.031.
- [220] X. Liu, X.-Q. Zeng, X.-Q. Li, Possible molecular structure of the newly observed  $Y(4260)$ , Phys. Rev. D72 (2005) 054023. arXiv:hep-ph/0507177, doi:10.1103/PhysRevD.72.054023.
- [221] A. Martinez Torres, K. P. Khemchandani, D. Gamermann, E. Oset, The  $Y(4260)$  as a  $J/\psi$  K anti-K system, Phys. Rev. D80 (2009) 094012. arXiv:0906.5333, doi:10.1103/PhysRevD.80.094012.
- [222] S.-L. Zhu, The Possible interpretations of  $Y(4260)$ , Phys. Lett. B625 (2005) 212. arXiv:hep-ph/0507025, doi:10.1016/j.physletb.2005.08.068.

- [223] C.-F. Qiao, One explanation for the exotic state  $Y(4260)$ , Phys. Lett. B639 (2006) 263–265. arXiv:hep-ph/0510228, doi:10.1016/j.physletb.2006.06.038.
- [224] E. van Beveren, G. Rupp, Is the  $Y(4260)$  just a coupled-channel signal? arXiv:hep-ph/0605317.
- [225] E. van Beveren, G. Rupp, The  $X(4260)$  and possible confirmation of  $\psi(3D)$ ,  $\psi(5S)$ ,  $\psi(4D)$ ,  $\psi(6S)$  and  $\psi(5D)$  in  $J/\psi$   $\pi^+$   $\pi^-$  arXiv:0904.4351.
- [226] E. van Beveren, G. Rupp, Interference effects in the  $X(4260)$  signal, Phys. Rev. D79 (2009) 111501. arXiv:0905.1595, doi:10.1103/PhysRevD.79.111501.
- [227] Z.-G. Wang, Lowest vector tetraquark states:  $Y(4260/4220)$  or  $Z_c(4100)$ , Eur. Phys. J. C78 (11) (2018) 933. arXiv:1809.10299, doi:10.1140/epjc/s10052-018-6417-5.
- [228] E. M. Aitala, et al., Experimental evidence for a light and broad scalar resonance in  $D^+ \rightarrow \pi^- \pi^+ \pi^+$  decay, Phys. Rev. Lett. 86 (2001) 770–774. arXiv:hep-ex/0007028, doi:10.1103/PhysRevLett.86.770.
- [229] H. G. Dosch, E. M. Ferreira, F. S. Navarra, M. Nielsen, Semileptonic D decay into scalar mesons: A QCD sum rule approach, Phys. Rev. D65 (2002) 114002. arXiv:hep-ph/0203225, doi:10.1103/PhysRevD.65.114002.
- [230] B. Aubert, et al., Study of  $J/\psi \pi^+ \pi^-$  states produced in  $B^0 \rightarrow J/\psi \pi^+ \pi^- K^0$  and  $B^- \rightarrow J/\psi \pi^+ \pi^- K^-$ , Phys. Rev. D73 (2006) 011101. arXiv:hep-ex/0507090, doi:10.1103/PhysRevD.73.011101.
- [231] G. Buchalla, A. J. Buras, M. E. Lautenbacher, Weak decays beyond leading logarithms, Rev. Mod. Phys. 68 (1996) 1125–1144. arXiv:hep-ph/9512380, doi:10.1103/RevModPhys.68.1125.
- [232] M. Cleven, Q. Wang, F.-K. Guo, C. Hanhart, U.-G. Meißner, Q. Zhao,  $Y(4260)$  as the first  $S$ -wave open charm vector molecular state?, Phys. Rev. D90 (7) (2014) 074039. arXiv:1310.2190, doi:10.1103/PhysRevD.90.074039.
- [233] G. Pakhlova, et al., Measurement of the  $e^+ e^- \rightarrow D^0 D^{*-} \pi^+$  cross section using initial-state radiation, Phys. Rev. D80 (2009) 091101. arXiv:0908.0231, doi:10.1103/PhysRevD.80.091101.
- [234] G.-J. Ding, J.-J. Zhu, M.-L. Yan, Canonical Charmonium Interpretation for  $Y(4360)$  and  $Y(4660)$ , Phys. Rev. D77 (2008) 014033. arXiv:0708.3712, doi:10.1103/PhysRevD.77.014033.
- [235] B.-Q. Li, K.-T. Chao, Higher Charmonia and  $X,Y,Z$  states with Screened Potential, Phys. Rev. D79 (2009) 094004. arXiv:0903.5506, doi:10.1103/PhysRevD.79.094004.
- [236] C.-F. Qiao, A Uniform description of the states recently observed at B-factories, J. Phys. G35 (2008) 075008. arXiv:0709.4066, doi:10.1088/0954-3899/35/7/075008.
- [237] G. Cotugno, R. Faccini, A. D. Polosa, C. Sabelli, Charmed Baryonium, Phys. Rev. Lett. 104 (2010) 132005. arXiv:0911.2178, doi:10.1103/PhysRevLett.104.132005.
- [238] Yu. S. Kalashnikova, A. V. Nefediev, Spectra and decays of hybrid charmonia, Phys. Rev. D77 (2008) 054025. arXiv:0801.2036, doi:10.1103/PhysRevD.77.054025.
- [239] F. Close, C. Downum, C. E. Thomas, Novel Charmonium and Bottomonium Spectroscopies due to Deeply Bound Hadronic Molecules from Single Pion Exchange, Phys. Rev. D81 (2010) 074033. arXiv:1001.2553, doi:10.1103/PhysRevD.81.074033.
- [240] F.-K. Guo, C. Hanhart, U.-G. Meißner, Evidence that the  $Y(4660)$  is a  $f(0)(980)\psi$ -prime bound state, Phys. Lett. B665 (2008) 26–29. arXiv:0803.1392, doi:10.1016/j.physletb.2008.05.057.
- [241] S. Dubynskiy, M. B. Voloshin, Hadro-Charmonium, Phys. Lett. B666 (2008) 344–346. arXiv:0803.2224, doi:10.1016/j.physletb.2008.07.086.
- [242] D. Ebert, R. N. Faustov, V. O. Galkin, Excited heavy tetraquarks with hidden charm, Eur. Phys. J. C58 (2008) 399–405. arXiv:0808.3912, doi:10.1140/epjc/s10052-008-0754-8.
- [243] J.-R. Zhang, M.-Q. Huang, The  $P$ -wave  $[c\bar{s}][\bar{c}s]$  tetraquark state:  $Y(4260)$  or  $Y(4660)$ ?, Phys. Rev. D83 (2011) 036005. arXiv:1011.2818, doi:10.1103/PhysRevD.83.036005.
- [244] H. Sundu, S. S. Agaev, K. Azizi, Resonance  $Y(4660)$  as a vector tetraquark and its strong decay channels, Phys. Rev. D98 (5) (2018) 054021. arXiv:1805.04705, doi:10.1103/PhysRevD.98.054021.
- [245] G. 't Hooft, G. Isidori, L. Maiani, A. D. Polosa, V. Riquer, A Theory of Scalar Mesons, Phys. Lett. B662 (2008) 424–430. arXiv:0801.2288, doi:10.1016/j.physletb.2008.03.036.
- [246] R. D. Matheus, F. S. Navarra, M. Nielsen, R. Rodrigues da Silva, Do the QCD sum rules support four-quark states?, Phys. Rev. D76 (2007) 056005. arXiv:0705.1357, doi:10.1103/PhysRevD.76.056005.
- [247] J. L. Rosner, Threshold effect and  $\pi^+ \pi^- \psi(2S)$  peak, Phys. Rev. D76 (2007) 114002. arXiv:0708.3496, doi:10.1103/PhysRevD.76.114002.
- [248] D. V. Bugg,  $Z^+(4430)$  as a cusp in  $D^*(2010)D(1)(2420)$  arXiv:0709.1254.
- [249] C. Meng, K.-T. Chao,  $Z^+(4430)$  as a resonance in the  $D(1)(D(1)\text{-prime})D^*$  channel arXiv:0708.4222.
- [250] X. Liu, Y.-R. Liu, W.-Z. Deng, S.-L. Zhu, Is  $Z^+(4430)$  a loosely bound molecular state?, Phys. Rev. D77 (2008) 034003. arXiv:0711.0494, doi:10.1103/PhysRevD.77.034003.
- [251] X. Liu, Y.-R. Liu, W.-Z. Deng, S.-L. Zhu,  $Z^+(4430)$  as a  $D(1)\text{-prime} D^* (D(1) D^*)$  molecular state, Phys. Rev. D77 (2008) 094015. arXiv:0803.1295, doi:10.1103/PhysRevD.77.094015.
- [252] G.-J. Ding, W. Huang, J.-F. Liu, M.-L. Yan,  $Z^+(4430)$  and analogous heavy flavor molecules, Phys. Rev. D79 (2009) 034026. arXiv:0805.3822, doi:10.1103/PhysRevD.79.034026.
- [253] J.-R. Zhang, M.-Q. Huang,  $Q$  anti-quanti- $Q(\text{-prime})q$  molecular states, Phys. Rev. D80 (2009) 056004. arXiv:0906.0090, doi:10.1103/PhysRevD.80.056004.
- [254] G.-Z. Meng, et al., Low-energy  $D^{*+} D_0(1)$  Scattering and the Resonance-like Structure  $Z^+(4430)$ , Phys. Rev. D80 (2009) 034503. arXiv:0905.0752, doi:10.1103/PhysRevD.80.034503.
- [255] L. Maiani, A. D. Polosa, V. Riquer, The Charged  $Z(4433)$ : Towards a new spectroscopy arXiv:0708.3997.
- [256] L. Maiani, V. Riquer, R. Faccini, F. Piccinini, A. Pilloni, A. D. Polosa, A  $J^{PG} = 1^{++}$  Charged Resonance in the  $Y(4260) \rightarrow \pi^+ \pi^- J/\psi$  Decay?, Phys. Rev. D87 (11) (2013) 111102. arXiv:1303.6857, doi:10.1103/PhysRevD.87.111102.
- [257] L. Maiani, F. Piccinini, A. D. Polosa, V. Riquer, The  $Z(4430)$  and a New Paradigm for Spin Interactions in Tetraquarks, Phys. Rev. D89 (2014) 114010. arXiv:1405.1551, doi:10.1103/PhysRevD.89.114010.

- [258] F. S. Navarra, M. Nielsen, J.-M. Richard, Exotic Charmonium and Bottomonium-like Resonances, *J. Phys. Conf. Ser.* 348 (2012) 012007. arXiv:1108.1230, doi:10.1088/1742-6596/348/1/012007.
- [259] S. Patel, M. Shah, P. C. Vinodkumar, Mass spectra of four-quark states in the hidden charm sector, *Eur. Phys. J. A50* (2014) 131. arXiv:1402.3974, doi:10.1140/epja/i2014-14131-9.
- [260] M. R. Hadizadeh, A. Khaledi-Nasab, Heavy tetraquarks in the diquark–antidiquark picture, *Phys. Lett. B753* (2016) 8–12. arXiv:1511.08542, doi:10.1016/j.physletb.2015.11.072.
- [261] Z.-G. Wang, Analysis of the  $Z(4430)$  as the first radial excitation of the  $Z_c(3900)$ , *Commun. Theor. Phys.* 63 (3) (2015) 325–330. arXiv:1405.3581, doi:10.1088/0253-6102/63/3/325.
- [262] S. S. Agaev, K. Azizi, H. Sundu, Treating  $Z_c(3900)$  and  $Z(4430)$  as the ground-state and first radially excited tetraquarks, *Phys. Rev. D96* (3) (2017) 034026. arXiv:1706.01216, doi:10.1103/PhysRevD.96.034026.
- [263] C. Deng, J. Ping, H. Huang, F. Wang, Systematic study of  $Z_c^+$  family from a multi-quark color flux-tube model, *Phys. Rev. D92* (3) (2015) 034027. arXiv:1507.06408, doi:10.1103/PhysRevD.92.034027.
- [264] L. Ma, X.-H. Liu, X. Liu, S.-L. Zhu, Exotic Four Quark Matter:  $Z_1(4475)$ , *Phys. Rev. D90* (3) (2014) 037502. arXiv:1404.3450, doi:10.1103/PhysRevD.90.037502.
- [265] T. Barnes, F. E. Close, E. S. Swanson, Molecular Interpretation of the Supercharmonium State  $Z(4475)$ , *Phys. Rev. D91* (1) (2015) 014004. arXiv:1409.6651, doi:10.1103/PhysRevD.91.014004.
- [266] X.-H. Liu, L. Ma, L.-P. Sun, X. Liu, S.-L. Zhu, Resolving the puzzling decay patterns of charged  $Z_c$  and  $Z_b$  states, *Phys. Rev. D90* (7) (2014) 074020. arXiv:1407.3684, doi:10.1103/PhysRevD.90.074020.
- [267] H. G. Dosch, G. F. de Téramond, S. J. Brodsky, Superconformal Baryon-Meson Symmetry and Light-Front Holographic QCD, *Phys. Rev. D91* (8) (2015) 085016. arXiv:1501.00959, doi:10.1103/PhysRevD.91.085016.
- [268] H. G. Dosch, G. F. de Téramond, S. J. Brodsky, Supersymmetry Across the Light and Heavy-Light Hadronic Spectrum, *Phys. Rev. D92* (7) (2015) 074010. arXiv:1504.05112, doi:10.1103/PhysRevD.92.074010.
- [269] S. J. Brodsky, G. F. de Téramond, H. G. Dosch, C. Lorcé, Universal Effective Hadron Dynamics from Superconformal Algebra, *Phys. Lett. B759* (2016) 171–177. arXiv:1604.06746, doi:10.1016/j.physletb.2016.05.068.
- [270] H. G. Dosch, G. F. de Téramond, S. J. Brodsky, Supersymmetry Across the Light and Heavy-Light Hadronic Spectrum II, *Phys. Rev. D95* (3) (2017) 034016. arXiv:1612.02370, doi:10.1103/PhysRevD.95.034016.
- [271] M. Nielsen, S. J. Brodsky, Hadronic superpartners from a superconformal and supersymmetric algebra, *Phys. Rev. D97* (11) (2018) 114001. arXiv:1802.09652, doi:10.1103/PhysRevD.97.114001.
- [272] M. Nielsen, S. J. Brodsky, G. F. de Téramond, H. G. Dosch, F. S. Navarra, L. Zou, Supersymmetry in the Double-Heavy Hadronic Spectrum, *Phys. Rev. D98* (3) (2018) 034002. arXiv:1805.11567, doi:10.1103/PhysRevD.98.034002.
- [273] M. Ablikim, et al., Determination of the Spin and Parity of the  $Z_c(3900)$ , *Phys. Rev. Lett.* 119 (7) (2017) 072001. arXiv:1706.04100, doi:10.1103/PhysRevLett.119.072001.
- [274] M. Ablikim, et al., Observation of  $Z_c(3900)^0$  in  $e^+e^- \rightarrow \pi^0\pi^0 J/\psi$ , *Phys. Rev. Lett.* 115 (11) (2015) 112003. arXiv:1506.06018, doi:10.1103/PhysRevLett.115.112003.
- [275] M. Ablikim, et al., Confirmation of a charged charmoniumlike state  $Z_c(3885)^\mp$  in  $e^+e^- \rightarrow \pi^\pm(D\bar{D}^*)^\mp$  with double  $D$  tag, *Phys. Rev. D92* (9) (2015) 092006. arXiv:1509.01398, doi:10.1103/PhysRevD.92.092006.
- [276] M. Ablikim, et al., Observation of a Neutral Structure near the  $D\bar{D}^*$  Mass Threshold in  $e^+e^- \rightarrow (D\bar{D}^*)^0\pi^0$  at  $\sqrt{s} = 4.226$  and  $4.257$  GeV, *Phys. Rev. Lett.* 115 (22) (2015) 222002. arXiv:1509.05620, doi:10.1103/PhysRevLett.115.222002.
- [277] L. Zhao, L. Ma, S.-L. Zhu, Spin-orbit force, recoil corrections, and possible  $B\bar{B}^*$  and  $D\bar{D}^*$  molecular states, *Phys. Rev. D89* (9) (2014) 094026. arXiv:1403.4043, doi:10.1103/PhysRevD.89.094026.
- [278] J. He, Study of the  $B\bar{B}^*/D\bar{D}^*$  bound states in a Bethe-Salpeter approach, *Phys. Rev. D90* (7) (2014) 076008. arXiv:1409.8506, doi:10.1103/PhysRevD.90.076008.
- [279] S. Prelovsek, L. Leskovec, Search for  $Z_c^+(3900)$  in the  $1^{+-}$  Channel on the Lattice, *Phys. Lett. B727* (2013) 172–176. arXiv:1308.2097, doi:10.1016/j.physletb.2013.10.009.
- [280] S. Prelovsek, C. B. Lang, L. Leskovec, D. Mohler, Study of the  $Z_c^+$  channel using lattice QCD, *Phys. Rev. D91* (1) (2015) 014504. arXiv:1405.7623, doi:10.1103/PhysRevD.91.014504.
- [281] Y. Chen, et al., Low-energy scattering of the  $(D\bar{D}^*)^\pm$  system and the resonance-like structure  $Z_c(3900)$ , *Phys. Rev. D89* (9) (2014) 094506. arXiv:1403.1318, doi:10.1103/PhysRevD.89.094506.
- [282] F. Aceti, M. Bayar, E. Oset, A. Martinez Torres, K. P. Khemchandani, J. M. Dias, F. S. Navarra, M. Nielsen, Prediction of an  $I = 1 D\bar{D}^*$  state and relationship to the claimed  $Z_c(3900)$ ,  $Z_c(3885)$ , *Phys. Rev. D90* (1) (2014) 016003. arXiv:1401.8216, doi:10.1103/PhysRevD.90.016003.
- [283] M. Karliner, J. L. Rosner, New Exotic Meson and Baryon Resonances from Doubly-Heavy Hadronic Molecules, *Phys. Rev. Lett.* 115 (12) (2015) 122001. arXiv:1506.06386, doi:10.1103/PhysRevLett.115.122001.
- [284] J. He, The  $Z_c(3900)$  as a resonance from the  $D\bar{D}^*$  interaction, *Phys. Rev. D92* (3) (2015) 034004. arXiv:1505.05379, doi:10.1103/PhysRevD.92.034004.
- [285] E. Wilbring, H. W. Hammer, U. G. Meißner, Electromagnetic Structure of the  $Z_c(3900)$ , *Phys. Lett. B726* (2013) 326–329. arXiv:1304.2882, doi:10.1016/j.physletb.2013.08.059.
- [286] Y. Dong, A. Faessler, T. Gutsche, V. E. Lyubovitskij, Strong decays of molecular states  $Z_c^+$  and  $Z_c'^+$ , *Phys. Rev. D88* (1) (2013) 014030. arXiv:1306.0824, doi:10.1103/PhysRevD.88.014030.
- [287] H.-W. Ke, Z.-T. Wei, X.-Q. Li, Is  $Z_c(3900)$  a molecular state, *Eur. Phys. J. C73* (10) (2013) 2561. arXiv:1307.2414, doi:10.1140/epjc/s10052-013-2561-0.
- [288] T. Gutsche, M. Kesenheimer, V. E. Lyubovitskij, Radiative and dilepton decays of the hadronic molecule  $Z_c^+(3900)$ , *Phys. Rev. D90* (9) (2014) 094013. arXiv:1410.0259, doi:10.1103/PhysRevD.90.094013.
- [289] A. Esposito, A. L. Guerrieri, A. Pilloni, Probing the nature of  $Z_c^0$  states via the  $c$  decay, *Phys. Lett. B746* (2015) 194–201. arXiv:1409.3551, doi:10.1016/j.physletb.2015.04.057.
- [290] D.-Y. Chen, Y.-B. Dong, Radiative decays of the neutral  $Z_c(3900)$ , *Phys. Rev. D93* (1) (2016) 014003. arXiv:1510.00829,

- doi:10.1103/PhysRevD.93.014003.
- [291] Q.-R. Gong, Z.-H. Guo, C. Meng, G.-Y. Tang, Y.-F. Wang, H.-Q. Zheng,  $Z_c(3900)$  as a  $D\bar{D}^*$  molecule from the pole counting rule, Phys. Rev. D94 (11) (2016) 114019. arXiv:1604.08836, doi:10.1103/PhysRevD.94.114019.
- [292] H.-W. Ke, X.-Q. Li, Study on decays of  $Z_c(4020)$  and  $Z_c(3900)$  into  $h_c + \pi$ , Eur. Phys. J. C76 (6) (2016) 334. arXiv:1601.03575, doi:10.1140/epjc/s10052-016-4183-9.
- [293] W. Chen, T. G. Steele, H.-X. Chen, S.-L. Zhu, Mass spectra of  $Z_c$  and  $Z_b$  exotic states as hadron molecules, Phys. Rev. D92 (5) (2015) 054002. arXiv:1505.05619, doi:10.1103/PhysRevD.92.054002.
- [294] J.-R. Zhang, Improved QCD sum rule study of  $Z_c(3900)$  as a  $\bar{D}D^*$  molecular state, Phys. Rev. D87 (11) (2013) 116004. arXiv:1304.5748, doi:10.1103/PhysRevD.87.116004.
- [295] C.-Y. Cui, Y.-L. Liu, W.-B. Chen, M.-Q. Huang, Could  $Z_c(3900)$  be a  $I^G J^P = 1^+ 1^+ D^* \bar{D}$  molecular state?, J. Phys. G41 (2014) 075003. arXiv:1304.1850, doi:10.1088/0954-3899/41/7/075003.
- [296] C. Deng, J. Ping, F. Wang, Interpreting  $Z_c(3900)$  and  $Z_c(4025)/Z_c(4020)$  as charged tetraquark states, Phys. Rev. D90 (2014) 054009. arXiv:1402.0777, doi:10.1103/PhysRevD.90.054009.
- [297] S. S. Agaev, K. Azizi, H. Sundu, Strong  $Z_c^+(3900) \rightarrow J/\psi\pi^+; \eta_c\rho^+$  decays in QCD, Phys. Rev. D93 (7) (2016) 074002. arXiv:1601.03847, doi:10.1103/PhysRevD.93.074002.
- [298] N. Mahajan, Interpreting  $Z(3900)$  arXiv:1304.1301.
- [299] M. Ablikim, et al., Observation of  $e^+e^-00h_c$  and a Neutral Charmoniumlike Structure  $Z_c(4020)^0$ , Phys. Rev. Lett. 113 (21) (2014) 212002. arXiv:1409.6577, doi:10.1103/PhysRevLett.113.212002.
- [300] M. Ablikim, et al., Observation of a neutral charmoniumlike state  $Z_c(4025)^0$  in  $e^+e^- \rightarrow (D^*\bar{D}^*)^0\pi^0$ , Phys. Rev. Lett. 115 (18) (2015) 182002. arXiv:1507.02404, doi:10.1103/PhysRevLett.115.182002.
- [301] A. De Rujula, H. Georgi, S. L. Glashow, Molecular Charmonium: A New Spectroscopy?, Phys. Rev. Lett. 38 (1977) 317. doi:10.1103/PhysRevLett.38.317.
- [302] N. A. Tornqvist, On deusons or deuteron - like meson meson bound states, Nuovo Cim. A107 (1994) 2471–2476. arXiv:hep-ph/9310225, doi:10.1007/BF02734018.
- [303] S. Dubynskiy, M. B. Voloshin, Possible new resonance at the  $D^*$  anti- $D^*$  threshold in  $e^+e^-$  annihilation, Mod. Phys. Lett. A21 (2006) 2779–2788. arXiv:hep-ph/0608179, doi:10.1142/S0217732306022195.
- [304] M. B. Voloshin, L. B. Okun, Hadron Molecules and Charmonium Atom, JETP Lett. 23 (1976) 333–336, [Pisma Zh. Eksp. Teor. Fiz.23,369(1976)].
- [305] F.-K. Guo, C. Hidalgo-Duque, J. Nieves, M. P. Valderrama, Consequences of Heavy Quark Symmetries for Hadronic Molecules, Phys. Rev. D88 (2013) 054007. arXiv:1303.6608, doi:10.1103/PhysRevD.88.054007.
- [306] R. Molina, E. Oset, The  $Y(3940)$ ,  $Z(3930)$  and the  $X(4160)$  as dynamically generated resonances from the vector-vector interaction, Phys. Rev. D80 (2009) 114013. arXiv:0907.3043, doi:10.1103/PhysRevD.80.114013.
- [307] F. Aceti, M. Bayar, J. M. Dias, E. Oset, Prediction of a  $Z_c(4000) D^*\bar{D}^*$  state and relationship to the claimed  $Z_c(4025)$ , Eur. Phys. J. A50 (2014) 103. arXiv:1401.2076, doi:10.1140/epja/i2014-14103-1.
- [308] J. Yamagata-Sekihara, J. Nieves, E. Oset, Couplings in coupled channels versus wave functions in the case of resonances: application to the two  $\Lambda(1405)$  states, Phys. Rev. D83 (2011) 014003. arXiv:1007.3923, doi:10.1103/PhysRevD.83.014003.
- [309] E. S. Swanson, Cusps and Exotic Charmonia, Int. J. Mod. Phys. E25 (07) (2016) 1642010. arXiv:1504.07952, doi:10.1142/S0218301316420106.
- [310] Y. Chen, et al., Low-energy Scattering of  $(D^*\bar{D}^*)^\pm$  System and the Resonance-like Structure  $Z_c(4025)$ , Phys. Rev. D92 (5) (2015) 054507. arXiv:1503.02371, doi:10.1103/PhysRevD.92.054507.
- [311] R. Molina, H. Nagahiro, A. Hosaka, E. Oset, Scalar, axial-vector and tensor resonances from the rho  $D^*$ , omega  $D^*$  interaction in the hidden gauge formalism, Phys. Rev. D80 (2009) 014025. arXiv:0903.3823, doi:10.1103/PhysRevD.80.014025.
- [312] Z.-G. Wang, Reanalysis of the  $Z_c(4020)$ ,  $Z_c(4025)$ ,  $Z(4050)$  and  $Z(4250)$  as tetraquark states with QCD sum rules, Commun. Theor. Phys. 63 (4) (2015) 466–480. arXiv:1312.1537, doi:10.1088/0253-6102/63/4/466.
- [313] C.-F. Qiao, L. Tang, Interpretation of  $Z_c(4025)$  as the hidden charm tetraquark states via QCD Sum Rules, Eur. Phys. J. C74 (2014) 2810. arXiv:1308.3439, doi:10.1140/epjc/s10052-014-2810-x.
- [314] Z.-G. Wang, Analysis of the  $Z_c(4200)$  as axial-vector molecule-like state, Int. J. Mod. Phys. A30 (30) (2015) 1550168. arXiv:1502.01459, doi:10.1142/S0217751X15501687.
- [315] W. Chen, T. G. Steele, M.-L. Du, S.-L. Zhu,  $D^*\bar{D}^*$  molecule interpretation of  $Z_c(4025)$ , Eur. Phys. J. C74 (2) (2014) 2773. arXiv:1308.5060, doi:10.1140/epjc/s10052-014-2773-y.
- [316] C.-Y. Cui, C.-Y. Cui, Y.-L. Liu, M.-Q. Huang, Could  $Z_c(4025)$  be a  $J^P = 1^+ D^*\bar{D}^*$  molecular state? Could  $Z_c(4025)$  be a  $J^P = 1^+ D^*\bar{D}^*$  molecular state?, Eur. Phys. J. C73 (12) (2013) 2661. arXiv:1308.3625, doi:10.1140/epjc/s10052-013-2661-x.
- [317] Y.-C. Yang, Z.-Y. Tan, H.-S. Zong, J. Ping, Dynamical study of  $S$ -wave  $\bar{Q}Q\bar{q}q$  system arXiv:1712.09285.
- [318] Z.-G. Wang, Reanalysis of the  $Y(3940)$ ,  $Y(4140)$ ,  $Z_c(4020)$ ,  $Z_c(4025)$  and  $Z_b(10650)$  as molecular states with QCD sum rules, Eur. Phys. J. C74 (7) (2014) 2963. arXiv:1403.0810, doi:10.1140/epjc/s10052-014-2963-7.
- [319] X. Liu, Z.-G. Luo, Y.-R. Liu, S.-L. Zhu,  $X(3872)$  and Other Possible Heavy Molecular States, Eur. Phys. J. C61 (2009) 411–428. arXiv:0808.0073, doi:10.1140/epjc/s10052-009-1020-4.
- [320] Y.-R. Liu, Z.-Y. Zhang, The Bound state problem of  $S$ -wave heavy quark meson-aitimeson systems, Phys. Rev. C80 (2009) 015208. arXiv:0810.1598, doi:10.1103/PhysRevC.80.015208.
- [321] Z.-G. Wang, Another tetraquark structure in the  $\pi^+$  ( $\chi(c1)$ ) invariant mass distribution, Eur. Phys. J. C62 (2009) 375–382. arXiv:0807.4592, doi:10.1140/epjc/s10052-009-1043-x.
- [322] V. M. Abazov, et al., Evidence for  $Z_c^\pm(3900)$  in semi-inclusive decays of  $b$ -flavored hadrons arXiv:1807.00183.
- [323] C. Deng, J. Ping, H. Huang, F. Wang, Hidden charmed states and multibody color flux-tube dynamics, Phys. Rev. D98 (1) (2018) 014026. arXiv:1801.00164, doi:10.1103/PhysRevD.98.014026.
- [324] Z. Guo, T. Liu, B.-Q. Ma, Light-front holographic QCD with generic dilaton profile, Phys. Rev. D93 (7) (2016) 076010. arXiv:1604.08463,

- doi:10.1103/PhysRevD.93.076010.
- [325] L. Zhao, W.-Z. Deng, S.-L. Zhu, Hidden-Charm Tetraquarks and Charged  $Z_c$  States, Phys. Rev. D90 (9) (2014) 094031. arXiv:1408.3924, doi:10.1103/PhysRevD.90.094031.
- [326] X.-Y. Wang, X.-R. Chen, Discovery Potential for the Neutral Charmonium-Like by Annihilation, Adv. High Energy Phys. 2015 (2015) 918231. arXiv:1509.08553, doi:10.1155/2015/918231.
- [327] X.-Y. Wang, X.-R. Chen, A. Guskov, Photoproduction of the charged charmoniumlike  $Z_c^+(4200)$ , Phys. Rev. D92 (9) (2015) 094017. arXiv:1503.02125, doi:10.1103/PhysRevD.92.094017.
- [328] L. Ma, W.-Z. Deng, X.-L. Chen, S.-L. Zhu, Strong decay patterns of the hidden-charm tetraquarks arXiv:1512.01938.
- [329] W. Chen, T. G. Steele, H.-X. Chen, S.-L. Zhu,  $Z_c(4200)^+$  decay width as a charmonium-like tetraquark state, Eur. Phys. J. C75 (8) (2015) 358. arXiv:1501.03863, doi:10.1140/epjc/s10052-015-3578-3.
- [330] J. Wu, X. Liu, Y.-R. Liu, S.-L. Zhu, Systematic studies of charmonium-, bottomonium-, and  $B_c$ -like tetraquark states arXiv:1810.06886.
- [331] M. B. Voloshin,  $Z_c(4100)$  and  $Z_c(4200)$  as hadrocharmonium arXiv:1810.08146.
- [332] Q. Zhao, Some insights into the newly observed  $Z_c(4100)$  in  $B^0 \rightarrow \eta_c K^+ \pi^-$  by LHCbar arXiv:1811.05357.
- [333] X. Cao, J.-P. Dai, The spin parity of  $Z_c^-(4100)$ ,  $Z_c^+(4050)$  and  $Z_c^+(4250)$  arXiv:1811.06434.
- [334] R. Aaij, et al., Search for the  $X(4140)$  state in  $B^+ \rightarrow J/\psi \phi K^+$  decays, Phys. Rev. D85 (2012) 091103. arXiv:1202.5087, doi:10.1103/PhysRevD.85.091103.
- [335] S. Chatrchyan, et al., Observation of a peaking structure in the  $J/\psi \phi$  mass spectrum from  $B^\pm \rightarrow J/\psi \phi K^\pm$  decays, Phys. Lett. B734 (2014) 261–281. arXiv:1309.6920, doi:10.1016/j.physletb.2014.05.055.
- [336] R. Aaij, et al., Amplitude analysis of  $B^+ \rightarrow J/\psi \phi K^+$  decays, Phys. Rev. D95 (1) (2017) 012002. arXiv:1606.07898, doi:10.1103/PhysRevD.95.012002.
- [337] N. Mahajan, Y(4140): Possible options, Phys. Lett. B679 (2009) 228–230. arXiv:0903.3107, doi:10.1016/j.physletb.2009.07.043.
- [338] X. Liu, The Hidden charm decay of Y(4140) by the rescattering mechanism, Phys. Lett. B680 (2009) 137–140. arXiv:0904.0136, doi:10.1016/j.physletb.2009.08.049.
- [339] F. Stancu, Can Y(4140) be a c anti-c s anti-s tetraquark?, J. Phys. G37 (2010) 075017. arXiv:0906.2485, doi:10.1088/0954-3899/37/7/075017.
- [340] X. Liu, S.-L. Zhu, Y(4143) is probably a molecular partner of Y(3930), Phys. Rev. D80 (2009) 017502, [Erratum: Phys. Rev. D85,019902(2012)]. arXiv:0903.2529, doi:10.1103/PhysRevD.85.019902, 10.1103/PhysRevD.80.017502.
- [341] T. Branz, T. Gutsche, V. E. Lyubovitskij, Hadronic molecule structure of the Y(3940) and Y(4140), Phys. Rev. D80 (2009) 054019. arXiv:0903.5424, doi:10.1103/PhysRevD.80.054019.
- [342] T. Branz, R. Molina, E. Oset, Radiative decays of the Y(3940), Z(3930) and the X(4160) as dynamically generated resonances, Phys. Rev. D83 (2011) 114015. arXiv:1010.0587, doi:10.1103/PhysRevD.83.114015.
- [343] Z.-G. Wang, Analysis of the Y(4140) with QCD sum rules, Eur. Phys. J. C63 (2009) 115–122. arXiv:0903.5200, doi:10.1140/epjc/s10052-009-1097-9.
- [344] W.-H. Liang, J.-J. Xie, E. Oset, R. Molina, M. Döring, Predictions for the  $\bar{B}^0 \rightarrow \bar{K}^{*0} X(YZ)$  and  $\bar{B}_s^0 \rightarrow \phi X(YZ)$  with X(4160), Y(3940), Z(3930), Eur. Phys. J. A51 (5) (2015) 58. arXiv:1502.02932, doi:10.1140/epja/i2015-15058-3.
- [345] C. Hidalgo-Duque, J. Nieves, M. P. Valderrama, Light flavor and heavy quark spin symmetry in heavy meson molecules, Phys. Rev. D87 (7) (2013) 076006. arXiv:1210.5431, doi:10.1103/PhysRevD.87.076006.
- [346] E. Wang, J.-J. Xie, L.-S. Geng, E. Oset, Analysis of the  $B^+ \rightarrow J/\psi \phi K^+$  data at low  $J/\psi \phi$  invariant masses and the X(4140) and X(4160) resonances, Phys. Rev. D97 (1) (2018) 014017. arXiv:1710.02061, doi:10.1103/PhysRevD.97.014017.
- [347] S. Narison, V. I. Zakharov, Duality between QCD Perturbative Series and Power Corrections, Phys. Lett. B679 (2009) 355–361. arXiv:0906.4312, doi:10.1016/j.physletb.2009.07.060.
- [348] R. Tarrach, The Pole Mass in Perturbative QCD, Nucl. Phys. B183 (1981) 384–396. doi:10.1016/0550-3213(81)90140-1.
- [349] R. Coquereaux, Dimensional Renormalization and Comparison of Renormalization Schemes in Quantum Electrodynamics, Annals Phys. 125 (1980) 401. doi:10.1016/0003-4916(80)90139-6.
- [350] P. Binetruy, T. Schucker, Gauge and Renormalization Scheme Dependence in GUTs, Nucl. Phys. B178 (1981) 293–306. doi:10.1016/0550-3213(81)90410-7.
- [351] S. Narison, Heavy Quark Mass in the MS Scheme: Revisited, Phys. Lett. B197 (1987) 405–408. doi:10.1016/0370-2693(87)90410-2.
- [352] S. Narison, Light and Heavy Quark Masses, Test of PCAC and Flavor Breakings of Condensates in QCD, Phys. Lett. B216 (1989) 191–197. doi:10.1016/0370-2693(89)91393-2.
- [353] N. Gray, D. J. Broadhurst, W. Grafe, K. Schilcher, Three Loop Relation of Quark (Modified) Ms and Pole Masses, Z. Phys. C48 (1990) 673–680. doi:10.1007/BF01614703.
- [354] J. Fleischer, F. Jegerlehner, O. V. Tarasov, O. L. Veretin, Two loop QCD corrections of the massive fermion propagator, Nucl. Phys. B539 (1999) 671–690, [Erratum: Nucl. Phys. B571,511(2000)]. arXiv:hep-ph/9803493, doi:10.1016/S0550-3213(99)00794-4, 10.1016/S0550-3213(98)00705-6.
- [355] K. G. Chetyrkin, M. Steinhauser, The Relation between the MS-bar and the on-shell quark mass at order alpha(s)\*\*3, Nucl. Phys. B573 (2000) 617–651. arXiv:hep-ph/9911434, doi:10.1016/S0550-3213(99)00784-1.
- [356] S. Narison, A. A. Pivovarov, QSSR estimate of the B(B) parameter at next-to-leading order, Phys. Lett. B327 (1994) 341–346. arXiv:hep-ph/9403225, doi:10.1016/0370-2693(94)90739-0.
- [357] K. Hagiwara, S. Narison, D. Nomura, B0(d,s) - anti-B0(d,s) mass differences from QCD spectral sum rules, Phys. Lett. B540 (2002) 233–240. arXiv:hep-ph/0205092, doi:10.1016/S0370-2693(02)02133-0.
- [358] A. Pich, E. De Rafael, K anti-K Mixing in the Standard Model, Phys. Lett. 158B (1985) 477–484. doi:10.1016/0370-2693(85)90798-1.
- [359] D. J. Broadhurst, Chiral Symmetry Breaking and Perturbative QCD, Phys. Lett. 101B (1981) 423–426. doi:10.1016/0370-2693(81)90167-2.
- [360] K. G. Chetyrkin, M. Steinhauser, Three loop nondiagonal current correlators in QCD and NLO corrections to single top quark production, Phys. Lett. B502 (2001) 104–114. arXiv:hep-ph/0012002, doi:10.1016/S0370-2693(01)00179-4.
- [361] K. G. Chetyrkin, M. Steinhauser, Heavy - light current correlators at order alpha-s\*\*2 in QCD and HQET, Eur. Phys. J. C21 (2001) 319–338.



- arXiv:hep-ph/0108017, doi:10.1007/s100520100744.
- [362] P. Gelhausen, A. Khodjamirian, A. A. Pivovarov, D. Rosenthal, Decay constants of heavy-light vector mesons from QCD sum rules, Phys. Rev. D88 (2013) 014015, [Erratum: Phys. Rev.D91,099901(2015)]. arXiv:1305.5432, doi:10.1103/PhysRevD.88.014015, 10.1103/PhysRevD.91.099901, 10.1103/PhysRevD.89.099901.
- [363] K. G. Chetyrkin, S. Narison, V. I. Zakharov, Short distance tachyonic gluon mass and  $1/Q^2$  corrections, Nucl. Phys. B550 (1999) 353–374. arXiv:hep-ph/9811275, doi:10.1016/S0550-3213(99)00167-4.
- [364] S. Narison, V. I. Zakharov, Hints on the power corrections from current correlators in  $x$  space, Phys. Lett. B522 (2001) 266–272. arXiv:hep-ph/0110141, doi:10.1016/S0370-2693(01)01274-6.
- [365] S. Narison, G. Veneziano, QCD Tests of  $G(1.6) = \text{Glueball}$ , Int. J. Mod. Phys. A4 (1989) 2751. doi:10.1142/S0217751X89001060.
- [366] S. Narison, Masses, decays and mixings of gluonia in QCD, Nucl. Phys. B509 (1998) 312–356. arXiv:hep-ph/9612457, doi:10.1016/S0550-3213(97)00562-2.
- [367] S. Narison, A fresh look into  $m_{c,b}$  and precise  $f_{D^{*(s)},B^{*(s)}}$  from heavy-light QCD spectral sum rules, Phys. Lett. B718 (2013) 1321–1333. arXiv:1209.2023, doi:10.1016/j.physletb.2012.10.057.
- [368] S. Narison, Improved light quark masses from pseudoscalar sum rules, Phys. Lett. B738 (2014) 346–360. arXiv:1401.3689, doi:10.1016/j.physletb.2014.09.056.
- [369] S. Narison, Improved  $f_{D^{*(s)}}, f_{B^{*(s)}}$  and  $f_{B_c}$  from QCD Laplace sum rules, Int. J. Mod. Phys. A30 (20) (2015) 1550116. arXiv:1404.6642, doi:10.1142/S0217751X1550116X.
- [370] S. Narison, QCD parameter correlations from heavy quarkonia, Int. J. Mod. Phys. A33 (10) (2018) 1850045. arXiv:1801.00592, doi:10.1142/S0217751X18500458.
- [371] E. G. Floratos, S. Narison, E. de Rafael, Spectral Function Sum Rules in Quantum Chromodynamics. 1. Charged Currents Sector, Nucl. Phys. B155 (1979) 115–149. doi:10.1016/0550-3213(79)90359-6.
- [372] B. L. Ioffe, K. N. Zyblyuk, Gluon condensate in charmonium sum rules with three loop corrections, Eur. Phys. J. C27 (2003) 229–241. arXiv:hep-ph/0207183, doi:10.1140/epjc/s2002-01099-8.
- [373] B. L. Ioffe, QCD at low energies, Prog. Part. Nucl. Phys. 56 (2006) 232–277. arXiv:hep-ph/0502148, doi:10.1016/j.pnpnp.2005.05.001.
- [374] G. S. Bali, C. Bauer, A. Pineda, Model-independent determination of the gluon condensate in four-dimensional SU(3) gauge theory, Phys. Rev. Lett. 113 (2014) 092001. arXiv:1403.6477, doi:10.1103/PhysRevLett.113.092001.
- [375] T. Lee, Renormalon Subtraction from the Average Plaquette and the Gluon Condensate, Phys. Rev. D82 (2010) 114021. arXiv:1003.0231, doi:10.1103/PhysRevD.82.114021.
- [376] E. Braaten, S. Narison, A. Pich, QCD analysis of the tau hadronic width, Nucl. Phys. B373 (1992) 581–612. doi:10.1016/0550-3213(92)90267-F.
- [377] S. Narison, A. Pich, QCD Formulation of the tau Decay and Determination of  $\Lambda(\overline{MS})$ , Phys. Lett. B211 (1988) 183–188. doi:10.1016/0370-2693(88)90830-1.
- [378] S. Narison, Strange quark mass from  $e^+e^-$  revisited and present status of light quark masses, Phys. Rev. D74 (2006) 034013. arXiv:hep-ph/0510108, doi:10.1103/PhysRevD.74.034013.
- [379] S. Narison, On the strange quark mass from  $e^+e^-$  and tau decay data, and test of the SU(2) isospin symmetry, Phys. Lett. B466 (1999) 345–354. arXiv:hep-ph/9905264, doi:10.1016/S0370-2693(99)01093-X.
- [380] H. G. Dosch, S. Narison, Direct extraction of the chiral quark condensate and bounds on the light quark masses, Phys. Lett. B417 (1998) 173–176. arXiv:hep-ph/9709215, doi:10.1016/S0370-2693(97)01370-1.
- [381] S. Narison, Gluon Condensates and precise  $\overline{m}_{c,b}$  from QCD-Moments and their ratios to Order  $\alpha_s^3$  and  $\int G^4$ , Phys. Lett. B706 (2012) 412–422. arXiv:1105.2922, doi:10.1016/j.physletb.2011.11.058.
- [382] S. Narison, Gluon Condensates and  $m_b(m_b)$  from QCD-Exponential Moments at Higher Orders, Phys. Lett. B707 (2012) 259–263. arXiv:1105.5070, doi:10.1016/j.physletb.2011.12.047.
- [383] R. A. Bertlmann, J. S. Bell, GLUON CONDENSATE POTENTIALS, Nucl. Phys. B227 (1983) 435, [435(1983)]. doi:10.1016/0550-3213(83)90567-9.
- [384] R. A. Bertlmann, H. Neufeld, Exponential QCD Moments for Charmonium Triplet  $s$  Wave Up to Order  $\langle G^4 \rangle$ , Z. Phys. C27 (1985) 437. doi:10.1007/BF01548649.
- [385] S. Narison, Determination of the  $D = 2$  'operator' from  $e^+e^-$  data, Phys. Lett. B300 (1993) 293–297. doi:10.1016/0370-2693(93)90368-R.
- [386] S. Narison, QCD tests from  $e^+e^- \rightarrow I = 1$  hadrons data and implication on the value of  $\alpha_s$  from tau decays, Phys. Lett. B361 (1995) 121–130. arXiv:hep-ph/9504334, doi:10.1016/0370-2693(95)01125-A.
- [387] F. J. Yndurain, Gluon condensate from superconvergent QCD sum rule, Phys. Rept. 320 (1999) 287–293. arXiv:hep-ph/9903457, doi:10.1016/S0370-1573(99)00079-4.
- [388] S. Narison, Heavy quarkonia mass splittings in QCD: Gluon condensate,  $\alpha_s$  and  $1/m$  expansion, Phys. Lett. B387 (1996) 162–172. arXiv:hep-ph/9512348, doi:10.1016/0370-2693(96)00954-9.
- [389] Y. Chung, H. G. Dosch, M. Kremer, D. Schall, Chiral Symmetry Breaking Condensates for Baryonic Sum Rules, Z. Phys. C25 (1984) 151. doi:10.1007/BF01557473.
- [390] H. G. Dosch, M. Jamin, S. Narison, Baryon Masses and Flavor Symmetry Breaking of Chiral Condensates, Phys. Lett. B220 (1989) 251–257. doi:10.1016/0370-2693(89)90047-6.
- [391] R. L. Jaffe, Multi-Quark Hadrons. 1. The Phenomenology of (2 Quark 2 anti-Quark) Mesons, Phys. Rev. D15 (1977) 267. doi:10.1103/PhysRevD.15.267.
- [392] S. Weinberg, Tetraquark Mesons in Large  $N$  Quantum Chromodynamics, Phys. Rev. Lett. 110 (2013) 261601. arXiv:1303.0342, doi:10.1103/PhysRevLett.110.261601.
- [393] M. Knecht, S. Peris, Narrow Tetraquarks at Large  $N$ , Phys. Rev. D88 (2013) 036016. arXiv:1307.1273, doi:10.1103/PhysRevD.88.036016.
- [394] G. Rossi, G. Veneziano, The string-junction picture of multi-quark states: an update, JHEP 06 (2016) 041. arXiv:1603.05830, doi:10.1007/JHEP06(2016)041.
- [395] S. Cho, et al., Exotic Hadrons from Heavy Ion Collisions, Prog. Part. Nucl. Phys. 95 (2017) 279–322. arXiv:1702.00486,

- doi:10.1016/j.pnpnp.2017.02.002.
- [396] C. Meng, H. Han, K.-T. Chao,  $X(3872)$  and its production at hadron colliders, *Phys. Rev. D*96 (7) (2017) 074014. arXiv:1304.6710, doi:10.1103/PhysRevD.96.074014.
- [397] A. Martinez Torres, K. P. Khemchandani, F. S. Navarra, M. Nielsen, L. M. Abreu, On  $X(3872)$  production in high energy heavy ion collisions, *Phys. Rev. D*90 (11) (2014) 114023, [Erratum: *Phys. Rev. D*93,no.5,059902(2016)]. arXiv:1405.7583, doi:10.1103/PhysRevD.93.059902, 10.1103/PhysRevD.90.114023.
- [398] B. D. Moreira, C. A. Bertulani, V. P. Goncalves, F. S. Navarra, Production of exotic charmonium in  $\gamma\gamma$  interactions at hadron colliders, *Phys. Rev. D*94 (9) (2016) 094024. arXiv:1610.06604, doi:10.1103/PhysRevD.94.094024.
- [399] V. P. Goncalves, B. D. Moreira, Probing the  $X(4350)$  in  $\gamma\gamma$  interactions at the LHC arXiv:1809.08125.
- [400] V. R. Debastiani, F. S. Navarra, A non-relativistic model for the  $[cc][\bar{c}\bar{c}]$  tetraquark arXiv:1706.07553.